IL-7 as a marker of a subset of bone marrow mesenchymal stromal cells

Sally L Clough

PhD

University of York

Biology

April 2013

Abstract

The organisation of a multitude of cellular niche components, their communication via many signalling pathways and their response to physical factors, protects and regulates haematopoietic stem cell (HSC) fate in adult bone marrow. Whilst the contribution of osteoblasts, endothelial cells and perivascular cells have been examined, the role of a second stem cell population in the bone marrow; mesenchymal stem cells, is not well understood due to the lack of distinctive markers to identify them *in vivo*. There is therefore a requirement to determine a characteristic that allows their prospective isolation. Under certain conditions, stromal cells and osteoblasts in the bone marrow express IL-7. The use of a novel IL7-Cre BAC transgenic mouse line has allowed more accurate IL-7 protein detection *in situ* and demonstrated IL-7 reporter expression in mesenchymal lineage cells in endosteal and vascular HSC niche locations. These cells were further characterised in this study in order to determine if IL-7 or nestin, an intermediate filament associated with a wide range of stem cell populations, is expressed by and could identify bone marrow derived MSCs.

YFP positive cells were analysed in sections of IL-7Cre Rosa26-eYFP mice. Interestingly, it was only a proportion of mesenchymal cells that expressed YFP, supporting the theory that subsets of MSCs exist and therefore, that they may have different roles in numerous bone marrow niches. IL-7 was not observed to have any effect on the proliferation or differentiation of human MSCs. Generation of MSC clones supported the suggestion that *in vitro* cultures of MSCs are a heterogeneous population and they displayed a wide range of IL-7 and nestin mRNA expression levels.

Contents

List of figures

List of tables

Acknowledgements

My sincere thanks go to my supervisors Paul Genever and Mark Coles for their guidance and support throughout my PhD. I would also like to thank Nathalie Signoret and Betsy Pownall for helpful suggestions as members of my training committee. Thank you to the wonderful staff in the Technology Facility, particularly to Graeme Park and Karen Hodgkinson for their training, assistance and patience. Thanks go to the MRC for financial support.

I would also like to thank all my fellow lab members, past and present, for their assistance in the lab. In particular: Jen Lee, Elen Bray, Tatjana Schilling and Fatima Saleh and more recently, Becky Mason and Sally 'the other one' James, for their continued guidance and lasting friendships. Thank you to all lab members for the almost constant stream of cakes and for generally making the biology department a lovely place to work!

To all those, too many to mention, that have rummaged in freezers and cupboards to find tissue samples and gladly shared reagents and technical advice – thank you. To those that provided tea, listened and consoled and to those who jumped to help proof-read this thesis - thank you. A special mention to Julie Knox, Hilary Jones and the Springboard network who helped me through to the end!

I would like to thank my husband, Dave, for his unwavering support and eternal optimism and to my beautiful little boy, Albi, the best remedy and an endless source of joy – thank you. Finally, I would like to thank my parents, Mary and David Jackson. Their support is immeasurable and words cannot express my gratitude. It is to them that I dedicate this thesis.

Declaration

No part of this degree has been submitted for any other degree to any other institution. I declare that I am the sole author of the work in this thesis except where clearly stated and recognise the contribution of others for the provision of tissue: Mark Coles, Amy Sawtell, Priyanka Narang and Anne Thuery harvested mouse tissue (section 2.1.4) and Bridget Glaysher isolated and purified human T cells (section 2.1.5).

Signed . . . . . .

Date . . . . . .

1. Introduction

1.1 Mesenchymal stem cells

The recapitulation of bone and bone marrow formation was demonstrated in the late 1960s by transplanting bone marrow fragments to heterotopic anatomical sites in mice (Reviewed by Tavassoli & Crosby, 1968). However, it is Friedenstein who is acknowledged with the discovery of bone marrow mesenchymal stem cells (MSCs) as his group demonstrated over a series of refined experiments that the osteogenic potential was confined to a small subset of bone marrow cells distinct from haematopoietic cells (Friedenstein et al, 1970). These cells were observed to adhere to tissue culture plastic with a fibroblastic morphology and could give rise to discrete colonies of cells when plated at clonogenic concentrations, subsequently termed colony-forming unit-fibroblasts (CFU-Fs). Additionally, single cells could be transplanted *in vivo* and demonstrated self renewal and skeletal differentiation capacity. Fulfilling the criteria for stem cells, the CFU-Fs were consequently named osteogenic stem cells and later stromal stem cells. Some years later the term mesenchymal stem cell was popularised for these stem cells *ex vivo* and remains, if a little controversially, in use today.

1.1.1 Nomenclature

Discrepancies exist around the term ‘mesenchymal stem cell’ that was originally conceived in 1991 by Caplan and given to multipotent bone marrow precursors (Caplan, 1991). The inclusion of the term “stem cell” suggests that alongside a multipotent ability to generate cells of bone, fat and cartilage (Figure 1.1), a single MSC may be transplanted and self renew appropriately to give rise to bone structure with accompanied host haematopoiesis. As many authors had used the term MSC to describe plastic-adherent cells that were multipotent *in vitro* but had not necessarily demonstrated *in vivo* self renewal capacity, the International Society for Cellular Therapy (ISCT) released a statement in 2005 to encourage the use of the term ‘multipotent mesenchymal stromal cell’ for these cells, reserving the ‘mesenchymal stem cell’ label for those that accomplished *in vivo* self renewal

(Horwitz et al, 2005). They recognised that the acronym MSC was widely accepted and sought to keep this for either population, as will be adopted in this report. However, this particular point has been disputed as causing more confusion in the field and therefore some designate different acronyms to try to acknowledge the 'stemness' of the cells they are reporting. As the identification and characterisation of MSCs in all their guises continues, this nomenclature is likely to shift further in the future and the most important points will concern the standardisation of their isolation and the accurate descriptions of their functionality and various subpopulations both *in vivo* and *in vitro*.

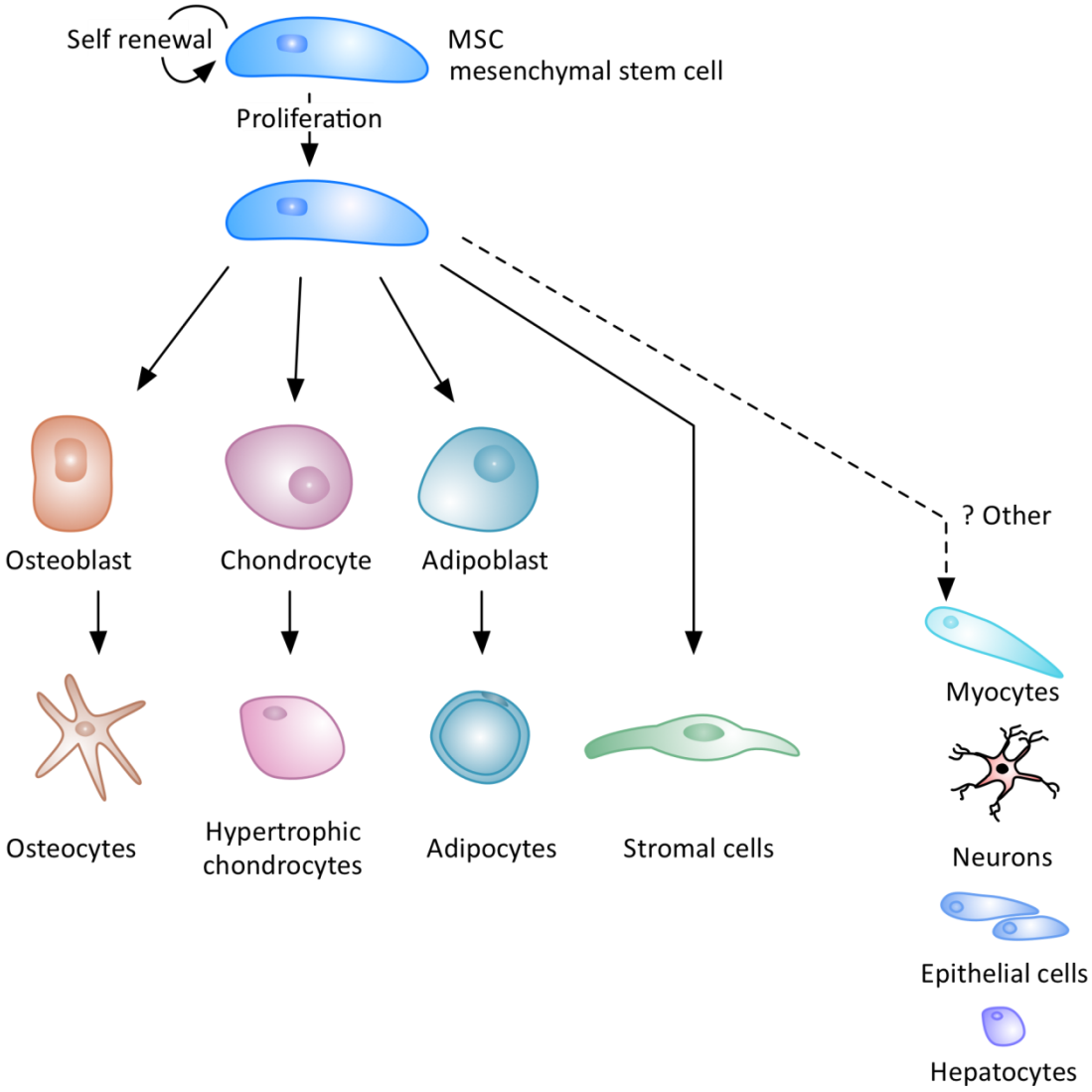

Figure 1.1 Lineage potential of mesenchymal stem cells
Mesenchymal stem cells are able to proliferate, self-renew and differentiate to give rise to cells of the bone, fat and cartilage. Evidence has also been reported to suggest their ability to differentiate into other lineages such as neural cells or liver cells although this remains controversial.

1.2 Developmental origin of MSCs

To date, a limited amount is known about the developmental origins of MSCs. MSCs have been isolated from numerous connective tissues in adult mammalian systems with a variation in their functional properties. The definition of their progenitor population may explain some of the current inconsistencies and allow directed differentiation of pluripotent stem cells and analysis for expanding MSC populations for therapeutic use.

Currently, bone marrow MSCs are predicted to arise from specific progenitors as skeletal tissue is derived from distinct embryonic regions. Neuroectodermal progenitors generate the craniofacial bones and cartilage, the limb skeleton originates from lateral plate mesodermal cells and axial skeleton develops from paraxial mesoderm (somites) (Olsen et al, 2000).

1.2.1 Mesoderm

Colony forming assays directing the differentiation of mouse embryonic stem cells (mESC) resulted in the identification of the haemangioblast, a bipotent precursor of haematopoietic and endothelial progeny (Choi, 1998). The haemangioblast was subsequently demonstrated in mouse embryos as a subpopulation of mesoderm prominently detected in the posterior primitive streak (Huber et al, 2004).

Previous derivation of MSCs from human ESCs (hESCs) with comparable potential to those isolated from adult bone marrow has been reported (Trivedi & Hematti, 2008) but the precursor population that gives rise to the MSCs remains poorly defined. Recent progress has been made in the designation of a mesenchymoangioblast as a direct MSC precursor with endothelial and mesenchymal potential. hESCs were subcultured with OP-9 (bone marrow-derived mouse stromal cell line) cells and directed towards a mesodermal specification. These hESCs were then plated in semi-solid media in the presence of fibroblast growth factor 2 (FGF2) and absence of serum. After a 2 day initial co-culture, this generated colonies that could be identified as mesenchymal (MS) by the surface marker pattern of $CD140a^{+}CD90^{+}CD56^{+}CD166^{+}CD31^{-}CD43^{-}CD45^{-}$ $CD146^{+}$. When

cells were initially co-cultured for 3 days, they formed more dispersed cell colonies (blast) that expressed haematopoietic commitment transcripts, as measured by RT-PCR. Both of these colony types were transient and could not be produced from hESCs co-cultured for more than 3 days before the colony assay or in the presence of serum (Vodyanik et al, 2010). The precursor for each colony was further specified as expressing apelin receptor (APLNR). APLNR was upregulated during co-culture mesodermal differentiation. Undetectable levels of APLNR were associated with undifferentiated hESCs that then increased to approximately 20% and 70% APLNR positive cells on days 2 and 3 of co-culture with OP-9 cells, respectively. Transcript analysis of $APLNR^+$ cells reported the absence of neural crest associated genes, in contrast to the presence of but no particular enrichment for, mesodermal genes. The treatment of co-culture cells with the Wnt agonist Dkk-1 or inhibitors of TGF-β signalling, both known to interrupt pathways mediating mesodermal differentiation, individually obliterated $APLNR^+$ expression. The authors therefore suggest that $APLNR^+$ cells represent a subpopulation of the mesoderm and further investigation will hopefully identify a unique marker for these cells (Vodyanik et al, 2010).

1.2.2 Neural crest

The neural crest is a mass of cells that arises at the neural fold during vertebrate development. Neural crest-derived stem cells (NCSCs) are able to differentiate to provide cells that constitute most of the peripheral nervous system (PNS) including neurons, glial cells and myofibroblasts. NCSCs also differentiate to chondrocytes, adipocytes and osteocytes that generate the bone structure and connective tissues in the head and neck. These tissues in the main body are widely attributed to cells of mesodermal origin and the differentiation of MSCs. The generation of transgenic mice have provided useful tools to investigate specific neural crest-derived cells. Protein zero (P0) or Wnt1 promoter or enhancer-driven Cre recombinase activity indelibly marks neural crest cells with a reporter transgene such as GFP (Danielian et al, 1998; Yamauchi et al, 1999). P0 is a cell adhesion molecule primarily associated with myelin sheaths in the PNS and at a transcript level has been

reported in neural crest cells after delamination from the neuroepithelium (Filbin et al, 1990) whilst Wnt1 expression is restricted to the neural plate and dorsal neural tube (Echelard et al, 1994). These transient expression windows make P0 and Wnt1 ideal candidates to demarcate cells of the neural crest. Additionally, Sox10 has been used in a similar way, as its expression is identified in the neural crest in the developing embryo in humans and rodents (Bondurand et al, 1998; Kuhlbrodt et al, 1998). Evidence suggests that these cells migrate to the developing thymus and differentiate into the cells associated with vasculature, indicating the contribution of neural crest derived mesenchymal cells to organs outside of the nervous system (Foster et al, 2008).

Emerging evidence suggests that NCSCs migrate to the adult bone marrow and contribute to the functional MSC population. GFP^+ cells were isolated from the bone marrow of adult Wnt1-Cre and P0-Cre/GFP transgenic mice and were able to self renew in sphere culture and differentiate into neural lineages (Nagoshi et al, 2008). Additionally, GFP^+ NCSCs were detected in the aorta-gonad-mesonephros (AGM) region, circulating blood and foetal liver as well as adult bone marrow, suggesting the NCSCs migrate to the bone marrow from the neural crest through the blood (Nagoshi et al, 2008). They also appeared in each tissue location to coincide with the concurrent arrival of haematopoietic stem cells (HSCs). As the stromal network of the niche is a supportive collaboration that is resident before the entrance of HSCs in order to guide and maintain the HSCs, this suggests that the NCSCs have intrinsic spatial and temporal roles on HSCs development. The NCSCs seem to retain the neuronal potential presumably gained at the site of generation in the neural crest, although it remains to be seen whether this is required for maintenance of sympathetic nerves in the bone marrow or whether it is a redundant pathway that can be reinstated in isolated cells *in vitro*.

Identification of NCSCs in bone marrow is hampered by the intrinsic problem of a unique characterisation marker for MSCs. P75 has been used to isolate rodent NCSCs from the sciatic nerve (Morrison et al, 1999) and although this marker had

been determined in multipotent cells obtained from tissue explants, *in vivo* BrdU incorporation experiments demonstrated the self renewal capabilities of these cells (Morrison et al, 1999). More recent advances utilise the Wnt1-Cre transgenic mouse model allowing neural crest-derived cells to be determined and examined in tissues outside the central nervous system (CNS). NCSCs have been located in the adult murine cornea (Yoshida et al, 2006), heart (Tomita et al, 2005) and gut (Kruger et al, 2002), indicating their migration and retention throughout adult life. Comparison between the adult and foetal NCSCs reported a reduced efficiency and more restricted multipotency in adult stem cells from the cornea (Yoshida et al, 2006) and gut (Bixby et al, 2002) (Kruger et al, 2002) prompting the requirement for classification and further understanding of this cell population.

Neuroepithelium cells have also been proposed as a common progenitor for bone marrow MSCs. $Sox1^+$ neuroepithelial cells differentiate into MSCs as detected in embryonic stem cell culture and Sox1-Cre/GFP transgenic embryo analysis (Takashima et al, 2007). Further investigation reported that somitic PDGFRα^+ cells present in E9.5 embryos could not give rise to MSCs *in vitro* but could differentiate into adipocytes, suggesting that the first MSC progenitors in this murine model are from a neuroepithelium source and not from the mesoderm. Further analysis concluded that $Sox1^+$ progeny could not account for all of the MSCs present in neonates and suggests that they only represent an initial wave of MSC supply which is supplemented from as yet undescribed sources (Takashima et al, 2007).

Another study using transgenic mice with neural crest specific GFP expression (P0-Cre/Floxed-eGFP) found that GFP positive and negative MSCs isolated from adult bone marrow were comparable in their ability to differentiate down tri-lineage mesenchymal pathways and into neuronal cell types under appropriate instruction (Morikawa et al, 2009b). MSCs were sorted as populations with the phenotype PDGFRα^+Sca-1^+CD45^-TER119^-, as alterations to this pattern led to lack of a fully differentiating or CFU-F forming potential (Morikawa et al, 2009b). Bone marrow-derived NCSC and MSC clones could be differentiated into osteocytes and

chondrocytes but NCSCs required pre-treatment with Wnt1 before successful adipogenic differentiation, which was not necessary for MSCs (Wislet-Gendebien et al, 2012). MSCs were only seen to differentiate into Tuj-1-expressing cells when cultured in contact with cerebellar granule neurons whereas NCSCs spontaneously differentiated into neural lineage cells in normal or induction media (Wislet-Gendebien et al, 2012). Taken together, these studies support the theory that bone marrow MSCs are comprised of cells from at least two origins: neural crest and mesodermal. However, the confinement of neural differentiation potential to MSCs derived from the neural crest is still disputed.

HSCs have also controversially been proposed as the origin of bone marrow fibroblasts and their precursors (Ebihara et al, 2006). Further investigations will be important to determine the full potential of each of these cells to generate MSCs and any physiological differences in MSCs that arise from different developmental origins.

1.2.3 Surface markers of MSCs

Identifying tissue resident MSCs will naturally facilitate the isolation of their precursors. MSCs represent a rare population inhabiting a complex bone marrow environment. Their characterisation is further hampered by the lack of a unique identifying cell surface marker. Currently, isolated and cultured MSCs are commonly distinguished *in vitro* by a panel of cell surface markers. In 2006 the International Society for Cellular Therapy (ISCT) produced a specification of markers that should determine plastic-adherent MSCs *in vitro* (Dominici et al, 2006). This included expression of CD105, CD90, and CD73. MSCs should also be negative for a vast array of markers; haematopoietic markers CD45 and CD34, monocytic markers CD14 and CD11b, B cell markers CD79a and CD19 and HLA class II. They must also be able to differentiate *in vitro* into osteoblasts, adipocytes and chondrocytes as part of the minimum suggested criteria. Despite these attempts to standardise the cell populations used to study MSC biology, issues remain surrounding alterations in expression that may occur due to *in vitro* culture before analysis. For example,

CD44, routinely used to characterise MSCs (Herrera et al, 2007; Sun et al, 2003) has been reported to be acquired in culture in murine and human populations as prospectively isolated MSCs were found to be $CD44^-$ (Qian et al, 2012).

Isolation from multiple tissue sources and the determination of multipotentiality *in vitro* contributes to the reported differences in MSC characterisation and the difficulty in confidently isolating a single cell type. It has been suggested that the heterogeneous properties of *in vitro* MSCs are not consistent with those in the *in vivo* environment. Cultures of MSCs can appear homogeneous for the expression of a range of cellular markers but have functional heterogeneity as demonstrated by clonal line production of Stro-1^+ VCAM-1^+ MSCs (Gronthos et al, 2003). Isolation of the monoclonal antibody Stro-1 led to recognition of a cell surface antigen on bone marrow cells that were capable of CFU-F generation and classic tri-lineage differentiation *in vitro* (Simmons & Torok-Storb, 1991). Although Stro-1 enriched the MSC population, the antibody also cross-reacts with glycophorin-A-positive nucleated red cells and B-lymphocytes, which meant contaminating cells prevented a homogeneous culture. This was partly overcome by using the combination of Stro-1 with vascular cell adhesion molecule-1 (VCAM-1/CD106), which generated a purer population but still showed varying clonogenic potential (Gronthos et al, 2003).

CD146 expression was detected in human bone marrow-derived subendothelial cells that were able to transfer ectopic bone and bone marrow when transplanted into irradiated mice hosts suggesting its use for prospectively isolating stromal progenitors *in vivo* (Sacchetti et al, 2007). In human bone marrow sections, CD146 labelling was restricted to adventitial reticular cells (ARCs) that were observed lining sinusoidal vessels with extended cellular processes. This localisation was supported by evidence that CD146 is upregulated in normoxic conditions but down regulated in hypoxia (Tormin et al, 2011). CD271 has been used to prospectively isolate bone marrow MSCs (Jones et al, 2002). CD271 is also known as $p75^{NTR}$ (a low affinity neurotrophin receptor), which is expressed on NCSCs that are capable of neuronal and mesenchymal differentiation (Lee et al, 2007; Stemple & Anderson, 1992). As is

common with other prospective markers, there is some cross reaction with other cell types. In this case, CD271 has been reported at low levels on erythroid cells that can be removed from the MSC culture by selecting CD45 negative cells (Cuthbert et al, 2012). CD271 had been used in conjunction with CD146 to identify subpopulations of MSCs. Similar CFU-F ability and morphological appearance was observed when cultured *in vitro* between $CD271^{+}/CD45^{-}/CD146^{-/low}$ and $CD271^{+}/CD45^{-}/CD146^{+}$ cells (Tormin et al, 2011). Additional markers CD105, CD90, and Stro-1, as well as PDGFR-β were expressed by each population. Interestingly, immunodetection in human bone marrow sections determined the $CD271^{+}/CD45^{-}/CD146^{-/low}$ population as bone lining cells whilst $CD271^{+}/CD45^{-}/CD146^{+}$ cells were associated with the sinusoids as previously reported for $CD146^{+}$ cells (Tormin et al, 2011). Isolated $CD146^{+}$ cells have also been reported to support *in vitro* haematopoiesis in long term cultures through the expression of adhesion molecules and cytokines (Sorrentino et al, 2008).

Murine MSCs are comparatively more difficult to culture *in vitro* due to a high level of haematopoietic cells contaminating the culture and the strict growth conditions that are required. Some surface markers detected on human MSCs cannot be conferred to mouse MSCs and additionally, the markers on mouse MSCs can vary between different mouse strains, adding an extra level of complexity when using these models to study MSCs. For example, Stro-1, mentioned above as an important human MSC marker, has no comparable antigen in mice. Another human marker, CD90 is also inconsistently reported with negative, (Anjos-Afonso et al, 2004) heterogeneous (Morikawa et al, 2009a) and positive (Chan et al, 2009) expression associated with MSCs despite using the same mouse strain (C57BL/6). This may be due to the inability to accurately define MSCs generally and therefore the identification of true MSCs or progenitors using CD90 as a marker *in vitro*. Therefore, slightly different candidates are considered in mice alongside those markers determined on human MSCs and whilst not completely compatible, the use of murine models can provide a useful understanding of the physiology of MSCs.

In murine studies, prospectively isolated PDGFRα^{+}Sca-1^{+}CD45^{-}TER119^{-} were identified in a perivascular region in adult mouse bone marrow with mesenchymal differentiation potential when transplanted into immunodeficient recipients (Morikawa et al, 2009a). The highest expression levels of HSC maintenance genes angiopoietin-1 (Ang-1) were detected in PDGFRα^{+}Sca-1^{+} cells, with abundant CXCL12 expression detected in PDGFRα^{+}Sca-1^{-} cells (Morikawa et al, 2009a).
Nestin^{+}CD45^{-}CD31^{-} cells investigated in the bone marrow of Nes-GFP transgenic mice, in which cells express GFP under regulatory elements of the nestin promoter (Mignone et al, 2004), have also been shown to contain the MSC capacity of the bone marrow. Nes-GFP^{+} cells were able to self renew *in vivo* and differentiated down mesenchymal lineages that were incorporated into bone and cartilage tissue, as analysed by lineage tracing studies (Mendez-Ferrer et al, 2010).

Despite progress to characterise the MSCs, the use of a multiple set of markers is problematic, as other cell types express individual markers, each marker may not have continuous roles throughout the life of MSCs and there are clear differences between expression of the markers used in mouse and human studies that requires a cautionary approach. Therefore, identifying a unique marker would be a very powerful tool to isolate specific MSC populations in order to provide consistent results and potential sources for therapeutic use.

1.3 The stem cell niche concept

Whilst MSCs can be isolated by their ability to adhere to plastic and studied *in vitro*, the restrictions of studying representative behaviour and not just culture artefact, requires that MSCs be identified *in vivo*. Confidently identifying MSCs begins with considering where they reside in the bone marrow.
The concept of the stem cell niche was proposed in 1978 to describe an environment that would accommodate and regulate the action of stem cells by maintaining the properties of self renewal and multipotent differentiation (Schofield, 1978). This idea was corroborated by the existence of stem cell niches in Drosophila, which demonstrated regulation of germ line stem cells by the stromal

cells in the ovary and asymmetric division (Xie & Spradling, 2000). This explained the apparent immortality of the HSCs despite the replenishment of mature bone marrow cells that had intrigued Schofield and colleagues. Further work has continued to examine the regulation of stem cell fate by its immediate environment as the cellular components and their interactions are still unclear.

1.3.1 Bone marrow microenvironment

Bone is a complex, specialised tissue that provides the body with mechanical support, protection of internal organs and a resource for ions such as calcium and phosphate. Skeletal bones have an outer layer of compact bone surrounding an inner trabecular bone. Bone matrix is continually replaced and remodelled, controlled by osteoblastic and osteoclastic action and is therefore a dynamic and organised structure. The bone marrow is contained within the bone cavities and encompasses a vast network of blood vessels supplying access and nutrients to undifferentiated and mature haematopoietic and stromal cells.

In mammalian bone marrow, two stem cell populations, HSCs and MSCs are evident. Their respective niches are intertwined and much niche investigation has been modelled using HSCs as it is a well characterised stem cell population with defined transplantation end point assays. In this way, most of the proposed niche components are presumed to be in close contact with the HSCs. Multipotent, long-term HSCs (LT-HSCs) are able to expand the stem cell pool for the life time of an organism to maintain and replace the haematopoietic system. By the process of asymmetric division these cells also give rise to differentiated short-term HSCs (ST-HSCs) or lineage restricted cells known as multipotent progenitors (MPPs) that proliferate and differentiate to produce the mature cells of the blood. HSCs have been identified in perivascular, endosteal and stromal compartments in the bone marrow (Kiel et al, 2005). In the continually remodelled bone marrow environment, it remains to be seen how much these niches overlap and the extent to which they might themselves be remodelled in the process of regulating HSC and MSC fate.

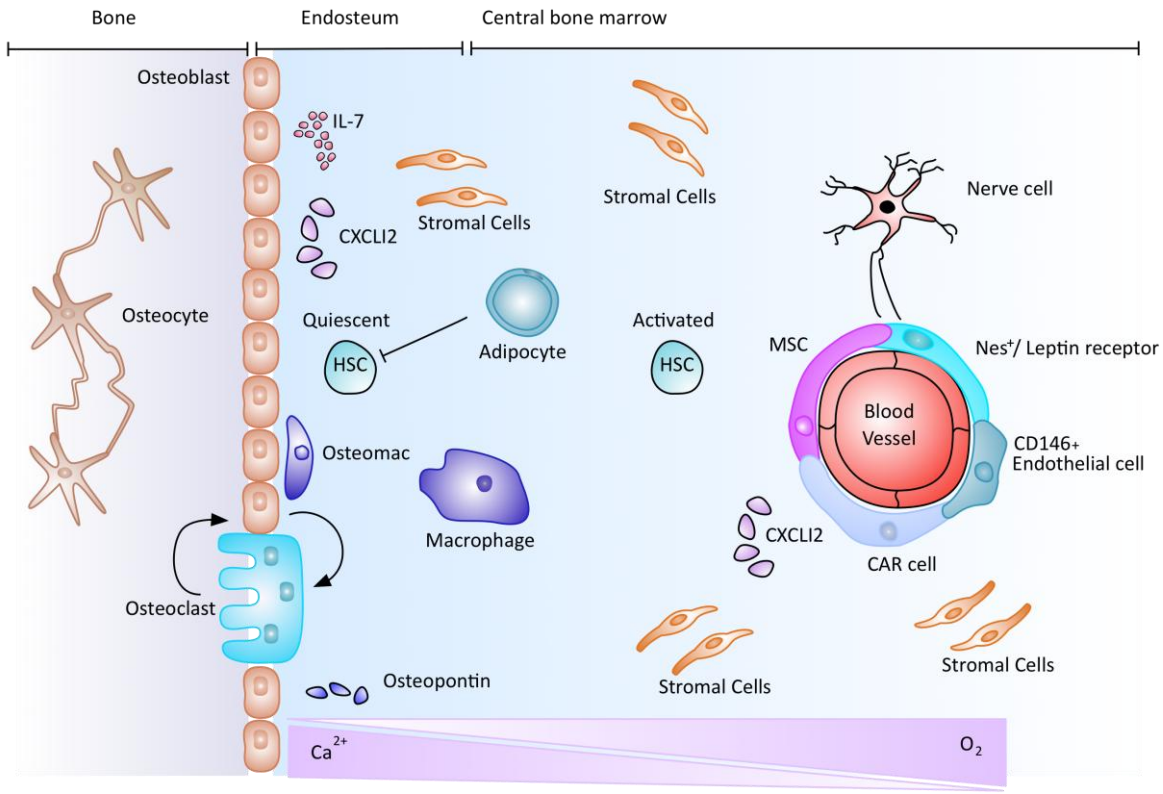

Figure 1.2 The bone marrow microenvironment

The bone marrow environment comprises multiple cellular components and a complicated cross-talk to regulate HSC fate.

Stromal cells are an important element of the HSC niche in vascular and endosteal locations and interact with osteoblasts and osteoclasts at the endosteum. Osteoblasts are implicated in retaining HSCs in the bone marrow. Expression of nestin, leptin receptor, CD146 and CXCL12 have all been described as potentially distinct markers of MSCs in the bone marrow HSC niche. Abbreviations: HSC; Haematopoietic stem cell, Ca^{2+}; calcium, O_2; oxygen, CAR cell; CXCL12 abundant reticular cell, MSC; mesenchymal stromal cell.

1.3.2 Perivascular niche

HSCs are closely associated with vascular tissue throughout their development. Haematopoietic cells are first detected in the extra-embryonic tissue of the yolk sac and then migrate to the foetal liver and bone marrow, a highly vascularised tissue (Moore & Metcalf, 1970). HSCs are also present at extramedullary sites such as the liver in adult tissues. Lineage^{-}Sca-1^{+}c-kit^{+} (LSK, markers used to define HSC lineage) cells isolated from adult mouse liver could competently reconstitute irradiated mice (Taniguchi et al, 1996). Additionally, HSCs are detected in the adult peripheral blood during homeostasis (Goodman & Hodgson, 1962) and in response to chemokines that can mobilise HSCs within minutes of administration (Laterveer et al, 1995). It is a logical explanation that HSCs residing in contact to bone marrow sinusoids would be able to monitor exogenous signals in the blood and respond effectively to haematopoietic requirement. Taken together, these findings support the location of HSCs in a perivascular location (Figure 1.2).

The SLAM (signalling lymphocytic activation molecule) family contains 10-11 cell surface receptors that are involved in lymphocyte activation (Engel et al, 2003). SLAM-family members CD150, CD244 and CD48 were used to identify HSCs by immunohistochemistry on tissue sections and a vascular niche was identified in the bone marrow (Kiel et al, 2005). There is some debate whether the endosteal and perivascular niches that have been recognised are true niches that maintain the self-renewal properties of HSCs. Perhaps the perivascular niche is just a holding pen for the HSCs that are primed to differentiate and provide a multitude of mature cells for systemic dispersal and the endosteal niche is where the most immature HSCs reside. Further detailed analysis is therefore required to understand the role of the niche on HSC behaviour.

1.3.3 Endosteal niche

The endosteum is the margin between bone and bone marrow and as such is the site of bone turnover. It is populated by a range of osteoblastic cells at different stages of differentiation that contribute to bone formation. The co-operation

between the processes of bone remodelling and haematopoiesis and the relationships between the cells that are involved are gradually being uncovered (Figure 1.2). Since the HSC niche proposal, there has been an accumulation of evidence to demonstrate that HSCs are located in close proximity to the endosteum (Lord et al, 1975) and that HSCs in this region possess the highest proliferative and haematopoietic potential (Haylock et al, 2007). This has been facilitated by the development of techniques such as intravital microscopy and multiphoton microscopy to analyse HSCs *in situ*. Transplanted LSK $CD150^{+}$ $CD48^{-}$ cells could be viewed by two-photon microscopy in live, irradiated mouse calvarial bones. The cells homed to within 20 µm of the endosteum while more committed progenitors and HPCs (LSK $Flt3^{+}$ $CD34^{+}$) were observed to home to a position further from the endosteum. This homing to a greater distance from the endosteum was also the case for HSCs in non-irradiated mice, suggesting that the endosteal niche is a preferred site for HSCs but that they must be depleted before lodgement of HSCs can occur and that different niches exist for cells that are more mature (Lo Celso et al, 2009).

1.3.4 HSC mobilisation to and from the niche

The processes of homing and mobilisation are key to understanding what first attracts HSCs to their niche in the bone marrow and what subsequently stimulates their mobilisation out again. Just before birth, HSCs migrate from foetal liver to the bone marrow and are able to re-enter the peripheral circulation during homeostasis or in response to demands for blood cells (Christensen et al, 2004; Massberg et al, 2007; Wright et al, 2001). CXCL12, (also known as stromal cell–derived factor-1, SDF-1) is an essential chemoattractant of HSCs that express its receptor CXCR4. The CXCL12/CXCR4 axis is an important signalling mechanism in the process of HSC homing to the niche and their subsequent retention. Deletion of either gene leads to depletion of HSCs in the bone marrow (Sugiyama et al, 2006; Tzeng et al, 2011). Therefore, a thorough understanding of the process and the identification of niche cells that express CXCL12 will provide improved strategies to aid the mobilisation of HSCs into peripheral blood for harvest and subsequent therapeutic use.

Whilst the mechanism of HSC direction into the peripheral blood in homeostasis is largely unknown, it has been proposed that it is initiated by circadian oscillations of CXCL12 in the bone marrow that result in the rhythmic release of HSCs into the bloodstream, in mice at least (Mendez-Ferrer et al, 2008). Mice deficient for CXCL12 die perinatally due to extreme defects in haematopoietic and central nervous systems (Baune et al, 2011). This is due to the disruption of the homing and engraftment of HSCs to the bone marrow from the liver. Furthermore, elevated levels of plasma CXCL12 mobilised HSCs into circulation in severe combined immunodeficient (SCID) mice, an activity that can be exploited to improve the harvesting of HSCs for therapy (Hattori et al, 2001). In clinical trials, an antagonist of CXCR4, Plerixafor (AMD3100), mobilised HSCs and their progenitors to the peripheral blood (Fruehauf et al, 2009).

Granulocyte-colony-stimulating factor (G-CSF) has been traditionally used to mobilise HSCs but not all patients respond satisfactorily. G-CSF functions to induce the degradation of SDF-1 in the bone marrow and indirectly causes the upregulation of CXCR4 (Petit et al, 2002). A synergistic response is seen when the two chemokines are used in combination to stimulate HSCs to enter the circulation and AMD3100 can be used as an alternative stimulant where G-CSF fails (Uy et al, 2008; Watt & Forde, 2008); an attractive benefit resulting from increased understanding of the roles of niche components. Entering and exiting the stem cell niche is a tightly controlled process which is adaptive to changes detected in the microenvironment.

1.3.5 Cellular candidates of the HSC niche

Whilst the cellular components of the niche may depend on the physical location in the bone marrow, a common theme is the skeletal progenitors that are reported at each site. Cells implicated in the HSC niches include osteoblasts, CXCL12-abundant reticular (CAR) cells and MSCs (Figure 1.2).

1.3.5.1 HSCs regulate their own niche

Mature cells derived from HSCs such as osteoclasts and macrophages (described below) have been implicated in regulating the stem cell niche and therefore indirectly influencing the fate of HSCs. Evidence also exists to support the theory that HSCs are able to regulate the niche directly. Using an *in vitro* co-culture system with HSCs and mesenchymal cells, steady state HSCs were observed to direct osteoblastic differentiation of bone marrow stromal cells and this osteogenesis was increased in conditions where the HSCs were derived from acutely stressed mice. The HSCs mediated the response through secretion of bone morphogenic protein (BMP)-2 and BMP-6, as detected by cDNA screening and RT-PCR (Jung et al, 2008).

1.3.5.2 Osteoclasts

Bone forming osteoblasts and bone resorbing osteoclast numbers and function are tightly regulated in order to maintain the structural integrity of bone. Osteoblasts are responsible for initiating the maturation of osteoclasts with the production of receptor activator of NF-κB ligand (RANKL). The haematopoietic origin of osteoclasts is indicated by the ability of RANKL to initiate their generation from the differentiation of macrophage progenitors (CFU-M) (Miyamoto et al, 2001). Following RANKL activation in mice, osteoclasts promote the release of haematopoietic progenitors into circulation (Kollet et al, 2006). However, osteoclasts have been shown to be non-essential for this role as their targeted depletion in mouse models had no effect on G-CSF induced HSC mobilisation (Miyamoto et al, 2011). In fact, another action of osteoclasts suggests the reverse of this role as during bone resorption, calcium is released from the bone into the endosteal region, which has a reported role in HSC retention (Adams et al, 2006) .

1.3.5.3 Macrophages

Macrophages and monocytes are implicated in the retention of HSCs within their niche. Endosteal macrophages or 'osteomacs' have a reported osteoblast supportive role and their depletion results in the mobilisation of HSCs and was concomitantly associated with a reduction in endosteal osteoblast numbers and a

significant reduction of CXCL12, stem cell factor (SCF also known as kit ligand), and Ang-1 mRNA levels at the endosteum (Winkler et al, 2010). This is similar to the effects observed by G-CSF administration. F4/80^{+} macrophages in mice and CD68^{+} macrophages in human bone sections are both observed at the endosteal surface (Chang et al, 2008). Addition of bone marrow macrophages to osteoblast differentiation cultures *in vitro* increases mineralisation, indicating their role in regulating osteoblast function and the consequential niche adaptation (Chang et al, 2008). In order to more specifically identify the macrophage cells responsible for HSC retention, CD169^{+} macrophages have been investigated. Specific depletion of CD169^{+} macrophages resulted in HSC mobilisation to the peripheral blood (Chow et al, 2011). Similar to the effects of 'osteomac' depletion (Winkler et al, 2010), the depletion of CD169^{+} macrophages was also associated with almost a 50% reduction in CXCL12 mRNA detected in total bone marrow (Chow et al, 2011). In this instance, the reduction was attributed to the nestin^{+} stromal cells, as CD169^{+} macrophages themselves do not produce CXCL12. CXCL12 associates with its receptor CXCR4 which is expressed on HSCs and functions to attract and retain HSCs in the niche (Lapidot & Petit, 2002). The subsequent loss of CXCL12 therefore explains the exit of HSCs into the circulation and reinforces the control of CXCL12 in the stem cell niche.

1.3.5.4 MSCs

MSCs have been reported to be an essential component in initiating the formation of the niche. CD45^{-}Tie2-α^{+}CD105^{+}Thy1.1^{-} cells isolated from foetal mouse bones produced bone with bone marrow when transplanted under the kidney capsule, through a transitional stage of cartilage formation known as endochondral ossification (Chan et al, 2009). Only bone was derived from cells with a similar phenotype isolated from foetal calvarial tissue and CD105^{+}Thy1^{+} progenitors from foetal bone, indicating that the mechanism of endochondral ossification is essential for HSC niche formation and that it is orchestrated by specific MSC populations.

Stromal cells expressing GFP under the control of nestin regulatory elements were observed in the murine bone marrow (Mendez-Ferrer et al, 2010). Differentiation

studies attributed tri-lineage potential only to nestin$^+$ stromal cells that could also contribute to osteochondral lineages when transplanted *in vivo*. Thus, nestin$^+$ stromal cells were proposed to be MSCs. These nestin$^+$ MSCs were located in the central marrow and at the endosteum near to HSCs and in contact with adrenergic nerve fibres of the sympathetic nervous system (SNS) which are known to regulate the mobilisation of HSCs (Katayama et al, 2006). Depletion of nestin$^+$ MSCs led to a reduction in HSC number and decreased their ability to home to the bone marrow when transplanted into irradiated mice. These studies indicate that MSCs contribute to the homing of HSCs to the niche and their retention and maintenance once in the bone marrow.

1.3.5.5 Osteoblasts

The differentiated progeny of MSCs are also widely regarded as niche components. The location of the endosteal niche suggests the involvement of osteoblastic cells in the regulation of HSC fate. Osteoblasts line the bone margin and secrete unmineralised matrix in the process of bone formation and control osteoclast activation (Mackie, 2003). *in vitro*, osteoblasts have been shown to maintain the immature phenotype of HSCs and support limited expansion of progenitors (Taichman et al, 1996). This supports the notion that osteoblasts are capable of promoting *in vivo* stem cell survival and self renewal. Osteoblasts secrete a number of haematopoietic cytokines including G-CSF, M-CSF, IL-1, IL-6 (Taichman & Emerson, 1994), IL-7 (Weitzmann et al, 2000) and CXCL12 (Ponomaryov et al, 2000) that have a significant role in the retention and maintenance of HSCs.

Two reports reinforced these initial *in vitro* findings by identifying osteoblasts as a key component in HSC regulation in mouse models. In the first of the simultaneously released articles, an increase in osteoblast numbers in response to stimulation by parathyroid hormone (PTH) was associated with an increase in the number of HSCs, which do not themselves express the receptor for PTH (Calvi et al, 2003). In the second study, depletion of BMP receptor 1A in haematopoietic cells and stromal cells resulted in the expansion of the HSC population and an increase in

osteoblast numbers (Zhang et al, 2003). Mice deficient in BMPR1A had abnormal bone formation and a 2-fold increase in functional LT-HSCs, whilst the number of progenitor cells remains the same as controls, indicating the increase in stem cells was not caused by an obstruction to differentiation (Zhang et al, 2003) Furthermore, N-cadherin expressing, spindle shaped osteoblasts were increased in number in the deficient mice and were closely associated with HSCs. Also using a mechanism involving N-cadherin, osteoblasts expressing Ang-1 attach to tyrosine kinase receptor (Tie2) positive HSCs, regulating the quiescent state of the stem cells (Arai et al, 2004). However, other work disputes the importance of the expression of N-cadherin in the niche as its deletion in mouse models does not alter the size of the HSC population or haematopoiesis and others are unable to detect any N-cadherin^{+} HSCs (Kiel et al, 2008). Méndez-Ferrer *et al* report that N-cadherin positive osteoblastic cells are distinct from nestin^{+} MSCs (Mendez-Ferrer et al, 2010). However, others have shown low nestin staining in some osteoblasts lining the trabeculae and these were proposed to be an immature osteoblastic cell type (Calvi et al, 2012). Osteoblast deficiency also leads to a reduced number of HSCs and their progenitors in the bone marrow and increased haematopoiesis at extramedullary sites. This could be reversed with the reappearance of osteoblasts, accompanied with local sites of haematopoiesis (Visnjic et al, 2004).

The roles of osteoblasts in HSC survival and proliferation has also been demonstrated in human studies in which CD34^{+} cells derived from cord blood were co-cultured with osteoblasts from trabecular bone. Co-cultures were able to promote survival and expansion of an increased number of haematopoietic precursors compared to controls. After 14 days of co-culture with osteoblasts, the CD34^{+}CD38^{-} cells were examined by flow cytometry. It was noted that haematopoietic cell expression of markers for monocyte/macrophage differentiation (CD14 and CD163) were increased and the number of cells positive for erythroid commitment was reduced, indicating a role for osteoblasts in the differentiation decision of haematopoietic cells (Salati et al, 2013).

Although significant niche function has been attributed to osteoblasts, they are not thought to be essential for all HSC niches as functional HSCs can be found in extramedullary sites such as spleen and liver that do not contain osteoblasts (O'Malley, 2007). Clearly, there are some inconsistencies and questions remaining about the identity and role of osteoblasts in the HSC niche.

1.3.5.6 Adipocytes

Adipocytes have been shown to maintain HSCs in a quiescent state and have an overall negative impact on haematopoiesis with reduced HSCs and progenitors isolated from the more fatty marrow of tail vertebrae (Naveiras et al, 2009). A-ZIP/F1 'fatless' mice cannot produce adipocytes as they express a dominant-negative form of the C/EBP under the adipocytic fatty-acid-binding protein 4 (Fabp4) promoter (Moitra et al, 1998). Using these mice confirmed that adipocytes were the negative regulators of haematopoiesis, as the process was restored in tail vertebrae in these mice. There was no difference in the number of HSCs isolated from the tail vertebrae compared to the thoracic vertebrae and furthermore, when irradiated, marrow engraftment was enhanced in these fatless mice compared to wild-types (Naveiras et al, 2009).

1.3.5.7 Endothelial cells

Endothelial cells line the blood vessels in the bone marrow and are well placed to interact with HSCs when they enter the bone marrow during development and when they enter peripheral blood during homeostasis and in response to stress. *In vitro*, endothelial cells effectively support HSCs (Li et al, 2004). Selective deletion of sinusoidal endothelial cells was achieved by administration of neutralising antibodies of vascular endothelial cadherin (VE-cadherin) into myelosuppressed mice. The subsequent disruption to the vascular niche inhibited thrombopoiesis (Avecilla et al, 2004), indicating the important role for endothelial cells in haematopoiesis.

Haematopoiesis has been promoted *in vitro* by bone marrow endothelial cells that express G-CSF, granulocyte-macrophage-CSF (GM-CSF), SCF and interleukin 6 (IL-6) (Rafii et al, 1997). *in vivo* studies utilised the expression of SLAM markers to distinguish HSCs in histological sections of spleen and bone marrow. These observed HSCs were in contact with sinusoidal endothelium (Kiel et al, 2005). Human subendothelial cells derived from haematopoietic marrow were able to generate bone and marrow when subcutaneously transplanted into immunocompromised mice, unlike cells from trabecular bone or periosteal cells which only formed bone and skin fibroblasts which failed to generate bone or marrow. CD146 expression was not detected in any of the cell types apart from the subendothelial cells and was therefore used to characterise these cells (Sacchetti et al, 2007). CD146 was expressed at a higher level in human umbilical cord perivascular cells which have a higher proliferative potential and similar differentiation ability than bone marrow MSCs (Baksh et al, 2007) thus confirming the ability of CD146 to be used as a putative stem cell marker.

SCF is a recognised mediator of HSC maintenance, which is proposed to be expressed by a variety of cells including endothelial cells and osteoblasts. However, in a series of depletion experiments, HSC number and function was not perturbed when SCF was specifically depleted from osteoblasts or nestin^{+} cells. In contrast, using Cre-mediated deletion of SCF in perivascular cells under the control of the Leptin receptor and by Tie2 in endothelial cells, HSC activity was affected (Ding et al, 2012). Despite nestin^{+} cells reportedly having high mRNA levels of SCF (Mendez-Ferrer et al, 2010), its deletion in these cells did not alter HSC numbers in the bone marrow, although the spleen population was reduced; nestin^{+} cells were also found in distinct vascular locations to those expressing GFP under the control of SCF. This could perhaps be explained by the subsequent analysis of nestin expression in different mouse models using different transgenes that showed some variation. In particular Nestin-GFP expression was reported around larger blood vessels whilst nestin Cre expression was associated with perisinusoidal stromal cells that resembled the SCF-GFP expression pattern (Ding et al, 2012).

Another important mechanism of endothelial control in the niche is through the IL-6 family receptor subunit gp130. Tie-2 Cre; $gp130^{fl/fl}$ mice showed defects in the bone marrow including hypocellularity and expanded sinusoidal spaces in the vascular niche. These abnormalities could not be rescued by a HSC transplant from wild type mice. In fact, HSC number and function was normal in Tie-2 Cre; $gp130^{fl/fl}$ mice and could themselves reconstitute irradiated hosts, indicating that the intrinsic factor within the HSC niche was endothelial cells (Yao et al, 2005).

1.3.5.8 CXCL12 abundant reticular cells (CARs)

Cells expressing GFP under the control of the CXCL12 promoter were identified as the main source of CXCL12 in the bone marrow and were thus termed CXCL12 abundant reticular (CAR) cells (Sugiyama et al, 2006). They are distributed throughout the bone marrow and were in contact with $CD150^{+}CD48^{-}CD41^{-}$ cells in endosteal and vascular niches as well as in the central marrow. CAR cell depletion leads to a reduction in HSC number and cell cycling, suggesting their role in controlling population size and proliferation (Sugiyama et al, 2006). These niche functions were also attributed to CAR cells in another study after their short term ablation in a mouse model. As well as being more quiescent, HSCs in CAR cell depleted mice had an increase in genes involved in myeloid differentiation. CXCL12-GFP cells were analysed by flow cytometry and the population was relatively homogeneous for expression of VCAM-1, CD44, CD51 (αv integrin), PDGFRα and PDGFRβ. These cells could also differentiate into osteoblastic and adipocytic cells *in vivo* (Omatsu et al, 2010).

$Nestin^{+}$ MSCs share many features with CAR cells such as their perivascular location, morphology and expression of CXCL12, SCF and VCAM-1. The extent to which these two populations overlap has yet to be defined. It has been suggested that $nestin^{+}$ MSCs may represent a more primitive niche cell as increased CFU-F activity and a greater differentiation potential is attributed to them (Ehninger & Trumpp, 2011).

The intercalation of the physical environment and the processes of haematopoiesis and bone remodelling is a complicated system that centres around two stem cell populations. HSCs and MSCs share the same anatomical space and are intrinsically linked to support and regulate each other's function as well as that of the niche. MSCs and their progeny are commonly implicated in maintaining HSC self-renewal and proliferation and have close interactions with committed HSC progenitors to provide an effective niche in the dynamic tissue of bone marrow. Therefore, further study is required to fully dissect the contribution of each cell to the niche and their relationship to each other.

1.3.6 Non-cellular components of the HSC niche.

1.3.6.1 Osteopontin

Osteopontin is secreted by a number of different cells in the bone marrow but most prominently by osteoblasts and at the endosteal surface. HSCs express CD44 and integrin α4 both known to interact with osteopontin (Schmits et al, 1997; Scott et al, 2003). Osteopontin-deficient mice have increased numbers of HSCs indicating that it is a negative regulator of the stem cell pool size. This response is attenuated in wild type mice by osteoblast activation by PTH (Nilsson et al, 2005; Stier et al, 2005). Furthermore, altered expression of Jagged-1 and Ang-1 in the absence of osteopontin suggests that it may regulate other niche components.

1.3.6.2 Calcium

Calcium (Ca^{2+}) ion levels at sites of bone resorption have been shown to reach 40 mM, a concentration much higher than the physiological level in serum (Silver et al, 1988). HSCs were found to express the G-protein coupled calcium receptor (CaR) and mice deficient in the receptor were unable to engraft to the endosteum, suggesting an important role for the calcium ion and its detection by HSCs to home to the niche (Adams et al, 2006).

1.3.6.3 Oxygen gradient

The lack of oxygen in some areas of bone marrow has been implicated in the regulation of haematopoiesis. Evidence suggests that HSCs are hypoxic and exist in sites of low oxygen concentration (Takubo et al, 2010). Mice injected with Hoechst dye 33342 (Ho) before cells were collected from the bone marrow provided cells with varying amounts of dye which were sorted using FACS analysis and transplanted into lethally irradiated mice. Those cells with the lowest Ho fluorescence (more likely to be furthest away from blood supply therefore least perfused) were able to repopulate the mice with fewer cells than those from high dye staining and contained 90-200 fold more HSCs, indicating that HSCs were more highly concentrated at the least perfused sites in bone marrow. These cells were also shown to have the highest staining of pimonidazole, a chemical marker of hypoxia (Parmar et al, 2007). These results agree with those of Ceradini *et al* who found areas of pimonidazole stained bone marrow were co-localised with the CXCL12 expression (Ceradini, Kulkarni et al. 2004).

1.4 The role of nestin in the HSC niche

As described above (section 1.3.5.4), nestin has been recently described in the field of niche biology after an unexpected finding that it is expressed by a subset of murine mesenchymal stem cells (Mendez-Ferrer et al, 2010). This section will focus on the current understanding of nestin expression and its potential as a marker of progenitor cells.

1.4.1 Nestin structure and transcriptional regulation

Intermediate filaments contribute to the cytoskeleton in combination with microtubules and microfilaments. Six sub-types of intermediate filament have been classified as determined by their structural properties. Nestin is a type V1 intermediate filament originally identified in rat neuroepithelial stem cells and previously known as Rat.401 (Cattaneo & McKay, 1990). Nestin is a 240 kDa protein comprised of an α-helical central rod with a short N-terminus and an unusually long C terminus which contains actin and microtubule binding domains to allow

interaction with other intermediate filaments. Nestin, unlike other intermediate filaments, is unable to self polymerise and consequently integrates into the cytoskeleton network via polymerisation with type III filaments such as desmin and vimentin.

The cellular distribution of nestin appears to be cell-type and cell cycle-stage specific. As well as a distinct cytoplasmic network of filaments, nestin expression in the cell nucleus has been reported in two cell lines derived from glioblastomas. Immunofluorescence and TEM confirmed its nuclear presence and as nestin depolymerised in mitotic cells, the protein was detected as a diffuse cytoplasmic staining (Veselska et al, 2006). Nuclear localisation of nestin is also reported in human neuroblastoma cells where it was reported to interact with DNA (Thomas et al, 2004).

Transcriptional control of nestin is cell-specific with enhancer elements in the second intron of the nestin gene regulating its expression in the CNS but less strongly associated with control on the PNS and the first intron controls the expression in muscle cells (Zimmerman et al, 1994). The first intron is also reported to control nestin expression in tumour epithelium (Aihara et al, 2004).

1.4.2 Nestin in the central nervous system

Nestin is now accepted as a marker of neural stem cells in embryonic development and in the adult brain. Nestin expression can be first detected in the mouse embryo at E7 in neuroectoderm and is highly expressed during early neurogenesis (Kawaguchi et al, 2001). In the adult brain, nestin expression is restricted to distinct regions of neurogenesis such as the subventricular zone (Kawaguchi et al, 2001).

Nestin knockout strategies result in murine embryo lethality. This is in contrast to knockout models of other intermediate filaments that show little or no change to their phenotype (Colucci-Guyon et al, 1994; Milner et al, 1996). Knockout mice were generated using homologous recombination to remove exon 1 of the nestin gene and the resulting embryos were examined to establish the critical point of

nestin expression (Park et al, 2010). The lack of nestin expression was confirmed with RT-PCR, western blotting and immunofluorescence of forebrain sections of E11.5 embryos that showed no positive cells in the $nes^{-/-}$ animals. Embryonic stages of the mice were examined to determine the point of lethality for the knockout mice. By stage E8.5 and beyond, the $nes^{-/-}$ embryos were smaller than littermates and after E8.5 some of the embryos removed did not have a heartbeat suggesting they may have already died by this point. Despite a 50% reduction in nestin mRNA in $nestin^{+/-}$ embryos, these mice survived and were comparable to wild type littermates throughout their development. A severely defective neural tube was associated with $nes^{-/-}$ embryos although other than this and their small size, no other major organ defect was detected. NSCs within the neural tube were reduced in number in $nes^{-/-}$ embryos and although they had a similar proliferation status to those in E11.5 littermates, there was increased apoptosis of cells in the neural tube as early as E9 specifically in the NSC fraction. Microarray analysis carried out on $nes^{-/-}$ NSCs from E11.5 embryos found minimal changes in the gene expression. Only 16 genes had more than a 2-fold change in expression, indicating that nestin is unlikely to have a role in the regulation of gene expression in NSCs. Nestin was found to co-localise with vimentin in wild type NSCs and the polymerisation of vimentin was normal in nestin knockout mice but nestin was not able to polymerise in $vimentin^{-/-}$ embryos (Park et al, 2010). No defect in NSCs from vimentin knockout mice was observed as might be expected from studies of normal development in these mice (Colucci-Guyon et al, 1994). Therefore, the role of nestin in the self-renewal and survival of NSCs does not depend on its incorporation into the intermediate filament network.

1.4.3 Nestin as a marker of stem cells

Nestin expression measured in embryoid bodies (EBs) cultured *in vitro* showed abundant protein expression that localised to the periphery of the ectodermal rim of cells at day 2 of culture. After 5 days, nestin expression in spindle shaped cells at the edges of the colonies indicated nestin in migratory, proliferating cells. Upon differentiation, EBs showed an initial, transient co-expression of nestin with lineage

specific intermediate filaments such as glial fibrillary acidic protein (GFAP) in neurons and desmin in mesodermal cells. Continued differentiation resulted in the loss of nestin altogether (Wiese et al, 2004). These observations are consistent with the theory that nestin is a marker for stem cells and progenitors and is not expressed on terminally differentiated cells.

As well as the recognised population of nestin$^+$ neural stem cells discussed above, an increasing number of reports are identifying regions outside the CNS that contain nestin positive cells including: developing cardiomyocytes (Kachinsky et al, 1995), dental follicles, pancreas, eyes, skin (Wang et al, 2006) and skeletal muscle . Its expression is frequently attributed to stem and progenitor cells with functional roles in stem cell fate rather than solely a characteristic stem cell marker.

1.4.4 Nestin expression in MSCs

Controversy remains about the extent of differentiation potential of bone marrow derived MSCs. Mesenchymal lineages of osteogenic, adipogenic and chondrogenic cells are accepted pathways for MSCs to follow, with more limited studies to support the probability of bone marrow MSCs to generate progeny of muscle (Ferrari et al, 1998), neuronal (Tropel et al, 2006) and hepatocytic classification.

Evidence has been presented to suggest neuronal capabilities of MSCs and that this differentiation strategy was confined to nestin$^+$ cells isolated from rat bone marrow. Initial attempts at characterising nestin-positive and negative MSCs using microarray data found approximately 400 genes to be significantly different between the two populations with nestin positive cells expressing higher levels of stem cell and neural cell related genes and lower levels of epithelial, haematopoietic and mesenchymal fate genes (Wislet-Gendebien et al, 2012). However, they failed to satisfactorily determine if nestin expression identified separate stem cell populations from the bone marrow or simply reflected cells of the same population at various stages of differentiation (Wislet-Gendebien et al, 2012). Using a Wnt1-Cre/R26R transgenic mouse model, NCSCs and MSCs were isolated from the adult bone marrow and clonal populations of each were

compared. An increase in nestin expression from 20% to 90% of cells within each clone was observed in MSCs that were serum starved but no difference was detected in NCSCs which all expressed nestin (Wislet-Gendebien et al, 2012). This indicates that nestin is distinctively regulated in different cell types. Additionally, 50% of *in vitro* cultured mMSCs expressed nestin, which increased to 90% after bFGF treatment, indicating the neural potential of a large proportion of MSCs. Neurofilament (NF-L) and beta III tubulin (β3-tub) were also upregulated in treated mMSCs although GFAP and other mature neural markers were not, indicating an inability to progress beyond an immature neural cell fate. However, these differentiated neural cells were functional, as established by calcium signalling in response to glutamate treatment (Wislet-Gendebien et al, 2012).

Nestin expression was heterogeneous in examined murine clones generated *in vitro*. Clonally generated murine mMSCs were all positive for nestin, which was maintained or increased after bFGF treatment. Three out of the 17 clones tested had tri-lineage potential and showed high expression of nestin that was maintained upon bFGF treatment. However, expression of neural marker β-tub was only limited after treatment and reported as low expression in one clone. Other MSCs with restricted differentiation potential were able to upregulate neural specific markers with greater ease, suggesting that mesenchymal cells that are perhaps already committed are more susceptible to the treatment and neuronal differentiation than stem cells (Tropel et al, 2006).

Nestin expression in bone marrow MSCs has been reported by some to depend on *in vitro* factors. Serum removal and extended cell passaging is required for nestin expression in culture. Nestin is inhibited when the cells are plated at high densities (Wautier et al, 2007). Thrombin has been suggested as the factor present in serum that inhibits nestin expression, as individually it has been reported to decrease the level of nestin expressed in MSCs in a dose dependent manner (Wautier et al, 2007). Thrombin has wide ranging roles in inflammation and tissue remodelling and is implicated in brain development with an increase of thrombin resulting in the

contraction of processes on neural cells and thereby altering their actin cytoskeleton (Reviewed by Grand et al, 1996).

1.4.5 Nestin in the HSC niche

Studies using transgenic mouse models have identified nestin$^+$ stromal cells to be MSCs with a key role in the HSC niche (Mendez-Ferrer et al, 2010).

Analysis of bone marrow sections of nestin-GFP transgenic mice located GFP$^+$ cells closely associated with HSCs. 80% of HSCs were within 5 cell diameters of a GFP$^+$ cell. Real time PCR identified a high level of expression of genes important for HSC maintenance: IL-7, SCF, Ang1 and VCAM-1.

In vivo depletion of nestin$^+$ cells using inducible tamoxifen/diphtheria toxin mice led to a reduction in the number of HSCs in the bone marrow, giving a clear indication that nestin positive cells are important for the maintenance of HSCs in the bone marrow (Mendez-Ferrer et al, 2010). Further analysis of the nestin$^+$ MSC population found them to be involved in attracting and retaining HSCs *in vivo*. When purified HSCs were transplanted into irradiated hosts, they localised to nestin positive cells. Conversely, when nestin positive MSCs were depleted, the ability of HSCs to home to the bone marrow was almost completely ablated.

Depletion of SCF in nestin-positive cells specifically using a Nes-Cre mediated removal of SCF resulted in a decreased number of HSCs in the spleen, although bone marrow HSCs were unaffected (Ding et al, 2012). This indicates that HSCs in the bone marrow do not require SCF from nestin$^+$ cells or that it can be sourced elsewhere in its absence and that nestin$^+$ cells may have an intrinsic role in HSC niche function in the spleen through the action of SCF.

1.4.6 The role of nestin-positive cells in tissue repair

Nestin$^+$ cells have been reported at sites of injury and remodelling, highlighting their stem cell attributes in the ability to proliferate and contribute mature cells in response to stress. One such tissue that has received a lot of attention is the infarcted heart. In normal rat heart tissue, nestin-positive stem cells have been isolated and could be induced to a neuronal or glial phenotype and to form cellular

spheres in culture in a similar fashion to NSCs (El-Helou et al, 2008). They are a resident cardiac cell population and express cardiac progenitor transcription factors. Nestin has also been detected in human and murine heart tissue (Beguin et al, 2011) (Tomita et al, 2005). Initially, cardiac nestin$^+$ cells were proposed to originate from the bone marrow, however, when irradiated rats were transplanted with GFP–labelled bone marrow cells and subsequently subjected to an induced myocardial infarction, only 20% of the nestin positive cells in the region also co-expressed GFP. (El-Helou et al, 2005). Therefore, the numbers could not account for all of the nestin-expressing cells detected in the heart. It remains to be seen whether the cells were nestin positive in the bone marrow and were attracted to the site of destruction or whether the expression of nestin was induced in the damage environment once in situ. The bone marrow population may represent a subset of cells required to regenerate the damaged tissue and the resident cells be a reservoir of stem cells. In the infarcted heart, resident nestin positive cells have been observed to migrate to the sites of damage and contribute to the repair of cardiac tissue by sympathetic innervation and angiogenesis (El-Helou et al, 2008). Nestin mRNA is increased following myocardial infarction (Scobioala et al, 2008). Nestin protein is reported in endothelial cells of the new blood vessels of the recovering heart and may represent a marker of the neovascularisation (Beguin et al, 2009) (El-Helou et al, 2008) (Reviewed by Calderone, 2012).

Reactive astrocytes are a key modulator of lesion repair in the brain and proliferate and upregulate GFAP in response to damage. Quiescent astrocytes in healthy tissue do not express nestin, however, these cells were found to re-express nestin after lesions were performed. Using a transgenic mouse with lacZ expression under the control of the same regulatory elements reported to promote nestin expression in the developing CNS, a close relationship between the adult astrocytes and neuro-progenitor is implied. Immunohistochemical staining confirmed that lacZ cells expressed nestin and GFAP, suggesting the astrocytic phenotype but not all of the GFAP$^+$ astrocytes expressed nestin (Lin et al, 1995). So, rather than astrocytes reverting to a more immature phenotype, the reactive astrocytes were proposed to

originate from a pool of stem cell precursors, as lacZ$^+$ cells were found near to the lesion site and also in a subependymal region known to contain a stem cell pool in the adult brain (Morshead et al, 1994).

1.4.7 Nestin expression in tumours

The initiation of tumours is thought to arise from cancer stem cells that function similarly to stem cells in their ability to self renew and produce large numbers of differentiated progeny. Their existence was demonstrated in acute myeloid leukaemia (Bonnet & Dick, 1997) and has since been recognised in a range of solid tumours. Concomitant with its expression amongst tissue stem cells, nestin is being recognised as a characteristic marker of tumour stem cells. Indeed, nestin expression is seen in many tumours, especially those derived from the CNS such as astrocytomas and gliomas, reflecting the original identification of nestin in the neural tissues. Tumours from other origins known to express nestin include cervical carcinomas (Aihara et al, 2004) and malignant melanomas (Florenes et al, 1994). An examination of prostate cancers and matched bone marrow metastases found nestin$^+$ cells confined to the epithelial cells (Eaton et al, 2010) suggesting a potential role in tumour vascularisation, which is consistent with the nestin expression detected in epithelial cells in the infarcted rat heart (El-Helou et al, 2008). Each prostate cancer sample was from established metastatic disease, therefore early onset upregulation of nestin for initiation of the primary tumour may not have been possible to detect in these samples. Appearance of cancer stem cells may be due to the mis-regulation and mutation of normal stem cells or the acquisition of the self renewal property in progenitor cells. Aberrant nestin expression may contribute to the transformation of these cells or be a subsequent consequence of the transformation which has yet to be addressed. Certainly, nestin expression is strongly correlated to the malignant grade of tumours as seen in angiosarcomas and gastrointestinal stromal tumours (Yang et al, 2008) where stronger nestin expression was detected by immunohistochemistry in human tumour samples.

Nestin expression within tumours has been specifically associated with proliferative endothelial cells (Sugawara et al, 2002). Almost 80% of 82 tumours from a range of sources examined by another group were found to contain nestin-positive intra-tumour epithelium (Aihara et al, 2004). Tumour epithelium is characterised by neovascularisation, therefore nestin may play a role in tumour progression by enabling angiogenesis for tumour growth. Normal uterine epithelium contained nestin positive cells confirming its association with cells involved in angiogenesis (Aihara et al, 2004). Although the function of increased nestin expression is still to be fully determined, it is clearly implicated in the roles of tumour initiation, metastatic progression and migration of cells in some tumours. Therefore, further research into the regulation of nestin expression on stem cells should help clarify and identify targets for disease intervention and conversely, the study of ectopic nestin expression in tumours may help identify roles in normal stem cell function.

1.5 IL-7

Interleukin-7 (IL-7) was originally identified in the late 1980s as a factor to promote murine B cell precursors in a long term culture system (Namen et al, 1988). Now IL-7 is recognised as a member of the type 1 cytokine family that is expressed by non-haematopoietic stromal cells in a range of organs including: lymph nodes, thymus, skin, liver and bone marrow. IL-7 plays critical roles in lymphopoiesis and T cell development. Murine T and B cell numbers are dramatically increased on injection of IL-7 (Morrissey et al, 1991). In contrast, injection of a neutralising IL-7 antibody results in the inhibition of B cell development in the bone marrow (Grabstein et al, 1993). These cell types are resident in the bone marrow, therefore alteration by and consumption of IL-7 impacts the niches they inhabit.

1.5.1 IL-7 signalling

1.5.1.1 IL-7R

The IL-7 receptor is composed of two subunits; the IL-7R alpha chain (IL-7Rα or CD127) and the common chain (γc). This common chain, as the name suggests, is shared by several other cytokines including: IL-2 (Takeshita et al, 1992), IL-4, IL-9

(Russell et al, 1994), IL-15 (Giri et al, 1994) and IL-21 (Habib et al, 2002). IL-7Rα is a member of the type I cytokine receptor family, which are characterised by a structural composition containing two fibronectin-like domains, four conserved cysteine residues and a WS motif in their extracellular domain. Both receptor components are expressed on the cell surface independently and become dimerised upon ligand binding. Thymic stromal lymphopoietin (TSLP) shares structural homology with murine IL-7 and is capable of similar pre B cell supportive functions (Sims et al, 2000). TSLP signals through IL-7Rα, which dimerises with a TSLP receptor that shows some resemblance to the γc subunit (Park et al, 2000).

IL-7Rα is expressed by a wide range of haematopoietic cells including natural killer cells, dendritic cells, lymphoid precursors, developing B cells and mature T cells as well as bone marrow macrophages. IL-7Rα has also been detected in endothelial cells, bone marrow stromal cells as well as numerous cancer cell types.

In lymphoid stromal cells, the expression of IL-7 mRNA is not affected by fluctuating levels of IL-7 or lymphocyte cell number (Fry & Mackall, 2005). However, the surface expression of IL-7Rα is altered depending on the differentiation status of the cells (Mazzucchelli & Durum, 2007). IL-7Rα is not expressed on HSCs but is acquired during lymphopoiesis and is consequently expressed by common lymphoid progenitors (Reviewed by Bhandoola & Sambandam, 2006). IL-7Rα is initially required to promote cell survival and proliferation but then is downregulated on B cells at the small pre-B2 cell stage in order to allow differentiation to continue. Expression of IL-7Rα is comparable between mouse and human systems (Mazzucchelli & Durum, 2007).

In respect of T cell development, small variations occur between mouse and human systems with an earlier downregulation of IL-7Rα in human cells at the pre-T1 cell stage, which in mice still express the receptor. Once T cells mature, they express either CD4 or CD8 and are known as single positive T cells. Murine immature single positive T cells do not express the IL-7 receptor although it is unclear if their

immediate precursor does whilst in both human and mouse mature single positive T cells, IL-7Rα is re-expressed. The expression of IL-7Rα on mature T cells is further regulated depending on environmental factors and cytokine availability. The regulation of IL-7 is speculated to be via its rate of consumption. IL-7 levels are thought to be at a level sufficient to maintain the resident T cell population with cells using only the IL-7 they require for homeostasis, thereby allowing each cell to harness the available IL-7. In response to IL-7 exposure, mature T cells downregulate IL-7Rα. This would support the view that after receiving adequate IL-7 signal for survival, the receptor is downregulated thereby preventing its own consumption of IL-7 and subsequently IL-7 is made available to other, non-stimulated T cells (Mazzucchelli & Durum, 2007). This theory has yet to be confirmed and will require some technical advancement of the detection of IL-7 protein which is currently too low to be detected accurately in mouse tissue.

IL-7R signalling is essential in T cell survival which is mediated by upregulation of the expression of pro-survival proteins Bcl2 (B cell lymphoma-2) and MCL1 (Myeloid cell leukaemia sequence 1). Withdrawal of IL-7 consequently leads to T cell death (Khaled & Durum, 2002).

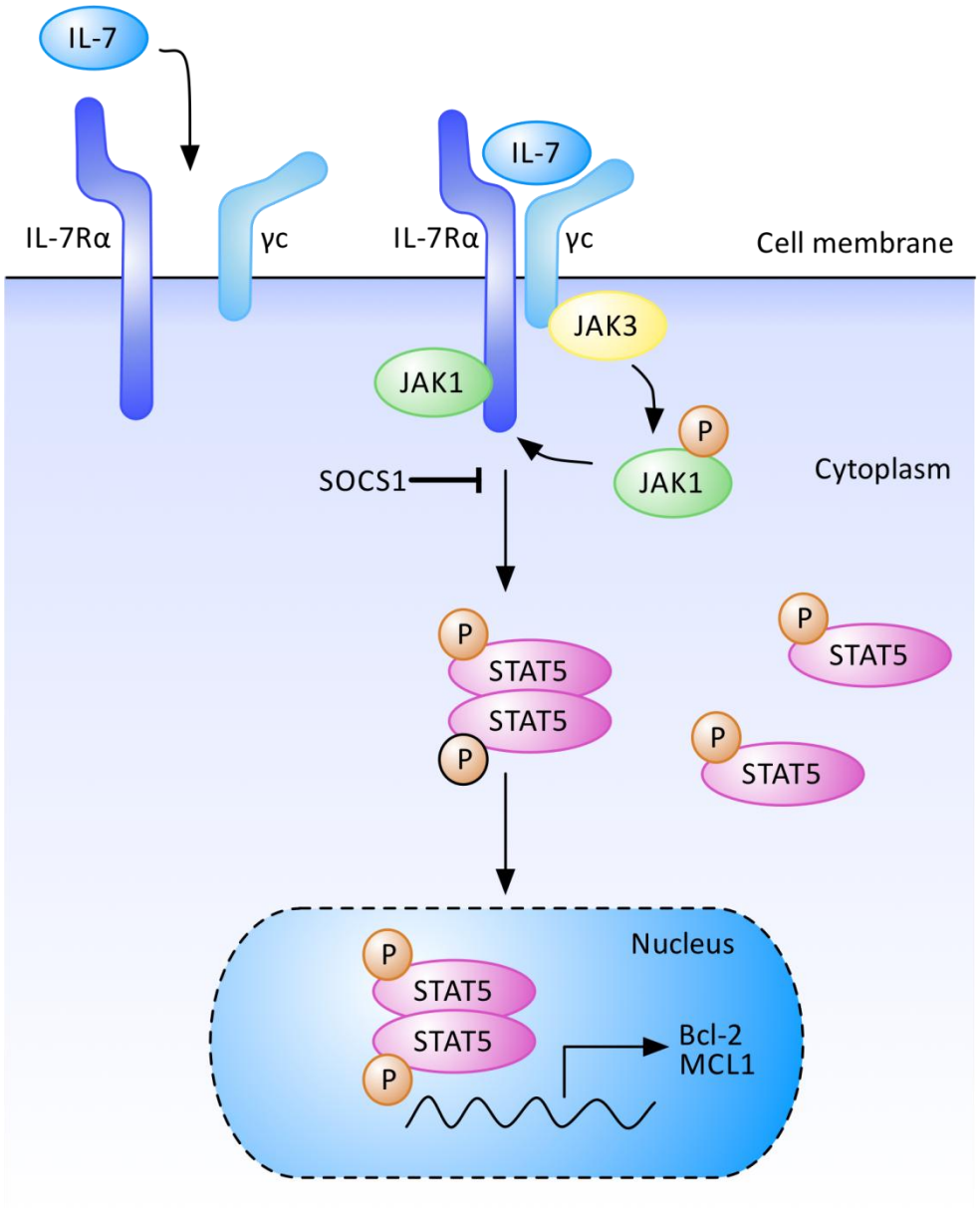

Figure 1.3 IL-7 signalling
IL-7 binding to its receptor IL-7Rα and common chain co-receptor initiates a signalling cascade through JAK and STAT proteins that results in the upregulation of pro-survival genes Bcl-2 and Mcl-1.

1.5.1.2 JAK-STAT pathways

IL-7 is known to signal through the heterodimerisation of the α and γ chains of its receptor resulting in a cascade of phosphorylation events orchestrated by janus kinases (JAKs) and signal transducers and activators of transcription (STATs). Upon IL-7 binding, JAK3, which is already associated with the γc, is activated to phosphorylate both the γc receptor and JAK1 which subsequently phosphorylates the α chain (Figure 1.3) (Khaled & Durum, 2002).

JAK3 is an essential transducer of cytokine signals. JAK3 and γc knockout mice show similar defects in lymphoid development and mutations in the human JAK3 gene also result in a disease almost identical to XSCID (X-linked recessive severe combined immune deficiency) (Nosaka et al, 1995). Lack of different JAK-STAT signalling components leads to similar phenotypes between mice and humans, suggesting their functions are highly conserved (Leonard, 2001).

STAT5a and b are two isoforms of STAT5 that become phosphorylated and may form homo or heterodimers which then translocate to the nucleus to bind DNA and induce gene activation. IL-7 induces STAT5 phosphorylation which is then altered during T cell development and correlates with thymocyte survival. STAT5a and b deficiencies in mice display different phenotypes (Teglund et al, 1998). A combined deficiency in STAT5a and b does not result in the inhibition of T cell development, suggesting other downstream components may be able to compensate for the STAT deficiency, although the exact signalling mechanism is yet unknown.

Cytokine signalling is negatively regulated by the protein family of suppressors of cytokine signalling (SOCS). These proteins can bind to JAKS, competitively bind STAT proteins or target proteins for degradation to inhibit the cytokine signalling pathway (Starr & Hilton, 1998). Eight SOCS proteins have been reported and SOCS1 is responsible for the inhibition of IL-7. IL-7 induces SOCS1 expression in B cells in a negative feed-back regulation of its own signalling (Corfe et al, 2011). SOCS1 deficient mice die perinatally due to extreme inflammation (Marine et al, 1999).

IL-7 has also been reported to initiate signalling mechanisms in cells that do not express IL-7R as it can associate with Flt3 and c-kit (Cosenza et al, 2002), although this remains controversial.

1.5.2 Mouse models of IL-7

Recently, a number of bacterial artificial chromosome (BAC) transgenic mice have been generated in order to study the *in vivo* expression of IL-7 (Reviewed by Kim et al, 2011). Detection of IL-7 protein is difficult using traditional immunodetection methods and relatively little is known about its promoter. The BAC reporter strategy provides an advantageous solution to locate IL-7 reporter expressing cells *in vivo* that can be further characterised to understand the role of IL-7 regulation in these cells and tissues.

1.5.2.1 BAC transgenesis

Transgenesis introduces exogenous DNA sequences or transgenes into the genome of an organism. BAC transgenes are employed to report spatial and temporal expression of endogenous genes at the physiological level. BACs are derived from single-copy functional fertility plasmid (F factor) of Escherichia coli (Shizuya et al, 1992). Replication of the F factor is tightly controlled and is only present in the cell as one or two copies, restricting recombination of DNA fragments and the DNA appears stable. Large genomic fragments can be cloned into these vectors, which made them a useful tool in the construction of DNA libraries allowing their subsequent sequencing. The ability to modify the BAC construct further improved its usefulness and cell-specific expression of reporters was possible by manipulation of the reporter gene by homologous recombination within bacteria (Yang et al, 1997). As demonstrated in Drosophila studies, enhancers and promoters may lie some distance away from the gene of interest (Dillon & Grosveld, 1993; Kennison, 1993) therefore, the faithful expression of transgenes to the endogenous gene expression is likely to be dependent on the incorporation of these areas in the

relatively large (300 kb) segments of DNA that are used to avoid integration site induced varied expression.

1.5.2.2 IL-7 reporter BAC mice

The IL-7 BAC transgenic mice insert a reporter gene into the IL-7 locus immediately after the ATG start codon of exon-1 (Figure 1.4).

The first IL-7 reporter mouse used yellow fluorescent protein (YFP) cDNA in the BAC construct and demonstrated identification of YFP^+ thymic epithelial cells TECs in the foetal thymus that persisted into adult tissues (Alves et al, 2009). They were either cortical or medullary and negative for epithelial or fibroblast markers. Cortical and medullary TECs are believed to have a common progenitor, which was postulated to be the distinct subsets of cells expressing YFP for each cell type. The TECs were also located in a specialised region of the adult thymus and were noted to have high expression of factors important for T cell development such as CXCL12 and CCL25 (Alves et al, 2009). This first report of an IL-7 BAC transgenic mouse only detected reporter expression in the thymus despite indications that IL-7 is expressed in other organs demonstrating a limitation in the detection of IL-7 using this method. To investigate this disparity, mRNA levels between cells known to express IL-7 and YFP^+ cells were compared. When compared against the levels of IL-7 transcript in fibroblastic reticular cells from the lymph node which did not express the reporter but are a known source of IL-7, the level of IL-7 in YFP positive TECs was found to be much higher. Thus they suggest a critical threshold limit for the expression of the YFP reporter that is only reached in cells with the highest expression of IL-7 transcript (Alves et al, 2009) and explains the lack of detection of YFP in peripheral tissues. A low level of IL-7 transcript was found in YFP negative TECs indicating heterogeneity within the cell type.

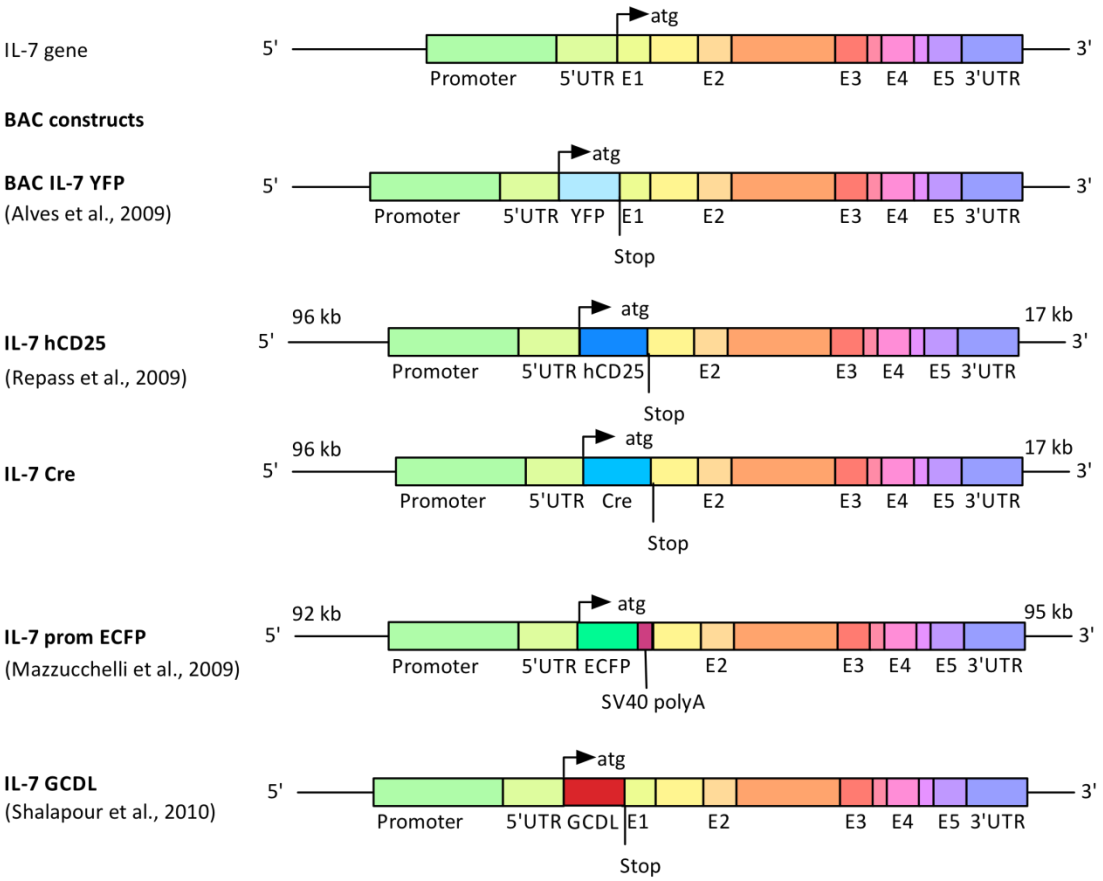

Figure 1.4 BAC constructs used to generate transgenic mice
Four independent groups have generated 5 different IL-7 BAC transgenic mice by inserting a transgene into the IL-7 locus.
Diagram modified from Kim et al (Kim et al, 2011).

Repass *et al* devised two models that used either human CD25 or Cre recombinase as a reporter of IL-7 (Repass et al, 2009). Both transgenes were inserted into position one of the IL-7 exon 1 and were composed of the whole 43kb IL-7 locus as well as 96kb of the 5' and 17kb of the 3' flanking sequences in order to include as many regulatory elements as possible. The IL-7.hCD25 transgene could then be detected by anti human CD25 antibodies. hCD25 staining was detected in E13.5 foetal thymus but not in those from non-transgenic mice. In foetal thymus cell suspensions, hCD25 was not detected on haematopoietic cells but was detected in almost a third of the stromal population. Of the non-haematopoietic cells that were isolated, only the hCD25-positive cells expressed hCD25 mRNA. Additionally, IL-7 mRNA was detected only in these cells and not in hCD25 negative cells. To confirm transgene expression was faithful to that of endogenous IL-7 expression, hCD25 expression was measured by flow cytometry. Lymph nodes, liver, small intestine, thymus and brains of adult mice were analysed for hCD25 and IL-7 expression by qPCR. In adult tissues that were analysed, IL-7 mRNA was a similar level in hCD25 positive cells to that of endogenous IL-7 detected in non-transgenic mice and with the exception of liver tissue, displayed a uniform level of expression of transgene and endogenous IL-7. Expression was highest in the thymus and lymph nodes and IL-7 in bone marrow was not reported.

Expression of Cre from the transgenic mice was detected by crossing the mice with either Rosa26R or R26YFP reporter mice (Repass et al, 2009). This generated mice in which the stop cassette is removed by Cre recombinase and subsequent expression of lacZ or eYFP. These were then detected by whole mount staining with X-gal or anti-YFP antibodies in thymus, lymph nodes, liver and small intestine but not in the kidney. Bone marrow and skin tissue were also mentioned to contain reporter expression. Lymph node, thymus and spleen tissue from YFP mice were further characterised by flow cytometry and demonstrated that YFP positive cells were confined to CD45 negative cells in the lymph node and thymus but entirely absent from the spleen. Each mouse therefore presented IL-7 reporter expression

that was in line with previous reports of endogenous IL-7, which used in-situ hybridisation to detect IL-7 in E13.5 thymus (Zamisch et al, 2005), and reported IL-7 expression in the stromal fraction of lymphoid cells (Repass et al, 2009).

The Durum group generated a fluorescent reporter strain of mice which replaced exon 1 in this instance with an enhanced cyan fluorescence protein (eCFP) in the BAC clone (Mazzucchelli et al, 2009). The weak level of eCFP expression was overcome by staining with anti-eCFP and an appropriate fluorescent secondary antibody. Multi-photon microscopy also enabled visualisation of IL-7 reporter expression without the need for additional antibody staining. eCFP positive cells were not detected in the gut, lungs, skin, brain or blood platelets, which reiterates the limitation of the direct YFP reporter mice that they may also only be useful in detecting cells with the highest levels of IL-7 mRNA. ECFP-positive cells were detected in the thymus and were negative for markers of fibroblastic and endothelial cells and further to the characterisation reported by Alves *et al*; dendritic cells and myeloid cells were eCFP negative.

Bone marrow stromal cells that were eCFP positive displayed an epithelial cell morphology. CFSE-labelled memory T cells were intravenously injected into the reporter mice and homing could be monitored using intravital microscopy of the skull. Numerous T cells were detected close to IL-7 reporter cells and preferentially interacted with eCFP positive cells. In order to further examine the potential of IL-7 in this relationship the group generated a mouse that expressed the reporter but lacked IL-7 and repeated the T cell experiment. In this case, the number of T cells that was detected 24 hours later in the skull bone marrow was not reduced but in fact slightly higher than in control mice, so the role of IL-7 as a chemoattractant was ruled out. As memory T cells express CXCR4, they may be recruited to the bone marrow by cells expressing CXCL12. Therefore, the CXCR4 agonist AMD3100 was injected into the IL-7 reporter mice but this did not prevent the T cells entering the bone marrow and so CXCL12 was also eliminated as the potential attractant to the IL-7 producing cells (Mazzucchelli et al, 2009).

An alternative BAC transgenic mouse uses four genes under the control of the IL-7 promoter to simultaneously express enhanced green fluorescent protein (G), Cre recombinase (C), the human diphtheria toxin receptor (D) and click beetle green luciferase 99 (L) (Shalapour et al, 2010). The mice were therefore termed IL-7GCDL. Luciferin was injected into the mice and whole organs were examined for bioluminescence. This was most highly detected in the thymus, skin and intestine whereas low levels were detected in the lung, heart, kidney and liver and no increase from background levels could be detected in the spleen. IL-7 mRNA levels corresponded well with the amount of bioluminescence detected apart from in the lymph nodes where relatively high levels of IL-7 mRNA compared to low detected levels of bioluminescence attributed to their small size. Although the highest levels of bioluminescence detected were in the colon of the transgenic mice, eGFP reporter could not be detected and so a further mouse was generated by crossing the strain with an RA/EG mouse that expressed eGFP after Cre recombinase activity. In this way, eGFP could be detected in the intestinal epithelial cells in the gut (Shalapour et al, 2010).

There are some inconsistencies between the studies generally accepted to be due to the differences in the generation of each mouse model. Together, the data builds an extensive picture of the cells that express IL-7 that were previously inaccessible. Three out of the five mice generated reported IL-7 expression in the bone marrow where it has established roles in B cell lymphopoiesis.

1.5.3 IL-7 in bone marrow

A negative impact on bone has been attributed to the actions of IL-7. IL-7 is known to be expressed by stromal cells in the bone marrow but the precise identification of these cells and their functional role are still to be described adequately (Mazzucchelli et al, 2009). It has been reported that IL-7 KO mice have increased bone mass due to a lack of IL-7 stimulated T cell activation (Weitzmann et al, 2000). This activation would ordinarily lead to T cell secretion of RANKL and M-CSF and subsequent activation of osteoclasts to initiate bone resorption (Figure 1.5).

Therefore, the absence of IL-7 in the bone marrow disrupts the regulation of bone remodelling, resulting in higher bone mass. However, it was noted that the RANKL pathway was not the only one responsible for increased osteoclastogenesis as osteoprotegerin (OPG), which inhibits RANKL, did not reduce all osteoclast formation (Weitzmann et al, 2000). RANKL deficient mice have no osteoclasts or lymph nodes and display defective B lymphocyte development, indicating the critical role it plays in osteoclast differentiation (Dougall et al, 1999).

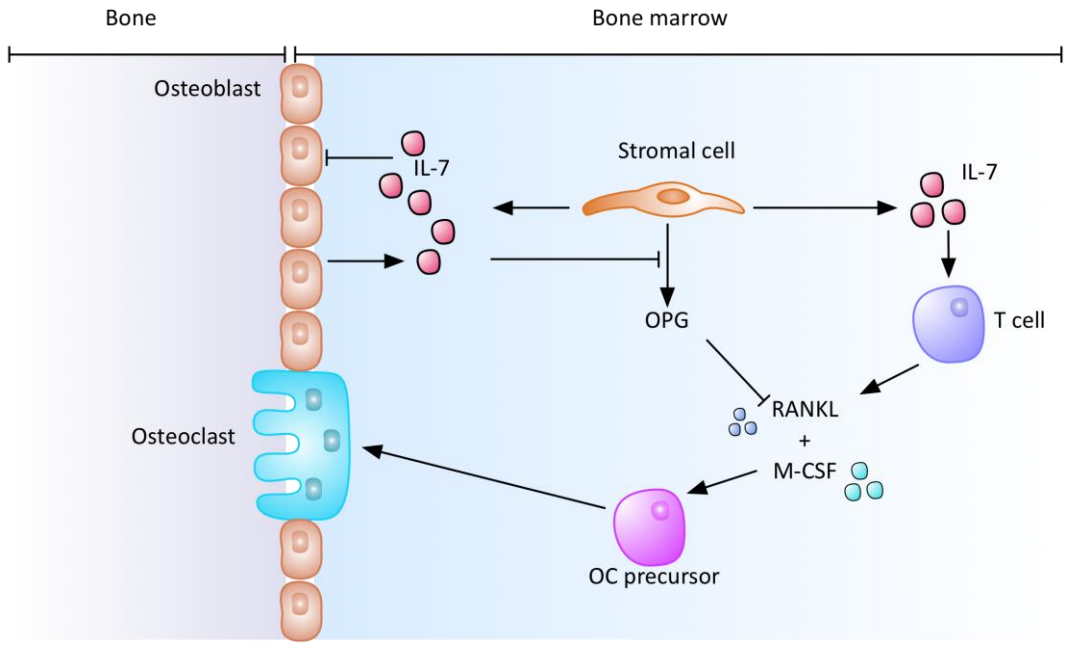

Figure 1.5 IL-7 interactions in bone
IL-7 is expressed by stromal cells and osteoblasts in the bone marrow and consequently initiates T-cell expression of RANKL and M-CSF that activate osteoclast maturation and activity. Stromal cells also express OPG, which is a soluble decoy receptor for RANKL and acts to antagonise OC activation. IL-7 negatively regulates OPG in order to increase OC maturation. IL-7 also suppresses bone formation by osteoblasts and therefore has a negative impact on bone.
Abbreviations: OPG; osteoprotegerin, RANKL; receptor activator of NF-κB ligand, M-CSF; macrophage colony stimulating factor, OC; osteoclast.

Gene inactivation of both IL-7 and IL-7R in mouse knockout models results in reduced size of both the thymus and spleen. When the bone marrow of these animals is examined, B lymphopoiesis is found to be perturbed. The overall number of B lymphocytes is greatly reduced compared to wild type mice and is a block to differentiation at the pro-B cell stage. Pre-pro B cells are unaffected but the number of pro-B cells reduced by a third and almost no cells transitioning from pro-B to pre-B cells were detected.

In mice that overexpress IL-7 under the control of a major histocompatibility complex (MHC) class II promoter, B cell development is greatly affected with no effect reported on T cell development (Fry & Mackall, 2002). The numbers of pro, pre and immature B cells are increased and myeloid cell numbers are extremely low. At 4-6 weeks, femur diameter is increased in the mice accompanied by a larger bone marrow cavity and focal osteolysis.

Direct administration of IL-7 into healthy mice results in B lymphopoiesis induction accompanied by bone loss (Miyaura et al, 1997). The mice examined in this study were females and an increased number of tartrate resistant acid phosphatase $(TRAP)^-$positive osteoclasts were observed that contributed to the loss of mineralised cancellous bone to the extent seen in mice with oestrogen deficiency (induced by ovariectomy). Bone loss was not observed in organ cultures of murine foetal long bones (Onoe et al, 1996) and so the resulting reduction in bone loss determined by radiological and histological analysis *in vivo* suggests that the alterations in B lymphopoiesis modify the microenvironment to stimulate bone resorption. Additionally, bone marrow derived $B220^+$ B cell precursors have been stimulated *in vitro* to generate osteoclasts themselves and may serve as a progenitor population (Manabe et al, 2001). However, despite an increase in $B220^+$ cells upon administration of IL-7, no increase in RANKL or bone loss was detected in T cell deficient nude mice (Toraldo et al, 2003). This suggests that the bone loss is T cell mediated and describes a clear relationship between IL-7, T cells and osteoclasts in the balance of bone remodelling.

IL-7 has been shown to be up-regulated in ovariectomised mice which have an oestrogen deficiency. This oestrogen deficiency leads to bone loss that can be prevented with IL-7 neutralisation. IL-7 was shown to promote osteoclastogenesis and suppress osteoblastic activity such that the result was an 'uncoupling' of the two processes as the balance is tipped, leading to the loss of bone. IL-7 blocked new bone formation of *in vitro* calvarial cultures that were stimulated with BMP-2 and *in vivo* intraperitoneal IL-7 administration (Weitzmann et al, 2002). Altogether, IL-7 has an overall negative impact on bone and clearly interacts with and is expressed by mesenchymal lineage cells.

1.5.4 IL-7 in arthritis

Rheumatoid arthritis (RA) is a chronic autoimmune disease characterised by inflammation and degradation of the bone joints which causes pain and stiffness in patients that can be debilitating. There is an increasing body of evidence to suggest the involvement of IL-7 in the activity and progression of this disease (Reviewed by Churchman & Ponchel, 2008). In human studies of RA, serum levels of IL-7 have been detected and measured that vary widely depending on the method of detection employed. In four separate studies, serum IL-7 concentrations have been reported at ranges between 1.5 – 3.8 pg/ml in one study and at the other end of the scale at 300 pg/ml. Serum levels were also measured in healthy controls and these were also found to differ between the reports. In a review of the studies, ELISAs from 5 different origins showed comparable levels of IL-7 in healthy controls of 13 ± 5 pg/ml with the exception of one which showed the lowest range of IL-7 mentioned above. The reported levels were found to be below the lower detection limit (3 pg/ml) of the ELISA. IL-7 detection from sources other than serum is also inconsistent. Whilst some report elevated levels of IL-7 in synovial fluid, others observe a reduction, although in general, studies agree that IL-7 levels are higher in rheumatoid arthritis compared to osteoarthritis. The increases in synovial fluid IL-7 measured in 44 RA patients was not correlated with age or sex and was not significantly different between groups that had rheumatoid factor present disease or not (van Roon et al, 2005). However, it has been shown that IL-7 is up-regulated

in human osteoarthritis chondrocytes as well as in normal chondrocytes with age (Long et al, 2008).

A small sample of human articular chondrocytes samples found IL-7 mRNA expression by RT-PCR in 2/6 osteoarthritis patients and in 2/3 RA patients. They also found that 1/5 normal infant chondrocyte samples expressed IL-7 whereas all balb/c mouse chondrocyte samples produced cytokine profiles including IL-7 (Tanabe et al, 1996). Another report published two years later found IL-7 mRNA to be exclusively detected in RA patients and absent from osteoarthritis and normal cartilage (Leistad et al, 1998).

As an auto-immune disease, antibodies such as rheumatoid factor and anti citrullinated peptides antibodies (ACPA) have been used to diagnose RA but show lack of specificity in the earliest stages of the disease. When examined as a potential biomarker for early onset RA, the median expression of serum IL-7 was found to be similar in 250 patient samples compared to 80 healthy controls. However, the lowest levels were detected in the samples from patients who were considered to have very early inflammatory arthritis symptoms. 108 patients progressed to RA and again the range of IL-7 serum levels measured was distributed at the lower end of the scale. Low IL-7 serum level (<10 pg/ml) predicted structural damage at follow-up in patients after two years but overall the sensitivity of IL-7 in predicting disease progression was lower than that of the currently used antibodies (Goeb et al, 2012). Low serum levels of IL-7 in RA patients were associated with lower IL-7 expression from bone marrow stromal cells cultured *in vitro* compared to healthy controls (Ponchel et al, 2005) suggesting a systemic defect in IL-7 regulation. However, peripheral blood mononuclear cells had the same proliferative response to IL-7 in RA and healthy patient samples indicating that the signalling pathway is still intact in these cells (Ponchel et al, 2005).

Lymphocytes extracted from the synovial fluid in RA patients proliferated at a greater rate at higher doses of IL-7 than those extracted from peripheral blood.

Culturing $CD4^+$ T cells from these sources *in vitro* with the addition of IL-7 led to their activation as MHC class II and CD25 were upregulated (van Roon et al, 2005).
In contrast to the low circulating levels of IL-7, it is reported to be high in arthritic joints. Immunodetection of IL-7 has been reported in human RA synovial tissue. This was reported to be co-localised with CD68 which is a glycoprotein expressed by macrophages, monocytes, activated T cells and fibroblasts. CD68 may be used as a measure of arthritis disease status and therefore the co-localisation of IL-7 may suggest a similar role. $CD68^+$ macrophage numbers are increased at the synovium of RA patients compared to controls and are reduced upon disease remission following successful treatment with a variety of disease modifying anti-rheumatic drugs (DMARDs) (Haringman et al, 2005). Macrophages and epithelial cells were also confirmed to be associated with extracellular IL-7 and collagen IV (Timmer et al, 2007). Samples from patients in clinical remission showed single sporadic IL-7 positive cells detected by immunohistology compared to an extensive area of IL-7 expression in a sample from active disease. These results correlated with the detection of high IL-7 mRNA levels from synovial fibroblasts cultured from patients with the highest inflammation scores measured at arthroscopy (Churchman & Ponchel, 2008). Low IL-7 serum levels return to normal levels in disease remission and the high levels of IL-7 observed at tissue sites also reverses in clinical remission. This may be due to the sequestering of IL-7 at the sites of inflammation and consequently, a reduced amount of free IL-7 in the circulation.

Approximately one quarter of patients with RA have an organised structure in the affected joint synovium which resembles that in the lymph node and are consequently referred to as ectopic lymphoid structures (Takemura et al, 2001). Infiltrated B and T cells are arranged in distinct areas and the presence of a network of follicular dendritic cells within the B cell areas leads to the formation of germinal centres (Takemura et al, 2001). Other patients have more diffuse infiltrations of cells or singular B or T cell type accumulations. These structures are common to a number of other chronic inflammatory conditions including chronic hepatitis (Mosnier et al, 1993), multiple sclerosis (Serafini et al, 2004) and Crohn's disease

(Kaiserling, 2001). Analysis of IL-7 within these lymphoid structures showed that IL-7 was secreted and positioned around the structure, possibly to promote the survival of T cells and subsequent B cell activation. In diffuse or aggregated cell infiltrations into synovial tissues, IL-7 detection was exclusively cellular. In RA synovial tissues with lymphoid areas, gene expression analysis of microarray data showed an upregulation in the JAK/STAT pathway and in particular each component of the IL-7R, compared to tissue that did not contain lymphoid structures (Timmer et al, 2007). Collectively this suggests a role for IL-7 in the organisation and maintenance of the lymphoid structures presented in RA in a similar manner to the IL-7 signalling mechanism in lymphoid tissue inducer cells that initiate lymph node development.

Evidence to suggest that IL-7 may be responsible for cartilage destruction in osteoarthritis disease has been presented. S100A4 is a calcium binding protein and has been found at elevated levels in both rheumatoid and osteoarthritis. On addition to chondrocytes cultures it promotes the chondrocyte hypertrophy and the expression of matrix metalloproteinase 13 (MMP-13). Ankle articular chondrocytes stimulated with 10 ng/ml IL-7 showed an increased expression in S100A4. This secretion appeared to be moderated by the JAK/STAT pathway as inhibition of JAK3, which was measured by immunoblotting and seen to be phosphorylated upon addition of IL-7, blocked the secretion of S100A4.

Arthritis is a progressive, debilitating disease characterised by damaged cartilage and bone around the joints. IL-7 involvement in human arthritis is contradictory, which indicates a requirement for standardised protocols to identify IL-7 and further study to identify the roles of IL-7 in the bone marrow cells involved in the arthritic process.

1.6 Thesis aims

MSCs are a rare population in the bone marrow that hold huge potential due to their ability to differentiate into skeletal lineages and therefore generate and maintain bone, fat and cartilage. As their developmental origin and functional contributions to the HSC niche are explored, it is becoming apparent that subsets of MSCs exist alongside each other in the bone marrow. Being able to accurately distinguish these subsets will be critical to understand not only MSC expansion and behaviour but also the factors that regulate HSC fate. However, to date, there is no agreement or demonstration of a marker to successfully isolate bone marrow MSCs. A number of potential candidates of unique markers have been proposed, among which, nestin is increasingly associated with stem cells and progenitor cells in a wide range of tissues and work continues to decipher its functional significance in the context of stem cell behaviour and potential.

IL-7 has essential roles in T and B cell development and has a negative impact on bone. The identity of IL-7 expressing stromal cells in bone marrow is currently unclear although significant advances have been made with the generation of transgenic mouse lines that allow the visualisation of IL-7 expressing cells. Detailed analysis and characterisation of the cells that express IL-7 may provide new insights into the processes of haematopoiesis and bone remodelling.

The aim of this study is to address the potential of nestin and IL-7 expression as markers of bone marrow derived MSCs and further examine the role of IL-7 expressing stromal cells in the bone marrow in the context of the stem cell niche, with the following objectives:

1. To examine the fate of murine IL-7 expressing cells in the bone marrow of IL-7CreRosa26-eYFP transgenic mice.
2. To develop a 3D *in vitro* model to assess IL-7 and nestin in the HSC niche.
3. To investigate the expression of IL-7 and nestin in primary human MSCs.
4. To investigate the role of IL-7 in MSC proliferation and differentiation.

2 Methods

2.1 Cell Culture

All cells were incubated at 37°C with 5% CO_2 in an atmosphere with 95% humidity unless otherwise stated. All plasticware was purchased from Corning and all reagents were purchased from Sigma-Aldrich (St. Louis, MO, USA) unless stated otherwise.

2.1.1 Isolation of primary mesenchymal stromal cells (MSCs)

Primary human mesenchymal stromal cells (MSCs) were extracted from femoral heads and knees obtained from Harrogate District Hospital and Clifton Treatment Centre, York, following informed consent and ethics approval from the University of York and NHS. Donors were anonymous and samples were identified with the prefix FH or K to denote donor site origin, followed by a unique number.

2.1.2 Isolation of cells from femoral heads

Bone marrow was removed from the femoral head using sterile instruments and collected into Dulbecco's Modified Eagle's Medium (DMEM, GIBCO, Life Technologies, Paiseley, UK) containing 100 ug/ml penicillin and 100 U/ml streptomycin (1% P/S). The fragments were minced with scissors and the supernatant removed once the large bone fragments had settled. The mincing process was repeated 3 times followed by vortexing the bone fragments for 1 minute and collecting the supernatant. The supernatant was centrifuged at 450 g for 5 minutes. The cell pellet was re-suspended in 16 ml DMEM and filtered through a 70 µm strainer into a fresh tube. This was then gently layered onto 12 ml Ficoll-Paque Plus (Amersham, GE Healthcare) in a falcon tube and centrifuged at 350 g for 30 minutes. The mononuclear fraction of cells could then be removed from above the Ficoll layer and washed in buffer A (phosphate buffered solution [PBS] containing 1% bovine serum albumin [BSA] and 5 mM

ethylenediaminetetracetic acid [EDTA, GIBCO]). Cells were seeded in DMEM containing 15% foetal bovine serum (FBS, batch tested for MSC growth) and 1% P/S into a 75cm^2 flask and cells allowed to adhere for 5 days.

2.1.3 Isolation of cells from knee bones

Knee bones were broken into pieces using sterile instruments, placed into a 10 cm petri dish and covered with DMEM containing 15% FBS and 1% P/S. Bone fragments were removed 5-7 days after seeding and the media changed to remove non-adherent cells and debris.

Adherent cells were termed passage 0 (P0) and once established, MSCs from both sources were maintained in DMEM containing 10% FBS and 1% P/S with media changes every 3-4 days. At 70% confluency the medium was removed, cells washed with PBS and harvested with 0.05% trypsin/0.02% EDTA. Cells were first seeded at a density of 1000 cells/cm^2 (P1) and thereafter at a 1:3 ratio.

2.1.4 Isolation and culture of primary murine stromal cells

IL-7cre Rosa26-eYFP mice were bred under specific pathogen free conditions in the Biological Services Facility at the University of York. All work was in accordance with ethical approvals from the University of York and Home Office Licence 60/4169 to Mark Coles. IL-7cre Rosa26-eYFP mice were schedule-1 killed and different long and flat bones were harvested by Priyanka Narang, Amy Sawtell and Anne Thuery. The rear femora and tibiae leg bones were scraped clean, the proximal and distal ends removed and PBS containing 2% FBS was flushed through using a 25 gauge (25 G) needle and syringe to collect the bone marrow. Separately, the bones were minced with scissors and washed in PBS containing 2% FBS to collect the cells. Settled bone fragments were incubated for 40 minutes at 37°C with gentle agitation in serum-free medium containing a collagenase cocktail to release the cells from the bone (Liberase TL, 1:40; Roche, Sussex, UK). DMEM containing 10% FBS was then added and the bones vortexed. The supernatant was removed to a fresh tube and centrifuged at 450g for 5 minutes to pellet the cells. All cells were washed and

filtered through a 70 µm cell strainer and maintained in DMEM with 10% FBS. After 4 days, non-adherent cells were removed and the medium changed every 3 days.

2.1.5 Primary cultures

Human adipose derived stem cells (ADSCs) were purchased from Invitrogen (Carlsbad, Ca, USA) and cultured in MesenPRO medium (Invitrogen) supplemented with 10% FBS.

Human T cells were isolated from peripheral blood cones (Blood Transfusion Service) by Dr Bridget Glaysher using the T cell purification kit RosetteSep (STEMCELL Technologies, Grenoble, France) which separates T cells using antibody mediate red cell resetting and a density gradient centrifugation.

Embryonic day 12.5 liver in murine foetal development is considered highly enriched for stem and progenitor cells and therefore the isolated cells have consequently been termed mouse haematopoietic progenitor cells (HPCs). Additionally, very few, if any mature myeloid or lymphocyte lineage cells are found at this stage in development. Mouse HPCs were isolated by Dr Mark Coles from day 12.5 embryos by removal of the foetal liver. Briefly, day 12.5 embryos were isolated from timed pregnancies and the foetal liver isolated by micro-dissection and placed in 10% DMEM. The foetal livers were teased apart through passage in a 19.5 gauge needle and finally filtered through a 70 uM mesh cell strainer. The cells were centrifuged and either frozen in 10% DMSO/FCS or used fresh in the spheroid and culture systems.

2.1.6 Culture of cell lines

The multipotent, murine mesenchymal cell line C3H10T1/2 (ATCC) and the human embryonal carcinoma stem cell line NTERA2/D1 were cultured in DMEM with 10% FBS. AFT024, a temperature sensitive mouse stromal cell line was maintained in DMEM with 10% FBS, 50 µM 2-mercaptoethanol and 1% P/S at 33°C. Mouse stromal cell line OP-9 was cultured in Minimum Essential Medium Eagle Alpha Modification (α-MEM, GIBCO) containing 20% FBS, 1% P/S, 1% L-glutamine and 1% non-essential amino acids (NEAA). Media was changed for each cell line every 3-4

days and cells passaged by trypsinisation at a ratio of 1:6 upon reaching 90% confluency.

2.1.7 Mycoplasma testing

All cells were subject to regular testing for mycoplasma. Cells were seeded into 24 well plates and allowed to adhere. Cells were washed with PBS and fixed for 5 minutes in methanol. Cells were washed with PBS and then incubated with 200 µl DAPI (1 µg/ml) for 5 minutes at room temperature. The DAPI was removed and the cells washed and viewed under UV light. Clear, defined nuclear staining was indicative of a negative result.

2.2 Colony forming unit assays

2.2.1 Colony forming unit – fibroblast (CFU-F) assay

To obtain clonal lines of MSCs from single cells, 10 cells/cm^2 were seeded out into 6 cm petri dishes and allowed to grow for 10-14 days with media changes every 3-4 days. MSCs of passages 0-7 were initiated, with passage 3 and 4 yielding enough clones to further analyse for donors FH408 and K6, respectively. DMEM with 20% HyClone FBS (GE Healthcare) and 1% P/S was used. Discrete colonies typically containing 200-300 cells were isolated using cloning cylinders sealed around each colony with sterile vacuum grease and harvested by trypsinisation. Cells were seeded into 48 well plates and transferred to larger vessels as the cell numbers increased.

2.2.2 Colony forming cell (CFC) assay

In order to quantify the potential of HPCs, cells were seeded into a semisolid medium (complete MethoCult; StemCell Technologies) containing cytokines and growth factors (rmSCF, rmIL-3, rhIL-6, rhEpo) to facilitate the proliferation and differentiation of progenitor cells into colonies of cells of the haematopoietic lineage such as granulocytes, erythroid cells and monocytes. HPCs were washed in Iscove's Modified Dulbecco's Media (IMDM) with 2% FBS, counted and adjusted to 10x the final concentration required (5 x 10^4 cells). 0.3 ml of cell suspension was

added to 3 ml of MethoCult media and vortexed to allow thorough mixing before seeding 1.1 ml into 35 mm dishes. Triplicate dishes were incubated in a humidified chamber at 37°C for 9 days and resulting colonies were identified according to descriptions and images provided with the MethoCult.

2.3 Spheroid culture

2.3.1 Spheroid media

A semi-solid media was prepared for the culture of cells in 3D spheroids as follows; 6 g methyl-cellulose was autoclaved and then stirred for 20 minutes to dissolve in 150 ml DMEM which had been pre-heated to 60°C. A further 100 ml media was added and stirred for 2-3 hours at 4°C. The mixture was finally centrifuged at 3600 g for 2 hours at room temperature to provide a stock solution of methyl-cellulose. The stock was diluted 1:7 in DMEM containing 10% FBS and 1% P/S and mixed thoroughly to provide a working solution of spheroid media.

2.3.2 Spheroid formation

Cell suspensions were seeded into non-adherent, U-bottomed 96 well plates in 200 µl spheroid media. Cells aggregated spontaneously over 24 hours to form a spheroid structure. Half media changes were carried out every 3-4 days.

2.3.3 Enzyme digestion of spheroids

To produce a single cell suspension from the 3D mesenchymal – haematopoietic cell spheroids they were enzymatically digested. Spheroids were collected into a 1.5 ml eppendorf and allowed to settle. Media was removed and the spheroids washed twice with PBS. Spheroids were re-suspended in 100 µl PBS and 5 µl Liberase TL (Roche, Sussex, UK) (2.5 mg/ml stock) added. Tubes were incubated with gentle agitation at 37°C for 20 minutes to disaggregate the spheroids. 1 ml DMEM containing 10% FBS was added and the sample then passed several times through a 25G needle to remove any clumps.

2.3.4 Fluorescent labelling of cells

In order to visualise the arrangement of cells within spheroids, cells were labelled with fluorescent probes; CellTracker green or red (Molecular probes, Invitrogen). Media was aspirated from monolayer cultures and replaced with 5 µl of 10 mM stock CellTracker probe diluted in 10 ml of serum-free media. Cells were incubated for 45 minutes at 37°C followed by a further 30 minutes in normal medium containing serum. Cells were then washed with PBS to remove any excess probe and replenished with normal media until further use.

2.3.5 LIVE/DEAD cell viability assay

To allow the analysis of viability of cells within spheroids, a LIVE/DEAD assay (Invitrogen) was used and the manufacturer's protocol was followed. Medium was removed from around the spheroid and replaced with 100 µl PBS containing 8 µM each of calcein-AM and ethidium homodimer-1 (EthD-1) as supplied. After incubating for 40 minutes in the dark at 37°C the spheroids were washed with PBS and fixed in 4% paraformaldehyde (PFA) for 15 minutes before imaging on a LSM510 confocal microscope (Carl Zeiss). Viable cells are able to convert calcein-AM to calcein by intracellular esterase activity and appeared fluorescently green whereas EthD-1 passes into cells with damaged plasma membranes and binds nucleic acids, resulting in an increase of a red fluorescence.

2.4 Cell proliferation

Cell proliferation of MSCs was determined using the colourimetric assay Cell Counting Kit-8 (CCK-8, Dojindo, Kumamoto, Japan). Cellular dehydrogenase activity reduces the tetrazolium salt WST-8 to give a soluble yellow coloured formazan product. The amount of formazan produced is directly proportional to the number of living cells. MSCs were seeded at 2 x 10^4 cells/cm^2 into 96 well plates. At days: 0, 3, 5 and 7, 100 µl of fresh medium was added to each well and inoculated with 10 µl CCK-8 reagent. The plate was incubated at 37°C for 100 minutes and the absorbance read at 450 nm on a plate reader (Dynex Technologies MRX II).

2.5 Cell differentiation

All differentiation reagents were obtained from Sigma-Aldrich unless stated otherwise.

2.5.1 Osteogenic differentiation

For monolayers, cells were seeded at 2 x 10^4 cells/cm^2 and allowed to adhere overnight. These adhered cells were designated day 0. Medium was replaced on day 0 with DMEM containing osteogenic factors: 5 mM β-glycerophosphate, 10 nM dexamethasone and 50 μg/ml L-ascorbic acid-2-phosphate. Cells were cultured up to 21 days and the medium was replaced every 3 days throughout.

2.5.1.1 Alkaline phosphatase and von Kossa staining

To visually determine alkaline phosphatase enzyme activity as a marker of osteogenic differentiation, the cells were washed twice in PBS and then stained for 2 minutes in a solution containing 1 mg/ml Fast red TR and 0.2 mg/ml napthol AS-MX phosphate dissolved in 1% N,N-dimethylformamide diluted in 0.1M Tris buffer at pH 9.2. von Kossa staining was subsequently used to visualise mineralisation. Cells were washed twice and fixed for 5 minutes in 4% PFA and then washed once in PBS and again in dH_2O. 1% silver nitrate solution was added to the cells and incubated for 60 minutes under strong light. After 3 washes in dH_2O, 2.5% sodium thiosulphate was added for 5 minutes before two final washes in dH_2O. Staining was visualised using a DM IRB light microscope (Carl Zeiss).

2.5.1.2 Alizarin Red staining

Cells were washed 3 times in PBS and fixed in 4% PFA for 20 minutes at room temperature. The cells were then washed 3 times in PBS and stained with 40 mM alizarin red at pH 4.2 for 20 minutes at room temperature. Thorough washing with PBS and then tap water whilst the plates were gently shaken removed residual stain and the cells were air dried before imaging on a stereo microscope (Stereo lumar, Carl Zeiss). Red staining indicated the presence of calcium after osteogenic differentiation. Differentiation was quantified by eluting alizarin red stain with

100 µl 10% w/v cetylpyridium chloride in sodium phosphate buffer (pH 7). Monolayers were incubated for 25 minutes with gentle agitation to release the stain. 96 well plates were then read at 570 nm (Dynex Technologies MRX II).

2.5.2 Adipogenic differentiation

Cells were seeded at 2 x 10^4 cells/cm^2 and allowed to adhere overnight. These adhered cells were designated day 0. Medium was replaced on day 0 with DMEM containing adipogenic factors: 500 µM 3-isobutyl-1-methylxanthine (IBMX), 1 µg/ml insulin, 1 µM dexamethasone, and 100 µM indomethacin. Cells were cultured up to 21 days and the medium was replaced every 3 days.

2.5.2.1 Oil Red O stain

A working solution of Oil Red O stain was prepared by first making a 0.5% stock solution of Oil Red O in 99% isopropanol. The stock was diluted with dH_2O to a 0.3% working dilution, left overnight and filtered before use to remove any solid residue. Cells were washed once in PBS and fixed for 5 minutes in 4% PFA and then washed in dH_2O. Cells were then left in 60% isopropanol for 5 minutes followed by a 10 minute incubation in 0.3% Oil Red O working solution. Cells were then washed once in 60% isopropanol to remove excess stain and 3 times in dH_2O before counter staining for 2 minutes in haematoxylin. Staining was visualised using a DM IRB light microscope (Carl Zeiss). In order to quantify the amount of Oil Red O staining on monolayers in 96 well plates, the haematoxylin stain was omitted and after cells were washed in dH_2O, the stain was released from the cells by the addition of 50 µl 100% isopropanol and incubation for 15 minutes at room temperature. The absorbance of Oil Red O in solution was then measured at 450 nm on a microplate reader (Dynex Technologies MRX II).

2.5.3 Chondrogenic differentiation

Cells were seeded at 2 x 10^5 cells into a universal in 500 µl of media. These cells formed pellets overnight and 24 hours after seeding the media was changed to serum-free DMEM containing chondrogenic factors: 100 nM dexamethasone,

50 µg/ml L-ascorbic acid-2-phosphate, 40 µg/ml L-proline, 1% ITS^{+}1 supplement and 20 ng/ml TGF-β3 (Peprotech). Control pellets were cultured in identical media with the omission of TGF-β3.

2.5.3.1 Alcian blue staining

The presence of sulphated glycosaminoglycans (GAGs) was detected by alcian blue staining to indicate chondrogenic differentiation. Slides were fixed in ice cold acetone for 10 minutes; monolayers in 96 well plates were fixed for 5 minutes with 4% PFA. The fixative was removed and the sample washed twice with dH_2O before incubation with 1% alcian blue (ph<1) for 30 minutes. Excess stain was removed with a 10 second wash in 1% acetic acid followed by rinsing in dH_2O. The sample was then covered with 10% glycerol and imaged on a DM IRB light microscope or stereo microscope (Carl Zeiss).

2.5.3.2 Collagen II staining

Using the Vectastain ABC kit (Vector Laboratories), the manufacturer's protocol was followed. Briefly, the sections were incubated in freshly prepared 10 mM sodium phosphate buffer for 2 minutes followed by 20 minutes in normal serum (provided in kit) in buffer. The serum was then removed and the slides were incubated overnight at 4°C in primary antibody (rabbit polyclonal anti-collagen II, Abcam, ab53047) diluted 1:200. The following day, the sections were washed 3 x 5 minutes in buffer and incubated with biotinylated secondary antibody (supplied) for 30 minutes at room temperature. Meanwhile, the Vectastain ABC reagent was prepared by adding equal drops of reagents A and B into buffer and mixing. Once the secondary antibody was removed, the slides were washed with buffer for a further 3 x 5 minute washes and incubated for 30 minutes with ABC reagent. This was removed and the slides washed before a final incubation in peroxidase substrate, NovaRED for 10 minutes until the colour developed. The sections were rinsed with tap water. The samples were then covered with 10% glycerol and imaged on a DM IRB light microscope (Carl Zeiss).

2.5.4 Spheroid differentiation

Spheroids were seeded at 4 x 10^4 cells per well in 96 well plates and then treated the same as the monolayer cultures but with spheroid media. 10 µm sections of cryo-preserved spheroids were taken before von Kossa and Oil Red O staining were carried out on slides.

2.6 Histology and immunofluorescence

2.6.1 Monolayers

13 mm glass coverslips were sterilised in 100% IMS, allowed to dry and placed individually into each well of a 24 well plate. Cells were seeded at 1 x 10^4 per well and allowed to adhere overnight. Staining was carried out in the plate and then the coverslips were removed and mounted with Vectashield (Vector Laboratories) onto glass slides and sealed with nail polish.

2.6.2 Vibratome sections

IL-7cre Rosa26-eYFP embryos were mounted in 8% agarose and set at 4°C. The embryo was cut into 250 µm thick longitudinal sections collected into PBS using a Vibratome (Leica Microsystems).

2.6.3 Tissue sample freezing and cryosectioning

Mouse bones from IL-7cre Rosa26-eYFP mice for immunohistochemistry were fixed in 4% PFA overnight. After fixation, bones were placed in 30% sucrose solution for 15 minutes at room temperature followed by 15% sucrose overnight at 4°C. Bones were then coated with 10% PVA and frozen in cooled isopropanol on dry ice. They were then fully mounted in 10% PVA and stored at -80°C.

Spheroids were embedded in OCT (Tissue-Tek, Sakura Finetek) and frozen by immersion in liquid nitrogen and stored at -80°C before sectioning. All samples were acclimatised to the chamber temperature (-30°C) of the cryostat (Bright Instrument Co.) before 10 µm sections were taken. Sections were collected onto Superfrost glass slides (Menzel-Gläser) and stored at -20°C until use.

2.6.4 Cytospin preparations

200 µl of cell suspension at a concentration of 1 x 10^5 cells/ml was added to the cytospin chamber (Cytospin 3, Shandon Scientific) and centrifuged for 5 minutes at 850 rpm with LO acceleration onto Superfrost slides. Slides were kept at -20°C until use.

2.6.5 Haematoxylin and Eosin (H&E) staining

Sections were fixed in 4% PFA for 5 minutes followed by 2 washes in dH_2O. Sections were incubated in Mayer's haematoxylin for 15 minutes and washed thoroughly with tap water. Unspecific staining was removed by addition of acid alcohol (0.25% hydrochloric acid in 50% ethanol) for 10 seconds followed by washing in dH_2O. Sections were then incubated in Scott's tap water for 5 minutes and washed well with tap water. One percent eosin was added for 5 minutes followed by thorough washing in tap water and then dehydration in 70% IMS for 2 minutes and then 100% IMS for a further 2 minutes. Sections were then cleared in xylene for 2 minutes and mounted in DPX mountant. Morphology was observed using a DM LA light microscope (Carl Zeiss).

2.6.6 Immuofluorescent staining

Samples were initially fixed in 4% PFA for 5 minutes at room temperature followed by 2 washes in PBS. To detect nestin, an intracellular protein, samples were permeabilised at this point with a 10 minute incubation in 0.25% Triton X-100 in PBS (PBS-T). Samples were then washed in PBS for 5 minutes several times. All samples were then blocked for 30 minutes in PBS containing 10% animal serum of the same species that the secondary antibody was raised in. Primary antibodies (Table 2.1) were added at the appropriate dilution in PBS and incubated in a humidified chamber overnight at 4°C. The primary antibody was washed off the next day with 3 x 5 minute PBS washes. If required, samples were incubated for 45 minutes at room temperature with a conjugated secondary antibody. The washing steps were repeated. Samples were counter-stained with DAPI for 5 minutes.

Negative controls were carried out by replacing the primary antibody with the appropriate immunoglobulin G (IgG). Samples were mounted with Vectashield (Vector Laboratories) and imaged using a LSM710 invert confocal microscope (Carl Zeiss). In order to quantify YFP expressing cells, 3 random areas of interest per region (central bone marrow, endosteum etc) were counted. Cells were counted manually and expressed as a percentage of total nucleated cell number which were counted using DAPI stain. n = 5 mice.

Target	Clone	Conjugate	Dilution	Supplier
Rat anti mouse Nestin	polyclonal	purified	1:800	abcam
GFP	polyclonal	Alexa Fluor 488	1:500	Invitrogen
Rabbit anti mouse CD169	MOMA-1	purified	1:50	AbDserotec
VCAM-1	429	APC	1:200	Invitrogen
Rat	polyclonal	Alexa Fluor 647	1:500	Invitrogen
Rabbit	polyclonal	Cy3	1:800	Sigma-Aldrich

Table 2.1 Antibodies for immunofluorescent staining
Primary antibodies used on mouse tissue were either directly conjugated or detected with an appropriate secondary antibody that detected the species that the primary was raised in.

2.6.7 Ki67 staining

Proliferation was analysed by Ki67 immunofluorescent staining. Primary Ki67 antibody was used diluted at 1:250 (ab15580, Abcam) whilst the secondary; Alexa Fluor 488 goat anti-rabbit was used at 1:5000 (A11008, Sigma-Aldrich). Cells were counter stained for 5 minutes in DAPI (1 µg/ml).

2.6.8 F4/80 staining

The presence of mature macrophages was determined using marker F4/80 using immunofluorescence described in section 2.6.6 with some modification. The antibody was Alexa Fluor 647 conjugated (clone BM8, ebioscience) and used at a concentration of 1:200 for 45 minutes at room temperature rather than overnight. Slides were mounted in Prolong gold (Invitrogen) and imaged using a LSM510 invert confocal microscope (Carl Zeiss).

2.6.9 Whole mount staining

For embryo sections taken on the Vibratome (section 2.6.2), immunostaining was extended. Sections were blocked in 10% rabbit serum for 1 hour at room temperature followed by antibody staining with Alexa Fluor 647 conjugated anti-GFP and Cy3 labelled anti-SMA (each 1:1000; Invitrogen) in 400 µl volume in a 24 well plate. The sections were incubated for 72 hours at 4°C followed by 24 hours of washing in PBS, replacing the PBS 3 times throughout the day. Sections were then fixed for 20 minutes at room temperature in 4% PFA followed by several PBS washes. Whole mounts were transferred to glass pots and covered in progressively stronger methanol solutions (25, 50, 75, and 100%) for 15 minutes each at room temperature. A final 100% methanol incubation for 1 hour completed their dehydration. A 50:50 solution of methanol: BABB (benzyl alcohol: benzyl benzoate; Sigma-Aldrich) was added for 15 minutes and then replaced with BABB for a further 2 hours to clear the sections. Sections were mounted in BABB in thick metal slides sealed between glass coverslips and viewed with a LSM510 confocal microscope (Carl Zeiss).

2.7 Flow cytometry

2.7.1 Flow cytometric analysis of human MSC surface antigen expression.

Isolated MSCs from human donors were analysed to confirm the expression of a panel of stromal cell surface markers commonly used to describe MSCs. Antibodies were previously titrated for optimal dilution for use by flow cytometry. Media was

removed from cultured MSCs which were then washed twice with PBS and harvested using FACS buffer (buffer A, see section 2.1.2) at 37°C. Cells were collected by centrifugation at 450 rpm for 5 minutes and the supernatant removed. Approximately 5 x 10^4 cells for each marker were resuspended in separate eppendorf tubes in 100 µl FACS buffer containing the appropriate dilution of primary antibody (Table 2.2) and incubated on ice for 30 minutes. Cells were then washed twice with 1 ml FACS buffer and centrifuged at 450 rpm for 5 minutes. Cells incubated with purified primary antibodies were incubated further for 20 minutes on ice in the dark with the appropriate dilution of secondary antibody followed by 2 FACS buffer washes. All samples were then re-suspended in 400 µl FACS buffer and kept on ice before processing on a cyAn flow cytometer and analysed using Summit software (v4.3; Beckman Coulter). 1 x 10^4 events per sample were collected.

Target	**Clone**	**Conjugate**	**Dilution**	**Supplier**
CD45	HI30	FITC	1:100	Caltag labs
CD166	3A6	PE	1:50	BD Pharmingen
CD44	G44-26	FITC	1:10	BD Pharmingen
CD90	ebio5E10	PE-Cy5	1:100	eBioscience
CD105	SN7	APC	1:100	eBioscience
CD29	MAR4	Purified	1:100	BD Pharmingen
CD73	AD2	Purified	1:100	BD Pharmingen
CD34	AC136	FITC	1:50	Miltenyi Biotec
Goat anti-mouse	polyclonal	Alexa Fluor 488	1:200	Invitrogen

Table 2.2 Antibodies for human MSC flow cytometry

2.7.2 Flow cytometric analysis of murine stromal cell surface antigen expression.

Following the protocol in section 2.7.1, stromal cells isolated from murine bones were analysed for cell surface markers in Table 2.3. Cells were analysed fresh or from cultured cells.

Target	Clone	Conjugate	Dilution	Supplier
F4/80	BM8	647	1:200	ebioscience
Ter-119	TER-119	PE	1:100	ebioscience
CD73	eBioTY/11.8	PE	1:100	ebioscience
CD90.2	30-H12	APC	1:100	ebioscience
CD45	30-F11	Biotin	1:200	ebioscience
CD127 (IL7Rα)	A7R34	PE	1:50	ebioscience
CD54 (ICAM-1)	YN1/1.7.4	PE	1:1000	ebioscience
CD106 (VCAM-1)	429	647	1:1000	ebioscience
CD105	MJ7/18	PE	1:100	ebioscience
Hamster anti mouse Gp38	eBio8.1.1	purified	1:800	ebioscience
Streptavidin	Not applicable	Pacific blue	1:400	Invitrogen
Goat anti hamster	Polyclonal	647	1:500	Invitrogen

Table 2.3 Antibodies for mouse MSC flow cytometry

2.7.3 MACs depletion of cells

Freshly harvested murine bone marrow cells were first depleted for CD45 cells by Magnetic affinity cell sorting (MACS) flow cytometry. Briefly, red cells were lysed in ACK buffer (0.15M, ammonium chloride [BDH lab supplies], 1 mM sodium hydrogen carbonate [Fisher], 0.1 mM EDTA [GIBCO] in dH_20); remaining cells were blocked for 10 minutes with F_c block (1:1000) and incubated with primary biotin conjugated CD45 antibody (1:200). After 2 PBS washes, cells were incubated with anti-biotin MACS microbeads (20 µl per 10^7 cells) before magnetic separation through a MACS column. The depleted cell fraction was then labelled for analysis.

2.7.4 Identification of HSCs

An antibody lineage cocktail (lin), c-kit and sca-1 (Table 2.4) were used to identify HSCs within the population of HPCs by flow cytometry (see section 2.7).

Target	Clone	Conjugate	Dilution	Supplier
c-kit	2B8	PE	1:100	ebioscience
Sca-1	D7	APC	1:100	ebioscience
lineage markers: (CD3, CD45R, CD11b, Ter-119, Gr-1)	145-2C11, RA3-6B2, M1/70, TER-119, RB6-8C5	Biotin	1:200	ebioscience
Streptavidin	Not applicable	Pacific blue	1:400	Invitrogen

Table 2.4 Antibodies to detect HSCs by flow cytometry

2.7.5 Cell sorting by flow cytometry

To purify the YFP expressing stromal cells from murine line IL-7cre Rosa26-eYFP, cells were sorted and collected on a MoFlo sorter (Beckman Coulter). Isolated cells from bone marrow and bone digests were incubated in 1 ml ACK buffer to lyse any red blood cells. Cells were then washed in buffer A (see section 2.1.2) and filtered through a 70 µm cell strainer. Cells were incubated with APC conjugated CD45 at

1:1000 dilution for 20 minutes on ice. Cells were washed twice in buffer A and re-suspended at a concentration of 1 x 10^7 cells/ml. Only cells that were CD45 negative were collected to remove haematopoietic cells from the sort and YFP positive and negative cells were then collected separately into tubes of DMEM + 20% FBS. Tubes of collected cells were centrifuged for 20 minutes at 450 rpm.

2.7.6 IL-7 binding assay

Binding of biotinylated recombinant IL-7 to human MSCs was detected using a Fluorokine kit (R&D systems) following manufacturers' guidelines. Briefly, cells were removed from adherent culture with buffer A, centrifuged at 500g for 5 minutes followed by 2 x PBS washes and re-suspension in PBS at a final concentration of 4 x 10^6 cells/ml. Cells were incubated with 10 µl biotinylated IL-7, a negative control protein (soybean trypsin inhibitor), both provided in the kit, or no protein for 45 minutes at 4°C. In a separate tube, 10 µl biotinylated IL-7 was incubated with 20 µl of an anti-IL7 blocking antibody to confirm specificity of the test. Cells were then stained with avidin-FITC for 30 minutes at 4°C in the dark, washed in the RDF1 buffer (a buffered saline and protein solution) provided and analysed by flow cytometry.

2.8 Gene expression analysis

All reagents were from Invitrogen unless stated otherwise.

2.8.1 RNA extraction

RNA was extracted from cells using TRIzol reagent following the manufacturer's protocol. For adherent cell cultures, 500 µl TRIzol reagent was added directly to a 25cm^2 cell culture flask to lyse the cells. For cells cultured in 3D, the spheroids were first digested as described in section 2.3.3 and centrifuged at 450 g for 5 minutes to pellet the cells. 500 µl TRIzol reagent was added to lyse the cells and then passed through a pipette several times. All samples were then incubated at room temperature for 5 minutes and treated in the same way. 200 µl chloroform (Sigma-

Aldrich) per 1 ml of TRIzol was added, vortexed for 15 seconds and incubated at room temperature for 5 minutes. Samples were then centrifuged at 12000 g for 20 minutes at 4°C. The RNA contained in the upper aqueous phase was removed to a fresh tube and precipitated using 500 µl of 100% isopropanol per 1 ml of TRIzol initially used. Samples were incubated at 4°C for 30 minutes and then centrifuged at 12000 g for 15 minutes at 4°C to pellet the RNA. The isopropanol was removed and the RNA washed with 1 ml 75% ethanol and centrifuged at 12000 g for 5 minutes. The supernatant was removed and the pellet allowed to air dry before being re-suspended in 12 µl of nuclease free H_20. RNA concentration was measured on a NanoDrop spectrophotometer (Thermo Scientific).

2.8.2 cDNA synthesis

First strand cDNA was synthesised from isolated mRNA using Superscript II reverse transcriptase. Briefly, reactions were carried out in duplicate for each sample with 1 µl oligo dt, 1 µg RNA and 1 µl 10 mM dNTPs (ATP, TTP, GTP, CTP) made up to 12 µl total reaction volume with nuclease free water. Samples were incubated at 65°C for 5 minutes followed by 2 minutes chilled on ice. Seven microlitres of a reaction mix containing 1^{st} strand buffer, 0.1M DTT and nuclease free water was added to each sample and incubated for 2 minutes at 42°C. One microlitre of Superscript II was then added to half the samples and 1 µl nuclease-free water was added to the duplicates to act as a no reverse transcriptase control (no RT control). Primer extension occurred during a 1 hour incubation at 42°C followed by 15 minutes at 72°C to inactivate the reverse transcriptase. cDNA was diluted 1:2 after synthesis with nuclease-free water and stored at -20°C until subsequent PCR amplification.

2.8.3 Reverse transcriptase polymerase chain reaction (RT-PCR)

PCR amplification of specific genes of interest was carried out using 2.5 µl cDNA template in a 25 µl total volume reaction containing the following components:

Component	Amount (µl)
Template cDNA	2.5
10 x PCR buffer	2.5
50 mM $MgCl_2$	0.75
10 mM dNTPs	0.5
Forward primer (10 µM)	0.5
Reverse primer (10 µM)	0.5
Taq DNA polymerase	0.25
Nuclease-free water	17.5

Table 2.5 Standard PCR reaction components

PCR amplification for GAPDH was carried out for each sample of cDNA produced to confirm successful synthesis. A water control was run for each gene within a PCR. Primers (Table 2.6) were designed using the NCBI Primer BLAST program, produced by Sigma-Aldrich and optimised using human T cell RNA.

Gene	Forward Primer	Reverse Primer	Product size
m/h GAPDH	GGTGAAGGTCGGWGTCAACGG	GGTCATGAGYCCTTCCACGAT	514
h IL2Rγ	CCTGCTGGGAGTGGGGCTGA	CCCGTGGGTCCTGGAGCTGA	359
h JAK1	ATGGCGTCTGTGTCCGCGAC	ACTGGCCTGCACCGGCTTTC	478
h STAT5B	TCAGTGGATCCCGCACGCACA	TGGCCAACTTCCAGGCTTCACG	379
h JAK3	TCCGGGAGGCGCAGACACTT	ATAGCGGCACAGCTCCACGC	437

Table 2.6 PCR primers

Samples were run on a DNA thermocycler (G-Storm) with the following conditions:

Step	Process	Temperature °C	Time
I	Initial denaturation	94	3 minutes
II	Denaturation	94	10 seconds
	Annealing	58 (GAPDH) or 62	20 seconds
	Extension	72	1 minute
III	Repeat step II		30 times
IV	Final elongation	72	5 minutes
V	Hold	12	-

Table 2.7 PCR conditions

2.8.4 Agarose gel electrophoresis

Agarose gel electrophoresis was used to verify the expected size of the PCR products. 1.5% agarose gels were made with TAE buffer (Tris, EDTA, acetic acid) with the addition of 5 µl SYBR safe to allow visualisation of the gel under UV light. The samples were run at 120v for approximately 45 minutes alongside a molecular weight marker (Hyperladder IV; Bioline). Images were acquired using an AlphaImager 2000 gel documentation system (Protein Simple).

2.8.5 Quantitative real time polymerase chain reaction (qRT-PCR)

Quantitative real time polymerase chain reaction (qRT-PCR) was used to measure the relative expression of genes of interest and was carried out in triplicate in a 96 well plate for each sample using reactions containing the components in Table 2.8.

Component	Amount (µl)
Template cDNA	5
Sybr green PCR master mix (Applied Biosystems)	12.5
Forward primer (10 µM)	1
Reverse primer (10 µM)	1
Nuclease free water	5.5

Table 2.8 Standard qRT-PCR components

Plates were covered with an adhesive lid and centrifuged at 3600 rpm for 1 minute 50 seconds before processing on an ABI7300 Prism System Detection System (Applied Biosystems) with the following cycle conditions:

Step	Temperature (°C)	Time
I	50	2 minutes
II	95	10 minutes
III	95	15 seconds
	60	1 minute
IV	Repeat step III	40 times

Table 2.9 qRT-PCR conditions

Results were analysed with the ABI7000 prism software based on the change in cycle threshold (ΔΔct) method. Target genes were normalised to the housekeeping gene and reported as relative expression as compared to the appropriate day 0 control. Controls were conducted for each primer set using nuclease free water and no reverse transcriptase template controls were run for the housekeeping gene.

Gene	Forward Primer	Reverse Primer
h RPS27A	TGGATGAGAATGGCAAAATTAGTC	CACCCCAGCACCACATTCA
m HPRT	CATCTTCTCAAAATTCGAGTGA	TGGGAGTAGACAAGGTACAAC
h IL-7	AGCCACGCCGTAGTGTGTGC	TCCGCGGAGTTGCCGAGTCT
m IL-7	CCTGTGACAGCCTTTCTGAAGA	AGGATAGGGAGCCTCAGACATAGG
h Nestin	CCTGTGACAGCCTTTCTGAAGA	AGGATAGGGAGCCTCAGACATAGG
h IL-7Rα	CCTGCTTAGCCTTGGGACTACA	GGGTTCAATGTCAGGATTCCA
m IL-7Rα	CCCACAGAGAAAACTACGACCAA	ACTCGCTCCAGAAGCCTTTG
h FABP4	TGTGCAGAAATGGGATGGAAA	CGCATTCCACCACCAGTTT
h PPARg	GGCTTCATGACAAGGGAGTTTC	AACTCAAACTTGGGCTCCATAAAG
h Runx2	AGTGATTTAGGGCGCATTCCT	GGAGGGCCGTGGGTTCT
h ALP	GGGAACGAGGTCACCTCCAT	TGGTCACAATGCCCACAGAT
h Sox 9	TTCCGCGACGTGGACAT	TCAAACTCGTTGACATCGAAGGT
h Collagen II	TTGCCTATCTGGACGAAGCA	CGTCATTGGAGCCCTGGAT
h IL-6	CCGGGAACGAAAGAGAAGCT	GCGCTTGTGGAGAAGGAGTT

Table 2.10 qRT-PCR primers

2.8.6 Primer optimisation

Primers were designed using ABI Primer Express software (Applied Biosystems) and are shown in Table 2.10. Newly designed primers were tested for equal qRT-PCR efficiency compared to the housekeeping gene by analysing 10 fold serial dilutions of cDNA by absolute quantification. In this example, cDNA from primary human T cells was used as the control sample to measure the efficiency of IL-7Ra primers. Reactions were carried out in triplicate and processed with the same conditions as for relative quantification (Table 2.9) with the addition of a dissociation step after step IV of 15 seconds at 95°C, 20 seconds at 60°C and a further 15 seconds at 95°C. Plots were generated using the ABI software of the threshold cycle (Ct) value against the log of the cDNA concentration (Figure 2.1 A). For primers to be acceptable for use and indicate equal efficiency the slope of the standard curve should be similar (Figure 2.1 C) and there must also only be a single peak in the dissociation curve (Figure 2.1 B). IL-7Rα was compared to the housekeeping gene ribosomal protein S27a (RPS27a).

2.9 Statistics

Data are expressed as mean ± SD. After testing for normal distribution (Kolmogorov-Smirnov normality test), control and treated or differentiated groups were compared using an independent samples t-test (for data with equal variance measured by a Levene's test). Statistically significant results were considered to have a p value < 0.05 and were annotated on graphs according to the following rule; $p \leq 0.05$ not significant (ns), $p < 0.05$ *, $p < 0.01$ **, $p < 0.001$ ***.

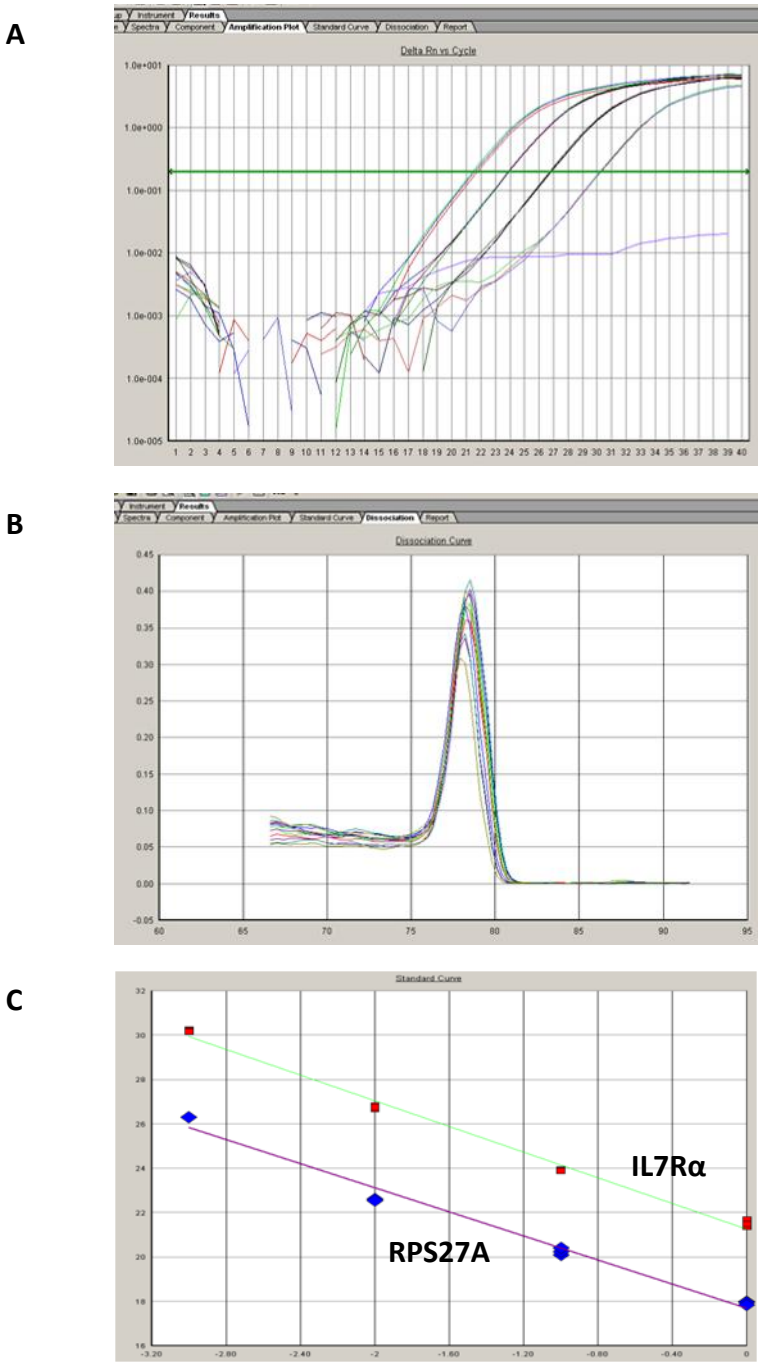

Figure 2.1 Optimisation of qRT-PCR primers
IL-7Rα primers were optimised using T cell RNA. Plots were generated of Ct values of serial dilutions of cDNA (A). No product was observed when RT was replaced with H_20 (no RT control). A single dissociation curve indicates a specific PCR product from all samples (B) and a standard curve produced from ct values and the log of DNA dilutions shows the same slope between the target of interest and the housekeeping gene (C).

3 Fate tracing of IL-7 expressing cells in the mouse bone marrow microenvironment

3.1 Introduction

IL-7 is a cytokine originally identified for its ability to stimulate B lymphopoiesis (Namen et al, 1988). Additionally, IL-7 is known to have an essential role in T cell survival and proliferation (Morrissey et al, 1991). These two fundamental roles of IL-7 are the best understood, although the detailed mechanisms of their regulation are still being investigated.

Investigations into the involvement of IL-7 in the murine system are hampered by the low levels of protein and transcript expression of endogenous IL-7 and the consequential lack of success of its detection by traditional methods such as immunohistochemistry (Mazzucchelli et al, 2009). To overcome this problem, several bacterial artificial chromosome (BAC) transgenic mice have been developed in which reporter genes were inserted into the IL-7 locus. Depending on the construct used, IL-7 reporter expression can then be assessed directly by fluorescent microscopy, using antibody staining or further crossing with reporter mice of Cre recombinase activity (Reviewed by Kim et al, 2011).

The Cre/lox system has been widely employed to manipulate gene expression in a tissue or temporal specific manner. Originally identified in bacteriophage, the recombination mediates circularisation and DNA replication during bacterial division. Cre recombinase is an enzyme that catalyses recombination between two loxP sites (locus of X-over of P1). These are specific 34-base pair (bp) sequences consisting of an 8-bp core sequence, where recombination takes place, and is flanked by two 13-bp inverted repeats. The recombination excises the DNA sequence between the loxP sites and can be used to produce gene deletions, or in combination with fluorescent proteins, to track Cre activity, as in the case of IL-7Cre

rosa26-eYFP mice. LoxP sites and the cre gene are not found in mice and are therefore introduced to produce the transgenic strains (Sauer, 1998). Detection of Cre mediated IL-7 reporter is located in the thymus, lymph nodes, bone marrow, liver and small intestines of IL-7Cre rosa26-eYFP mice (Repass et al, 2009).

IL-7 is known to be expressed by stromal cells in the bone marrow but the precise identification of these cells and their functional role are still to be described adequately. Overall, IL-7 has a negative impact on bone as knockout studies in mice report an increased bone mass due to a lack of IL-7 stimulated T cell activation and subsequent increased osteoclast number (Roland et al, 2011). Oestrogen is a critical regulator of bone mass and is involved in promoting survival of osteoblasts (Gohel et al, 1999) and suppressing osteoclast activity (Manolagas, 2000). Oestrogen deficiency leads to accelerated bone loss or osteoporosis. In order to provide effective treatment strategies for osteoporosis the mechanisms of this osteoclastogenesis must be understood. Ovariectomy induces oestrogen deficiency which is accompanied by bone loss. Interestingly, IL-7 production is increased in these mice and enhances the production of osteoclast precursors *in vitro* (Sato et al, 2007). Neutralisation of IL-7 *in vivo* prevented the ovariectomy induced bone loss by inhibiting osteoclastogenesis and stimulating bone formation, suggesting that IL-7 plays a role in the balance between bone formation and resorption in these conditions (Weitzmann et al, 2002). Together, these data suggest that IL-7 production is interlinked with the bone remodelling process and by extension, with haematopoietic stem cells (HSCs) and mesenchymal stem cells (MSCs).

3.2 Aims

In this chapter IL-7Cre Rosa26-eYFP BAC transgenic mice were used to determine the localisation of YFP positive cells in bone and bone marrow. Briefly, the activity of Cre recombinase under the control of IL-7 regulatory elements in IL-7Cre Rosa26-eYFP BAC transgenic mice leads to the genetic marking, by YFP expression, of cells that are either currently expressing IL-7, have previously expressed IL-7 or have been derived from a precursor that at one point expressed IL-7. These cells

were isolated and further characterised in order to gain a better understanding of the stromal cells that express IL-7.

3.3 Results

3.3.1 Localisation of YFP expressing cells

In order to define the location of YFP expressing cells from IL-7Cre Rosa26-eYFP mice, frozen sections of bones were immunostained with an anti-GFP antibody in order to amplify the YFP signal and counter stained with DAPI (see section 2.1.7). Serial image sections were acquired using confocal microscopy and are presented as a stacked projection of roughly 30-40 µm tissue.

YFP expressing cells were found throughout the central bone marrow (Figure 3.1) and represented approximately 4% of the total bone marrow cell population (Table 3.1). In some cases the YFP^+ cells were arranged in distinct patterns and associated with vessels within the bone marrow (Figure 3.2, B).

Additionally, YFP expressing cells were located in areas of cartilage such as articular chondrocytes at joint surfaces and hypertrophic chondrocytes in the growth plate of the bones that were identified by their characteristic appearance and location (Figure 3.1 A and B). YFP^+ cells were also present at the joint interface in the cartilaginous triangular meniscus extending into the synovium (Figure 3.1 B).

YFP expressing cells were also found closely associated with the bone. YFP^+ cells were found lining the bone at the junction with the bone marrow or endosteum, and particularly around trabeculae. A proportion of the osteocytes within the bone were YFP^+ (Figure 3.1 D). YFP expressing cells were also detected at the periosteum and in skeletal muscle attached to the bones (Figures 3.1 and 3.2 D).

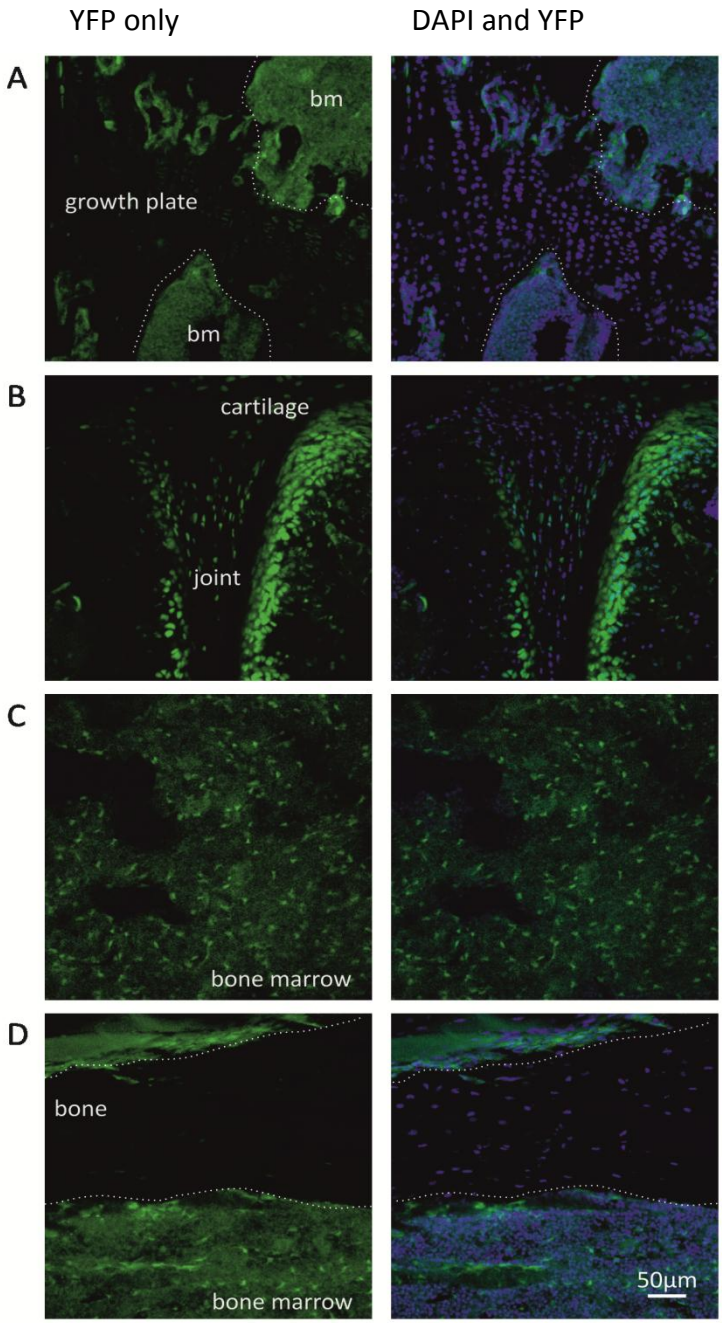

Figure 3.1 Detection of YFP expressing cells in the adult mouse femur
Representative images of 10 µm sections of snap frozen femur show YFP expressing cells (green) at the growth plate (A), joint (B), bone marrow (C) and endosteum (D). Slides were counter stained with DAPI (blue). bm, bone marrow.

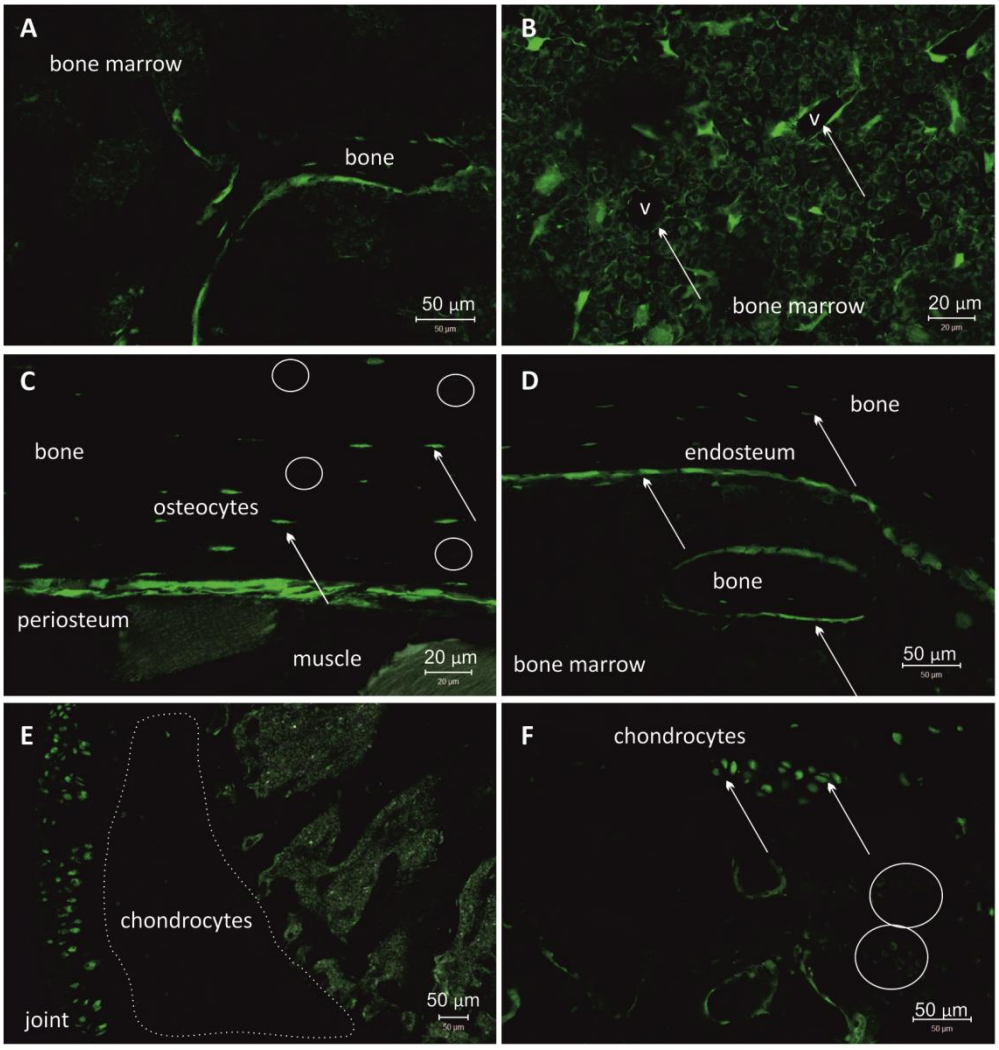

Figure 3.2 Detection of YFP expressing cells in the adult mouse tibia
Representative images of 10 µm sections of snap frozen tibia show YFP expressing cells (green) are located around trabeculae (A) and vessels (v, B), are osteocytes contained within bone (C), are at the endosteum (D) are articular chondrocytes (E) and hypertrophic chondrocytes (F, arrows). YFP is not expressed in all cells in which it is present. Circles in C and F indicate YFP negative osteocytes and chondrocytes, respectively.

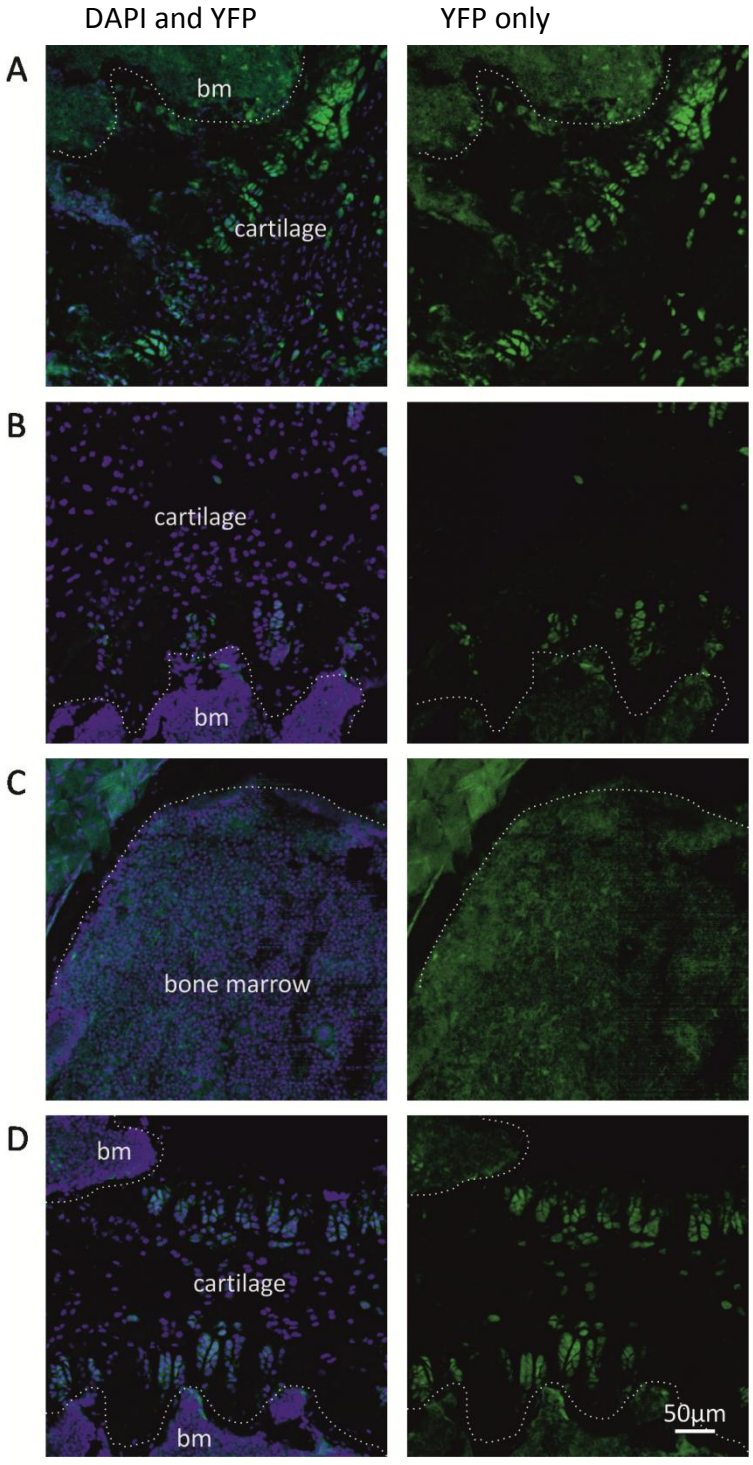

Figure 3.3 Detection of YFP expressing cells in the adult mouse sternum
Representative images of 10 µm sections of snap frozen sternum show YFP expressing cells (green) in regions of bone marrow and cartilage (A-D). Slides were counter stained with DAPI (blue). bm, bone marrow.

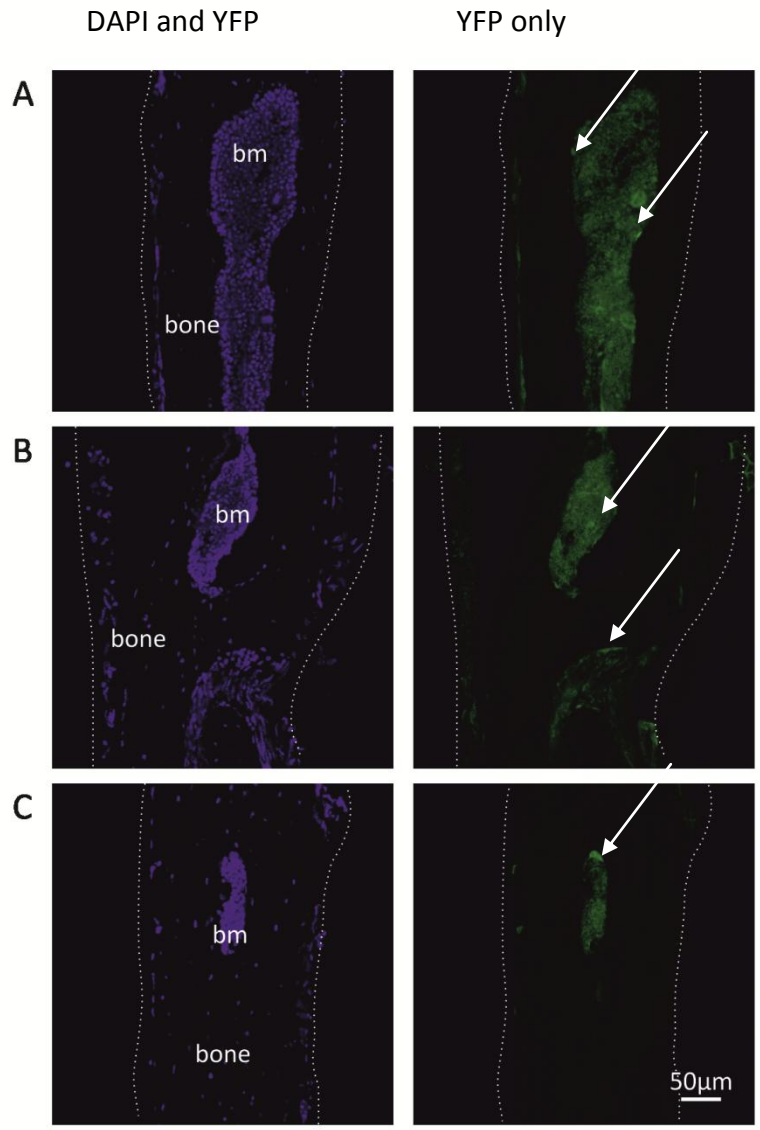

Figure 3.4 Detection of YFP expressing cells in the adult mouse calvaria
Representative images of 10 µm sections of snap frozen calvaria show YFP expressing cells (green) in the bone marrow and periosteum (dotted lines, A-C). Slides were counter stained with DAPI (blue). bm, bone marrow.

HSCs have been reported to be located at the endosteum. If YFP expression demarcates cells involved in the HSC niche we might expect their occurrence to increase within this area. The proportion of approximately 4% of YFP^+ cells increased slightly to between 5% and 6% in the long bones in the 20 μm endosteal region next to the bone, compared to the total area of the bone marrow. Additionally, the cells in this area appeared morphologically different as they were much more elongated than those found in the central marrow and therefore, the endosteum appeared a defined location for the presence of these cells (Figure 3.2, D).

Each of the cell types found to express YFP; stromal cells, chondrocytes and osteocytes arise from the differentiation of MSCs. As YFP expression is inherited, reporter expression allows a level of lineage analysis and indicates the possibility of an IL-7 expressing MSC progenitor that gave rise to these mature cells. The location of some of the remaining YFP expressing cells suggests that they may be also be differentiated cells of mesenchymal lineage, such as those lining the endosteum which could potentially be osteoprogenitors and osteoblasts. Interestingly, YFP was not universally expressed within each cell type identified and therefore if an IL-7 expressing MSC existed, it is likely to only represent a subset of the MSC population that differentiate and contribute to the skeletal lineages. Chondrocytes and osteocytes were identified by their location and histological appearance and approximately 60% of articular chondrocytes and 10% of osteocytes were YFP^+ in femoral sections (Table 3.1). Other cell types such as stromal cells contained in the central marrow could not be identified without further staining but it is probable that there were also YFP^- cells in this fraction.

As bones may develop by the processes of either endochondral or intramembranous ossification, the long bones and the sternum were harvested to represent these processes respectively to assess any difference in YFP appearance. The features of YFP expression and localisation within each bone were common to all adult femurs, tibiae (Figure 3.2) and sterna (Figure 3.3) analysed as YFP was

detected in chondrocytes, osteocytes and in marrow cells. Slight differences in the proportion of each cell type that were YFP^+ was exhibited in bones from different sources. Hypertrophic chondrocytes in the sternum were more frequently YFP^+ than in long bones. 30% of hypertrophic chondrocytes in the sternum were YFP^+ compared to only 14% in the femur and 4% in the tibia were YFP^+. Calvarial bones of the skull were also analysed as an example of bones that form by intramembranous ossification. Calvarial bones displayed a similar proportion of YFP^+ cells in the bone marrow but the distinction of the endosteal region was difficult as the thin width of the tissue meant this also overlapped with the central marrow (Figure 3.4).

Cell/Tissue	**Femur**	**Tibia**	**Sternum**	**Calvaria**
Central marrow	3.9	3.9	5.2	3.4
Endosteal region	5.4	6.0	8.5	2.2
Articular chondrocyte	60.0	54.0	11.1	nd
Hypertrophic chondrocyte	13.8	3.6	31.0	6.9
Osteocyte	9.5	22.9	nd	7.6

Table 3.1 Distribution of YFP positive cells in bone
Slides were manually scored for the number of YFP^+ cells per section as a percentage of total nucleated cells as stained by DAPI. nd, not determined. 4-7 sections were scored, n=3 mice. Sections were demarcated into appropriate regions of interest including marrow, chondrocytes or bone and therefore, in excess of 1000 cells may be counted, in the case of bone marrow, or as few as 50 osteophytes in regions of bone.

In order to determine the presence of YFP^+ cells in embryonic tissue, three E17.5 embryos were examined. YFP expression was not as widespread as in the adult tissues. Whole mount staining of 250 µm vibratome sections detected a small number of YFP^+ cells in the foot tissue (Figure 3.5). These cells were clustered together and showed an elongated, stromal like morphology. No YFP positive cells were detected in the sterna of the embryos (Figure 3.5, B).

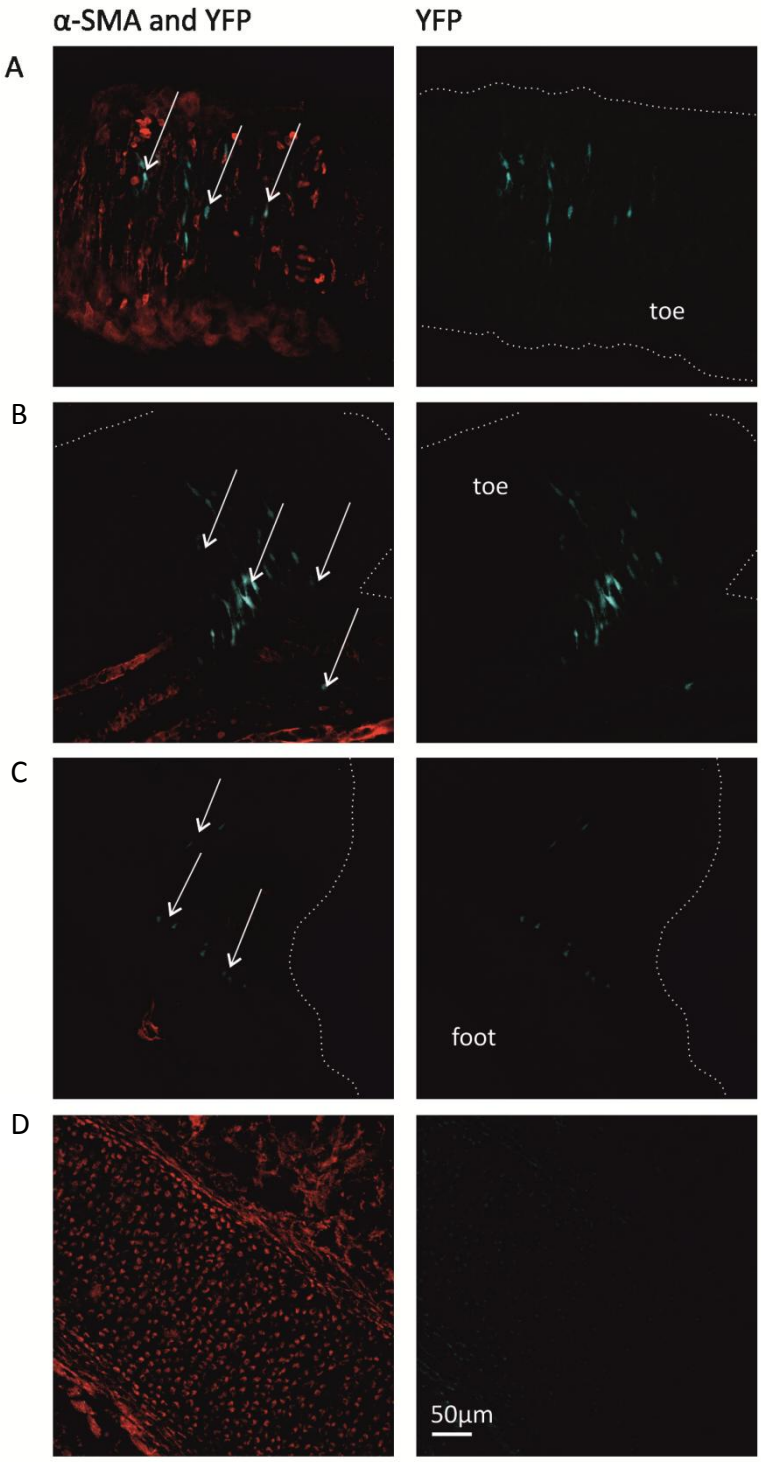

Figure 3.5 YFP expressing cells in embryonic tissue
Representative images of whole mount staining of 250 µm vibratome sections of E17.5 legs (A-C) and sterna (D). YFP expressing cells (turquoise, arrows) were detected in the toes and feet. Slides were stained with α-SMA (red) for visualisation. Dotted lines show tissue edge.

3.3.2 Localisation of YFP$^+$ cells with other niche cells

Femoral sections were further analysed for the presence of CD169 and CD146 in order to assess the relationship of YFP$^+$ cells with other cells that have been proposed as key niche components.

Bone marrow macrophages identified by CD169 expression are reported to have a key role in retaining HSCs in their niche by acting specifically on nestin$^+$ MSCs (Chow et al, 2011; Tormin et al, 2011). Lymph nodes were used as a staining control and CD169$^+$ cells could be clearly detected in the periphery of the nodes (Figure 3.6 A). CD169$^+$ cells were found throughout the bone marrow of IL-7 mice (Figure 3.6 B and C) in a distribution consistent with that reported in the literature. CD169$^+$ cells were not detected at the growth plate or joint areas of the long bones (Figure 3.6 D). In sternal sections, CD169$^+$ cells were also distributed throughout the bone marrow and not at the cartilaginous regions (Figure 3.7). CD169$^+$ cells were often in close proximity to YFP$^+$ cells due to this frequency and localisation. However, no co-localisation with YFP was observed.

It is reported that CD146 is expressed on human MSCs capable of reconstituting the murine HSC niche and are located perivascularly in the bone marrow (Sacchetti et al, 2007). CD146$^+$ cells has not been reported on murine MSCs but is widely expressed on endothelial cells which are considered a component of the HSC niche (Schrage et al, 2008). Therefore, CD146 was examined in IL-7Cre tissue sections. CD146$^+$ cells were detected sporadically in the central bone marrow (Figure 3.8 A-C). Consistent with reports in human bone marrow that CD146 is infrequently detected in cells lining the bone (Tormin et al, 2011), immunostaining presented here also demonstrate CD146 to be localised away from the endosteal region and not detected at the joint interface (Figure 3.8 C). No YFP$^+$ cells were stained with CD146 and although CD146 was initially detected in femoral sections, subsequent staining of additional sections failed to identify any further staining. Further work would be required to confirm the presence of CD146 in bone marrow.

Vascular cell adhesion molecule 1 (VCAM-1) may be found on bone marrow stromal and endothelial cells as well as B cells and macrophages. VCAM-1 has been shown to be expressed on murine nestin^{+} MSCs and is important in HSC maintenance (Mendez-Ferrer et al, 2010). Staining of IL-7 bone sections detected VCAM-1^{+} cells throughout the bone marrow, predominantly in the central marrow with fewer cells towards the diaphysis. VCAM-1^{+} was not expressed in chondrocytes. An average of 56% of the central marrow YFP^{+} cells also expressed VCAM-1 (Figure 3.9, n=4).

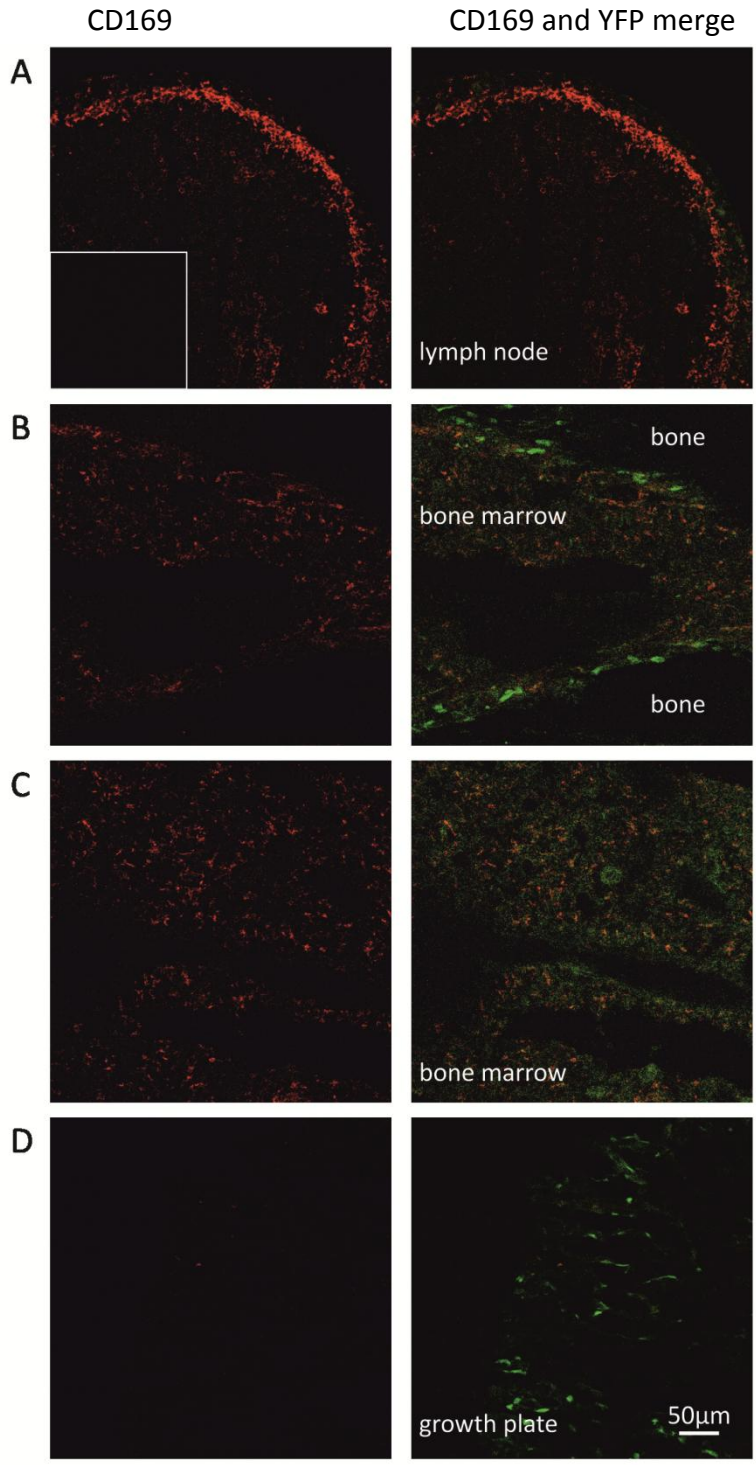

Figure 3.6 YFP expressing cells are in close proximity to CD169$^+$ cells
Lymph node (A) sections show expected CD169 distribution as a positive staining control. Inset image is antibody control.
Representative images of 10 µm sections of snap frozen femur show CD169$^+$ cells (red) close to YFP expressing cells (green) in the bone marrow (B-C) but not at the growth plate (D).

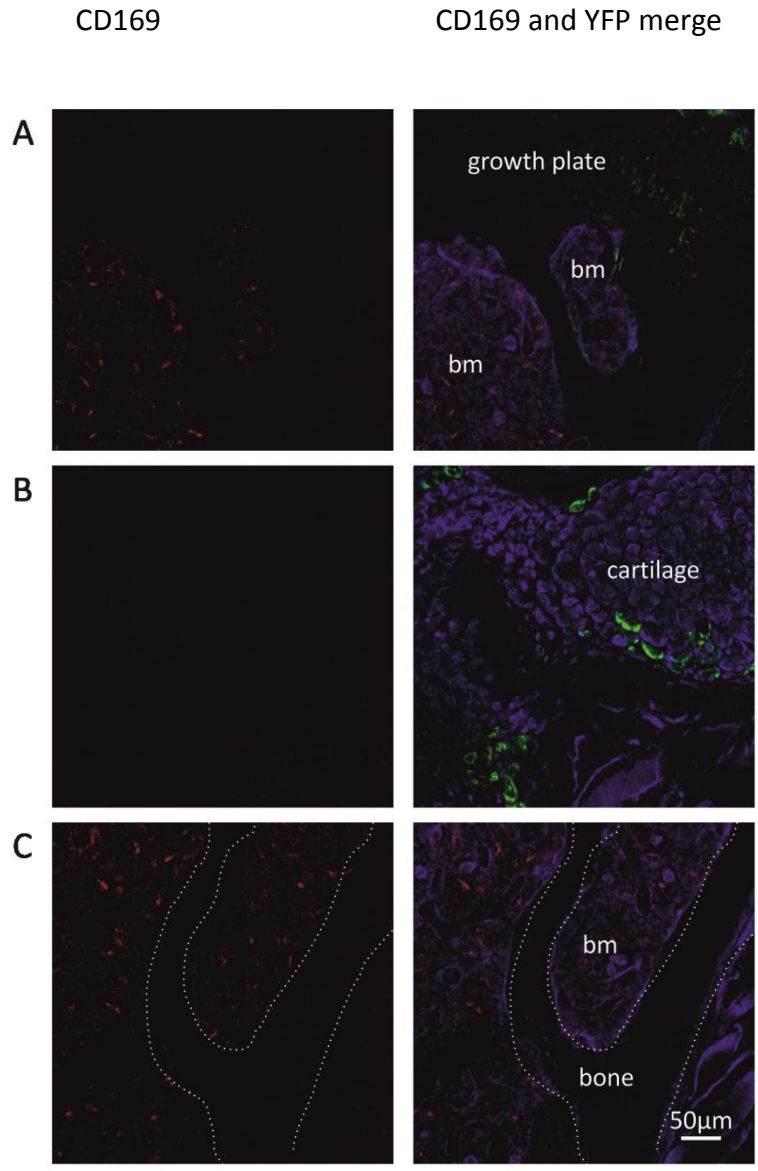

Figure 3.7 YFP expressing cells are close to CD169$^+$ cells in the adult sternum
CD169$^+$ cells (red) were detected close to YFP expressing cells (green) in the bone marrow (A, C) but not at the growth plate or cartilage (A, B) in adult sternum sections. bm, bone marrow.

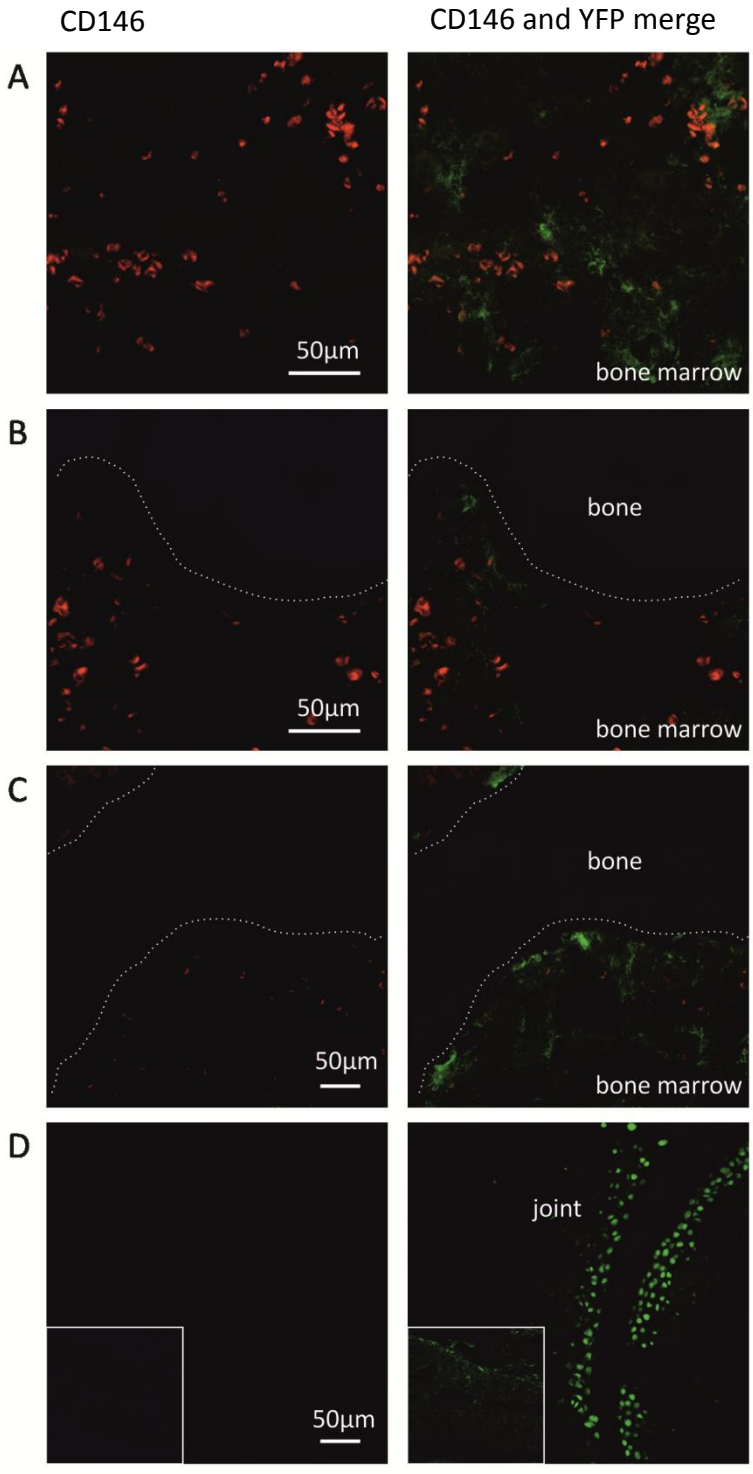

Figure 3.8 CD146$^+$ cells do not co-localise with YFP expressing cells
CD146$^+$ cells (red) were detected within the bone marrow of adult mouse femurs (A-C) but not at the joints (D). No co-localisation of CD146 with YFP expressing cells was detected.

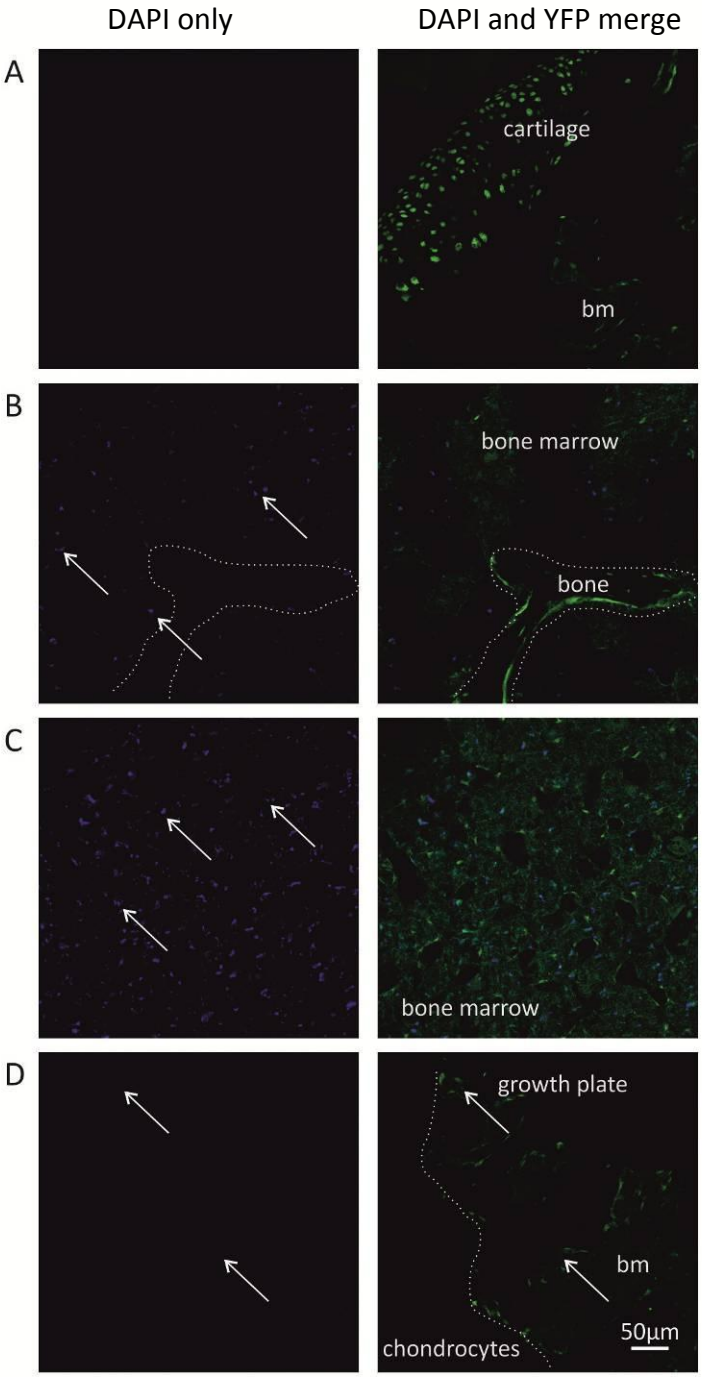

Figure 3.9 VCAM-1 detection on YFP expressing cells
YFP expressing cells (green) within the bone marrow also express VCAM-1 (blue, arrows). VCAM-1 was detected in the bone marrow (B-D) but not in areas of cartilage (A) or bone (B). bm, bone marrow.

3.3.3 Localisation of nestin

The distribution of YFP^+ cells observed in this study is strikingly similar to that of differentiated cells derived from $nestin^+$ MSCs described by Mendez-Ferrer *et al.* (2010). They identified $nestin^+$ MSCs to be essential haematopoietic stem cell niche constituents in the bone marrow. $Nestin^+$ MSCs were located near to HSCs *in vivo* and their depletion led to a reduction in number and activity of HSCs in the bone marrow. Due to the Cre recombinase YFP mechanism in the IL-7 mice, it is possible that the cells expressing YFP in our mouse model are doing so because they are descended from a common progenitor that expressed IL-7 and that these original $IL\text{-}7^+$ cells are MSCs. If so, they may represent the same population of MSCs identified by nestin expression or a discrete MSC sub-population. Therefore, nestin staining was performed on IL-7Cre Rosa26-eYFP sections to determine if a subset of YFP cells would also express nestin. Nestin was in fact only found in one set of sections from one mouse and staining did not co-localise with YFP. Nestin expression was found in femoral and calvarial sections (Figure 3.10 D and B). Nestin was not detected in regions of cartilage or those densely populated with chondrocytes. No other mice (n=4) showed nestin expression in the bone marrow. Mouse brain was used as a positive control and nestin staining was detected (Figure 3.10 A). Whilst nestin may be a marker for MSCs and could be detected in IL-7 mouse tissue it was not detected at a similar frequency to that reported in the literature or in a distribution pattern that may be expected of bone marrow MSCs. This may be due to the sensitivity of methods of detection in comparing immunostaining to a reporter mouse line where GFP expression was under the regulatory elements of the nestin promoter.

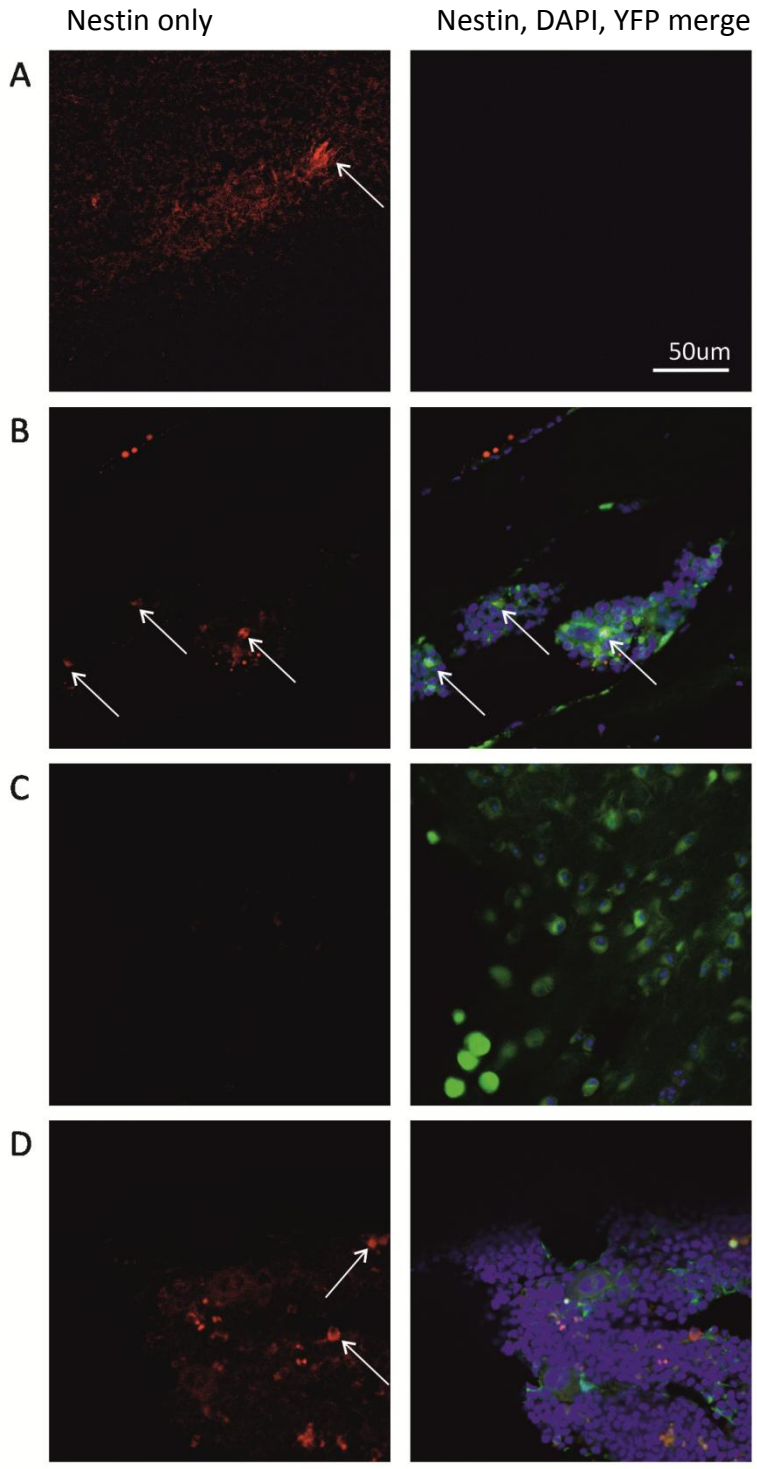

Figure 3.10 Nestin expression in adult mouse tissue
Nestin (red) expression was detected in adult mouse brain sections (A) and sporadically in bone marrow of calvaria (B) femurs (D). Co-localisation with YFP expressing cells (green) and detection in cartilaginous areas (C) was not detected.

3.3.4 Isolation of YFP expressing cells

There is still a lack of clarity about the location of the HSC niche. Controversy surrounds the distinction of endosteal and vascular sites as separate niches but immunohistology has located HSCs in both regions (Kiel et al, 2005). In accordance with this, the supportive cellular components of the niche are presumed to be in close physical contact with the HSCs. Analyses of serial bone marrow flushes and enyzymatically digested bone have supported the suggestion of an endosteal niche, as HSCs with higher differentiation potential have been identified nearest the bone (Haylock et al, 2007). Human studies have also reported an improved extraction of MSCs using collagenase digestion of femoral heads (Jones et al, 2010). In order to assess the distribution and potential of YFP positive cells in the long bones, cells flushed from the bone marrow were compared to cells isolated from crushed and digested bones that have already been flushed of their bone marrow. In order to compare the populations, cells were sorted on the basis of YFP expression by MACS flow cytometry. Cells were also sorted for YFP expression either immediately after extraction or after a period of *in vitro* culture.

FACS data for CD45 and YFP expression was gated based on forward scatter and side scatter properties to select for live cells. There were clear populations that were CD45 positive, and those that were CD45 negative could be segregated into YFP positive and negative samples that were subsequently collected. There were a small proportion of cells that appeared $CD45^+$ YFP^+ but these were not collected as the focus was on identifying stromal cells, known to be negative for CD45 (Figure 3.12, A).

In this way, cell sorting identified YFP^+ cells that represented approximately 1% of the CD45 negative population of bone marrow and a slightly higher (1.25%) proportion was found in bone digest cells harvested from the same mice. YFP^+ cells were not detected in control mice (Figure 3.11). The actual number of YFP^+ resident cells may be higher, as some could be lost through the process of extraction, especially of the bone digest which requires numerous steps and effective enzyme

digestion. Histological analysis had identified approximately 4% of total bone marrow cells to be YFP positive but did not take into account CD45 expression (Table 3.1). Of the cells that had been cultured, for an average 13 days, before sorting, an average of 0.4% ± 0.44% YFP^+ cells that were $CD45^-$ were recovered from the bone marrow (n=7 sorts). This indicates that the YFP^+ cells persist in culture for over 4 weeks. However, the smaller proportion of YFP^+ cells may indicate a loss of some of the YFP^+ cells in culture over time and/or a preferential outgrowth of those that are YFP^-. There was no remarkable decline seen over time between 7 different sorts and therefore alternative factors such as cell density, cell proliferation and paracrine and autocrine signalling mechanisms may play a part in regulating YFP expression and YFP^+ cell survival *in vitro*. In comparison, bone digest cells that had been cultured yielded an average of 1.15% ± 1.49% YFP^+ cells (n=5 sorts) when sorted which was similar to those from the fresh tissue (Figure 3.12, B). This suggests that the YFP^+ cells from bone regions are more stable in culture than those from the bone marrow. Similar to the cultured cells from bone marrow, there was no trend in YFP expression and time spent in culture in bone digest cells (Figure 3.12, B).

The number of $CD45^-$ YFP^- cells that were recovered from cells immediately sorted after extraction was approximately one third of the number of $CD45^-$ YFP^+ cells from both fresh bone and bone marrow. In cultured cells, this population increased and was generally at least twice the number of YFP^+ cells in either bone or bone marrow samples. YFP^- cells from the bone marrow had an average (n=5 sorts) of 1.6% ± 2.1% and in the bone the YFP^- cells were 7.5% ± 10.7% of the total cell number after a maximum of 30 days in culture.

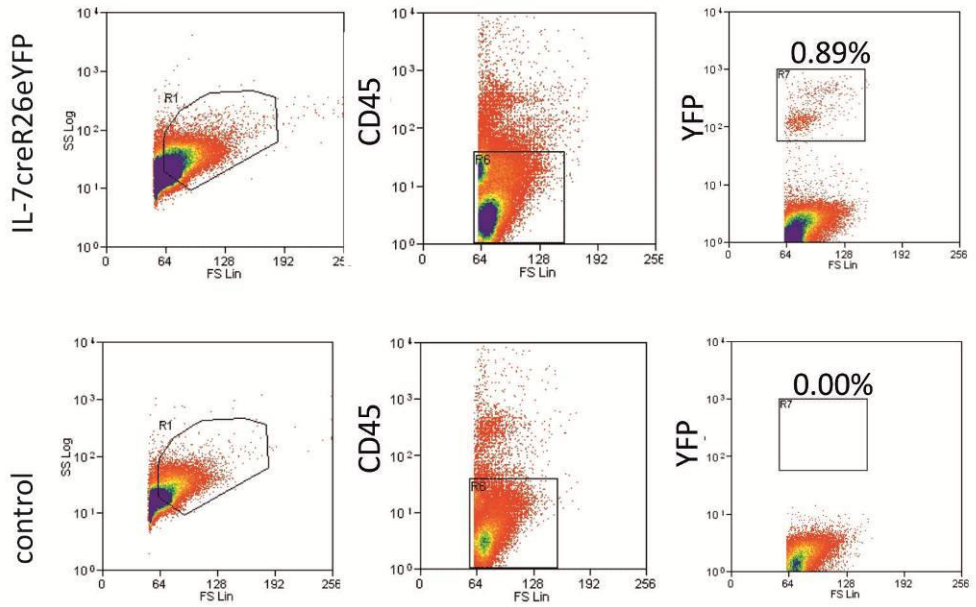

Figure 3.11 Detection of YFP$^+$ cells by flow cytometry
Cells were harvested from the bone marrow of IL-7Cre Rosa26-eYFP mice and the CD45$^+$ population depleted by MACs. The remaining cells were then stained with biotin labelled CD45 and then with pacific blue conjugated streptavidin secondary antibody and analysed by flow cytometry for YFP expression.
YFP$^+$ cells could be detected in the IL-7Cre Rosa26-eYFP samples but were not found in control mice.

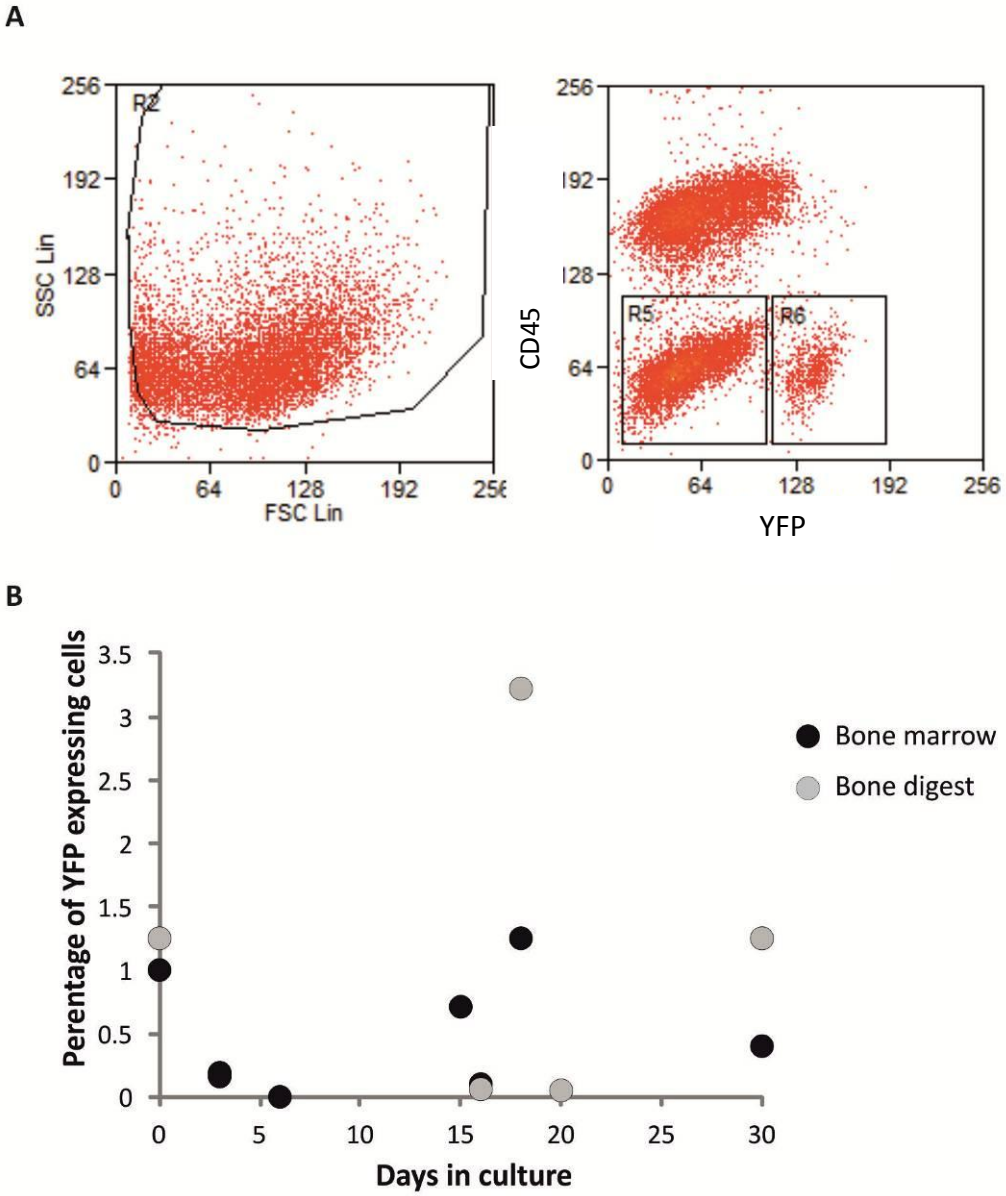

Figure 3.12 MoFlo sorting of YFP positive cells

Cells were harvested from mouse bones and incubated with APC conjugated CD45 antibody. They were then isolated using a MoFlo cell sorter and those cells that were CD45 negative and either YFP positive (gate R6) or negative (gate R5) were collected separately. Gating is shown in A. R2 determines the events that were collected based on size properties that excluded debris. Cells were sorted fresh or alternatively after being cultured for up to 30 days. The graph indicates the percentage of CD45 negative cells that were YFP^+ in each extraction. Each point represents an independent sort from an average of 7 mice per sort. The bone digest sorts correspond to the bone marrow at each time point (B).

3.3.5 Characterisation of YFP expressing cells

Cells harvested from the IL-7Cre Rosa26-eYFP bone marrow were analysed by flow cytometry to determine the expression of common stromal cell markers and further characterise the cells that expressed YFP. Cells were initially sorted to be $CD45^-$ (to exclude haematopoietic cells) and YFP^+ expressing cells were collected. These cells were found to widely express VCAM-1 and gp38. CD90 and ICAM-1 were barely detectable and a mixed population of CD105 expressing cells were observed (Figure 3.13).

RNA was extracted from mouse bone marrow $CD45^-$ cells that had been sorted for YFP expression and real time PCR performed to assess the expression of nestin and IL-7. YFP expressing cells showed 50% greater expression of IL-7 mRNA and a 30% greater expression of nestin mRNA as compared to samples extracted from those cells that were YFP^- (Figure 3.14). If IL-7 were purely a marker of a progenitor cell that gave rise to the mature cells in the bone marrow then it would be expected that the IL-7 levels would be the same between cells, regardless of their YFP expression. As an increased expression of IL-7 is observed, it is likely that, at the time of isolation, some of the YFP^+ cells expressed IL-7. As the isolated cells were a heterogeneous population, it is also possible that a progenitor population and even MSCs were enriched in the YFP expressing cell set. This is supported by the observed increase in nestin expression, which is reportedly expressed on a range of stem cells, in the YFP^+ cells compared to the YFP^- cells.

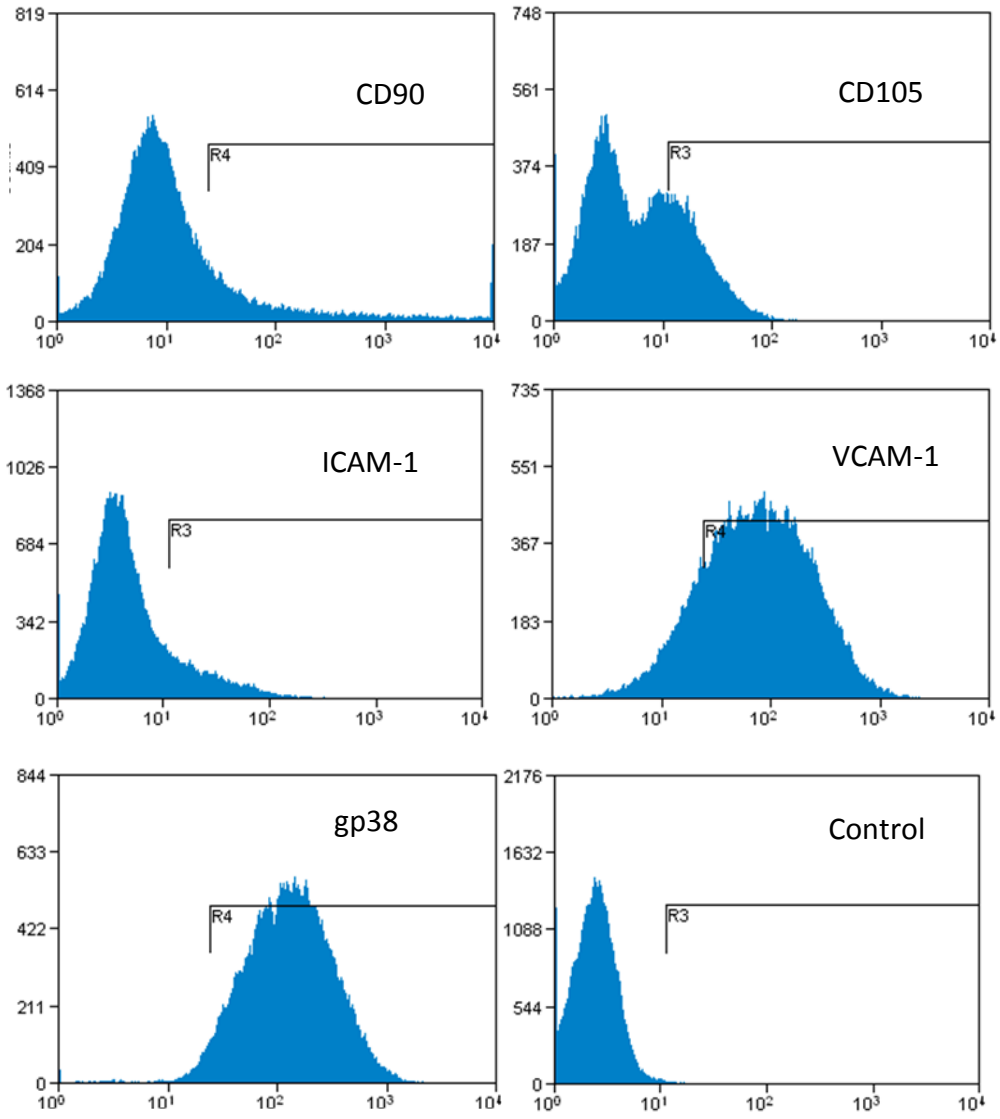

Figure 3.13 Cell surface markers expressed by YFP$^+$ cells
Murine bone marrow cells were isolated using MACS flow cytometry and the cells were sorted depending on their expression of CD45 and YFP. CD45$^-$ YFP$^+$ cells were further stained with stromal cell markers and analysed by flow cytometry. R3 and R4 determine the regions of positive marker expression compared to an unstained cell control.

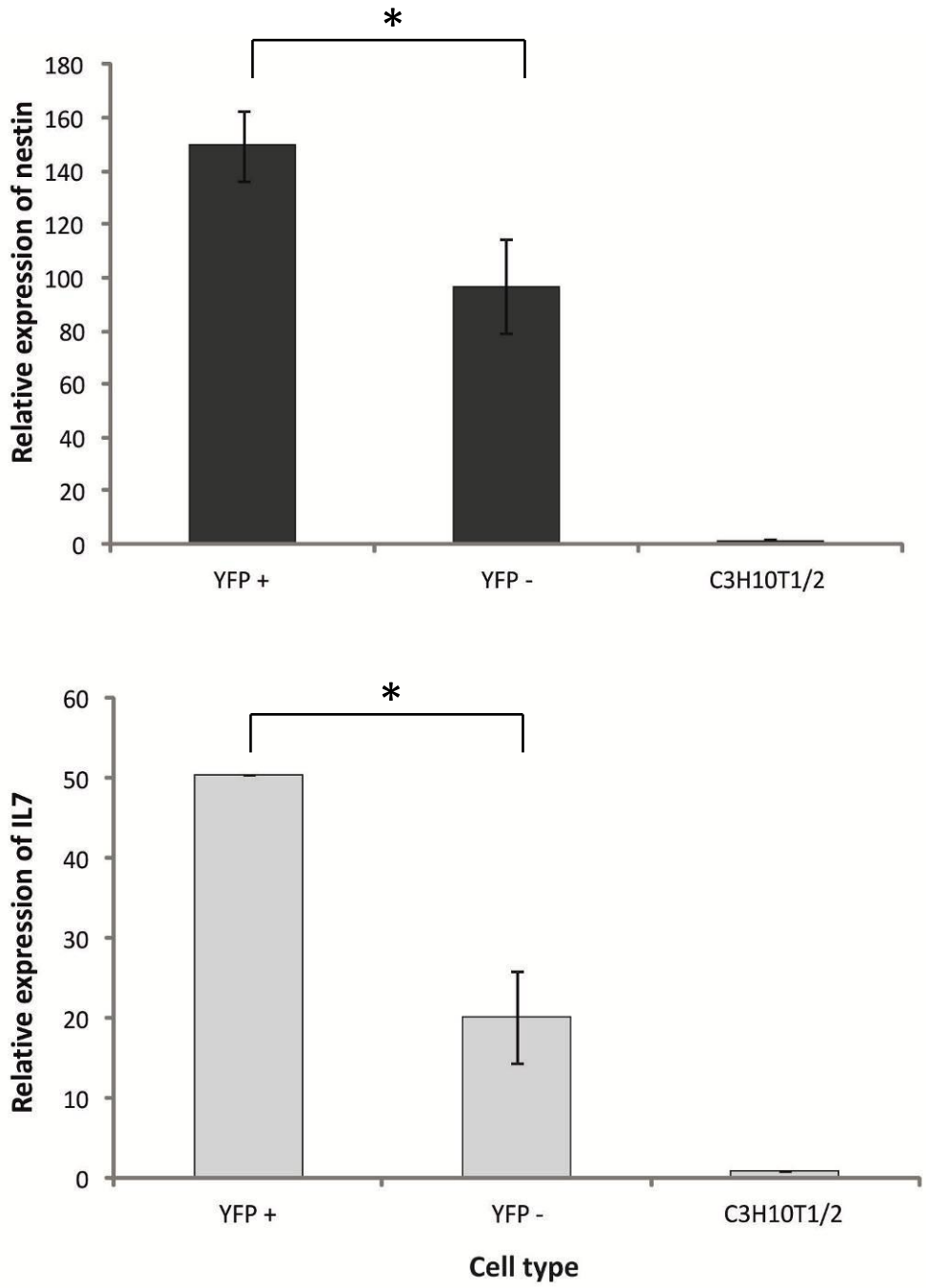

Figure 3.14 qRT-PCR analysis of nestin and IL-7 in bone marrow cells
IL-7Cre Rosa26-eYFP bone marrow cells were sorted with flow cytometry (MoFlo) into populations that were $CD45^-$ and either YFP^- or YFP^+. Extracted RNA from each population was subsequently analysed for nestin (top) and IL-7 (bottom) gene expression and presented relative to murine cell line C3H10T1/2. * indicates $p < 0.05$ determined by t-test.

3.4 Summary

While knockout studies have shown that IL-7 has a functional role in the regulation of T and B cell development in the bone marrow, little is known about the identity of stromal cells in the bone marrow that express IL-7. IL-7 is also involved in the mechanism of bone remodelling and negatively regulates bone formation, particularly in the context of oestrogen deficiency. Understanding the cells responsible for the contribution of IL-7 and their origin will therefore allow a greater understanding of the bone remodelling process and its interactions with T and B cell development. Using a transgenic mouse line (IL-7Cre Rosa26-eYFP) in which cells that have previously, or are currently expressing IL-7 are indelibly marked with YFP, the fate of IL-7 expressing cells was examined in the bone marrow to explore the hypothesis that IL-7 could identify MSCs. As IL-7 expression may be transient within stromal populations, this method of cell tracking allows the capture of a wider population of cells that contribute to the IL-7 expression in bone marrow. YFP expression was demonstrated in osteocytes within the bone, cells at the endosteum and cells associated with blood vessels. Whilst osteoblasts and perivascular cells have individually been proposed as IL-7 expressing cells in the literature, this study is able to consider the lineage relationship of these cells collectively.

The results in this chapter indicate that mesenchymal cell types express YFP and that potentially, an IL-7-expressing common progenitor was responsible for the differentiation of the YFP positive cells. As MSCs are a multipotent stem cell capable of giving rise to each of these cell types, they are strongly implicated as this precursor. Importantly, not all of the cells in a given population were YFP positive, suggesting that if IL-7 is indeed expressed on MSCs that have subsequently differentiated in the bone marrow, it is only expressed on a subset of them. These results will be discussed in more detail in chapter 6.

4 An *in vitro* murine model of the HSC niche

4.1 Introduction

Haematopoietic stem cell fate is believed to be regulated by the specialised microenvironment or 'niche' in which they reside. The niche comprises cellular components, secreted signalling molecules and chemical gradients that promote the retention of the stem cells, maintains them in an undifferentiated state and enables their transient differentiation when required in order to preserve long term stem cell function (Scadden, 2006).

HSCs are found in adult bone marrow and have been well characterised but the cells constituting their niche and their regulation of HSC fate are still not fully understood. The cellular fraction of the niche includes HSCs, MSCs, progenitor cells, osteoblasts, endothelial cells, adipocytes and CXCL12-abundant reticular (CAR) cells (For reviews see Lo Celso & Scadden, 2011; Mercier et al, 2012). MSCs indirectly control HSCs by supplying a range of mature cells that are constituents of the HSC niche. Nestin^{+} murine MSCs have been reported to have a direct effect on HSC function *in vivo*. Stromal cells expressing GFP under the control of nestin regulatory elements were identified in murine bone marrow. Further characterisation identified them as MSCs and depletion studies confirmed their requirement for homing and survival of HSCs (Mendez-Ferrer et al, 2010).

Complex communication between each of the cell components is orchestrated via multiple signalling pathways that are important in the regulation of the HSC niche including notch, Wnt and TGFβ (Reviewed by Chotinantakul & Leeanansaksiri, 2012). The involvement of IL-7 in this signalling network is less well understood but it is certainly implicated in the differentiation process of HSCs. B-lymphopoiesis occurs in the adult bone marrow in distinct niches depending on the differentiation stage of the B cells and is dependent on IL-7 (Parrish et al, 2009). IL-7 expressing cells are reportedly present in niches of the more proliferating stage of B cell development (Tokoyoda et al, 2004). Another study showed that mature osteoblasts that were stimulated with PTH, secreted IL-7 which led to B cell

differentiation of HSCs when co-cultured *in vitro* (Zhu et al, 2007). They also determined that cell contact between the osteoblasts and HSCs was required for initiation of lymphopoiesis and that VCAM-1 was implicated in the process, as its inhibition reduced the numbers of B lymphocytes produced in culture (Zhu et al, 2007). Reports using BAC transgenic mice have described IL-7 expressing cells concentrated around vascular networks in the bone marrow (Mazzucchelli et al, 2009) which was also observed in bone sections from IL-7CreRosa26-eYFP mice (examined in Chapter 3). Additionally, IL-7 reporter cells were located at the endosteum. IL-7 has an overall negative effect on bone and may therefore have a role in the physical modulation of the HSC niche.

Studies of IL-7 and its role in B cell development in the bone marrow niches *in vitro* predominantly use 2D cultures of cells, however, cellular morphology, proliferation and gene expression is markedly changed in cells cultured in a 3D environment compared to 2D, which may be explained by the altered mechanical forces and greater cell contact that are imposed in a 3D structure (Birgersdotter et al, 2005). Bone marrow is a complex structure and as such the niche is described as a 3D environment, therefore, the culture of MSCs in 3D may be more representative of their *in vivo* counterparts. Numerous methods to enable 3D interactions have been developed to study the niche *in vitro*. Cellular spheroids are widely employed and can be formed in a number of ways: by culturing cells in rotating vessels to form aggregates (Frith et al, 2010); by a hanging drop method originally employed to study embryoid bodies (Banerjee & Bhonde, 2006) and by centrifugal force in plates, as well as various techniques to prevent adherence to tissue culture plastic. An alternative technique is to provide a biologically relevant scaffold, which allows the inclusion of ECM components or bone-like tissue.

4.2 Aims

IL-7 has reported functions in lymphopoiesis and bone remodelling that occur in anatomically distinct regions of the proposed HSC niche. The experiments in this chapter are designed to build a simple cellular model of MSCs in the HSC niche that imitates the *in vivo* cellular interactions more faithfully than plastic adherent culture to allow the study of IL-7 and nestin in the bone marrow microenvironment.

4.3 Results

4.3.1 A simple model of the MSC niche

C3H10T1/2 cells are a murine multipotent stromal cell line and were used as a model of MSCs due to their functional similarity and ready availability to generate a model of the niche. Using C3H10T1/2 cells allowed a single species model, as the primary HPCs are also isolated from mice. This provided a format to study the proposed murine MSC marker nestin and investigate IL-7 whose expression was alluded to by reporter expression in IL-7Cre transgenic mice.

In order to study cellular interactions, cells were cultured in a 3D spheroid structure that formed spontaneously when cells were seeded in a viscous spheroid media. This method of spheroid production had been previously successful in producing consistent spheroids that were easy to manipulate (Saleh et al, 2012). Each spheroid was cultured individually in 96 well plates to make each one identifiable and accessible with the ability to control the cell number and growth conditions of each spheroid.

C3H10T1/2 cells were initially seeded at four different densities to examine a range of spheroid sizes and cultured for 10 days. 2, 4, 6 and 12 x 10^4 cells were seeded and formed spheroids over 24 hours in culture. In all cases spheroid diameter decreased by approximately 50% by day 7 which then stabilised and was maintained until day 10 (Figures 4.1 and 4.2). The largest of the spheroids maintained a doughnut like appearance throughout the 10 days of culture, as the

cells were predominantly located around the periphery of the structure leaving a less cell dense area in the centre. In contrast, this cellular distribution was altered after 3 days with the smaller spheroids which appeared uniformly arranged after this time. 2 x 10^4 cell spheroids formed aggregates with orbiting cells that remained close to but did not join the main spheroid over the 10 days.

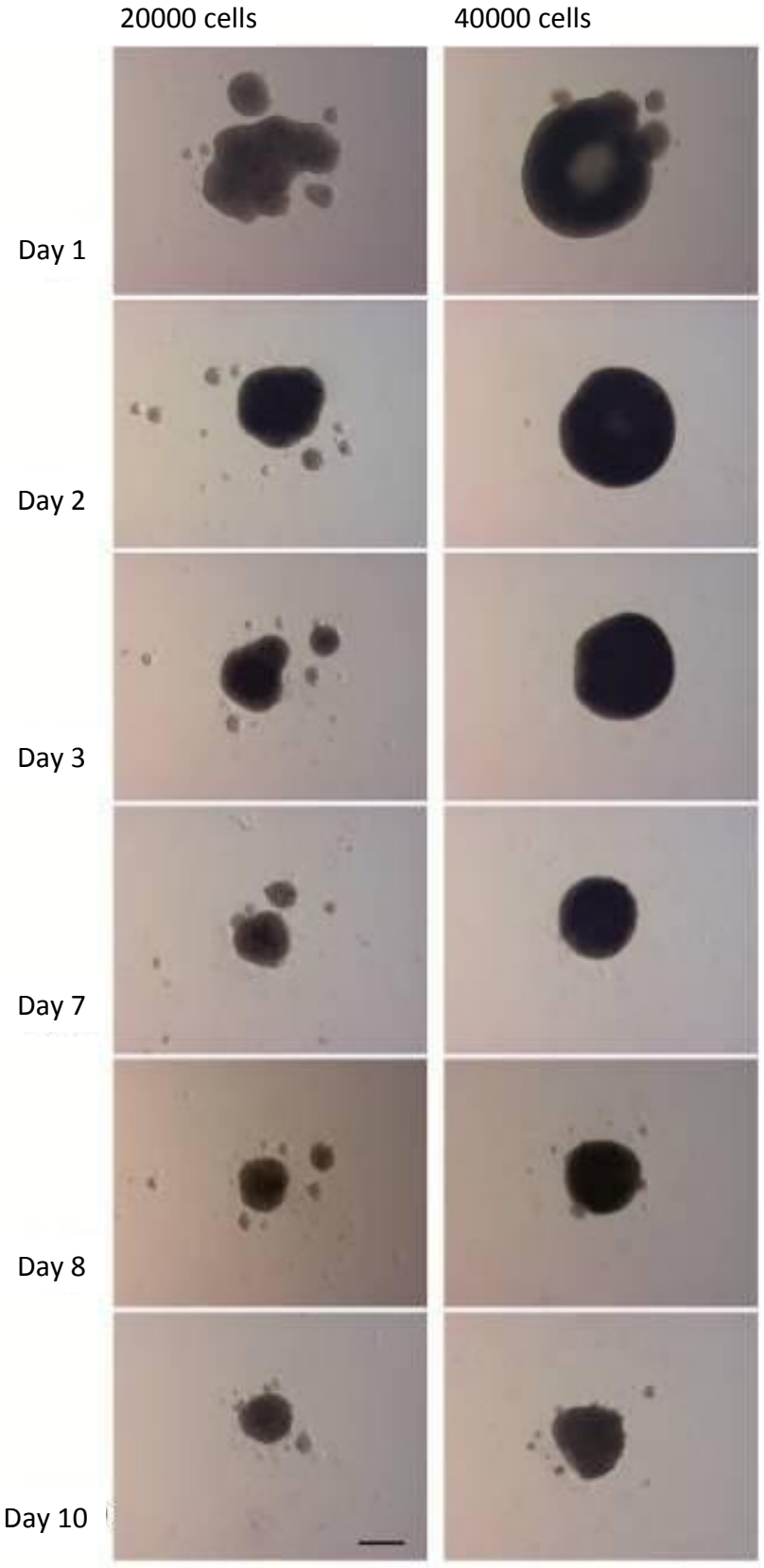

Figure 4.1 Determination of the optimal cell number for a spheroid model
C3H10T1/2 cells were seeded into methyl-cellulose media at 2 x 10^4 and 4 x 10^4 cells per well in 96 well plates. Spheroids formed spontaneously after 24 hours and were cultured for 10 days. Scale bar 200 µm.

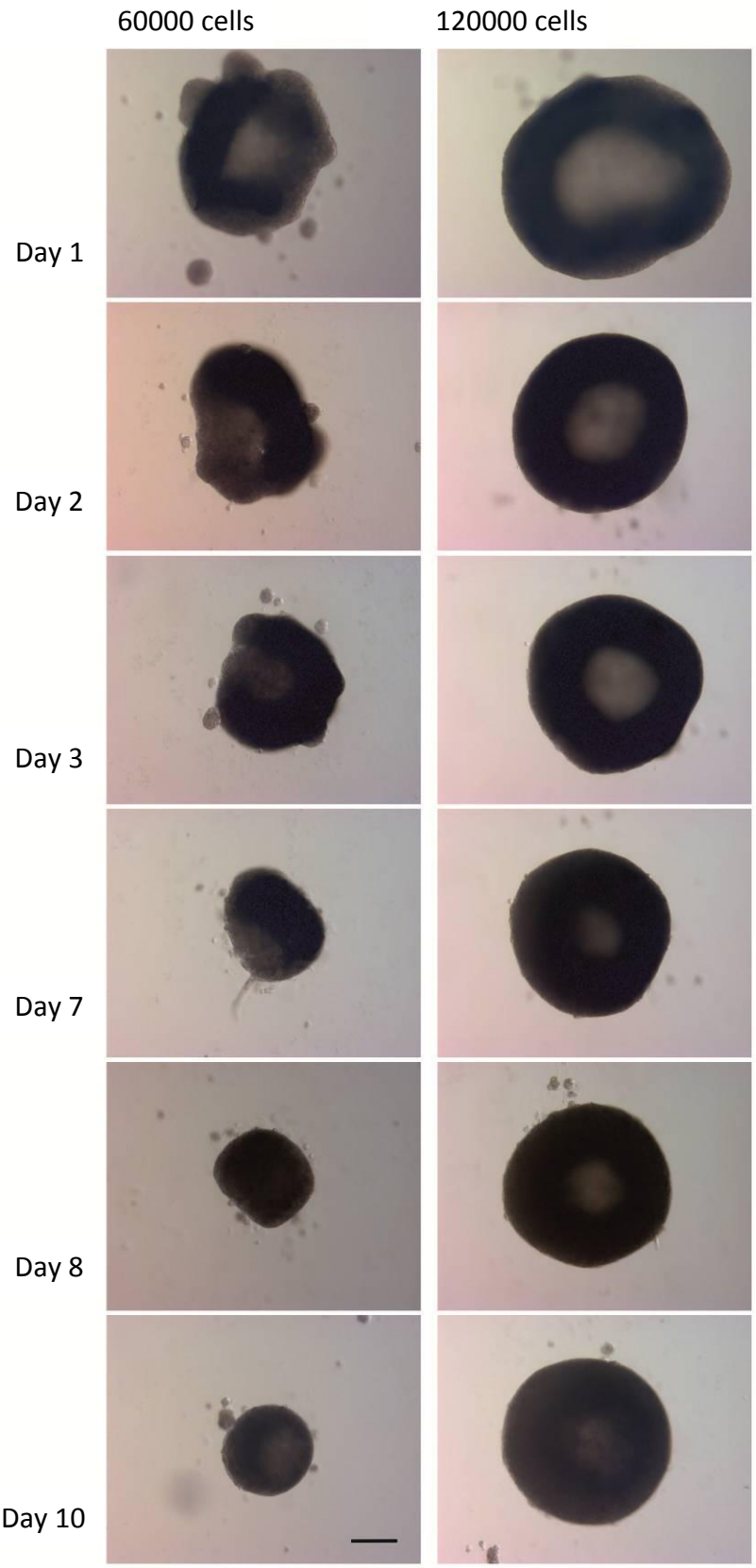

Figure 4.2 Determination of the optimal cell number for a spheroid model
C3H10T1/2 cells were seeded into methyl-cellulose media at 6 x 10^4 and 12 x 10^4 cells per well in 96 well plates. Spheroids formed spontaneously after 24 hours and were cultured for 10 days. Scale bar 200 µm.

Spheroids were snap frozen in liquid nitrogen and sectioned for further analysis. H&E staining showed densely packed cells within the spheroid encased by an outer layer of cells with a more elongated appearance (Figure 4.3, left). Immunofluorescent staining with proliferation marker Ki67 showed an average of 23% positive cells that were distributed throughout the spheroids at day 1. For all time points beyond one day, Ki67 positive cells were restricted to the outer layers of the spheroids and the percentage of positive cells decreased to fewer than 1% (n=3) on day 2 (Figure 4.3, centre), indicating that proliferation was dramatically reduced after only a short period of time in spheroid culture.

As the spheroids decreased in size over time, a LIVE/DEAD assay was performed to determine if cells were simply dying within the spheroids leading to a reduced cell number and decreased spheroid size. Reconstructions of confocal image stacks allowed identification of the cells throughout a deeper proportion of the spheroid than an individual image. Spheroids harvested at days 3, 6 and 8 confirmed the presence of only a small number of dead cells within each size of spheroid, indicating that cell death could not account for the reduction in spheroid size and that cell survival was maintained in this method of culture. The highest proportion of dead cells appeared in the smallest of the spheroids: each of the 2×10^4 spheroids over 8 days and the 4×10^4 spheroids at day 8 (Figure 4.4).

To confirm the ability of C3H10T1/2 spheroids to differentiate, spheroids were cultured in osteogenic, adipogenic or chondrogenic spheroid media for 14 days. Sections of snap-frozen spheroids were stained with von Kossa, Oil Red O and type II collagen that indicated successful osteogenic, adipogenic and chondrogenic differentiation respectively (Figure 4.5). Mineralisation, as determined by von Kossa staining, appeared localised to the central region of the spheroid and was most prominent at day 14. Oil Red O-positive lipid vesicles were distributed throughout the spheroid and showed a large proportion of cells within the spheroid staining positive at day 7 with larger, merged lipid vesicles consistent with more mature adipocytes at day 14. Immunohistochemical staining detected type II collagen at the

periphery of the spheroids at day 7 but expression was more uniformly detected throughout the spheroid at day 14. Little or no staining was detected in spheroids cultured in control medium for each condition indicating a lack of any spontaneous differentiation of MSCs when cultured in 3D.

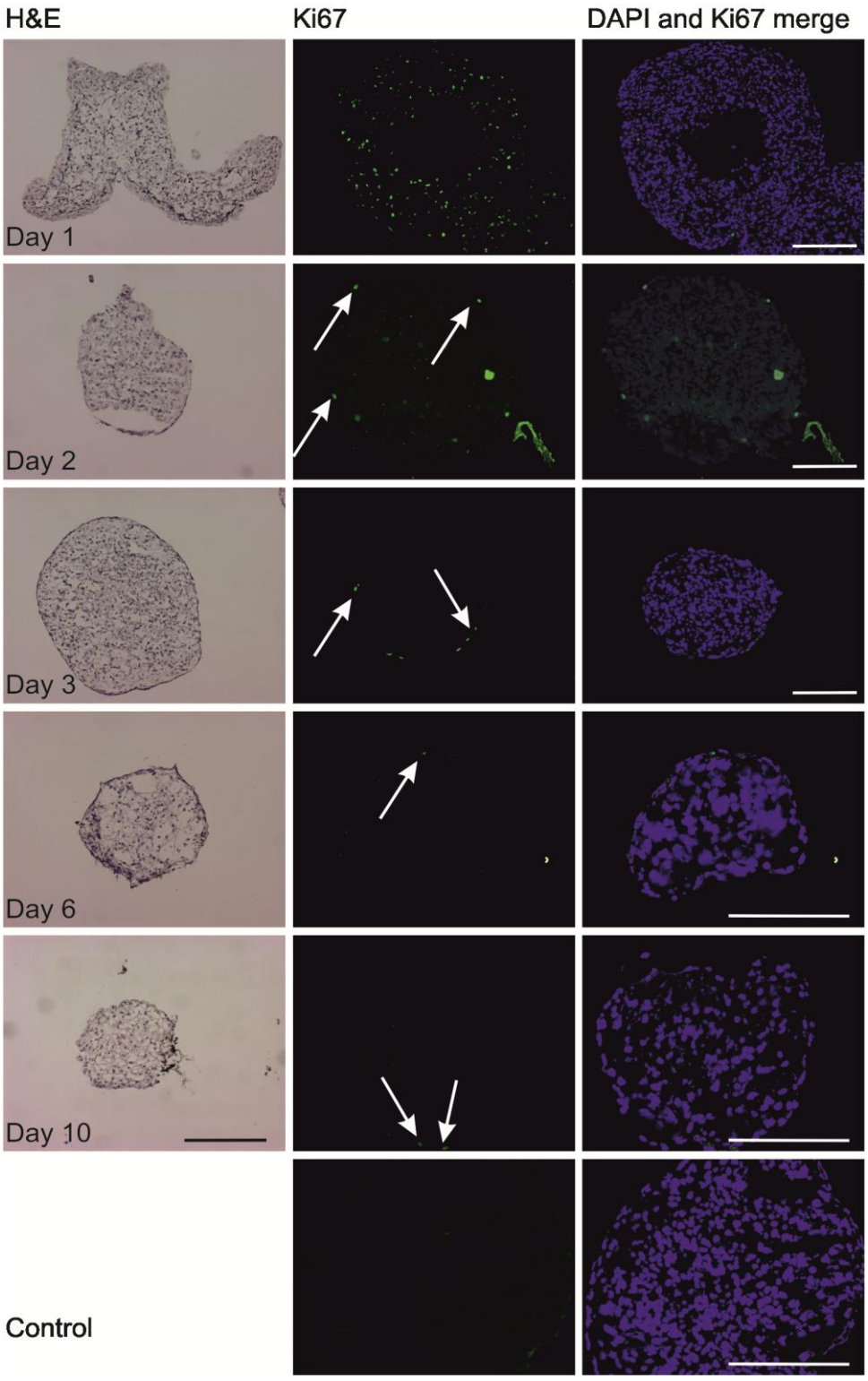

Figure 4.3 Cell proliferation within spheroids
C3H10T1/2 spheroids were snap frozen, sectioned and stained with haematoxylin and eosin (H&E) to visualise morphology (Left). Sections were stained with proliferation marker Ki67 (green, middle) and counter stained with DAPI (blue, right). Scale bars 200 µm.

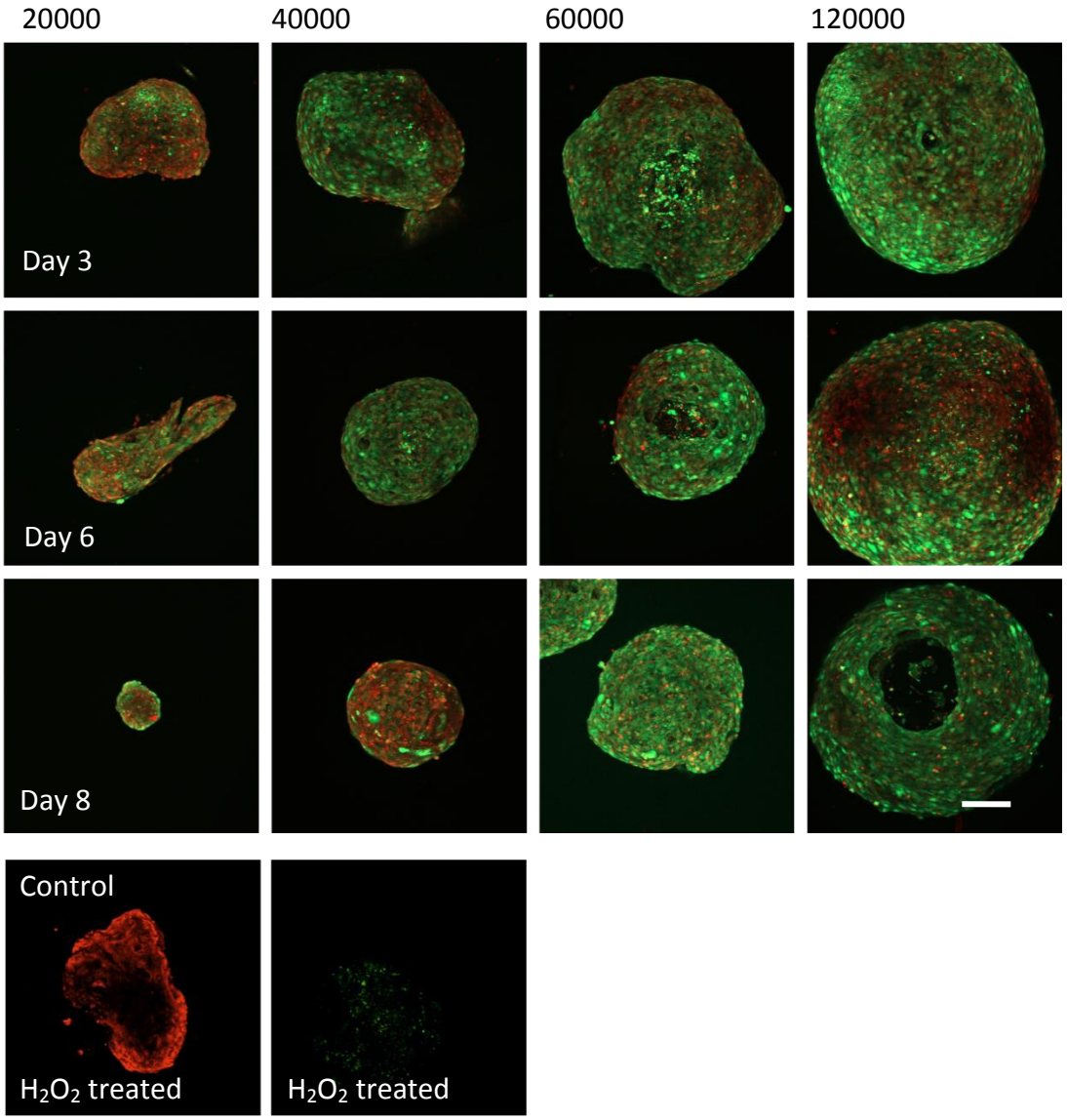

Figure 4.4 Viability of cells within spheroids
C3H10T1/2 spheroids were stained on days 3, 6 and 8 with calcein AM and ethidium homodimer-1 to identify live (green) and dead (red) cells, respectively. Hydrogen peroxide was used to kill cells within the spheroid and confirm specificity of the staining. Whole spheroids were imaged on an LSM 510 confocal microscope (Carl Zeiss). Projections of z-stack images are shown. Scale bar 200 µm.

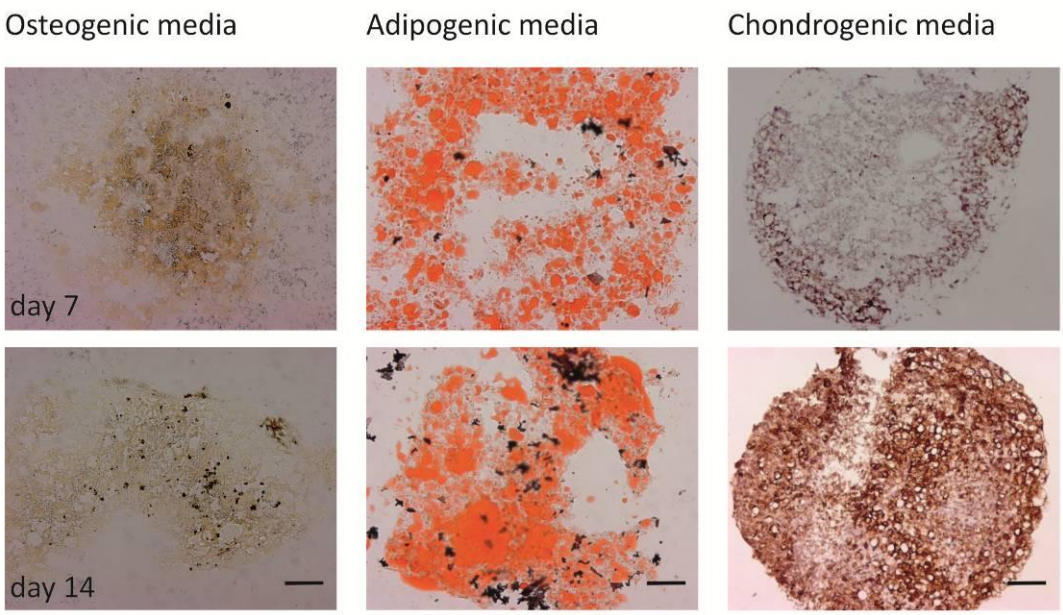

Figure 4.5 Differentiation of C3H10T1/2 spheroids
Spheroids were cultured in methyl-cellulose media containing osteogenic, adipogenic or chondrogenic factors. At days 7 and 14, spheroids were sectioned and stained with von Kossa for mineralisation (brown/black) of osteogenic spheroids, Oil Red O to detect lipid vesicles (red) or type II collagen (dark brown) to confirm chondrogenic differentiation. Scale bars 50 µm.

IL-7 gene expression was determined by real time PCR in spheroids that were differentiated for 7 and 14 days and compared to the respective day 0 control (Figure 4.6). In both osteogenic and adipogenic spheroids, IL-7 was significantly decreased upon differentiation. The reduction was evident at day 7 and was maintained at day 14. 2D monolayers of C3H10T1/2 cells were also induced for adipogenic differentiation and these followed the same pattern of decreased gene and therefore no statistical difference could be detected in IL-7 expression in 2D or 3D adipogenic differentiation. When compared to monolayer cultures at day 0, the spheroid sample had an approximately 30% decrease in IL-7 expression ($p= 0.04$), indicating differences in gene expression between the two methods of culture.

Chondrogenic differentiation in spheroids resulted in an increase in IL-7 at day 7 but was not determined at day 14 due to low quality of sample RNA. This would require repeating to determine the expression at day 14. Chondrogenic differentiation is carried out in serum-free medium, which may be responsible for some of the differences. Large cell pellets rather than monolayer cultures are routinely used for chondrogenic differentiation and were formed here with 5 times the number of cells in each spheroid. Subtle differences between pellet and spheroid culture include formation, as pellets are generated by centrifugal force and maintained in culture medium rather than the viscous spheroid medium that allows spontaneous cell aggregation into spheroids. The increase in IL-7 expression at day 7 in pellets was statistically significant compared to day 7 spheroids and to the day 0 control pellet. At day 14, the IL-7 expression level in the pellets was drastically reduced from the level observed at day 7 to below that even of the day 0 pellet.

4.3.2 Addition of HPCs to the niche model

Selecting a spheroid size of 4×10^4 cells for further study due to their consistent aggregation, stromal cells were cultured with the addition of 10-100% HPCs. HPCs were combined at the initial seeding stage and contributed to the total cell number, which remained at 4×10^4, to include both stromal cells and HPCs. For example, a spheroid with 50% HPCs would contain 2×10^4 C3H10T1/2 cells were used with 2 x

10^4 HPCs. HPCs alone were unable to form spheroids. As HSCs and progenitors are a rare population in the bone marrow they would not necessarily come into contact with each other *in vivo* and may therefore lack the adhesion molecules or integrins required to interact and so to form spheroids.

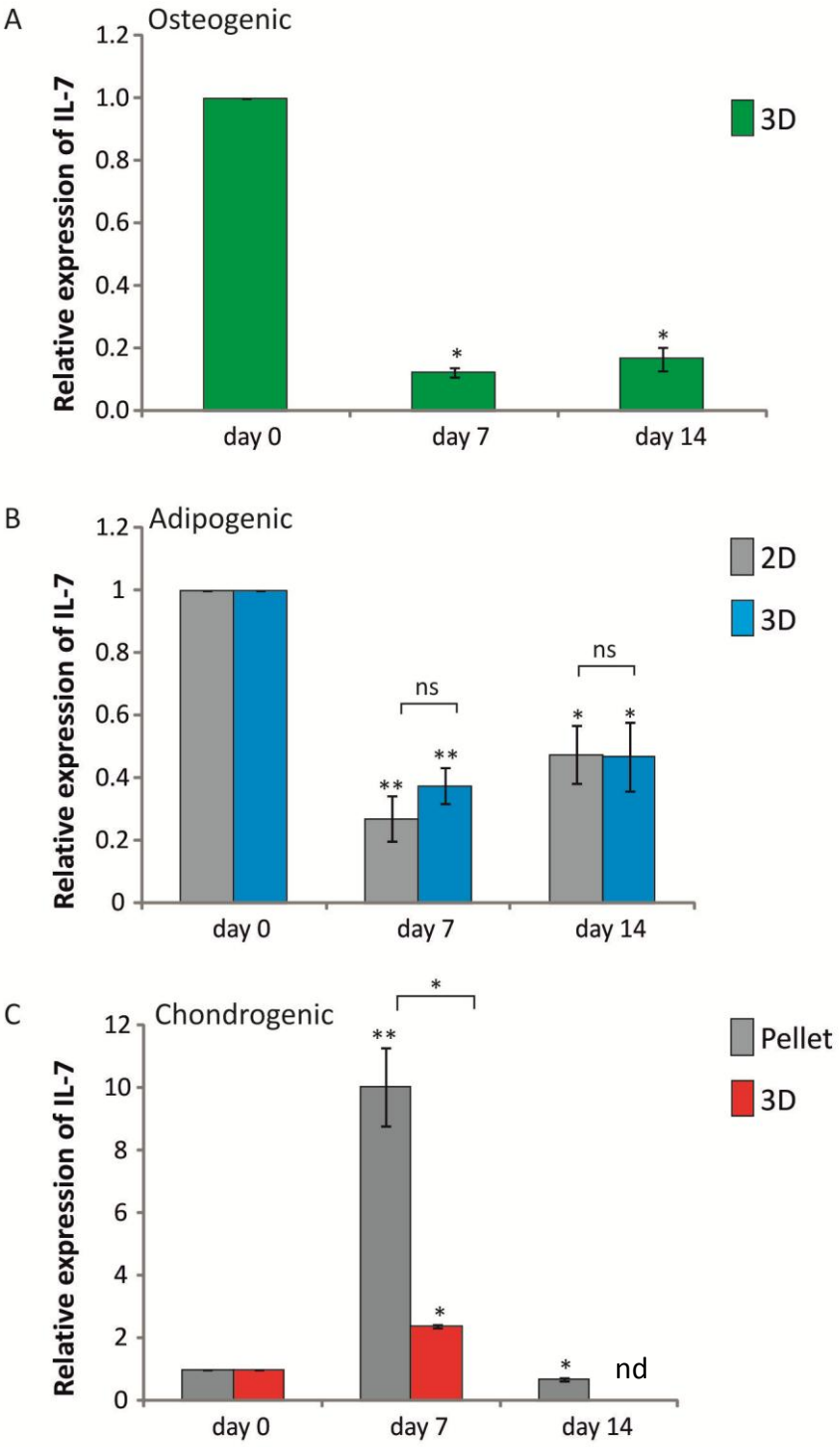

Figure 4.6 Expression of IL-7 during differentiation in 3D

Spheroids and monolayers were induced with osteogenic, adipogenic or chondrogenic media for 14 days. Spheroids were enzymatically digested and RNA extracted to analyse by real time PCR. Expression of IL-7 is shown relative to the appropriate day 0 control. Independent t-test determined statistical significances * p= <0.05. ** p=<0.01. nd, not determined.

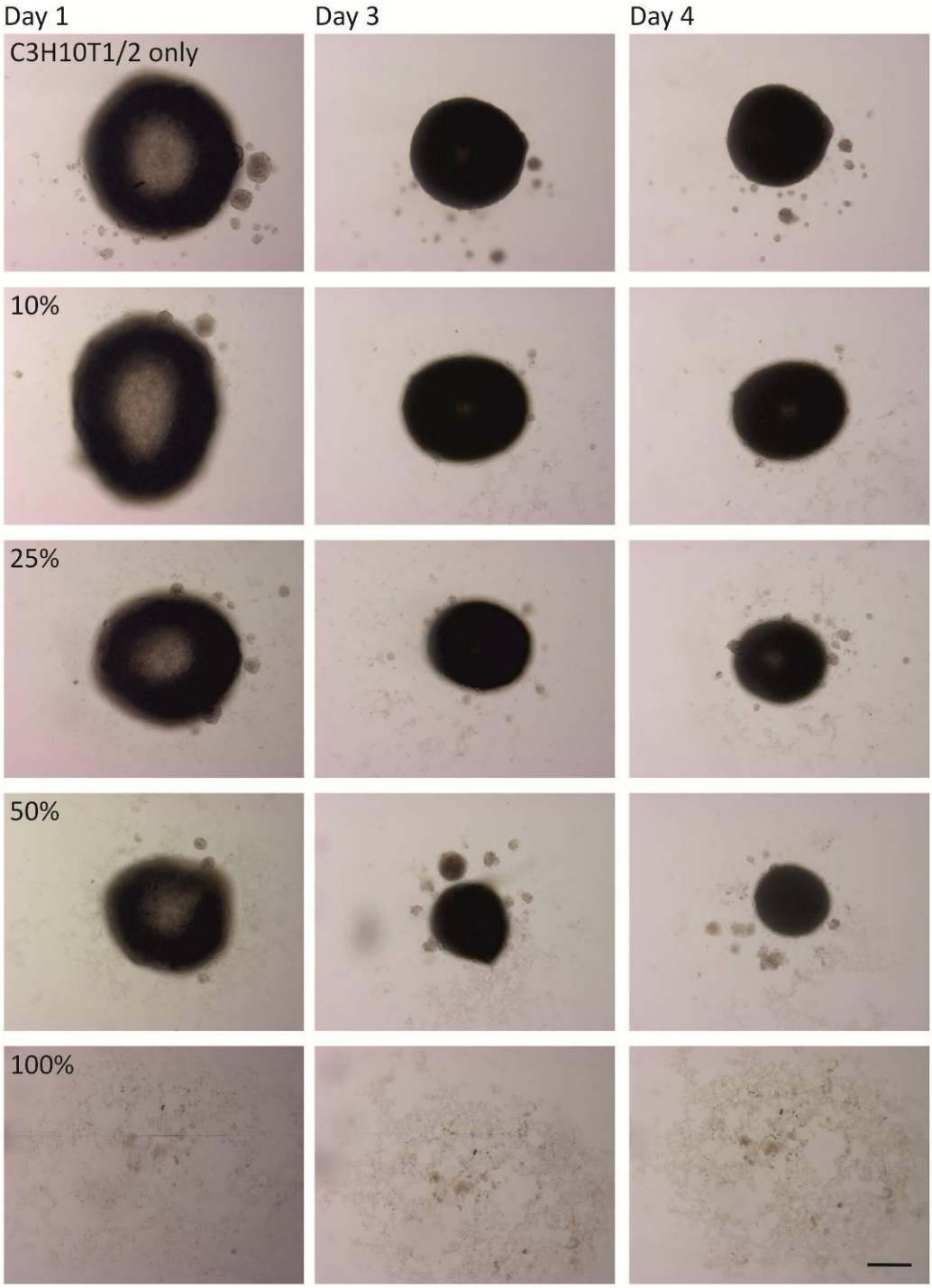

Figure 4.7 Addition of HPCs to the model
Spheroids with a total cell number of 4 x 10^4 were formed with between 10-100% of the total number composed of HPCs (as indicated) mixed with the C3H10T1/2 cells at seeding. Brightfield images are shown from days 1, 3 and 4.
Scale bar 50 µm.

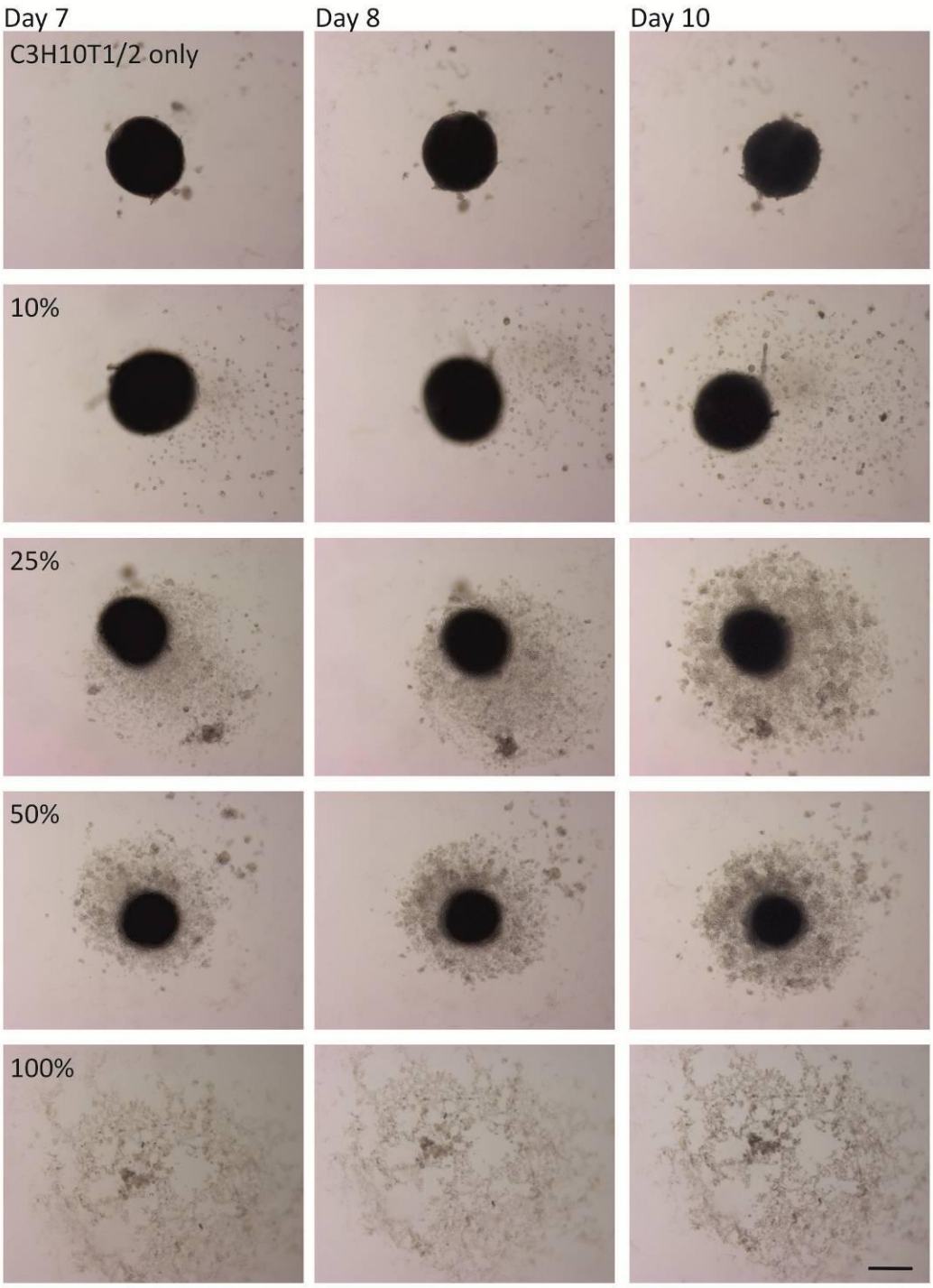

Figure 4.8 Addition of HPCs to the model
Spheroids with a total cell number of 4 x 10^4 cells were formed with between 10-100% HPCs (as indicated) mixed with the C3H10T1/2 cells at seeding. Brightfield images from days 7, 8 and 10 show an increasing outgrowth of cells from those spheroids containing HPCs. HPCs do not form spheroids on their own (bottom images). Scale bar 50 µm.

Owing to the smaller size of the HPCs, the co-culture spheroids were smaller than their stromal-only counterparts, which potentially could alter the microenvironment due to alterations in physical forces and diffusion of factors into the spheroids (Figures 4.7 and 4.8). After spheroid co-culture for 3-5 days, cells began to appear as an outgrowth encircling the main compact spheroid. Although the spheroids did not decrease in size after 7 days of culture, the cells surrounding the spheroids increased in number indicating the proliferation of this population of cells (Figure 4.8). These outgrowth cells were further examined by immunostaining and flow cytometry. After the spheroid was removed from the well, the cells remained adhered to the plastic (Figure 4.9 A) and could be harvested separately by trypsinisation. The cells were cytospun onto slides and stained with H&E which showed a cellular appearance typical of macrophages with bulky vacuolated cytoplasm, attributed to their phagocytic cell type (Figure 4.9 B). The majority of cells also stained positive for the trans-membrane protein F4/80, a marker of mature macrophages (Figure 4.9 C) and for common cell surface markers CD45 and CD11b when assessed by flow cytometry (Figure 4.9 D). Macrophages did not appear around the spheroids containing only stromal cells but were particular to those containing HPCs. Macrophages could have been introduced as a contaminant from the HPC population or, alternatively, differentiated from the HPCs once in spheroid culture. Subsequently, they migrated out of the spheroids and readily proliferated and preferentially adhered to the plate despite the untreated surface and the presence of spheroid media.

The use of CellTracker labelling also suggested that some HPCs exit the spheroids by day 6 after originally being contained within the spheroids (Figure 4.10). HPCs labelled by CellTracker Green were found throughout the C3H10T1/2 spheroid at day 3. A proportion of CellTracker labelled green cells were detected outside of the spheroid at day 6 and were located even further from the main spheroid body by day 8 whilst some still remained in the spheroid. As the C3H10T1/2 cells had originally been labelled with CellTracker Red, some red cells were also found external to the spheroid and were in the periphery of the well and associated with

the HPCs. Both cell types were observed to combine and remain as an intact spheroid after 24 hours, which suggests that the stromal cells and the HPCs exited the spheroid. Exit of the HPCs occurred concurrently with the stromal component of the spheroid. CellTracker Green is inherited in daughter cells; however, the extent of green cells detected in these spheroids does not account for the number of outgrowth macrophages observed surrounding the spheroid. This indicates that the label may be lost over time in highly proliferative macrophages. It also remains to be seen the extent to which the HPCs were able to re-enter the spheroid or whether the movement was unidirectional to determine how mobile these HPCs were in spheroid culture. HPCs are detected in adult peripheral blood and it is therefore plausible that entering and exiting a stromal niche would be achievable for these cells *in vitro*.

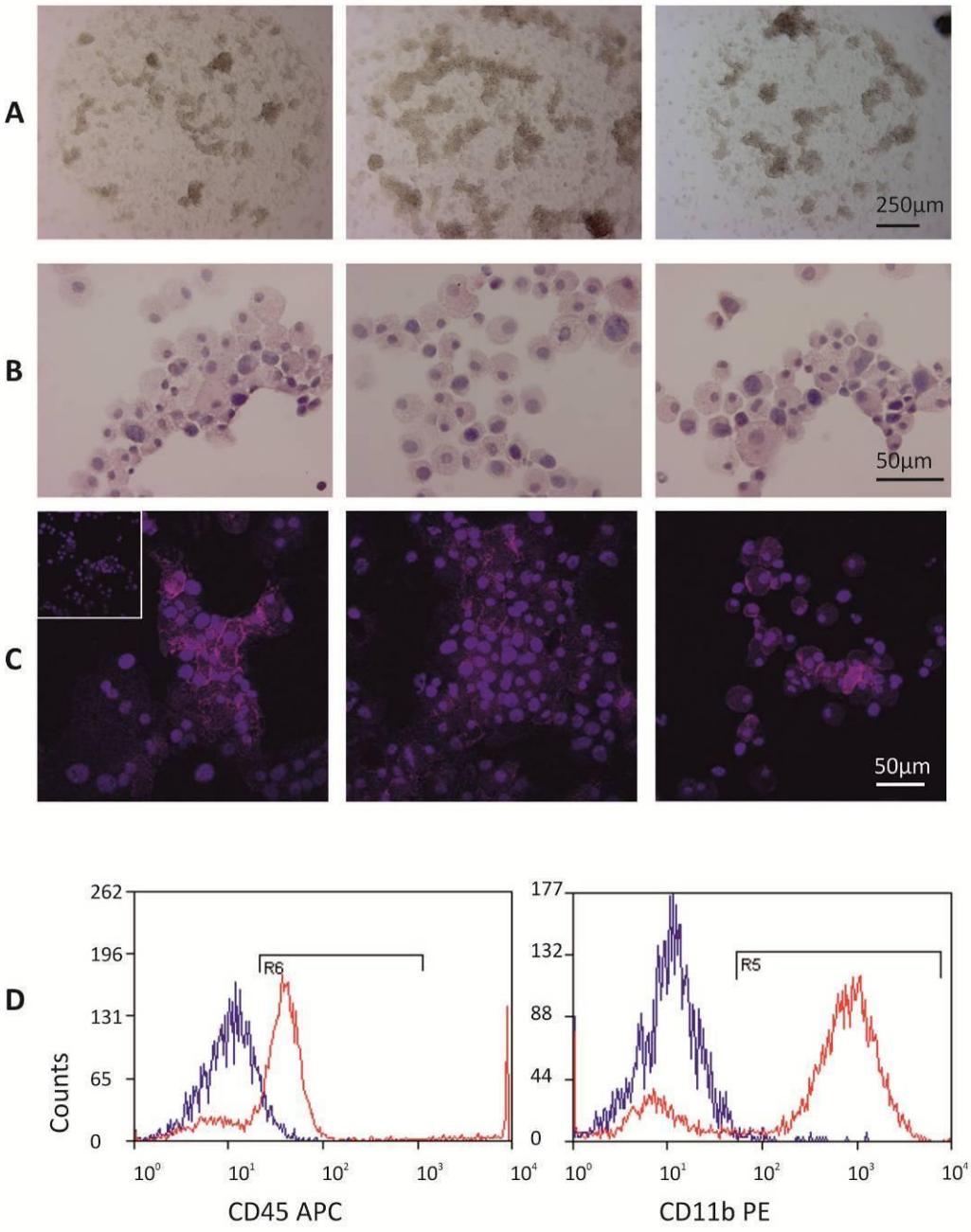

Figure 4.9 Characterisation of outgrowth cells
Co-culturing of C3H10T1/2 cells with HPCs leads to an outgrowth of cells that remain in the well once the spheroid is removed at day 8 (Brightfield images, A). These cells were collected and cytospun and stained with H&E (B) and the common macrophage marker F4-80 (pink, C) counterstained with DAPI (blue). Inset image represents antibody control. Expression of macrophage markers CD45 and CD11b was determined by flow cytometric analysis (D). Red line represents antibody stained, blue line is the isotype control.

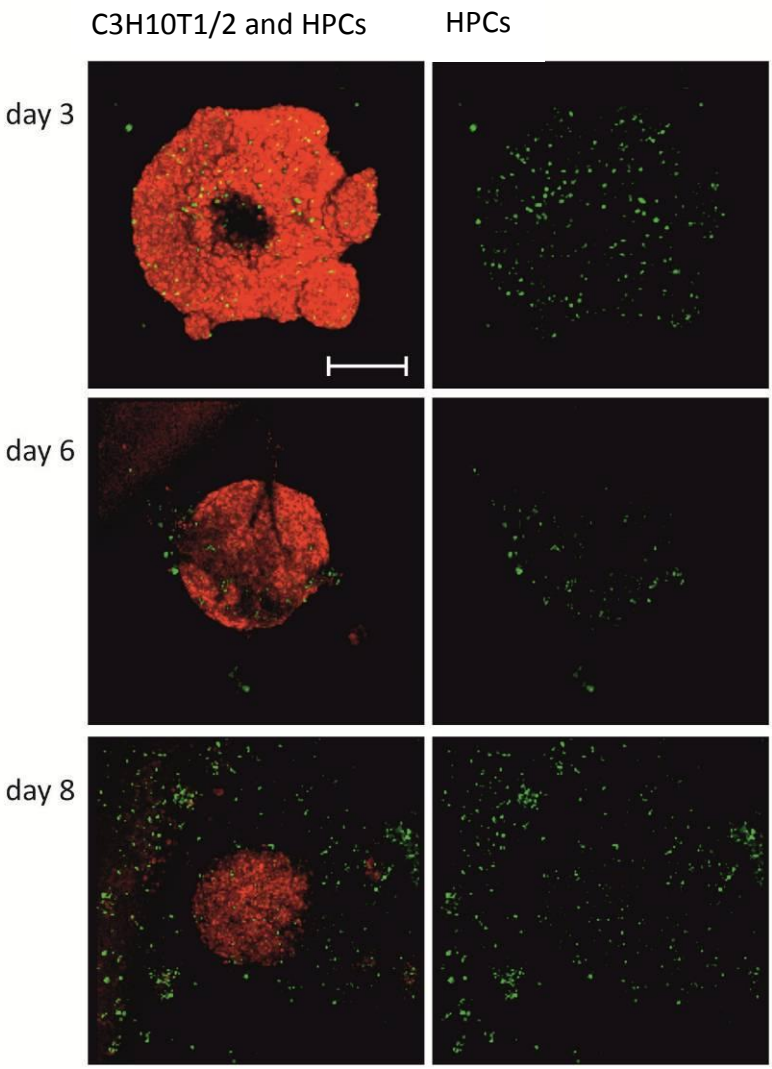

Figure 4.10 HPC detection within co-culture spheroids
HPCs and C3H10T1/2 cells were labelled with CellTracker red and green respectively and combined into spheroids. Confocal imaging detected HPCs within the spheroids at days 3, 6 and 8. Scale bar 200 µm.

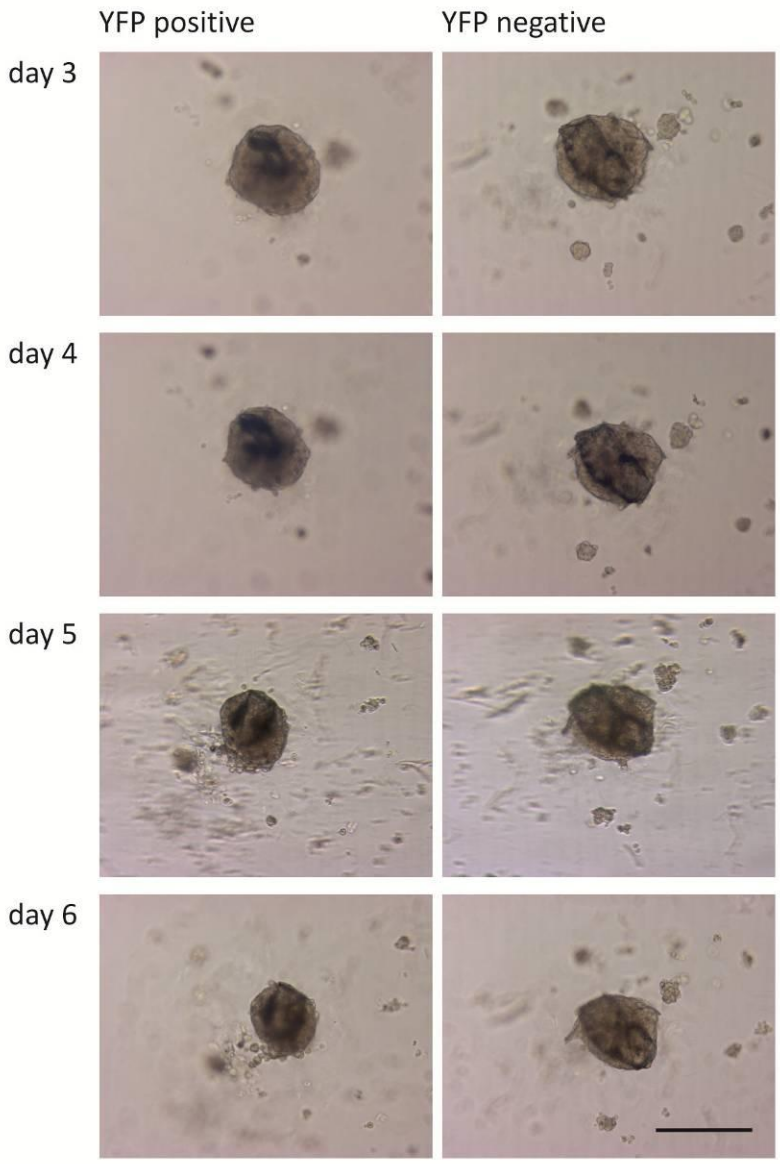

Figure 4.11 Formation of spheroids with primary stromal cells
Bone marrow cells were sorted by flow cytometry to be CD45 negative and either YFP positive or negative from IL-7CreRosa26eYFP transgenic mice. Both YFP^+ and YFP^- stromal cells were able to form spheroids that were maintained in culture for 6 days. Due to the small number of cells sorted, only 2.6 x 10^4 cells were used for each spheroid. Scale bar 250 µm.

As demonstrated in Chapter 3, IL-7Cre Rosa26eYFP transgenic mice are a novel reporter of IL-7 and YFP^+ cells were found to be a variety of mesenchymal cells located in the bone and bone marrow. Flow cytometric sorting of non-haematopoietic ($CD45^-$) cells isolated a small percentage (approximately 1%) of cells that were YFP^+. Both YFP positive and negative populations were successfully able to form spheroids that were maintained in culture for a week (Figure 4.11). Monolayer culture of these cells was not successful as after some initial adherence, the cells detached and were non-viable. These primary cells therefore appeared to prefer the 3D culture method, possibly due to the cross-talk that would be facilitated by the close interaction of cells.

in vivo, murine $nestin^+$ MSCs have been shown to support the HSC niche. Whilst co-culture of the C3H10T1/2 cells and HPCs has been determined to provide a physical model of such a niche, the next aim was to assess the ability of the stromal cells to maintain the HPCs functionality in culture. A sample of HPCs used in co-culture studies was cultured for 9 days in MethoCult, a semisolid media containing cytokines (rm SCF, rm IL-3, rhIL-6, rh Epo) to induce progenitor cells to proliferate and differentiate to produce colonies of cells (Figure 4.12). An expected number and range of myeloid and erythroid lineage colonies were produced by the foetal liver HPCs (Figure 4.12).

HPCs were analysed for cell surface markers after spheroid co-culture for 8 days. AFT024 cells are also widely used to support HSC cultures *in vitro* and were used alongside the C3H10T1/2 cells as alternative stromal cell line. The spheroids were disaggregated by enzyme digestion and examined by flow cytometry for expression of HSC markers: lineage markers (as a cocktail containing CD3, CD45R (B220), CD11b, Gr-1 (Ly-6G/C), 7-4, and Ter-119), c-kit and sca-1. The results showed that HPC cells predicted as having the profile lin^- $sca\text{-}1^+$ $c\text{-}kit^+$ could be detected as a small population within the disaggregated spheroids, suggesting their maintenance by each of the stromal cell lines (Figure 4.13, D and F). Expression of sca-1 was found in both the AFT024 and C3H10T1/2 stromal lines (Figure 4.13, C and E). From

the AFT024 co-culture spheroids there was a 1% population of live lin^- cells that were also $sca\text{-}1^+$ $ckit^+$. 2.6% of the lin^- cells were positive for c-kit but did not express sca-1. A similar pattern of expression was observed with C3H10T1/2 co-culture spheroids, with a slightly larger proportion (2.7%) of cells expressing both sca-1 and c-kit.

HPCs could be detected by flow cytometry after spheroid co-culture but when put into MethoCult colony assays, did not form haematopoietic colonies (data not shown). This was possibly due to the overgrowth of stromal cells and their consumption of growth factors as no sorting was done to separate HPCs from the stromal cells before colony assay. So, whilst HPCs could be detected in the spheroids after 8 days, their ability to form colonies was not demonstrated.

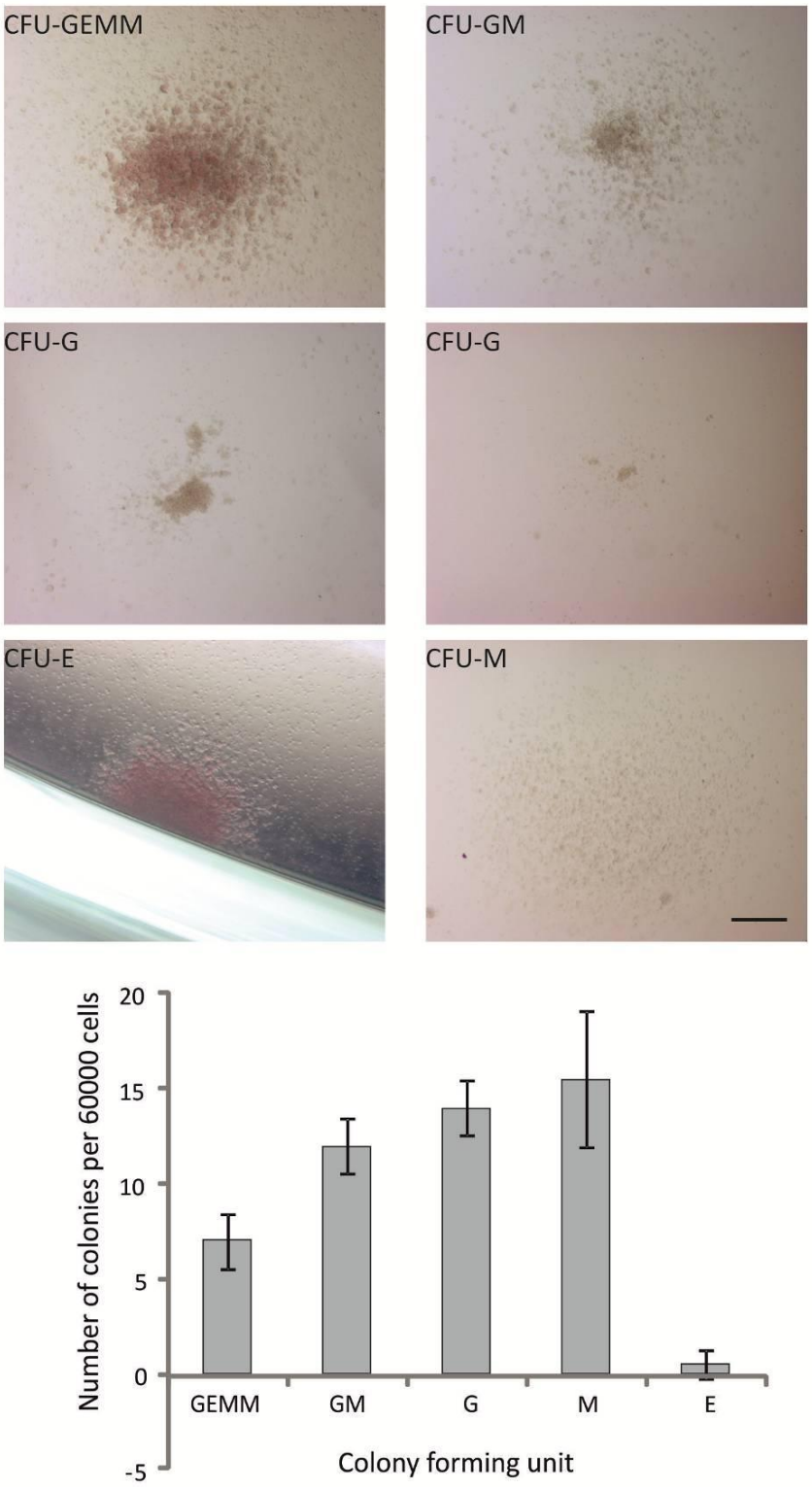

Figure 4.12 Colony forming cell assay
HPCs were cultured in Methocult and resulting colonies were identified microscopically (top images) and counted (presented in graph) on day 9. Scale bar 250 µm. CFU- Colony Forming Unit, -GEMM; granulocyte erythrocyte monocyte megakaryocyte, -GM; granulocyte, monocyte, -G; granulocyte, -E;erythroid, -M;monocyte. Error bars indicate standard deviation of the mean, n=3 technical replicates.

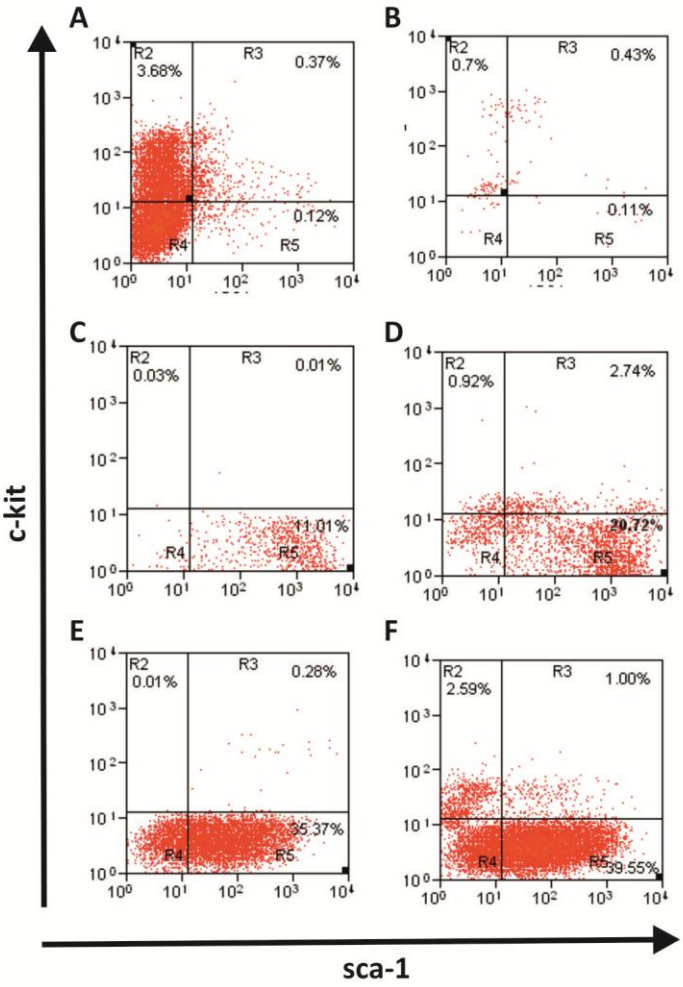

Figure 4.13 Expression of LSK markers in HPCs after spheroid culture
HPCs and stromal cells were cultured in spheroids for 8 days before disaggregation and flow cytometric analysis of cell surface markers of lineage (CD5, CD45R (B220), CD11b, Gr-1 (Ly-6G/C), 7-4, and Ter-119), c-kit and sca-1. Cells were gated to be lineage negative and numbers shown are percentage of population that are $lin^{-}ckit^{+}sca\text{-}1^{+}$. HPCs alone were assessed pre-spheroid culture (A) and after 8 days (B), C3H10T1/2 (C) and C3H10T1/2 with HPCs (D), AFT024 cells (E) and AF024 with HPCs (F) were assessed after spheroid culture.

4.4 Summary

The bone marrow microenvironment is a complicated tissue, therefore it is important to generate a 3D *in vitro* model in order to more accurately study stem cell proliferation, self-renewal and differentiation. The results of this chapter will be discussed in chapter 6. Briefly, C3H10T1/2 cells were able to spontaneously form spheroids in methyl-cellulose media and could differentiate efficiently when induced down osteogenic, adipogenic and chondrogenic lineages. Owing to the consistent spheroid shape, 4 x 10^4 cells was the number selected from a range of spheroid sizes to be further characterised. C3H10T1/2 cells organised into a dense network of cells in the spheroid which was surrounded by an outer layer of cells that arranged in spindle-shaped appearance to encase the spheroid. Only small numbers of cells in the peripheral layer of the spheroids were positive for proliferative marker Ki67, demonstrating that the cells adopt a quiescent state in the spheroids. Primary YFP^+ murine stromal cells are able to form spheroids and can be maintained in culture more successfully than in 2D, demonstrating the importance of a 3D environment to cells cultured *in vitro*. However, detection of LSK cells after 8 days of co-culture with C3H10T1/2 cells was not successful; indicating that C3H10T1/2 cells were ineffective at maintaining HPCs in this spheroid culture system and therefore, that further development of the model is required.

5 Characterisation of IL-7 and nestin in human MSCs

5.1 Introduction

Human MSCs are commonly distinguished *in vitro* by a panel of cell surface markers including CD90, CD105, CD73 and CD106 as well as Stro-1 (Simmons & Torok-Storb, 1991), although these may differ between investigating groups. As MSCs are routinely isolated and examined *in vitro*, culture dependent changes and the probability of examining a heterogeneous cell population contributes to the difficulty in isolating and characterising a single cell type. Currently, a number of markers such as CD271 and CD146 (human) and nestin (mouse) have been proposed to prospectively isolate MSCs with a high degree of purification (Jones et al, 2002; Mendez-Ferrer et al, 2010; Sacchetti et al, 2007). However, these proteins are also expressed on a population of differentiated cells and cannot account for the entire MSC ability of the bone marrow. This suggests subsets of MSCs exist with distinct profiles that are yet to be identified.

Nestin is recognised as a marker of stem and progenitor cells in an increasing number of human tissues and studies in mouse models report nestin^{+} MSCs to be critical in HSC survival in the bone marrow (Mendez-Ferrer et al, 2010). These MSCs expressed higher levels of IL-7 mRNA than nestin^{-} cells in the bone marrow. IL-7 is known to be expressed in human bone marrow cells but their relationship in the regulation of the HSC niche has not been determined.

Much of the work that has defined stem cell niche biology has been carried out in invertebrates and mouse studies and the systems involved are highly conserved. Therefore, results from the previous chapters together with these published reports suggest that IL-7 and nestin could be applicable to identifying human MSCs and as such the experiments in this chapter aim to determine IL-7 and nestin expression in human MSCs and examine their potential functional role.

5.2 Aims

- To determine expression of IL-7 and nestin in human MSCs

- To identify IL-7 and nestin expression patterns during human MSC differentiation
- To identify whether IL-7 has a functional role in MSCs

5.3 Results

5.3.1 Characterisation of human MSCs

MSCs obtained from patient femoral head samples were purified using a density gradient and centrifugation protocol. Additionally, MSCs were isolated from knee bone by simply placing the bone chip into a tissue culture dish with media. Cells which were adherent on tissue culture plastic could then be selected for further analysis. Cells were examined by flow cytometry for the expression of markers commonly used to identify MSCs (Figure 5.1). Cells were examined between passages 2-4 to allow sufficient proliferation from their original isolation and the loss of any contaminating haematopoietic cells. All donors (refers to K6, FH441, FH450 and FH181) were found to be negative for haematopoietic markers CD45 and CD34 and macrophage marker CD11b. Cells were positive for CD105, CD166, CD29, CD90, CD73 and CD44. CD271 was not detected. Donors from knee and hip sources showed an identical profile for these markers and were consistent with the expected expression on MSCs.

To confirm their differentiation capacity, each MSC donor was induced for 21 days. Adipogenic differentiation was detected by Oil Red O staining. By day 7, a large proportion of cells had visible lipid vesicles within the cytoplasm. The number of cells containing lipid vesicles increased over time and the individual vesicles became larger and merged together in mature adipocytes by day 21 (Figure 5.2). At day 21, one or two cells stained positive in the control samples indicating infrequent spontaneous differentiation events. Early osteogenic differentiation was determined at day 7 by staining for alkaline phosphatase (ALP) activity, which appeared as diffuse pink staining. ALP activity remained widespread and could also be detected at days 14 and 21. Mineralisation was detected by von Kossa staining and showed brown staining, which was most prominent at day 21 (Figure 5.3).

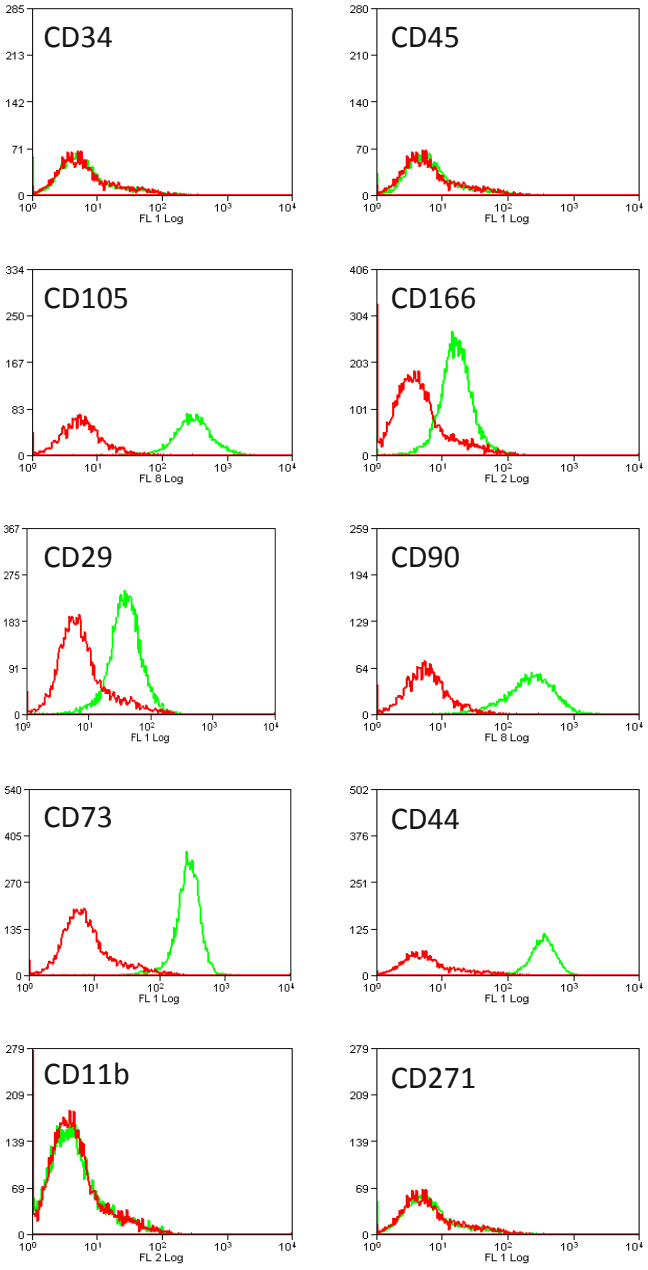

Figure 5.1 Expression of MSC cell surface markers
Overlay histograms of flow cytometry results show the expression of negative (CD34, CD45, CD11b) and positive (CD105, CD166, CD29, CD90, CD73, CD44) surface markers used to identify MSCs. CD271 was not detected on the MSCs. Donor FH441 shown as representative of those analysed: K6, FH181, FH450. Red lines indicate isotype control.

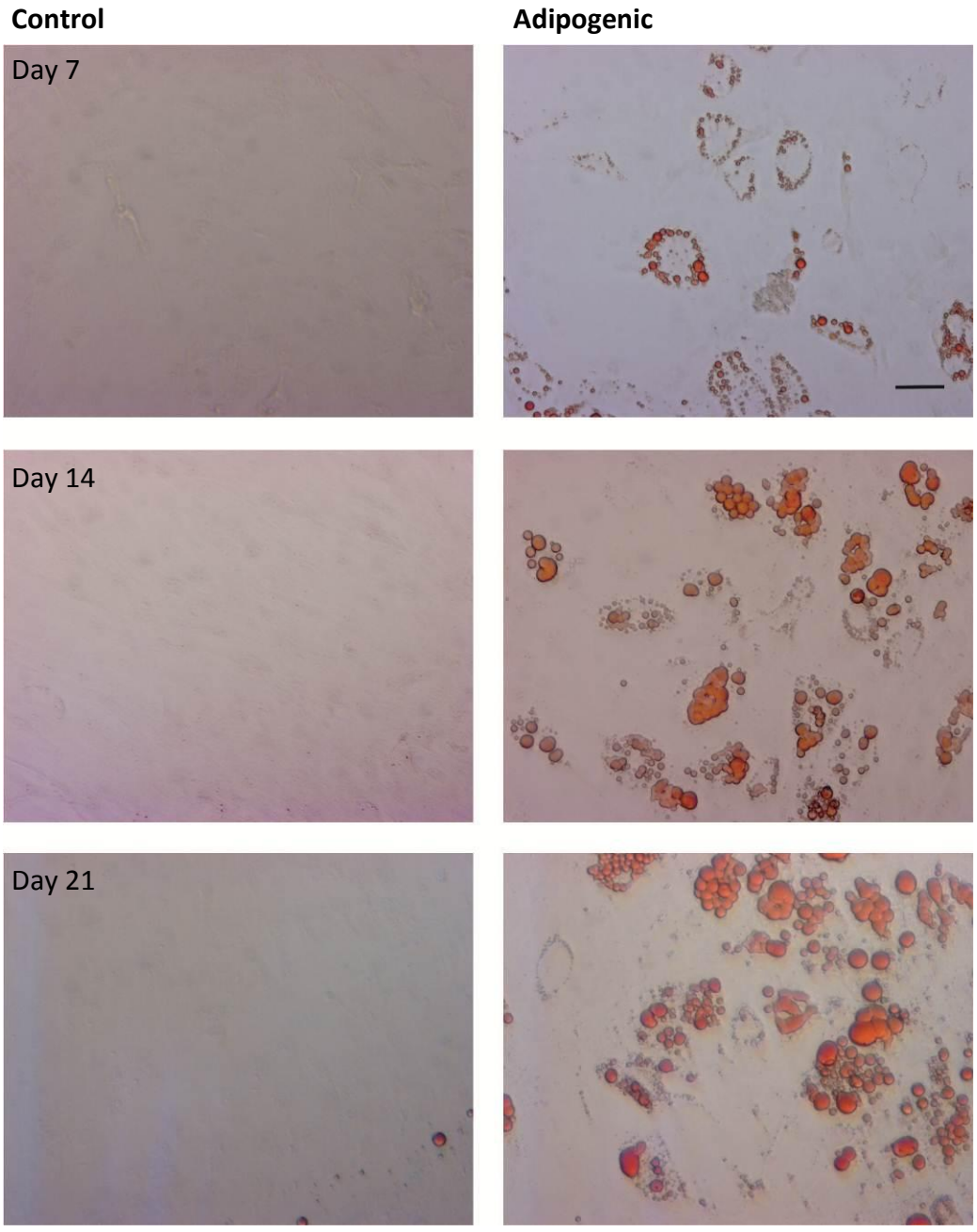

Figure 5.2 Adipogenic differentiation of MSCs
MSCs were cultured in normal basal media or media containing adipogenic factors for 21 days. At days 7, 14 and 21 samples were stained with Oil Red O (red) to determine the presence of lipid vesicles. Scale bar 50 µm. Donor K6 is shown.

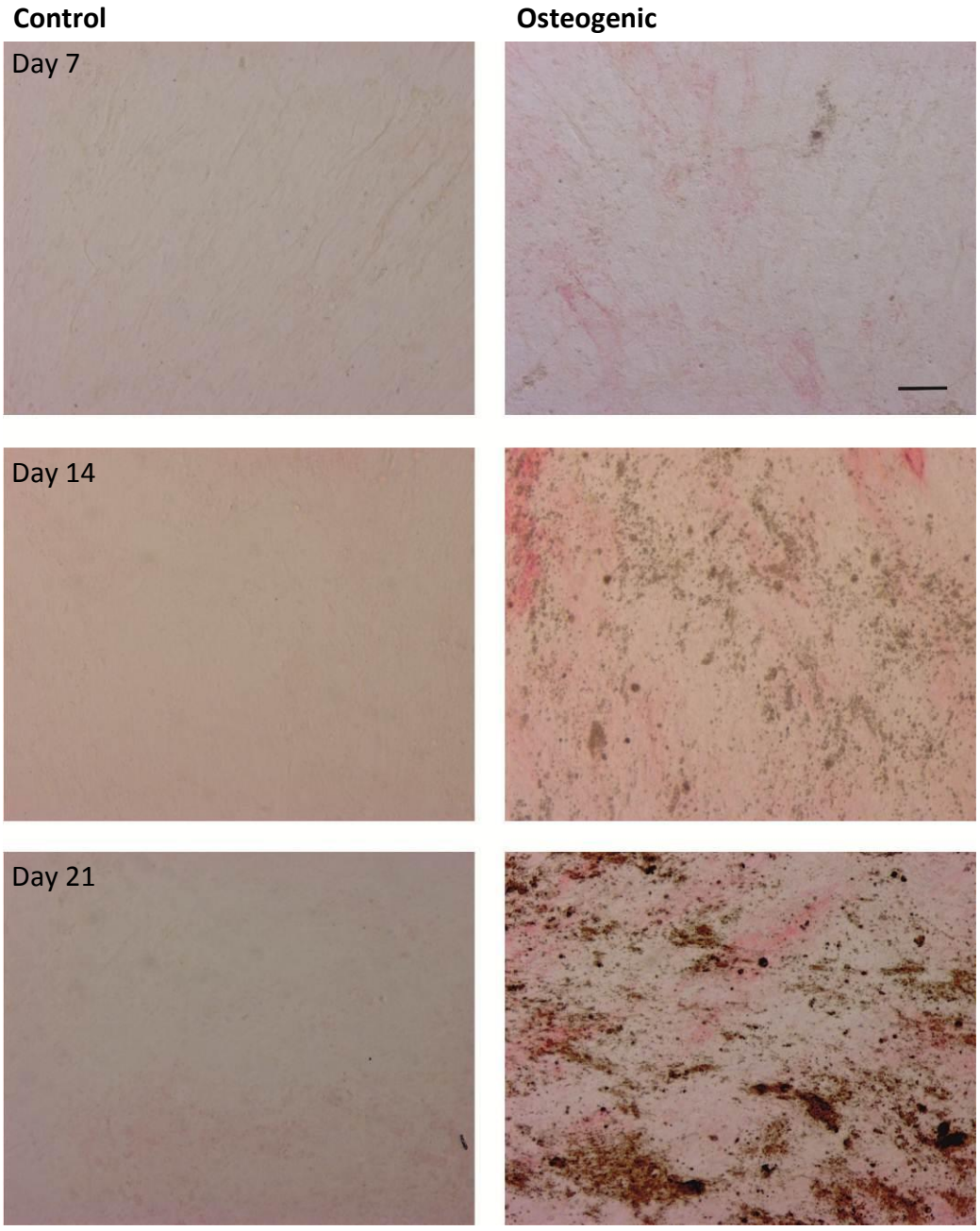

Figure 5.3 Osteogenic differentiation of MSCs
MSCs were cultured in basal or osteogenic media for 21 days. Samples were stained at weekly intervals for alkaline phosphatase activity (pink) and von Kossa staining (brown/black) to show mineralisation. Scale bar 50 µm. Donor FH450 is shown.

Similar to the adipogenic controls, the osteogenic control samples showed little or no staining. Each donor was found capable of multipotent differentiation. Quantitative real time PCR (qPCR) was used to examine gene expression in MSCs during differentiation. Genes indicative of osteogenic, adipogenic and chondrogenic lineage commitment were analysed as well as the two genes of interest; IL-7 and nestin. All genes were normalised to the housekeeping gene RPS27a and expression was compared to the appropriate day 0 control.

Adipogenic differentiation of MSCs led to the progressive increase in expression of fatty acid binding protein 4 (FABP4, Figure 5.4) and peroxisome proliferator-activated receptor gamma (PPARγ, Figure 5.5) in all donors. Donor FH441 varied slightly in that the expression of each marker was similar on day 7 and 14 before increasing to a maximum on day 21. Control samples at each time point had low or no expression in comparison.

Gene expression was more varied between donors during osteogenic differentiation. ALP was increased at day 7 and then further increased at day 21 in K6 and FH441 cells but the increase at day 7 in donor FH181 cells was followed by a reduction at later time points (Figure 5.6). Runx2 expression in FH181 cells was upregulated at day 7 which was maintained at day 14 before decreasing at day 21. The other three donors, particularly K6 cells, had similar expression of Runx2 in both the control and osteogenic cells (Figure 5.7). FH441 and FH450 only showed an increase in Runx2 expression compared to the control at day 21. Despite these variations in gene expression, all donors were similarly differentiated as determined by histology staining.

All donors examined for chondrogenesis had the greatest increase in collagen II expression at day 14, which was seen to decrease at day 21 in FH181 (Figure 5.8). Whilst Sox9 expression was increased compared to day 0 in donors FH441 and FH450, it was not distinctly different to the control at each time point apart from day 14 in FH450 cells (Figure 5.9). Sox9 expression even appeared reduced in FH181 cells.

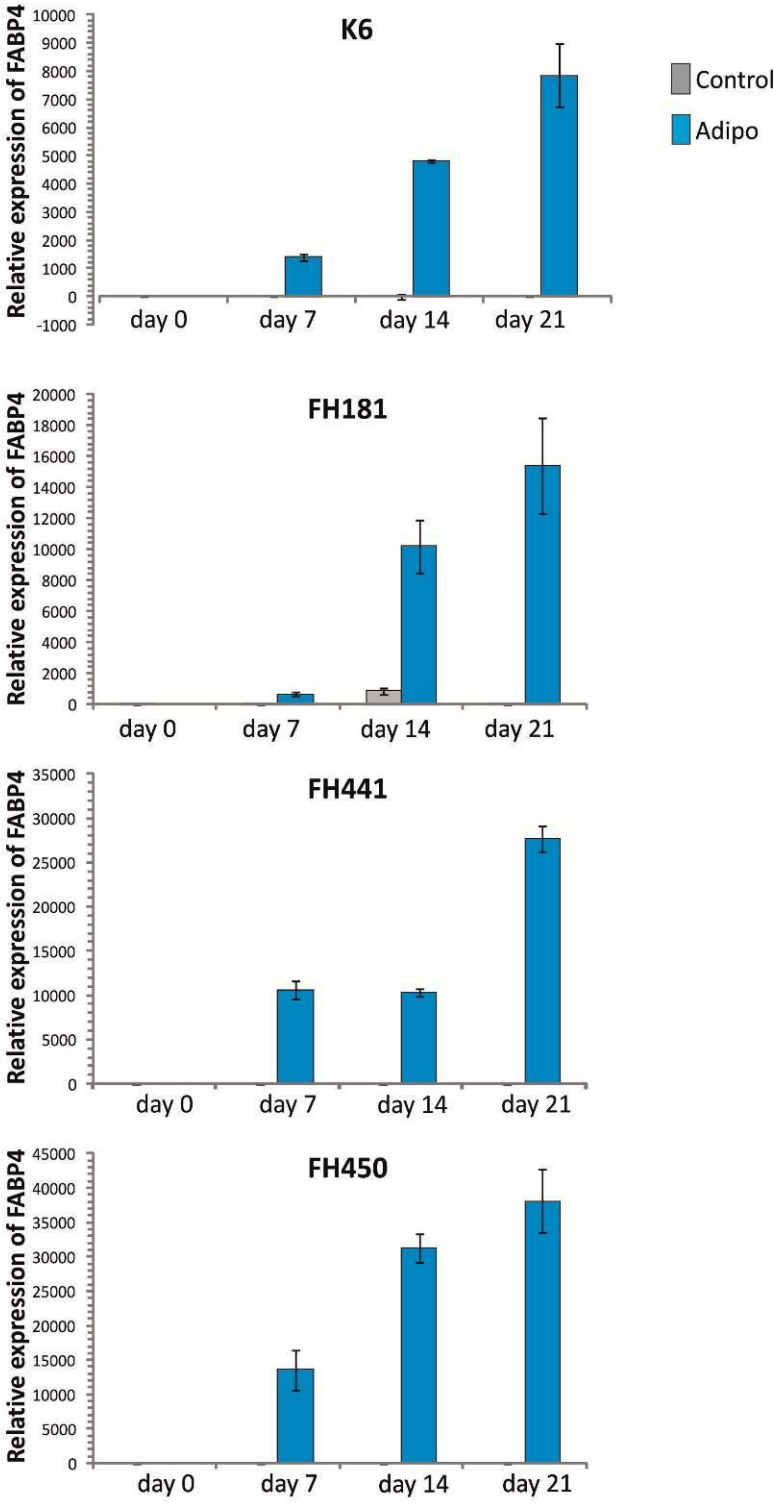

Figure 5.4 qRT-PCR analysis of adipogenic marker FABP4
RNA samples were extracted from monolayers undergoing adipogenic differentiation and examined for FABP4 expression. Error bars indicate sd.

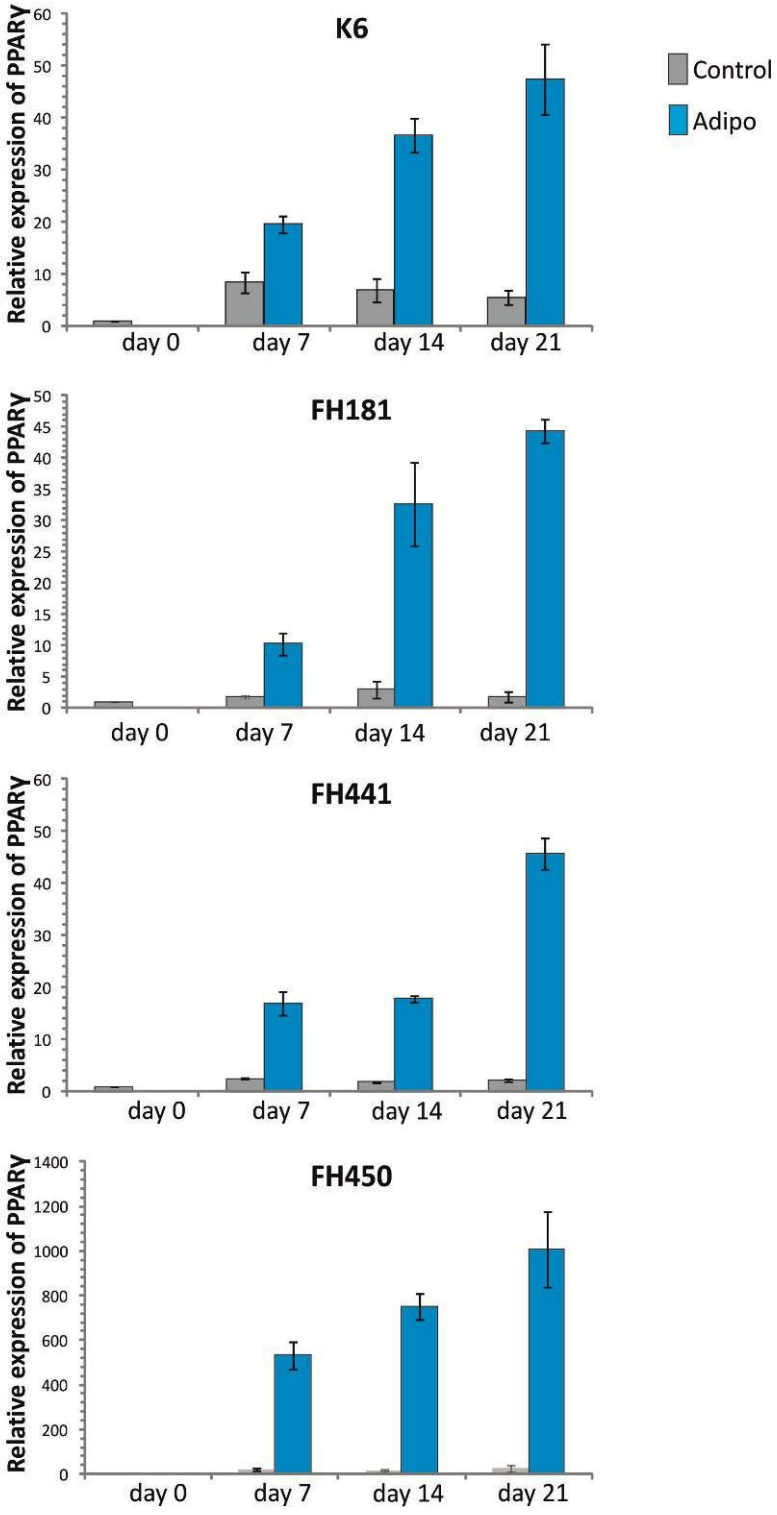

Figure 5.5 qRT-PCR analysis of adipogenic marker PPARγ
RNA samples were extracted from monolayers undergoing adipogenic differentiation and examined for PPAR expression. Error bars indicate sd.

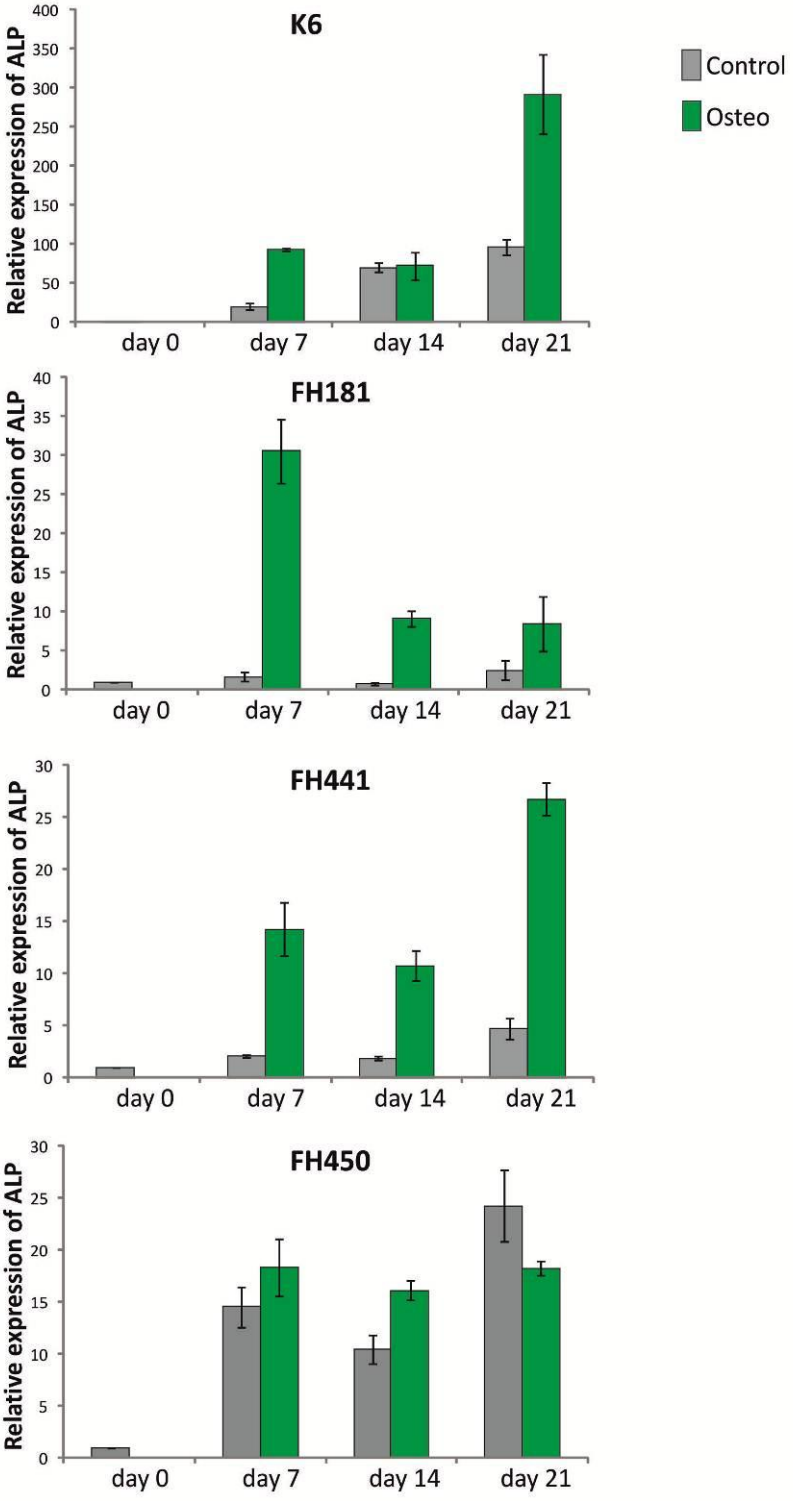

Figure 5.6 qRT-PCR analysis of osteogenic marker alkaline phosphatase (ALP)
RNA samples were extracted from monolayers undergoing osteogenic differentiation and examined for ALP expression. Error bars indicate sd.

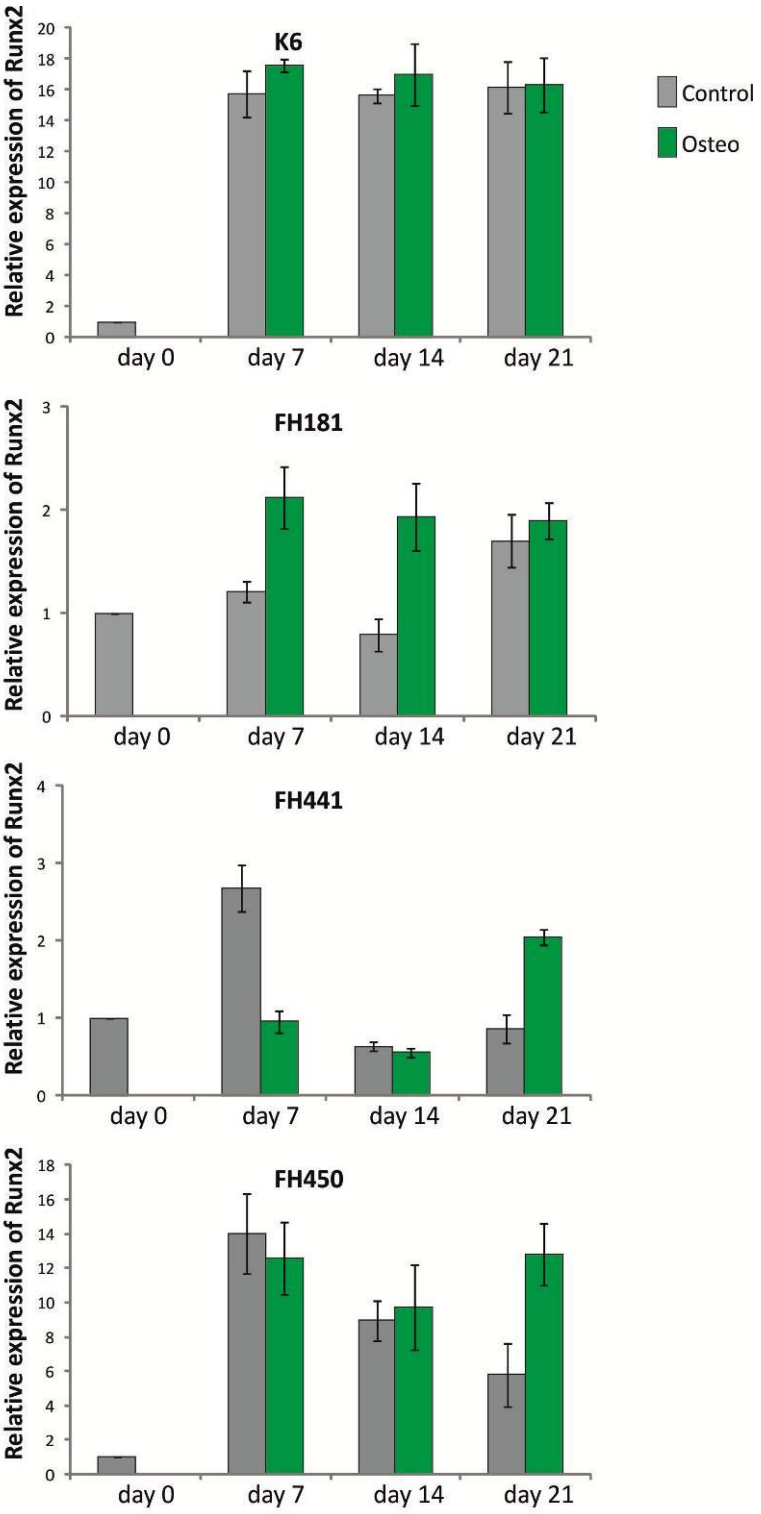

Figure 5.7 qRT-PCR analysis of osteogenic marker Runx2
RNA samples were extracted from monolayers undergoing osteogenic differentiation and examined for Runx2 expression by real time PCR. Error bars indicate sd.

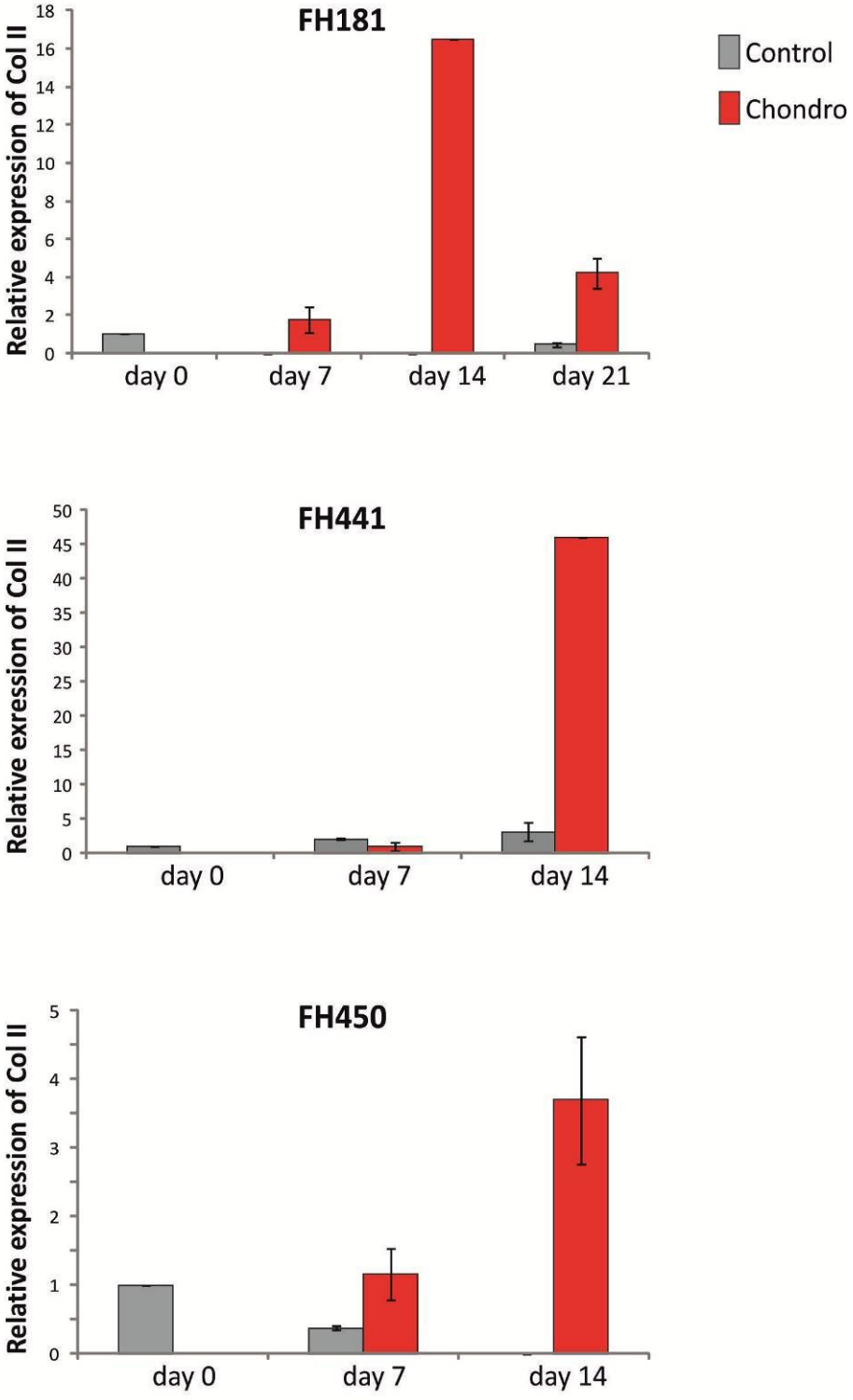

Figure 5.8 qRT-PCR analysis of collagen II during chondrogenic differentiation
RNA samples were extracted from cell pellets undergoing chondrogenic differentiation and examined for collagen II expression. Error bars indicate sd.

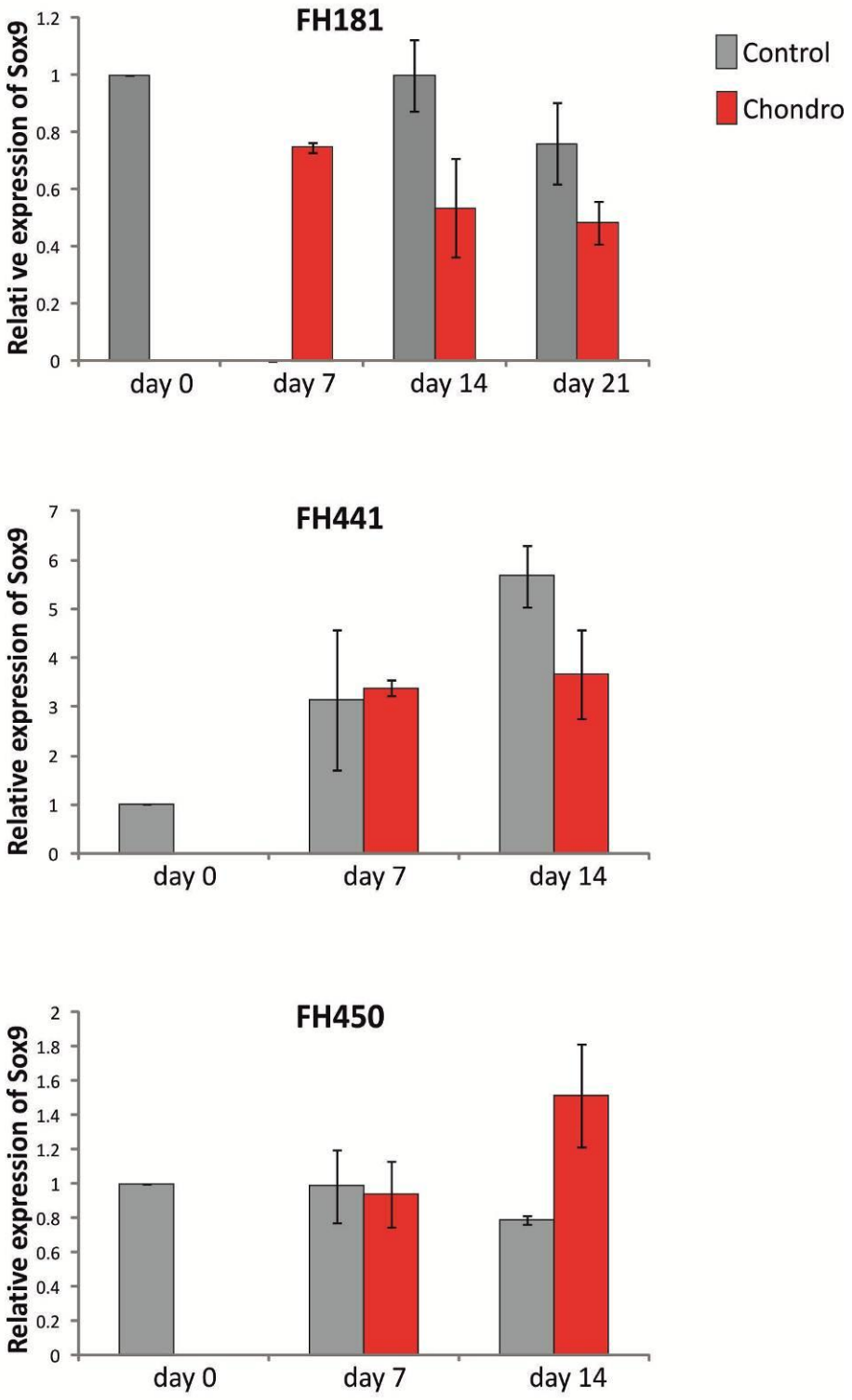

Figure 5.9 qRT-PCR analysis of Sox9 during chondrogenic differentiation
RNA samples were extracted from cell pellets undergoing chondrogenic differentiation and examined for Sox9 expression. Error bars indicate sd.

5.3.2 Expression of IL-7 and nestin during MSC differentiation

Nestin expression is reportedly downregulated in differentiated cells. Therefore, mRNA levels were analysed to detect if this expression profile of nestin was apparent in bone marrow MSCs as they differentiated down tri-lineage pathways. IL-7 expression was also analysed in these samples and would be expected to follow a similar pattern to that of nestin if IL-7 were a stem cell marker of MSCs. In chapter 3, bone marrow cells in transgenic mice expressed IL-7 reporter YFP and therefore, differentiated MSCs may potentially express IL-7. qPCR of samples collected at days 7, 14 and 21 during differentiation induction was used to determine IL-7 and nestin expression. IL-7 expression was primarily increased under both control and differentiation conditions in monolayer cultures over 21 days. With only a couple of exceptions in donor FH441, IL-7 expression was highest in the control samples compared to those that were differentiated at each time point (Figure 5.11). Nestin expression was also predominantly highest in control cells followed by osteogenic and adipogenic cells and was also usually lower in day 7, 14 and 21 when compared to day 0 (Figure 5.13).

Osteogenically differentiated cells generally showed a progressive increase in IL-7 expression although in FH181 cells; this decreased a little after day 14. Donor FH181 showed the least variation in expression from the day 0 control and control and osteogenic samples were quite similar throughout as noted by less than half of the osteogenic samples being statistically significant from their respective controls (Figure 5.11). Nestin expression increased in FH441 cells at days 7 ($p=0.006$) and 14 ($p=0.002$) compared to the control sample. The other 3 donors showed more variability but nestin was essentially expressed at day 7 slightly above the control level and then in day 14 and 21 osteogenic samples, nestin had decreased below the individual and day 0 controls (Figure 5.13).

IL-7 expression during adipogenic differentiation generally remained at a consistent level at all time points in each donor. In FH181 cells it was noticeably lower on days 7, 14 and 21 in comparison to the day 0 control and whilst in the other donors the

expression level was higher in each condition compared to day 0, IL-7 in the differentiated samples remained lower than the control at each time point (Figure 5.11). This was also the case with nestin expression; at each time point the level was statistically lower in adipogenic samples than the control apart from donors FH441 and FH181 at day 14. In an opposite effect to IL-7, rather than an increase compared to the day 0 control, nestin expression decreased and remained lower than this control in each of the adipogenic samples (Figure 5.13).

Cells were formed into pellets rather than monolayer culture for chondrogenic differentiation studies. IL-7 expression increased in control and chondrogenic samples over time with negligible difference between them at day 7. IL-7 was generally increased in chondrogenic samples compared to the control at the same timepoint although FH441 cells at day 14 showed a decrease in expression ($p=0.004$) (Figure 5.10). Conversely, nestin expression in cell pellets decreased compared to day 0 levels in both control and differentiated samples in FH181 cells and did not increase more than 2-fold in other donors. Compared to the respective day control sample, statistical significance was not detected between control and chondrogenic samples (Figure 5.13).

Cells cultured in 3D rather than 2D have been shown to have differences in their behaviour and gene expression. IL-7 was expressed at a higher level in the pellet samples compared to monolayer cultures in all 3 donors although, the difference between control and chondrogenic samples in donor FH441 was not considered statistically significant (Figure 5.10). However, nestin expression was significantly lower in day 0 monolayer cultures compared to day 0 cell pellets in donors FH181 and FH441, with no significance detected in donor FH450, indicating a general difference between the two culture methods (Figure 5.12).

5.3.3 Nestin is detected in human MSCS

After confirming the presence of nestin mRNA by qPCR and alterations in its expression during differentiation, MSCs were seeded onto coverslips and stained to

detect the presence of nestin protein (see section 2.6.6). NTERA2/D1 cells are derived from a human embryonal carcinoma and were used as a positive control as they are known to express nestin and showed strong cytoplasmic staining. Unexpectedly, K6 cells showed weak nuclear staining with some diffuse cytoplasmic staining. This was similar after 24 hours and 7 days (Figure 5.14). Conversely, two other donors showed initial nuclear staining which was replaced by more distinct cytoplasmic staining at day 7 (Figure 5.15). When differentiated for 7 days, K6 cells retained the nestin staining, perhaps a little weaker, which agreed with the mRNA expression detected. Ki67 staining showed similar low level proliferation events in osteogenic and adipogenic samples (Figure 5.16).

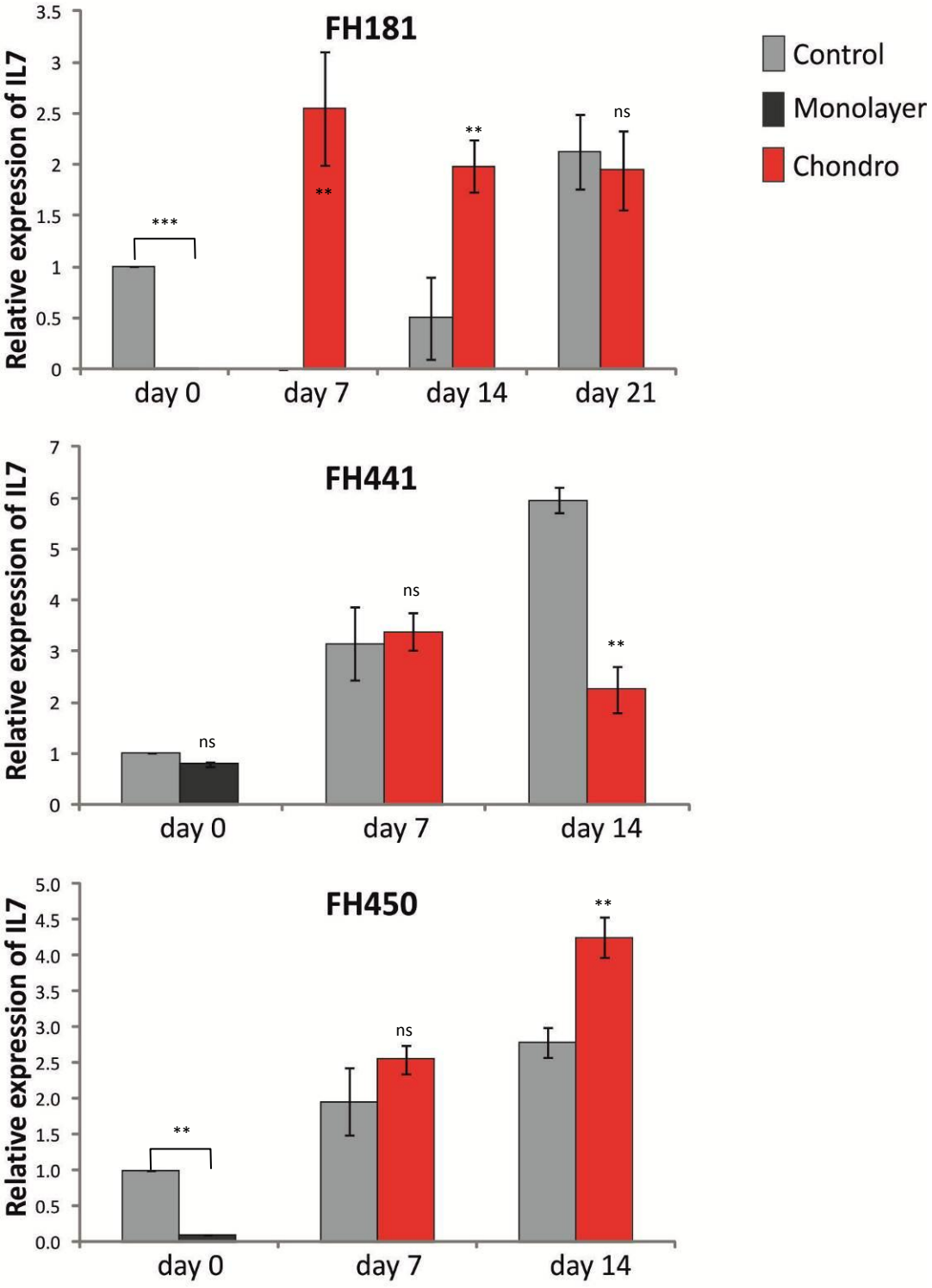

Figure 5.10 qRT-PCR analysis of IL-7 expression during chondrogenesis
RNA samples were extracted from cell pellets undergoing chondrogenic differentiation and examined for IL-7 expression. Error bars indicate sd.
$p \leq 0.05$ not significant (ns), $p < 0.05$ *, $p < 0.01$ **, $p < 0.001$ *** represents statistical significance determined by t-test.

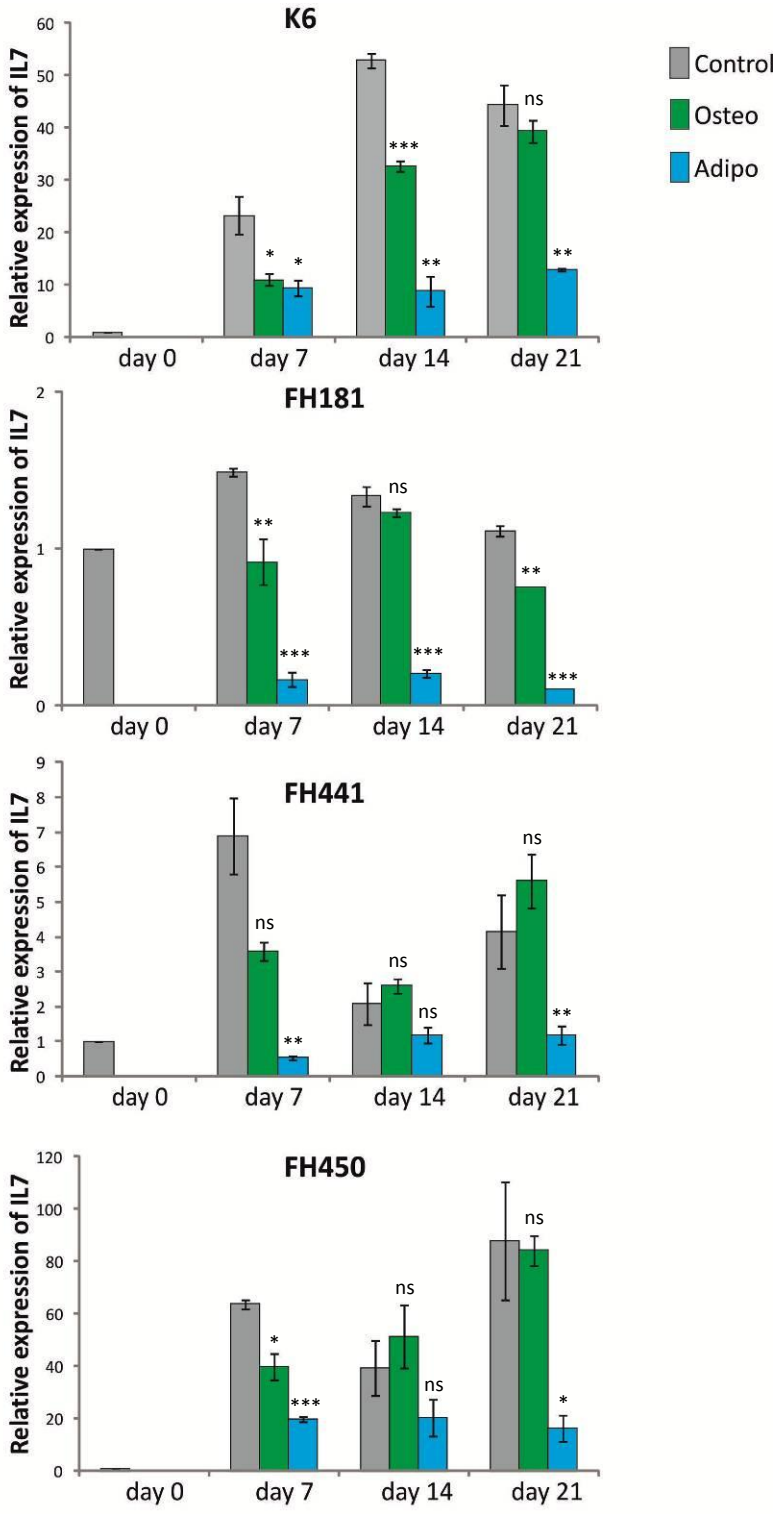

Figure 5.11 qRT-PCR analysis of IL-7 expression during differentiation
RNA samples were extracted from cells undergoing adipogenic or osteogenic differentiation and examined for IL-7 expression. Error bars indicate sd.
$p \leq 0.05$ not significant (ns), $p < 0.05$ *, $p < 0.01$ **, $p < 0.001$ *** represents statistical significance determined by t-test.

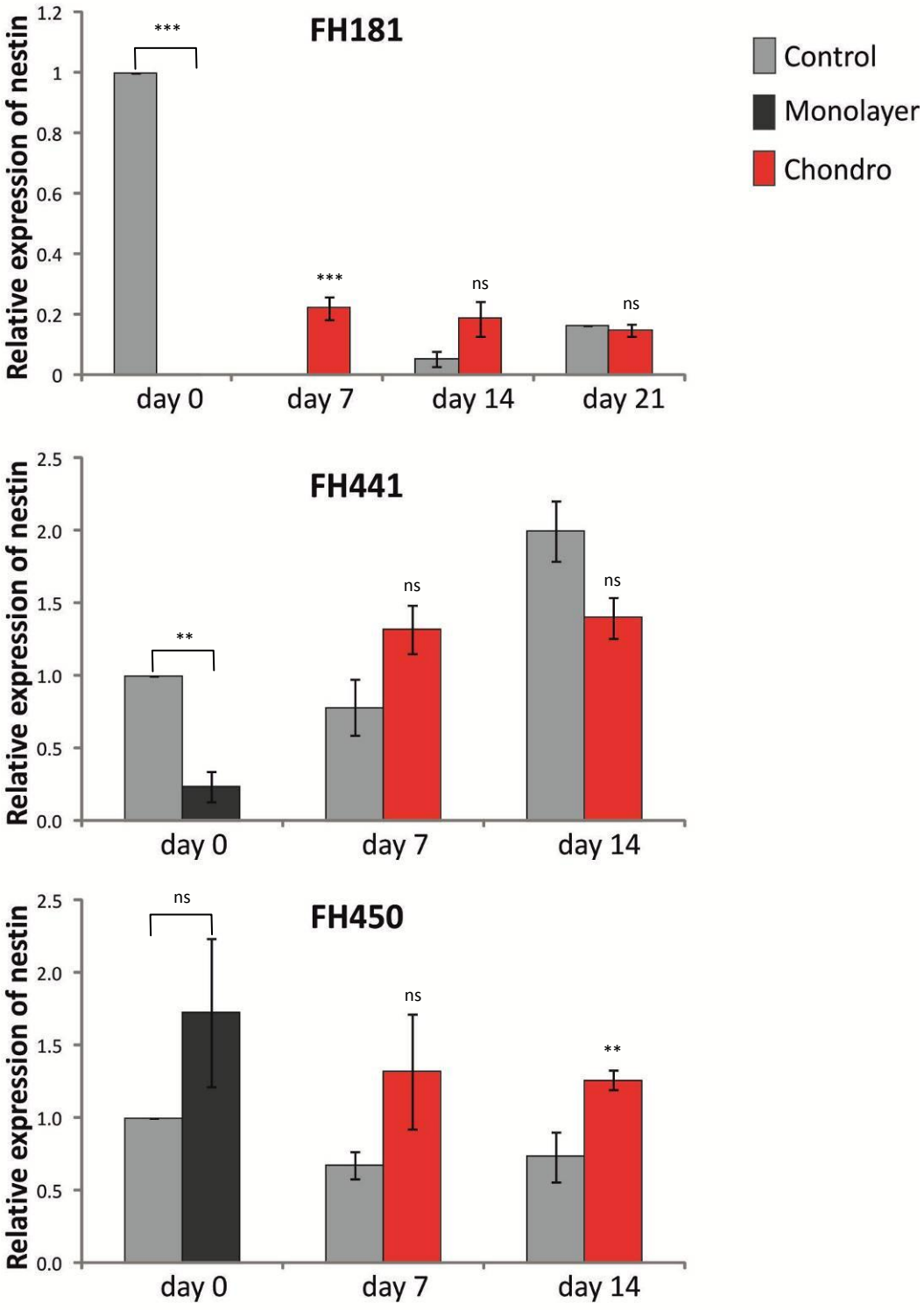

Figure 5.12 qRT-PCR analysis of nestin expression during chondrogenesis
RNA samples were extracted from cell pellets undergoing chondrogenic differentiation and examined for nestin expression. Error bars indicate sd.
$p \leq 0.05$ not significant (ns), $p < 0.05$ *, $p < 0.01$ **, $p < 0.001$ *** represents statistical significance determined by t-test.

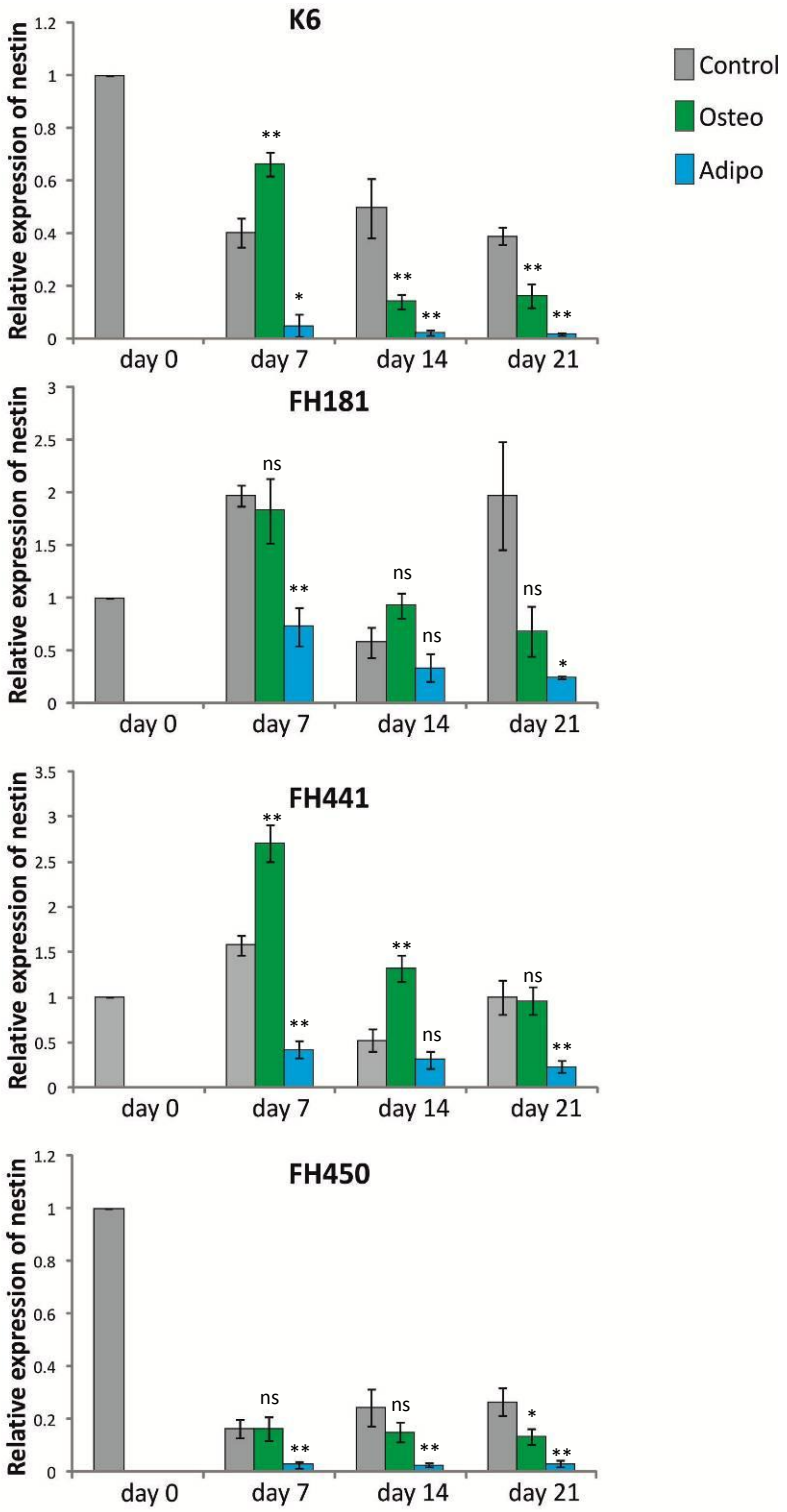

Figure 5.13 qRT-PCR analysis of nestin expression during differentiation
RNA samples were extracted from cells undergoing adipogenic or osteogenic differentiation and examined for nestin expression. Error bars indicate sd.
$p \leq 0.05$ not significant (ns), $p < 0.05$ *, $p < 0.01$ **, $p < 0.001$ *** represents statistical significance determined by t-test.

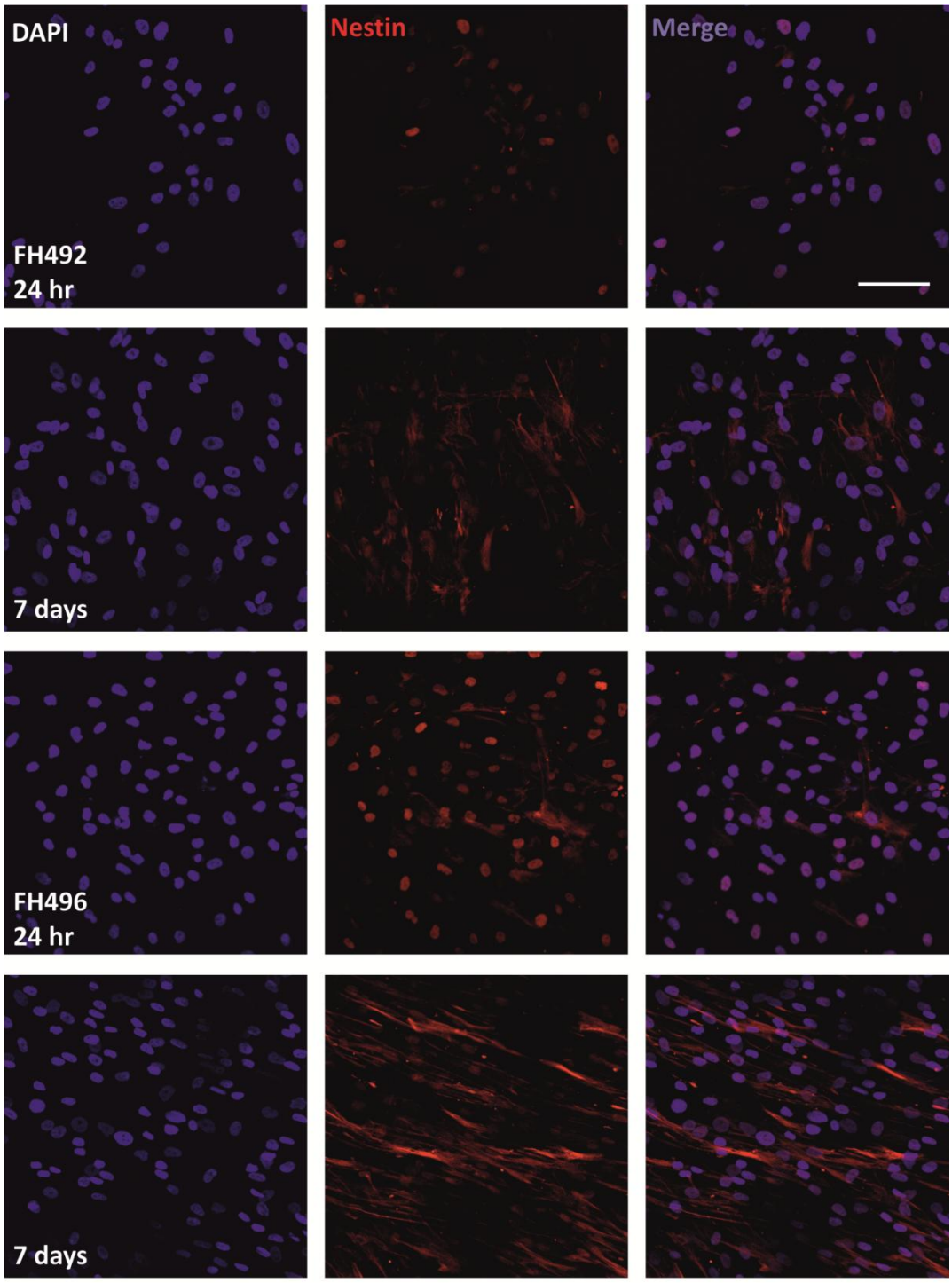

Figure 5.14 Immunofluorescent detection of nestin expression in MSCs (FH496 and FH492)
Cells were seeded onto coverslips at 2 x 10^4 cells/cm^2 and staining performed 24 hours and 7 days later. Nestin (red) could be detected in the nucleus of FH492 (top panels) and FH496 (bottom panels) MSCs. After 7 days, nuclear nestin staining was weaker whilst cytoplasmic staining increased. Cells were counterstained with Dapi (blue). Scale bar 100 µm.

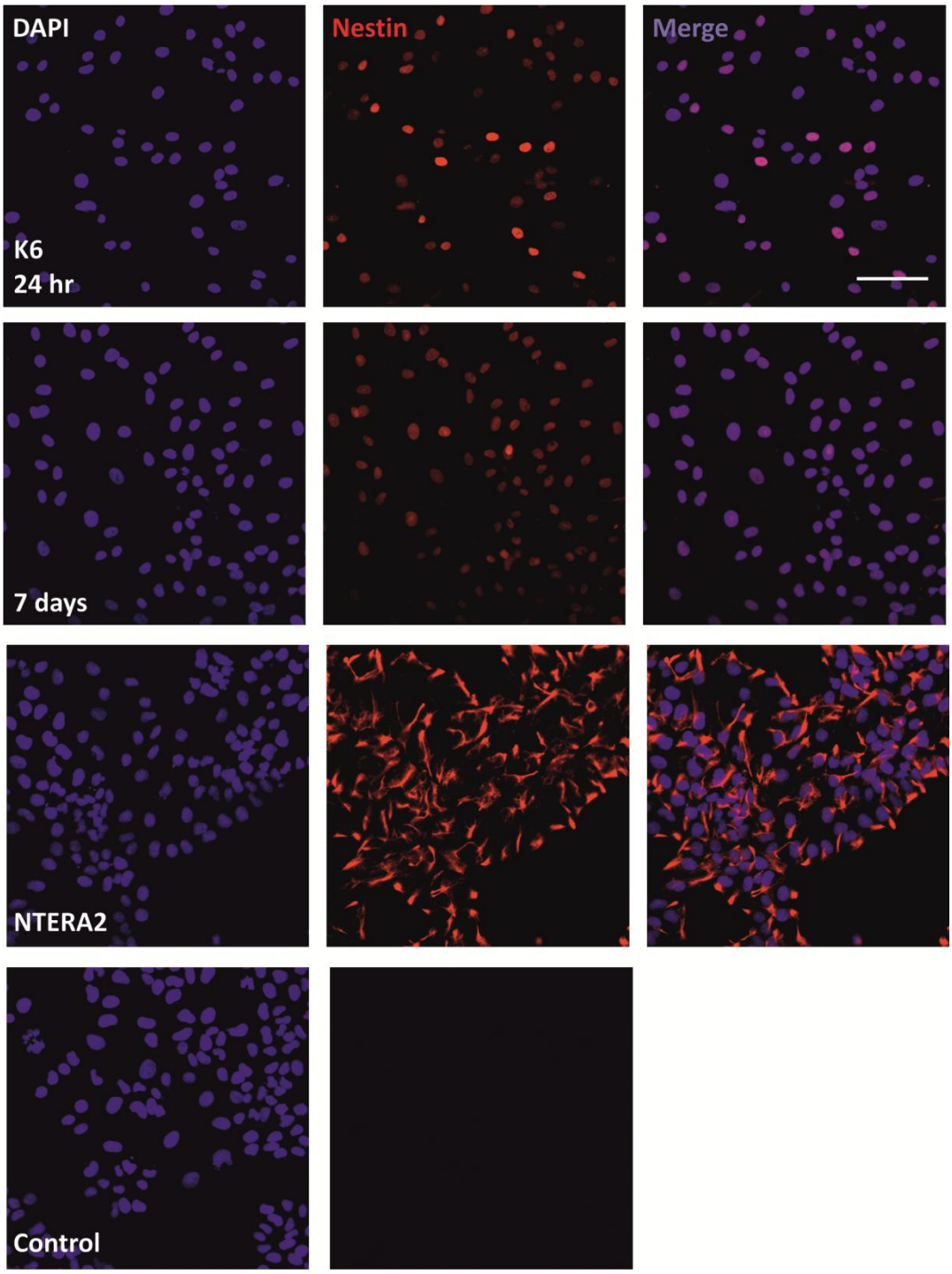

Figure 5.15 Immunofluorescent detection of nestin expression in MSCs (K6)
Cells were seeded onto coverslips at 2 x 10^4 cells/cm^2. 24 hours or 7 days later nestin (red) could be detected in the nucleus of K6 MSCs. NTERA2/D1 cells are known to express nestin and were used as a positive control. Rabbit IgG was used as an antibody control. Cells were counterstained with Dapi (blue). Scale bar 100 µm.

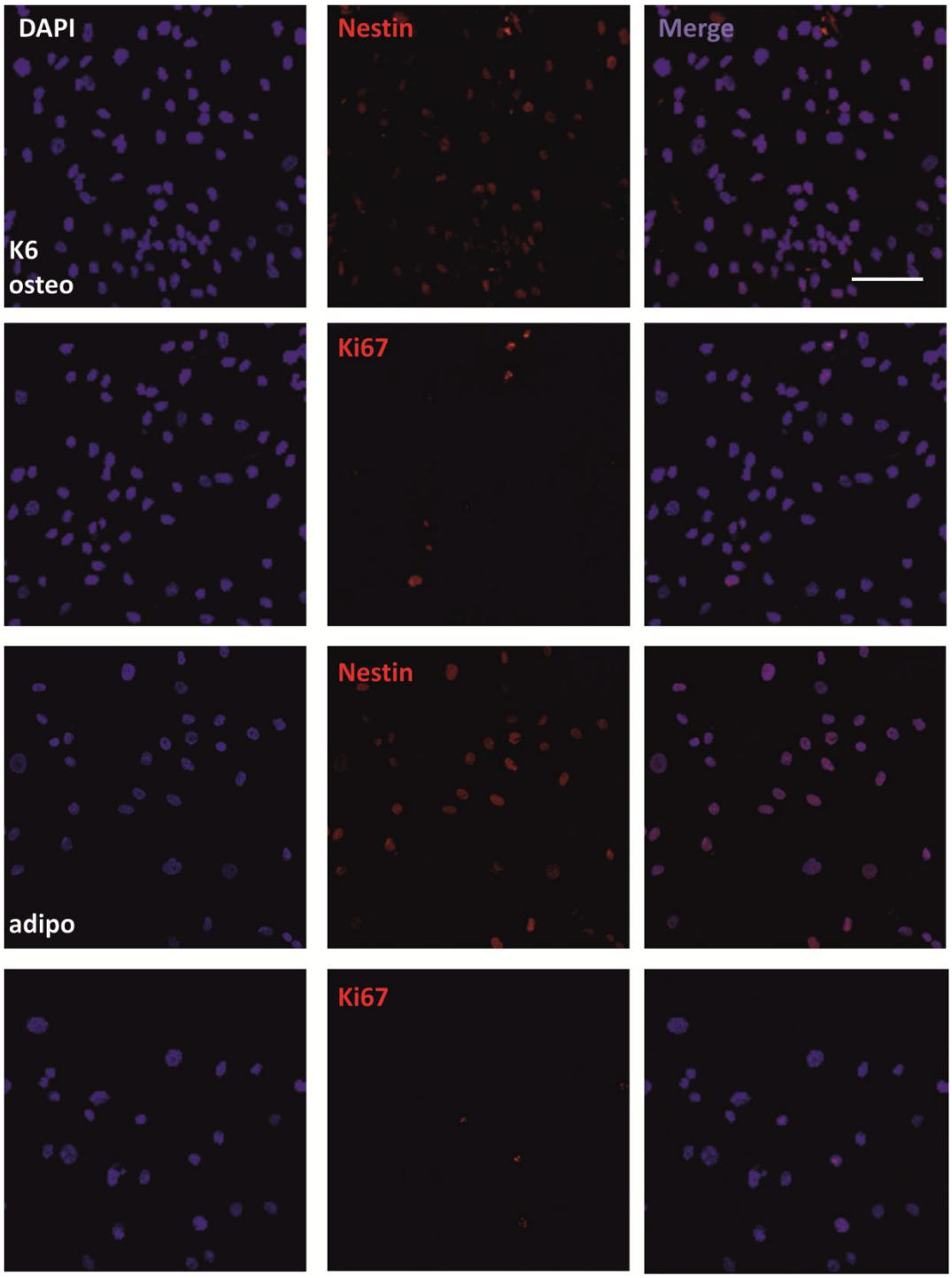

Figure 5.16 Nestin expression and proliferation in differentiated MSCs (K6)
Cells were seeded onto coverslips at 2 x 10^4 cells/cm^2. MSCs were differentiated for 7 days in osteogenic (top) or adipogenic (bottom) induction medium. Nestin (red) could be detected in the nucleus of K6 MSCs. Ki67 staining indicated a small proportion of proliferating cells in each sample. Cells were counterstained with Dapi (blue). Scale bar 100 µm.

5.3.4 IL-7 has no effect on MSC differentiation

To determine the effect of IL-7 addition on differentiating MSCS, cells were seeded into 96 well plates for adipogenic or osteogenic differentiation using 6 wells for each condition. Media was supplemented on day 0 with 20 pg or 20 ng/ml recombinant human IL-7, which was also replenished at each media change. Plates were stained on days 0, 7, 14 and 21 with alizarin red to detect mineralisation or Oil Red O to highlight lipid vesicles. Each of the stains could be eluted and quantified on a microplate reader (Dynex technologies) at 570 nm or 490 nm respectively.

IL-7 had no effect on the ability of cells to undergo adipogenesis (Figure 5.17). A large proportion of cells with lipid vesicles were detected in all wells cultured in adipogenic medium, with no visible difference between the conditions with IL-7 treatment (Figure 5.17, A) This was confirmed by quantifying the Oil Red O stain (Figure 5.17, B). Results shown are representative of 3 donors.

IL-7 also had no effect on the ability of cells to undergo osteogenesis (Figures 5.18 and 5.19). Alizarin red staining was detected in all osteogenic samples from day 7, which increased over time (Figure 5.18, A). No clear difference could be detected between those osteogenic samples with or without the addition of IL-7, which was confirmed with the measurement of the eluted stain (Figure 5.18, B and Figure 5.19). Control samples did not stain positive for alizarin red or Oil Red O at the same time points. No positive stain was detected in control samples that had been cultured with the addition of IL-7 (results not shown). To control for the lack of an effect, the recombinant IL-7 protein (same batch) was subsequently used in T cell survival assays (data not shown) to confirm that the IL-7 was bioactive.

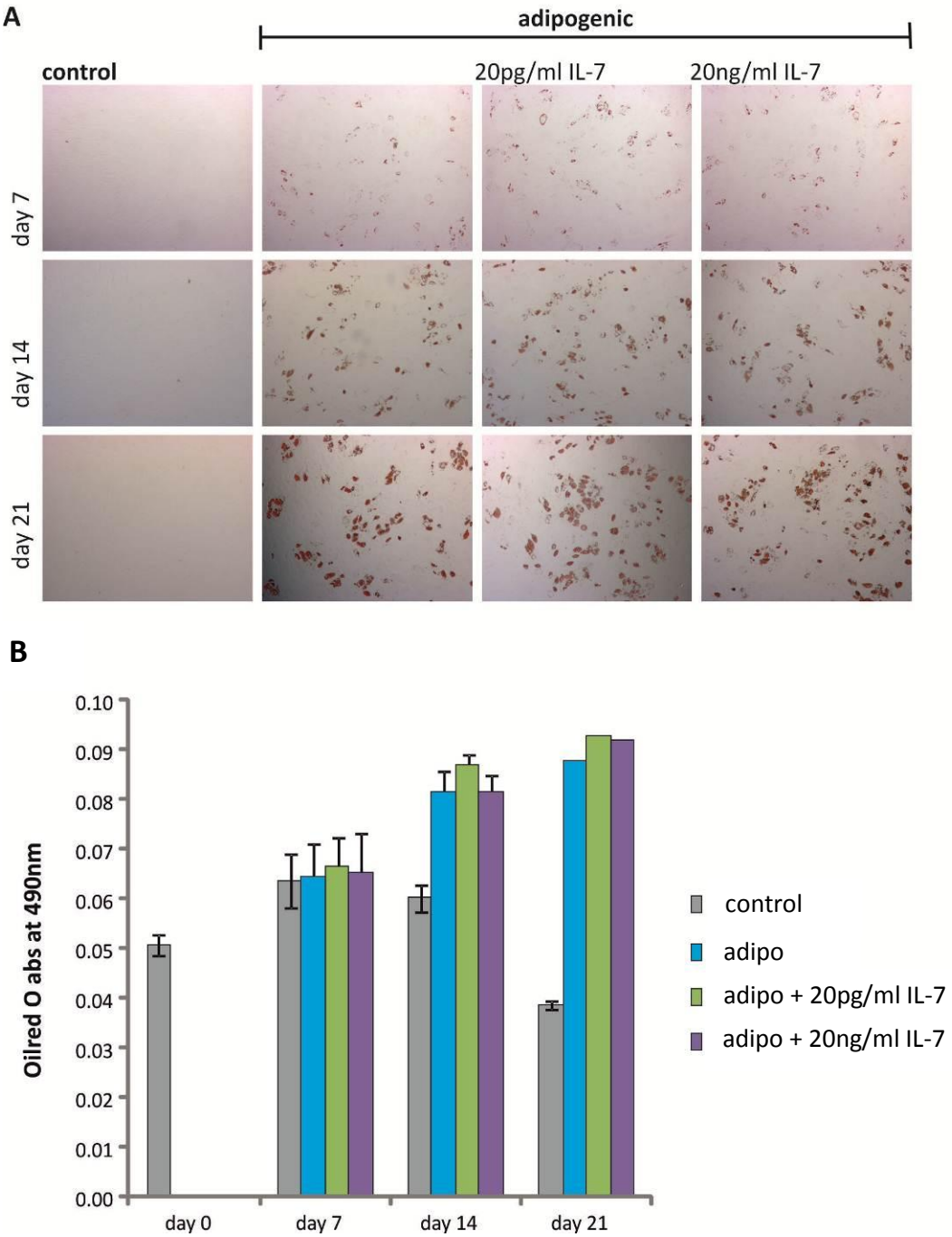

Figure 5.17 Effect of IL-7 on adipogenesis (K6)
MSCs were cultured in 96 well plates for 21 days in control media or adipogenic media. 6 wells were used for each condition. Adipogenic media was supplemented with 20 pg/ml or 20 ng/ml IL-7. Plates were then stained with Oil Red O (red) to detect lipid vesicles (A). Stain was eluted in 100% isopropanol and read on a plate reader at 490 nm (B). The addition of IL-7 had no effect on adipogenesis.

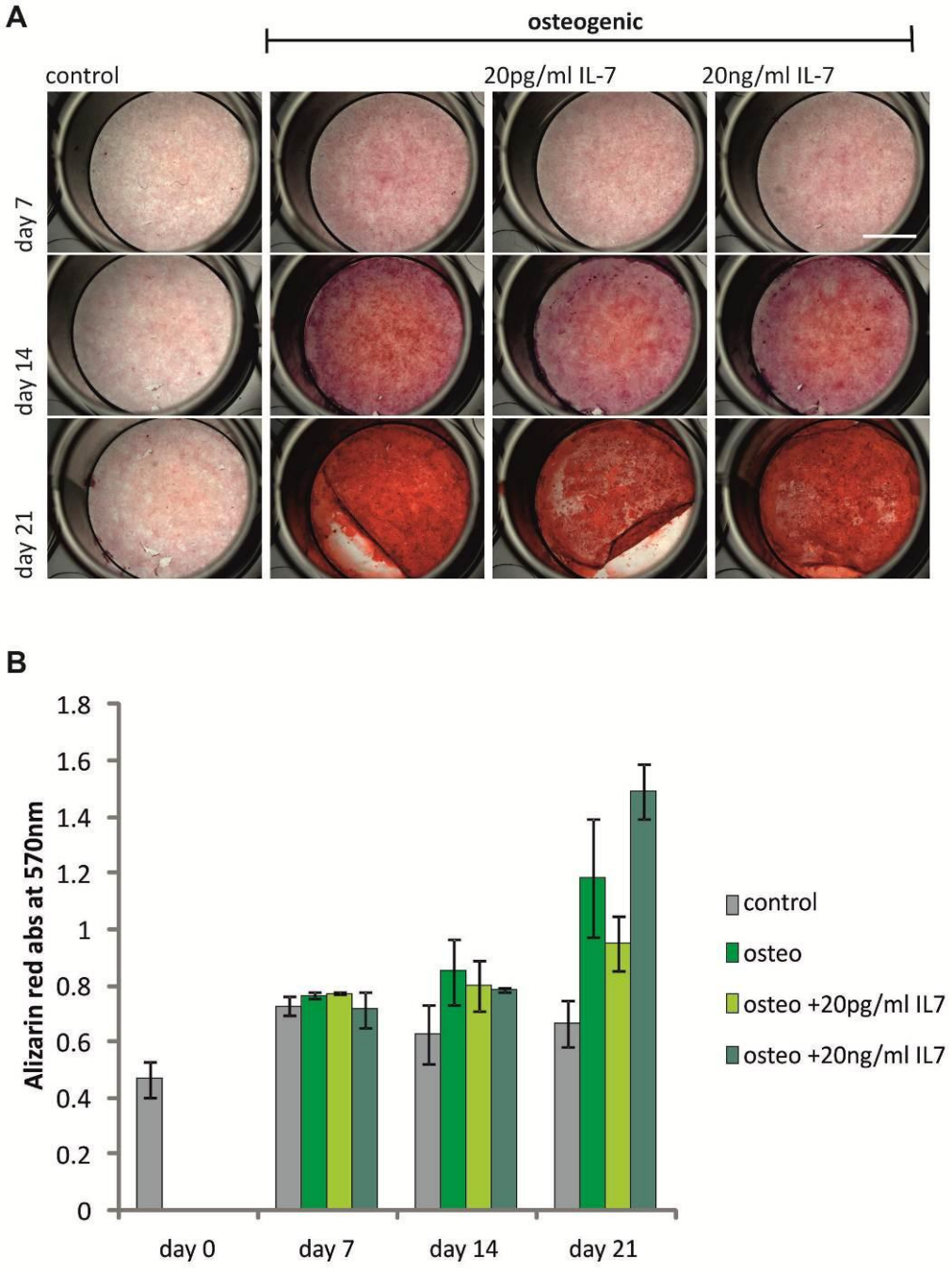

Figure 5.18 Effect of IL-7 on osteogenesis (K6)
Cells were cultured in 96 well plates for 21 days in control media or osteogenic media. 6 wells were used for each condition. Osteogenic media was supplemented with 20 pg/ml or 20 ng/ml IL-7. Plates were then stained with alizarin red (red) to detect mineralisation (A). Stain was eluted in 10% CPC and read on a plate reader at 570 nm (B). The addition of IL-7 had no effect on osteogenesis. Scale bar 500 µm.

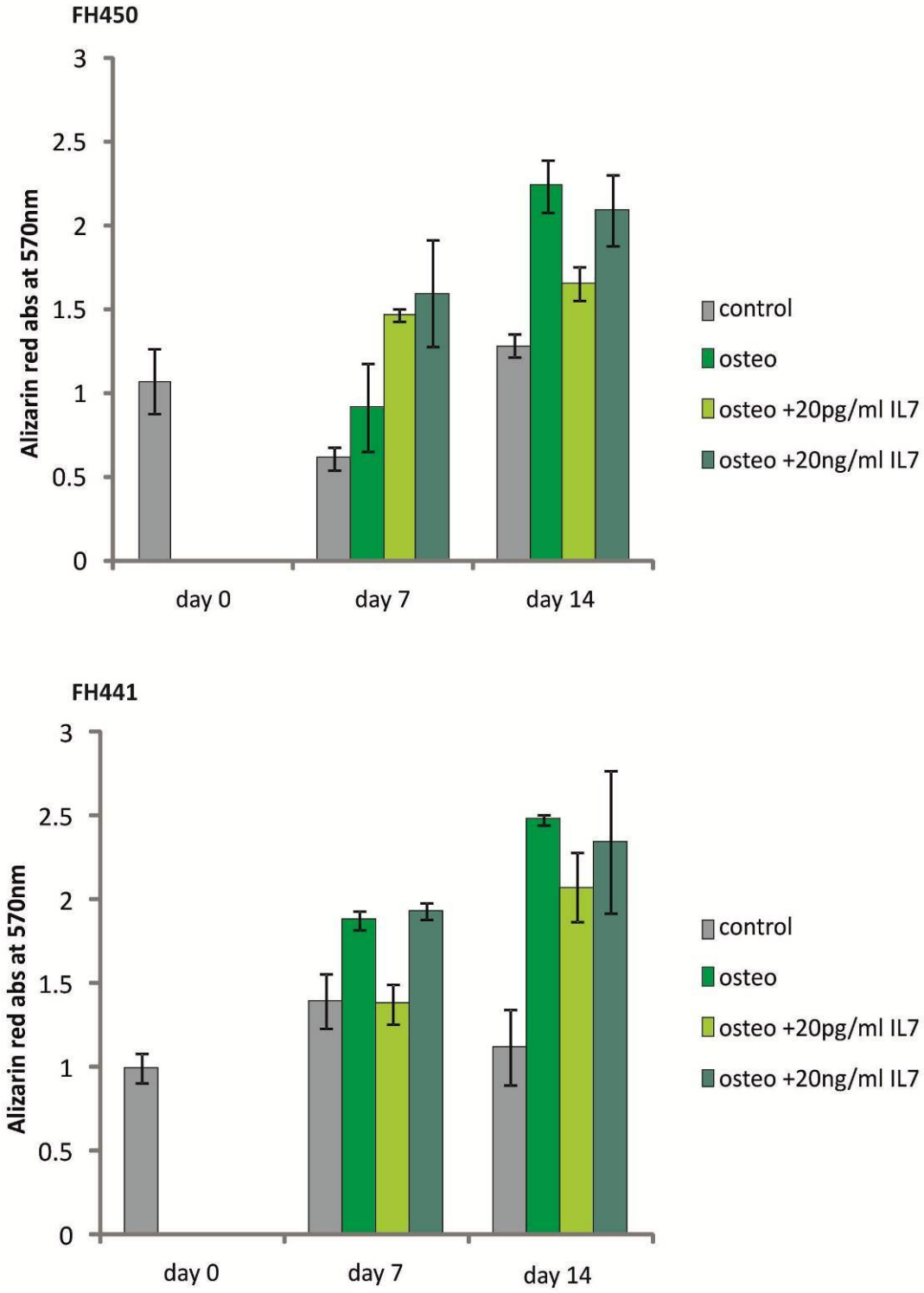

Figure 5.19 Effect of IL-7 on osteogenesis
MSCs (FH450, top and FH441, bottom) were cultured in 96 well plates for 14 days in control media or osteogenic medium. 6 wells were used for each condition. Osteogenic medium was supplemented with 20 pg/ml or 20 ng/ml IL-7. Plates were then stained with alizarin red to detect mineralisation, which was eluted and the absorbance measured at 570 nm.

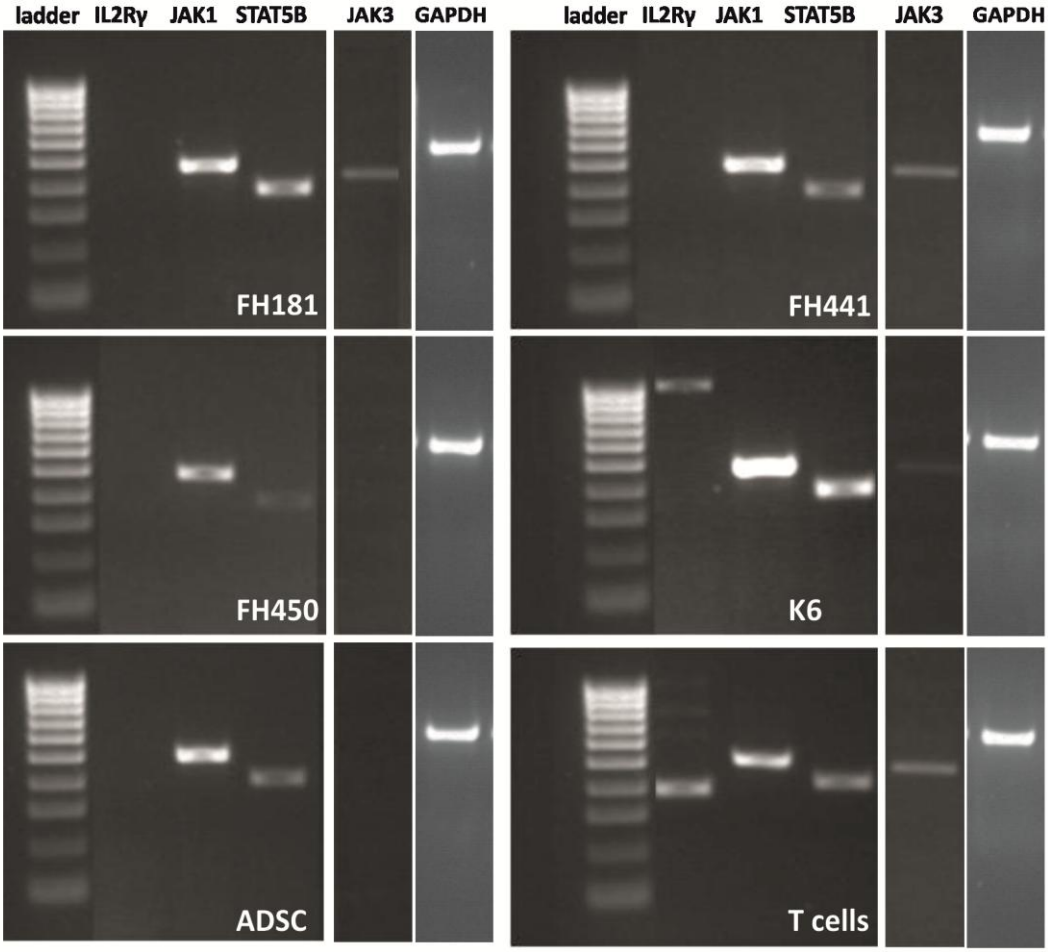

Figure 5.20 Expression of IL-7 signalling components
RT-PCR confirmed the presence of components of the JAK/STAT signalling pathway in MSCs. Human T cells were used as a positive control.

5.3.5 IL-7 signalling in MSCs

IL-7 is known to signal through the JAK/STAT pathway in B and T cells. Initially, IL-7 is bound by its receptor IL-7Rα, recruiting a second receptor subunit, the common γ chain (IL2Rγ) which is a binding subunit shared by many other cytokines. Initiation through JAK1 and JAK3 leads to the downstream phosphorylation and activation of STAT5. In order to assess the gene expression of these signalling molecules in MSCs, RNA was extracted from monolayers of MSCs seeded out 24 hours previously at 2 x 10^4 cells/cm^2. ADSCs were also included in the analysis to represent MSCs derived from an alternative source. RT-PCR confirmed the presence of some of the components of this signalling pathway; JAK1 and STAT5B were detected in human MSCs but IL2Rγ was only detected in human T cells. JAK3 was present in donors FH441, FH181 and K6 but it was not detected human ADSCs or donor FH450 (Figure 5.20). Knee and femoral head derived MSCs as well as ADSCs showed almost identical expression of each of the signalling components.

As the initial step in IL-7 signalling is the binding of IL-7 to its receptor, MSCs were then assessed for their ability to bind to IL-7. An assay was carried out using biotinylated IL-7 followed by incubation with FITC conjugated avidin that allowed the detection of bound protein by flow cytometry (see section 2.7.6). T cells are known to bind IL-7 and were used as a positive control. Donors FH441 and K6 were also able to bind IL-7 (Figure 5.21, green lines). Controls including a negative control biotinylated protein and a sample incubated with the addition of an anti-IL-7 blocking antibody did not show any positive FITC detection, indicating the specificity of the assay (Figure 5.21).

In order to address some of the reported downstream effects of IL-7, several experiments were carried out to look at altered gene expression. IL-7 is reported to have an impact on the inflammatory cytokine IL-6. An increase of IL-6 was detected by real time PCR after 3 hours and decreased again at 24 hours to levels observed before the addition of IL-7. This pattern of expression was identical in both control and treated samples (Figure 5.22, A). A possible explanation is the method of IL-7

addition to the MSCs. The culture medium was replaced at the beginning of the timecourse with fresh medium containing the IL-7; therefore, the increase may be the effect of fresh serum in the medium and not a true IL-7 mediated effect.

IL-7Rα was not detected by flow cytometry in bone marrow derived MSCs from four donors in control conditions or following treatment with 20 ng/ml or 20 pg/ml IL-7 for 24 hours (Figure 5.22, B). Additional concentrations of 0.1 and 10 ng/ml IL-7 were also used to treat MSCs for 24 hours and RNA was collected and examined by real time PCR for the expression of IL-7Rα, IL-7 and nestin. Compared to cells that received no IL-7 treatment, 20 pg/ml IL-7 reduced the expression of IL-7Rα ($p=0.002$) but higher concentrations of IL-7 did not alter the expression of the receptor. Conversely, the two highest concentrations of IL-7 (10 and 20 ng/ml) led to an increase in relative IL-7 expression. Nestin expression was not affected in an IL-7 dose dependent manner as 20 pg/ml slightly decreased nestin expression ($p=0.001$), 10 ng/ml decreased it further ($p=0.003$) but 20 ng/ml increased the expression ($p= 0.012$) compared to the control (Figure 5.23).

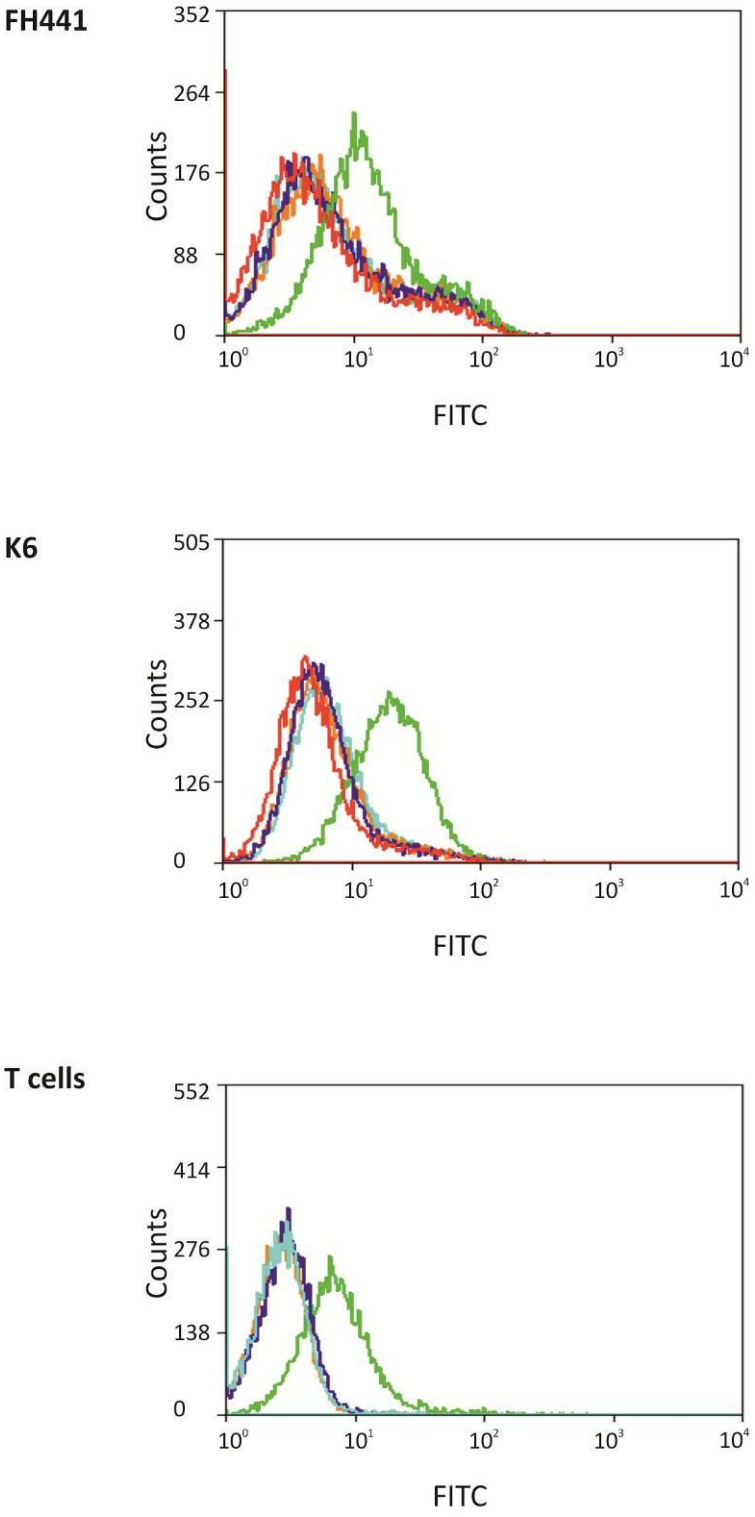

Figure 5.21 IL-7 binding assay
MSCs were incubated with IL-7 (green line), a negative protein control (blue line) or no protein control (turquoise line) followed by FITC-conjugated avidin. Bound protein could then be measured by flow cytometry. To test the specificity of the assay, some cells were also incubated with anti-IL-7 antibodies (orange line) which reduced the binding to control levels (red line).

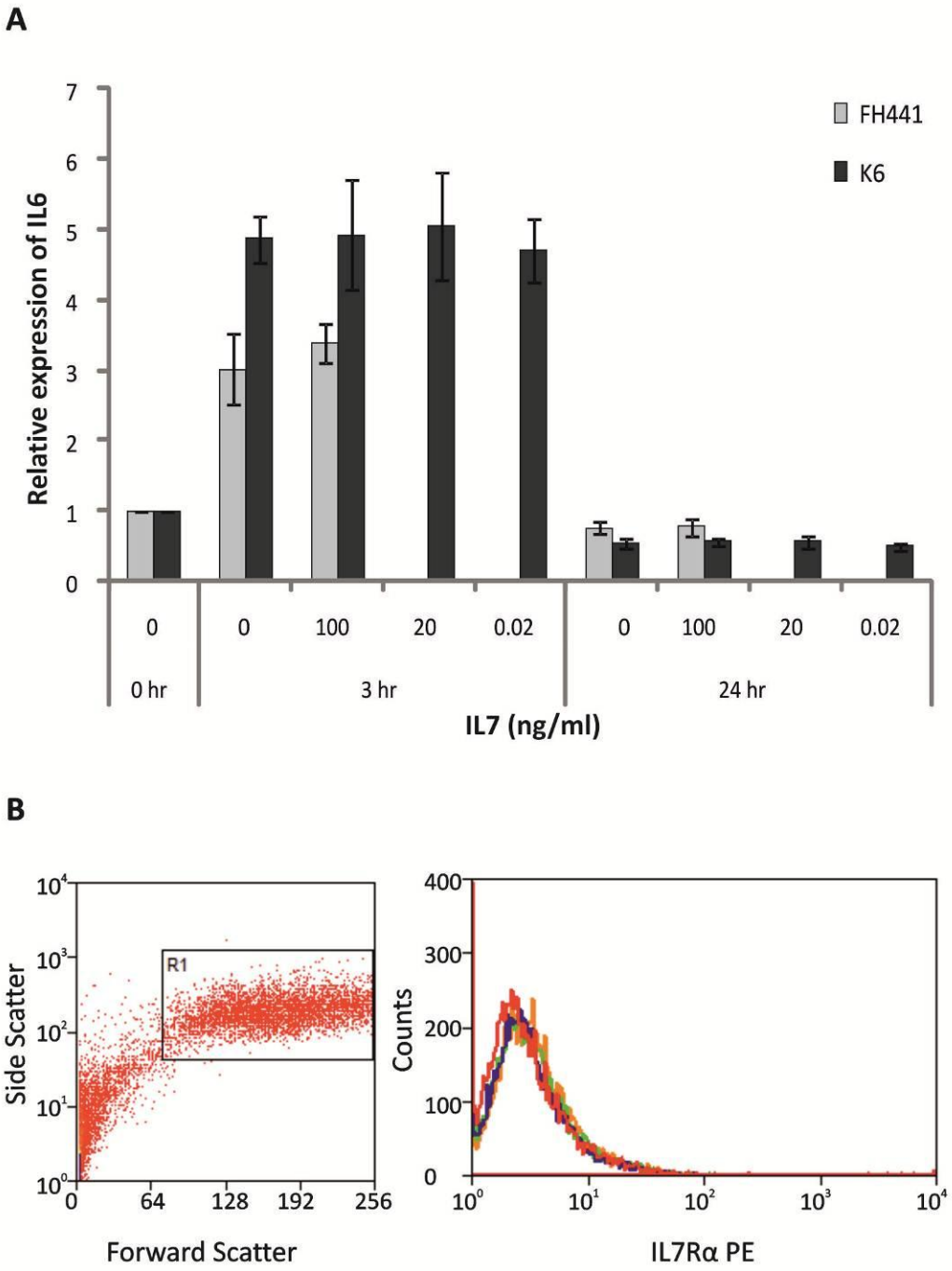

Figure 5.22 Effect of IL-7 on IL-6 and IL-7Rα expression
qRT-PCR was used to determine the expression of IL-6 after IL-7 treatment for 3 hours and 24 hours on MSC monolayers (A). The expression of IL-7Rα was determined by flow cytometry after 24 hour treatment with IL-7 (B). No expression was found in any donor (K6 shown) or after IL-7 treatment. Red line, cells only; blue line, IgG control; orange line, 20 pg/ml IL-7; green line, 20 ng/ml IL-7. PE-conjugated anti IL-7Rα was used.

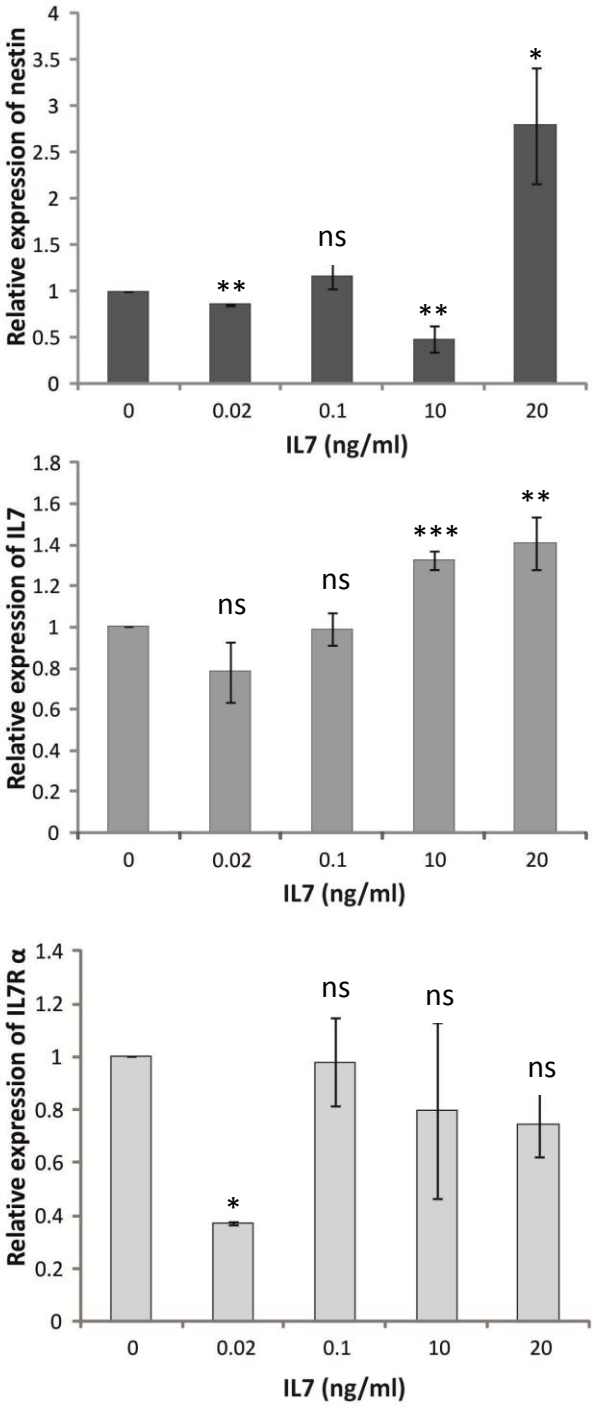

Figure 5.23 Effect of IL-7 on IL-7 and nestin expression in MSCs (K6)
Media was supplemented with IL-7 for 24 hours before RNA collection and qRT-PCR analysis for nestin (top graph) and IL-7 (bottom graph) mRNA expression.
$p \leq 0.05$ not significant (ns), $p < 0.05$ *, $p < 0.01$ **, $p < 0.001$ *** represents statistical significance determined by t-test.

5.3.6 IL-7 has no effect on MSC proliferation

IL-7 is known to enhance T and B cell proliferation. To examine if it has a similar impact on MSCs, cells were grown for 7 days in the presence of IL-7 and their proliferation assessed by a CCK-8 kit (Dojindo) on days 3, 5, and 7. This kit uses a colourimetric assay based on cellular dehydrogenase reduction of a tetrazolium salt to give an indication of the number of viable cells present. The amount of formazan produced is directly proportional to the number of living cells. An increase in absorbance was detected over 7 days in K6 cells and reached a stable level in FH441 cells by day 3 indicating that the cells had proliferated over 7 days. No increase was detected with the presence of IL-7 in either donor examined (Figure 5.24).

In experiments presented earlier in this chapter, IL-7 mRNA expression has been seen to increase in MSC cultures at day 7 and beyond, whilst nestin generally decreases upon culture and differentiation. In order to assess how quickly these changes in gene expression take place in control culture conditions, RNA samples were collected daily for 7 days and analysed for nestin and IL-7.

In donor FH450, nestin expression decreased on day 1 to 20% that of the day 0 sample and maintained a low expression level throughout the 7 days rising slightly to 40% on days 6 and 7 (Figure 5.25). IL-7 expression was determined in cells that had been seeded out at 2 initial plating densities. All cells had increased IL-7 expression compared to day 0. Those cells seeded out at the low density generally had higher IL-7 expression than their counterparts seeded at a higher density. In a repeat of the experiment, K6 cells were seeded out at a range of cell densities. Mitomycin C was added for 1 hour on day 0 to a series of cells seeded at 2×10^4 cells/well to arrest cell proliferation. Nestin was decreased as before to approximately 50% that of the day 0 level, which was maintained at days 5 and 7 in cells seeded out at 2×10^4/well and higher. Those cells seeded lower saw an increase in nestin expression over 7 days compared to their day 0 controls. Mitomycin C treatment also increased nestin expression at each time point.

IL-7 expression increased in the 2 highest seeding densities over 7 days with a peak on day 3 followed by a subsequent decrease. Cells seeded at lower densities showed a progressive increase in IL-7 over 7 days of culture. Mitomycin C treated cells had approximately half the level of IL-7 expression than those cells seeded out at the same density, which may indicate a role for IL-7 in proliferating MSCs.

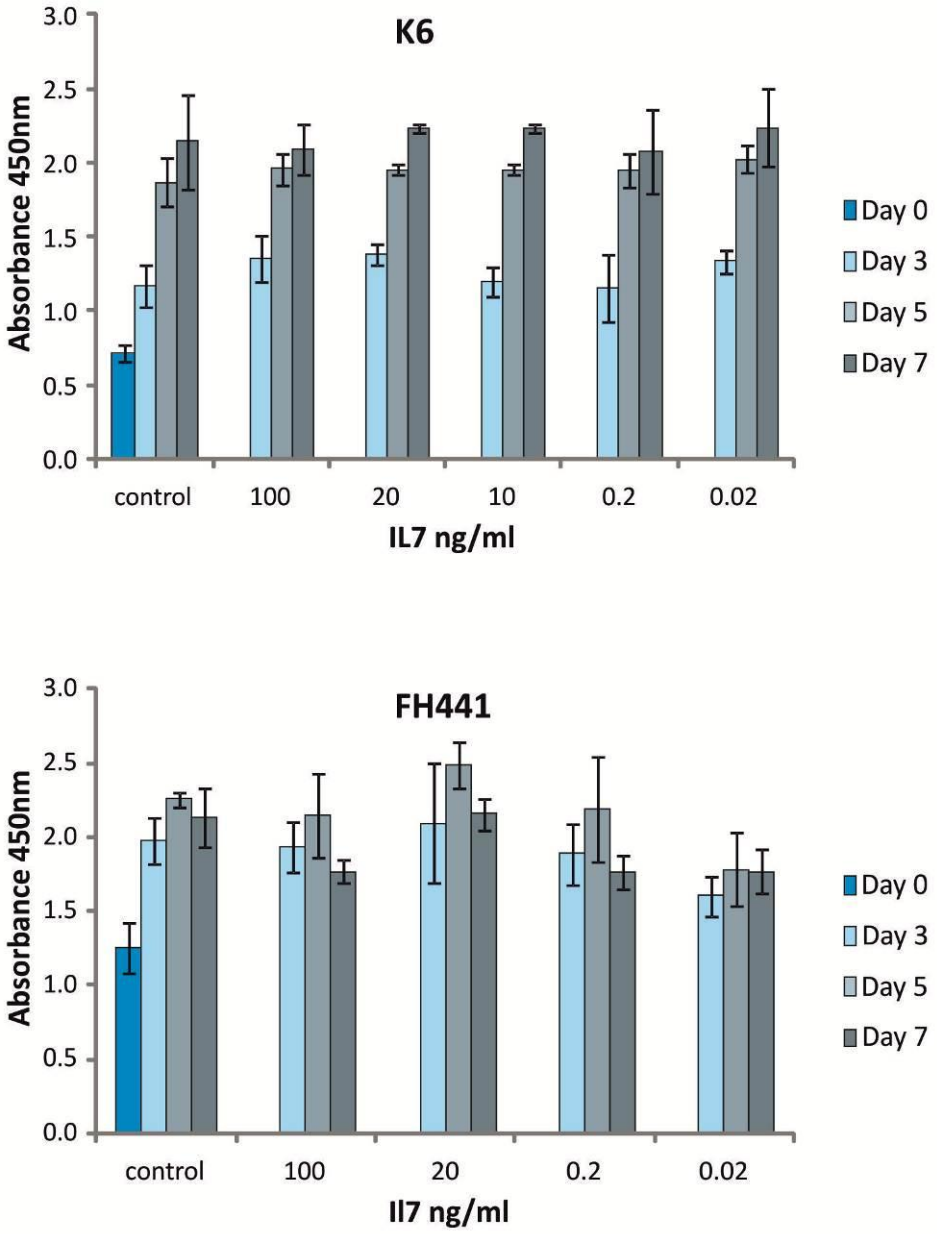

Figure 5.24 IL-7 treatment does not affect MSC proliferation
Cells were seeded into 96 well plates and cultured for 7 days with control media or media supplemented with IL-7, which was replenished with media changes. A colourimetric assay to measure cell proliferation (CCK-8) was carried out and the resulting absorbance, measured at 450 nm, was proportional to the number of viable cells.

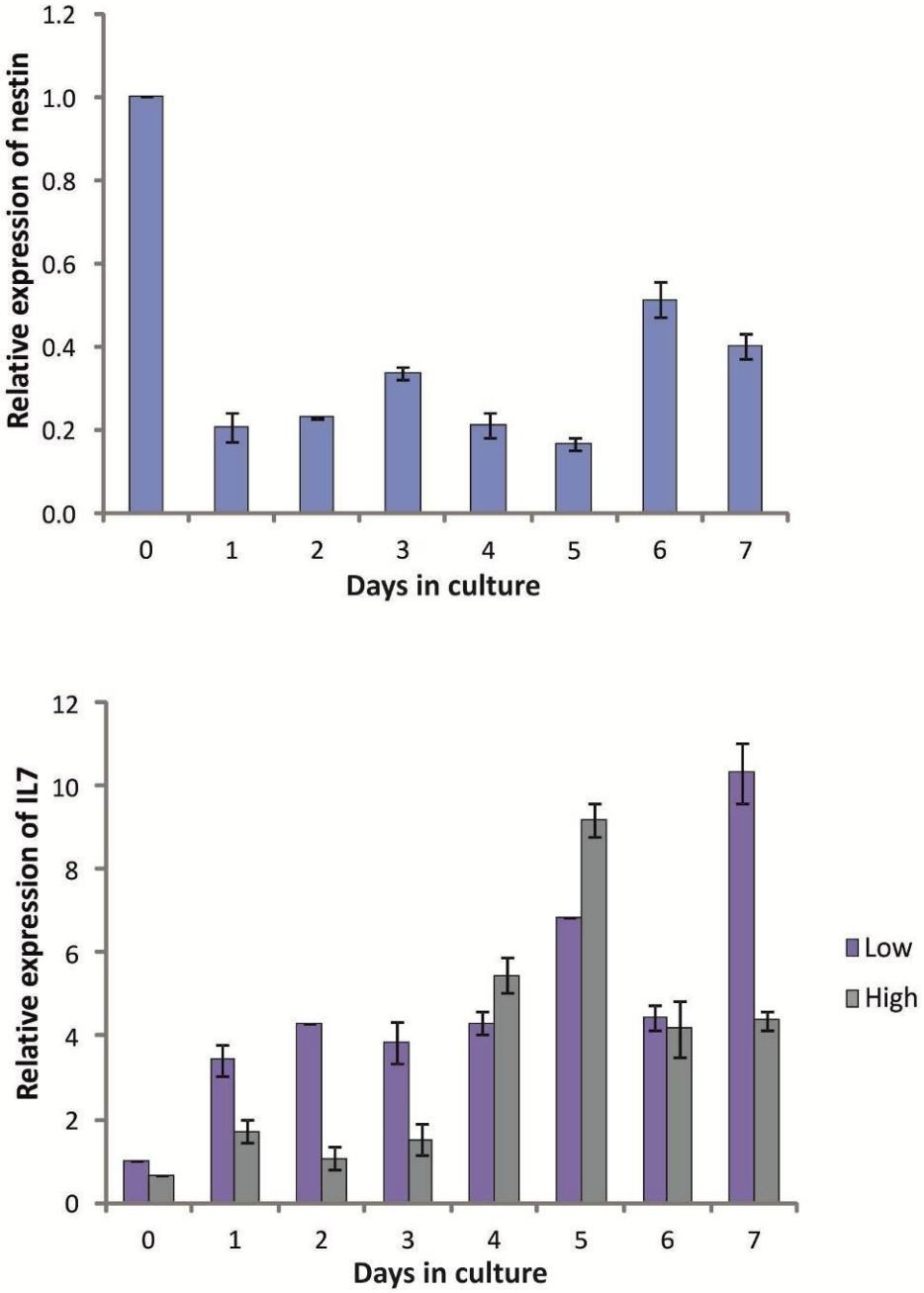

Figure 5.25 Nestin and IL-7 expression over 7 day culture (FH450)
MSCs were seeded out at high or low density and RNA collected over 7 days and examined by qRT-PCR for nestin (top) and IL-7 (bottom).

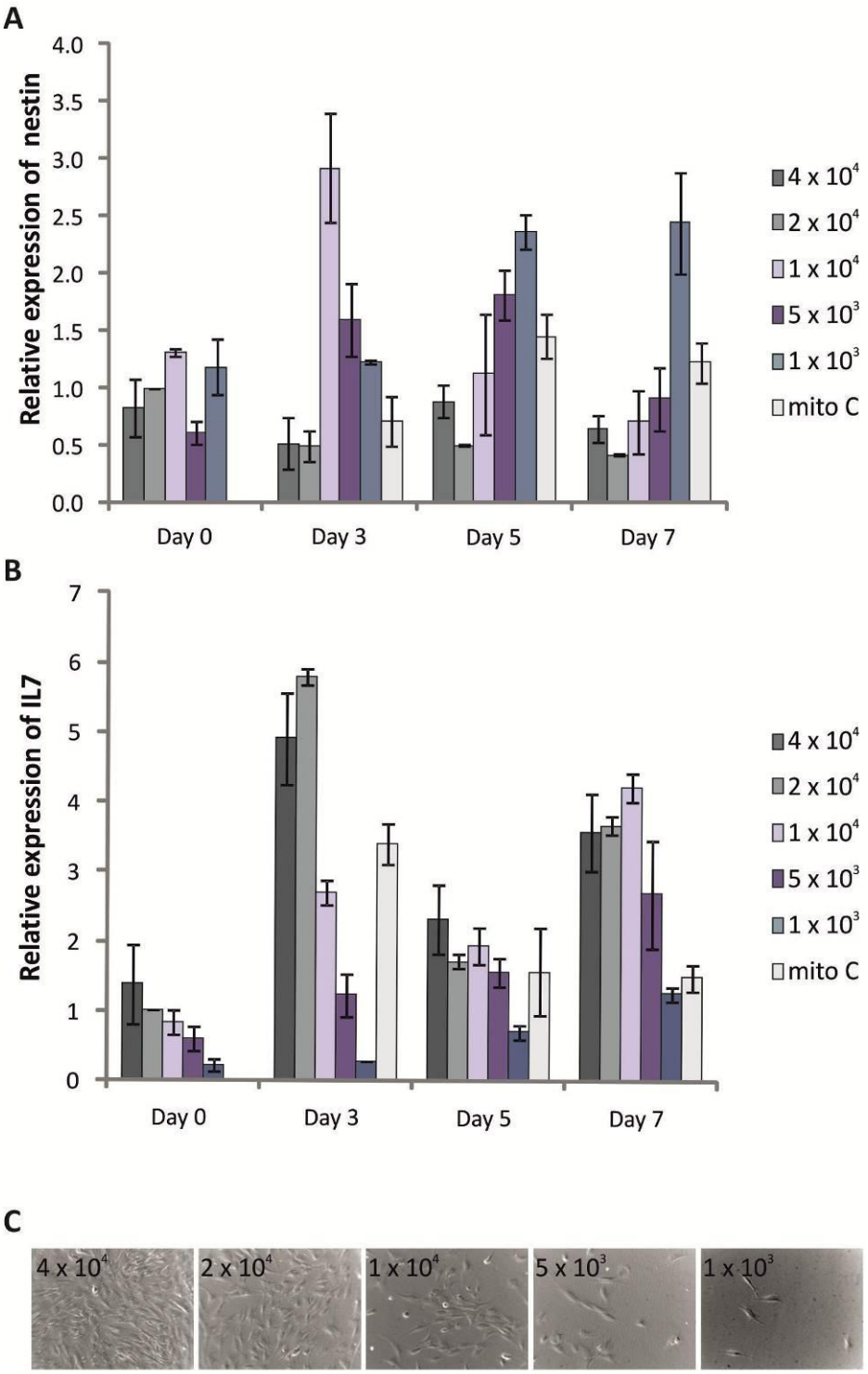

Figure 5.26 Effect of seeding density on Nestin and IL-7 (K6)
MSCs were plated at different densities and RNA collected over 7 days to examine nestin (A) and IL-7 (B) expression by qRT-PCR. Cells treated with mitomycin C were seeded at 2 x $10^4/cm^2$. Brightfield images show cells on day 0 (C).

5.3.7 Generation and analysis of MSC clones

By the nature of their isolation, MSC cultures are a heterogeneous population that may contain cells at various stages of commitment and varying levels of differentiation potential. In order to address the expression of IL-7 and nestin in cells derived from an individual progenitor, clonal lines were generated. MSCs were originally described by their ability to generate colony-forming units and this character was exploited to isolate clusters of cells that arose from an individual MSC.

MSCs seeded out at clonal density (10 cells/cm^2) led to the establishment of CFUs, which were harvested and expanded in culture. Many donors (n=6) were set up at different passages and into either dishes or wells of a 6-well plate. In several cases (62/142 plates), the colonies that were produced were not suitable for harvest due to close proximity to other cells or colonies which could lead to isolation of cells from multiple progenitors. Higher passage cells (5+) tended to produce an even outgrowth of cells in monolayer that did not form defined clusters of cells. In some cases, those colonies that were harvested did not: adhere when re-seeded into individual wells, expand in culture sufficiently or produce a large enough sample of clonal lines.

Two donors, K6 and FH408, yielded 19 and 17 clones respectively that could be expanded to sufficient number to extract RNA. K6 colonies had a 100% success rate of colony formation to cell expansion, while 59% of FH408 colonies harvested from one batch survived and proliferated enough to analyse further. Cells were cultured for 4 weeks after colony harvest and seeded into 6-well plates at 5 x 10^4 cells/well and RNA extracted 24 hours later. Real time PCR identified differences in gene expression amongst the clones. K6 clones were compared to RNA extracted from the parent line of the same passage and showed a range of expression of both nestin (Figure 5.27, A) and IL-7 (Figure 5.27, B). The pattern of expression was not the same for each gene and in some cases was opposite. Clone 19 showed the highest relative expression of IL-7 and high nestin expression whilst clone 3 had

highest level of IL-7 and barely detectable level of nestin and clone 13 had much higher levels of nestin than IL-7.

Cell numbers were counted as they were harvested to move to increasingly larger plates and flasks. The clones that proliferated most and produced the highest final cell number were 5, 16 and 19 (Figure 5.27, C). Clones 5 and 16 showed moderate expression of IL-7 and nestin and, as mentioned, clone 19 had high levels of both. Clones 1, 3, 7, 11, 12 and 15 were used solely for gene analysis as they had expanded to sufficient numbers for RNA extraction, but not for further differentiation culture. All other clones were also put into osteogenic differentiation studies in 96 well plates. Clones 5, 9 and 16 were seeded into 6 wells per condition of control or osteogenic media. Owing to the small number of cells, the remaining clones had between 1 and 4 wells per condition, so these results give an indication of their ability to differentiate but the comparisons are made mindful of the small sample number.

Alizarin red staining showed that all clones were capable of osteogenic differentiation. Clones 4, 5, 8 and 10 had the highest degree of staining after 21 days. Each of these clones had a similar, moderate expression of nestin (12 ± 1.9) and differed in their IL-7 expression. IL-7 was undetectable in clone 4, and negligible in clone 10 but comparable to the parental line in clones 5 and 8. The lowest level of staining was in clone 13, which had the second highest expression level of nestin and almost undetectable IL-7.

Additionally, 4 clones were analysed for adipogenic potential. Oil Red O staining of clones that had been cultured in adipogenic conditions showed that of the 4 clones that were analysed, clone 5 did not produce any visible lipid vesicles whilst clone 19 had many more cells staining positive (Figure 5.30, B). Quantification of the eluted stain did not show this clearly; perhaps due to the small amount of stain to be measured making small differences indeterminate (Figure 5.30, C). Cells were seeded to confluence in 96 well plates and cultured with chondrogenic media for 14

days, all of which stained faintly with alcian blue. Clone 16 cells detached from the bottom of the well and formed aggregates. Chondrogenesis would normally be measured in pellet culture but as not enough cells were available, monolayer culture was hoped to give an indication of differentiation. Alcian blue staining was weak but apparent in each of the wells with chondrogenic factors and not in control wells. An extended period of culture may have increased the differentiation but would certainly benefit from traditional pellet culture differentiation.

FH408 clones also showed a range of expression levels for nestin and IL-7 when analysed (Figure 5.31). Generally, the clones had low IL-7 expression levels and higher nestin levels. Fourteen clones were induced with osteogenic media and were all able to differentiate (Figure 5.32, A). Weaker alizarin red staining was observed in induced clones 4 and 9 indicating less differentiation (Figure 5.32, B). Clone 4 had the highest expression of nestin with a moderate IL-7 level but clone 9 showed a similar pattern to the expression levels of other clones. Again, this variation may simply be due to the small sample number. Analysis of more clones would allow greater prediction of outcome based on gene expression. Only 3 FH408 clones had sufficient cells to determine adipogenic differentiation. Clones 1, 4 and 6 all showed cells with lipid vesicles with clone 1 generating a greater number of positively-stained cells than clones 4 and 6 (Figure 5.32, C).

Donor	Passage	Dishes/wells	Colonies harvested
K6	1	10	9
	3	17	0
	4	17	19
	5	3	6
	6	12	0
	7	12	0
FH408	3	8	29
	4	9	13
FH441	1	5	20
	2	3	0
	3	5	0
FH496	3	18	0
FH492	1	3	0
	2	3	5
K61	0	17	8

Table 5.1 CFU-F assays

MSCs were seeded at clonal density (10 cells per cm^2) and cultured for 14 days before discrete colonies were harvested using cloning cylinders and trypsinisation. A large number were discounted due to apparent cell migration between colonies or close proximity to other colonies that could not be distinguished using the cloning cylinders.

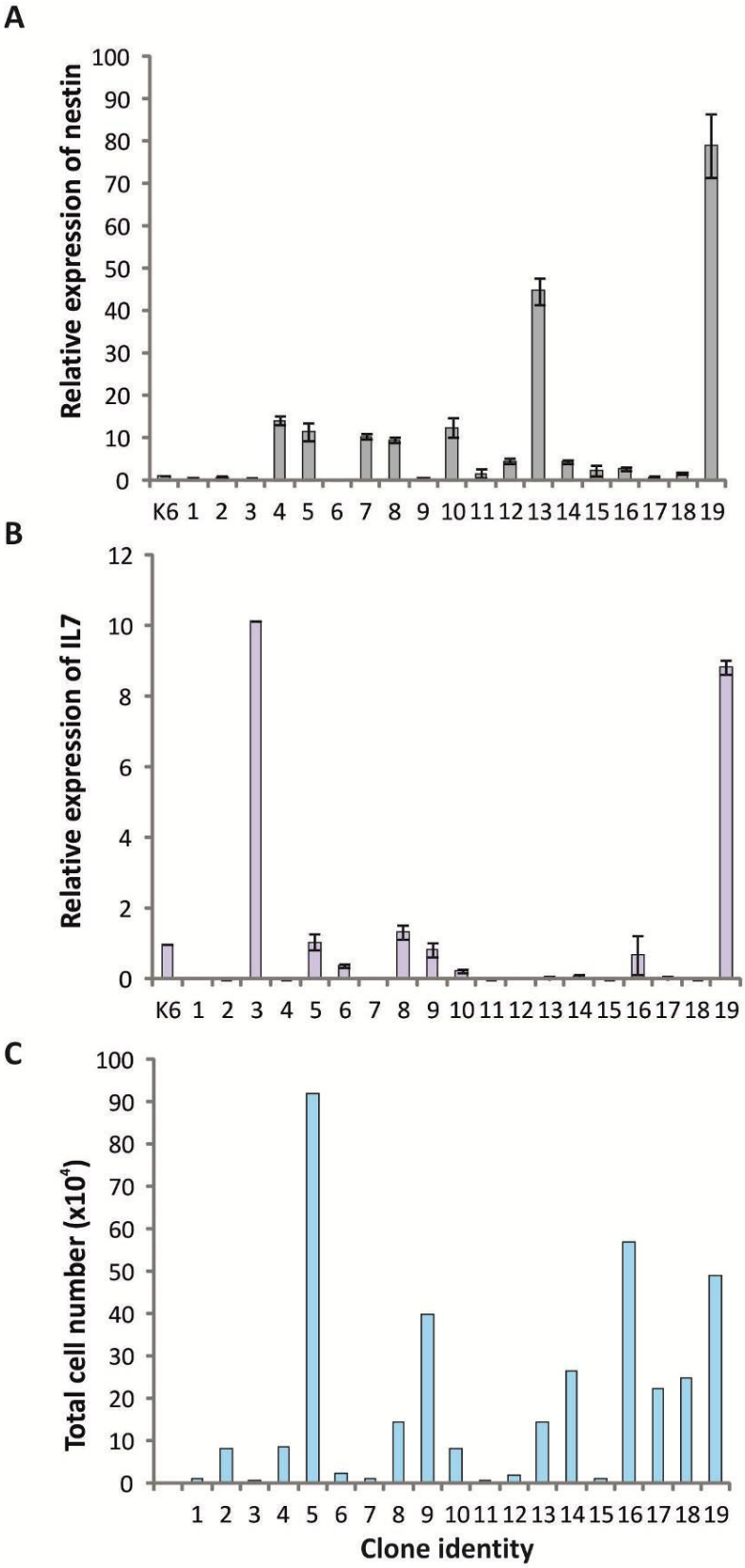

Figure 5.27 qRT-PCR analysis of K6 clonal lines

RNA was extracted from 19 clones and examined for expression of nestin (A) and IL-7 (B) mRNA. Cell numbers are represented as the total accumulated over 27 days culture after initial colony harvest (C).

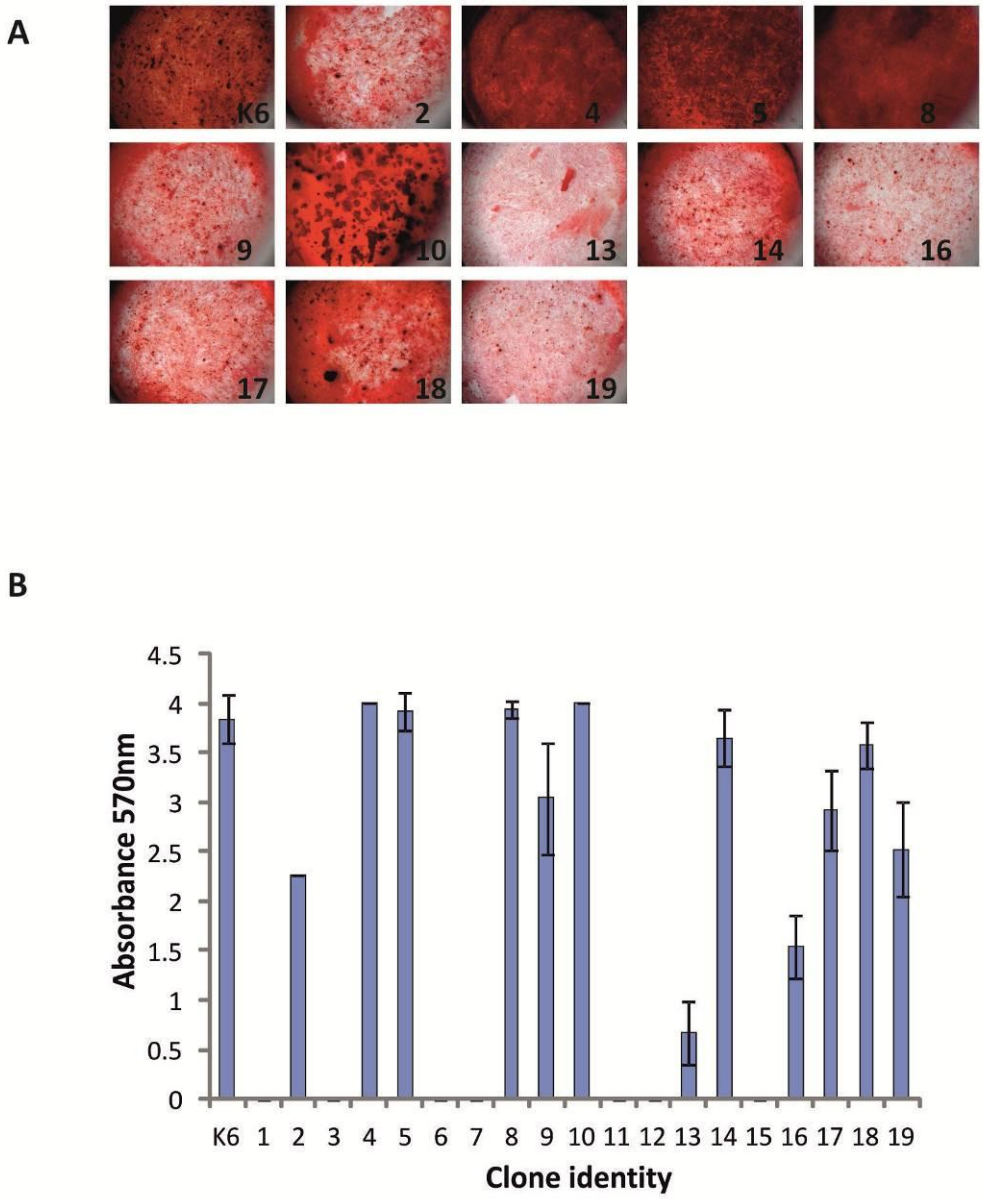

Figure 5.28 Osteogenic differentiation of K6 clones
Cells were cultured in 96 well plates for 21 days in control media or osteogenic media. Up to 6 wells were used for each condition. Plates were then stained with alizarin red (red) to detect mineralisation (A). Stain was eluted in 10% CPC and read on a plate reader at 570 nm (B). 12/19 clones were assayed for osteogenic ability.

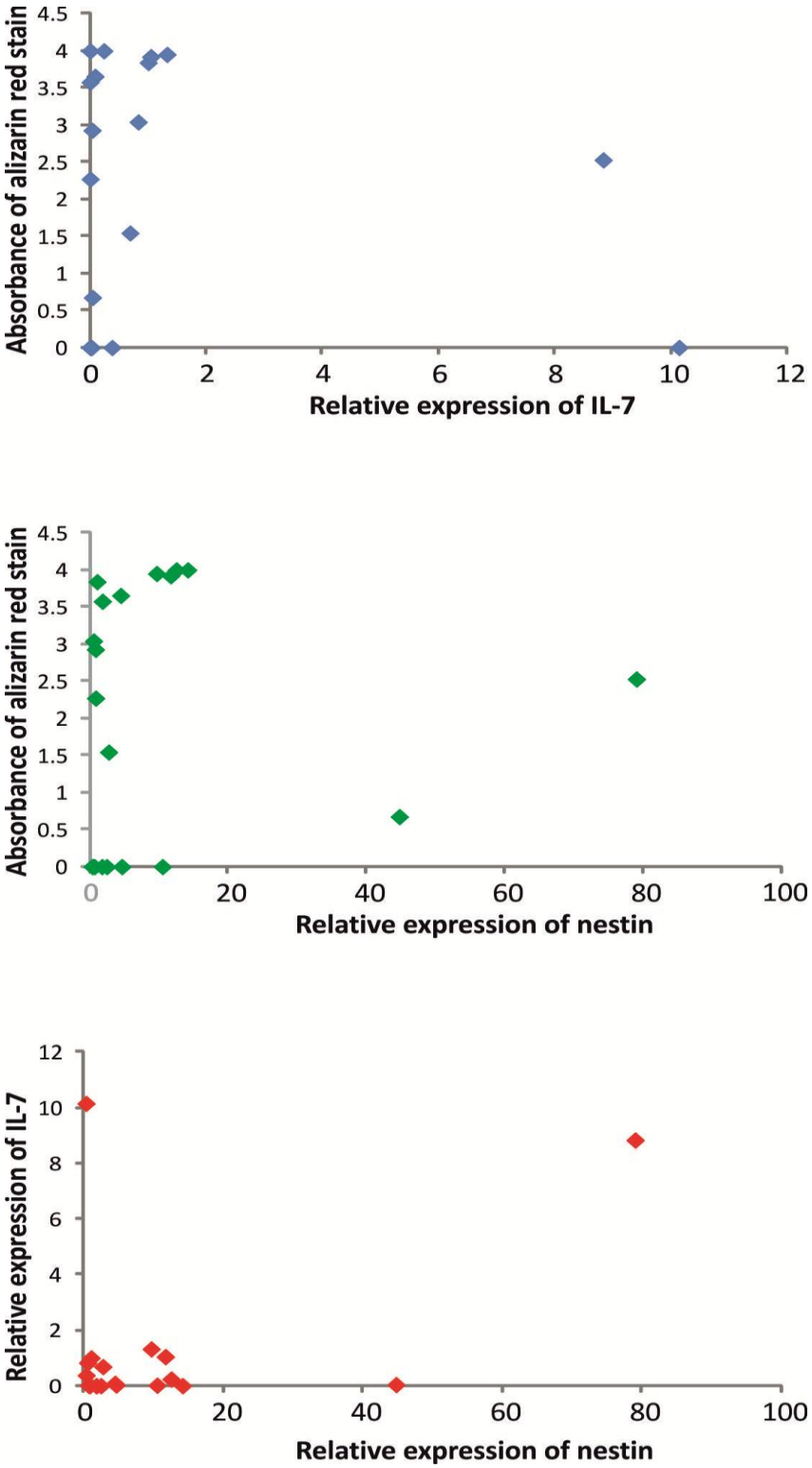

Figure 5.29 Osteogenic differentiation of K6 clones
Relationship between IL-7 and nestin gene expression and osteogenic differentiation performance of K6 clones.

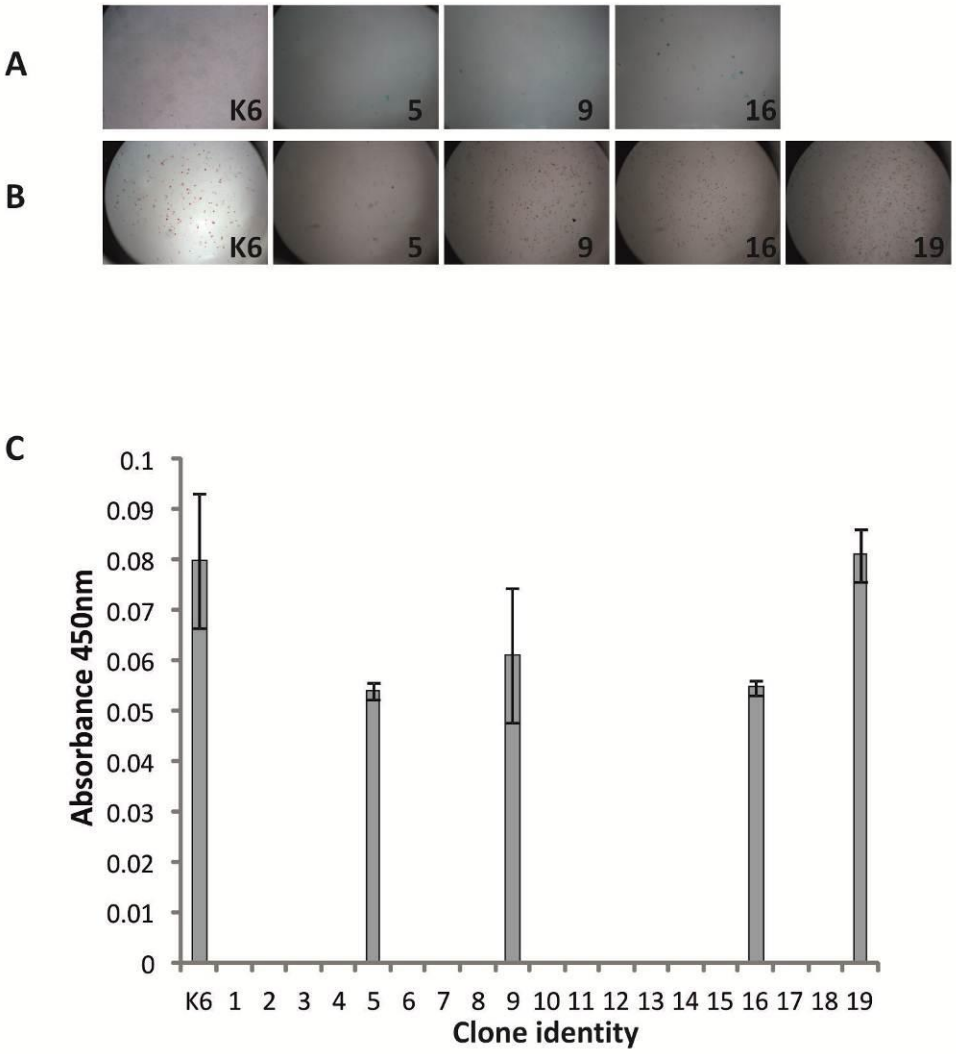

Figure 5.30 Adipogenic and chondrogenic differentiation of K6 clones
Cells were cultured in 96 well plates for 14 days in control media or chondrogenic or adipogenic media. Up to 6 wells were used for each condition. Plates were then stained with alcian blue (A) to detect chondrogenic differentiation or Oil Red O (red) to detect lipid vesicles (B). Oil Red O stain was eluted in 100% isopropanol and read on a plate reader at 490 nm (C).

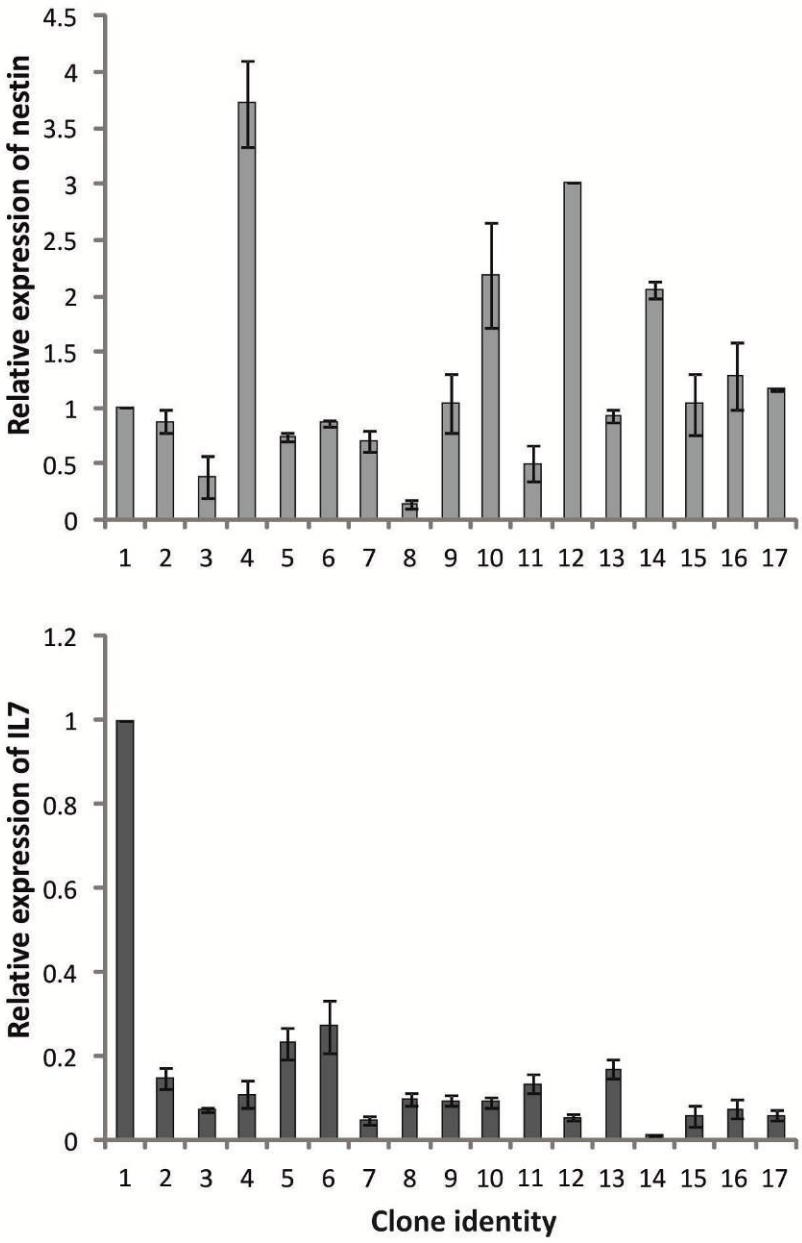

Figure 5.31 qRT-PCR analysis of FH408 clonal lines
RNA was extracted from 19 clones and examined for expression of nestin (top) and IL-7 (bottom) mRNA. Expression is represented relative to clone 1.

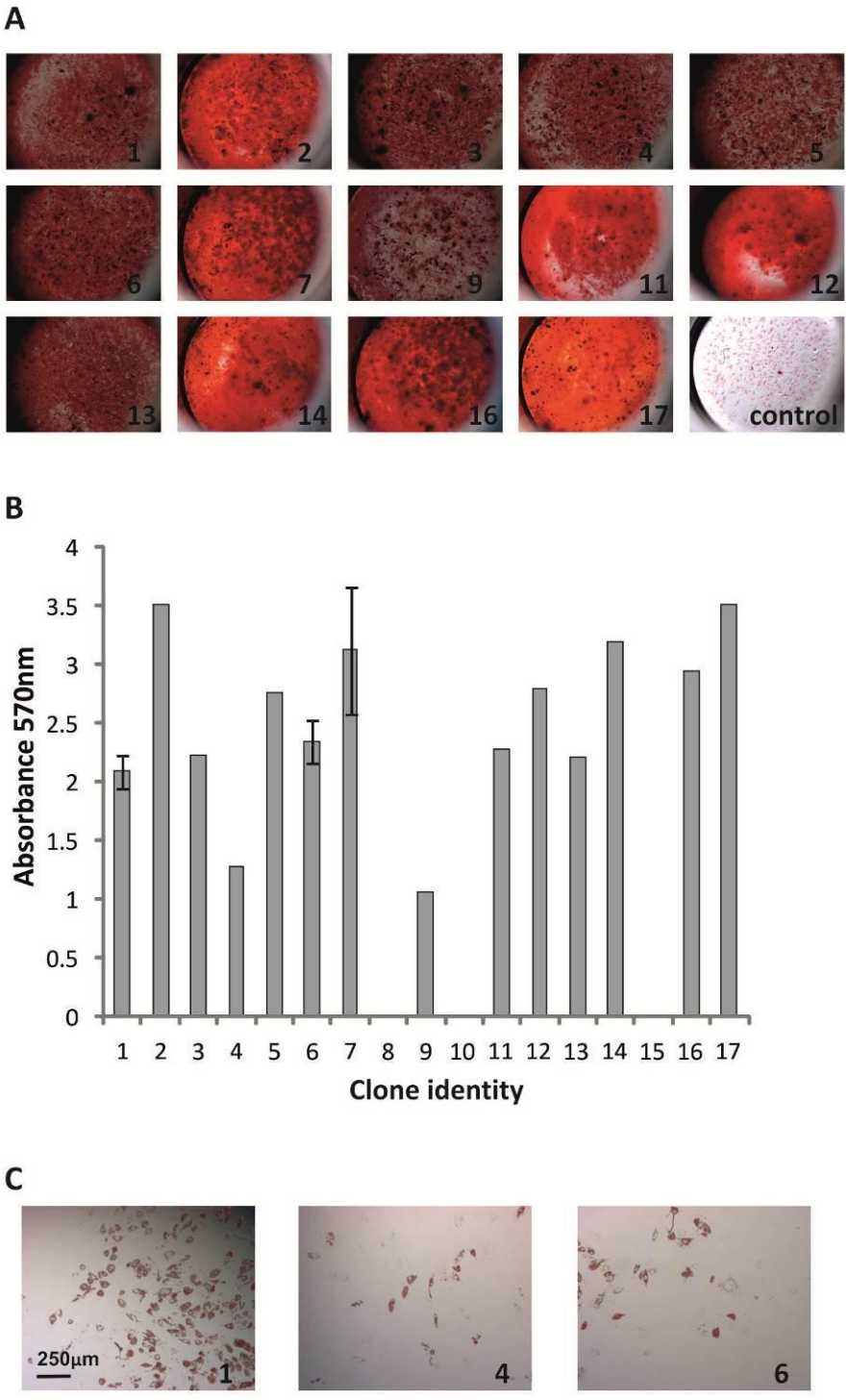

Figure 5.32 Differentiation of FH508 clones

Cells were cultured in 96 well plates for 21 days in control media or osteogenic media. Plates were then stained with alizarin red (red) to detect mineralisation (A). Stain was eluted in 10% CPC and read on a plate reader at 570 nm (B). 14/17 clones were assayed for osteogenic ability. 3/17 clones were assayed for adipogenic ability and stained with Oil Red O at day 14 to examine the presence of lipid vesicles (C).

5.4 Summary

The characterisation and understanding of HSCs was significantly improved by the discovery of a panel of SLAM receptors that could distinguish between stem cells and progenitors. It is hoped that the same can be achieved in MSC biology by the identification of markers that can be used to prospectively isolate MSCs. There is a lack of coherence in the field about which markers are best suited to assess MSCs as well as evidence to suggest that a number of different subsets of MSCs exist. Results presented in this study have identified murine mesenchymal cells that are potentially derived from an IL-7-expressing MSC and that these cells are able to form 3D spheroids in culture. Therefore, the experiments in this chapter were undertaken to explore the potential of IL-7 expression in human MSCs. Bone marrow derived MSCs could be differentiated in the presence of induction medium containing osteogenic, adipogenic and chondrogenic factors. During differentiation, levels of IL-7 were generally increased in comparison with day 0 controls, whereas nestin expression was decreased, which is in agreement with data reported for its downregulation in neuronal cells when differentiating from neural crest stem cells and indicative of it being used as a stem cell marker. However, IL-7 had no effect on osteogenic or adipogenic differentiation of MSCs *in vitro* and therefore MSCs may express IL-7 but not respond themselves to IL-7.

MSC isolation strategies give rise to heterogeneous populations of cells in culture that have varying differentiation potentials. This has been demonstrated by the analysis of clonal lines and was confirmed by the generation of MSC clones in this study. In order to determine the association between IL-7 and nestin expression and the efficiency of differentiation, clonally derived cells were differentiated *in vitro*. The hypothesis was that the MSC clones expressing the highest levels of each gene would represent true stem cells and be the most effective at tri-lineage differentiation. Owing to the small sample size, little can be drawn from the differentiation studies, although tentatively it was clear that high mRNA expression of IL-7 and nestin did not bestow a dramatic advantage in differentiation capacity.

6 General Discussion

This thesis has examined two proteins: nestin and IL-7, as potential markers for bone marrow derived MSCs in the context of MSCs providing a niche in the bone marrow for HSCs. Despite the existence of MSCs being demonstrated nearly 50 years ago, the accurate description of their *in vivo* location and prospective isolation has remained elusive. MSCs are able to extensively differentiate into fat, cartilage and bone and are an essential component in forming a niche for HSC maintenance in the bone marrow. Whilst nestin has already been described as a potential stem cell marker in a wide range of tissues and is detected on MSCs that have potentially been derived from the neural crest, the functional role of nestin in stem cells is yet to be determined. IL-7, on the other hand, is known to be expressed by stromal cells in the bone marrow and has a critical role in B cell development but the exact nature of the cells that express it is not fully understood. Therefore, studying the characteristics of MSCs, IL-7 and nestin could provide new insights into the regulatory mechanisms involved in the stem cell niche.

Using a novel mouse model in which Cre recombinase, under the control of IL-7 regulatory elements, drives YFP expression, IL-7-reporter expression was identified in mesenchymal-lineage cells in the bone and bone marrow. Immunodetection to enhance the signal determined YFP expression in bone lining cells, in central bone marrow cells and in cells closely associated with vasculature consistent with the location and morphology of cells expected to derive from mesenchymal progenitors. Interestingly, YFP was not detected in every cell of the same type at identical locations, for example only approximately 20% of osteocytes in the bone were YFP^+ (Table 3.1). It was therefore predicted that IL-7 had been expressed in a common progenitor that had given rise to the mature cells and that IL-7 could be used to identify a specific subset of MSCs in the bone marrow. This supports observations of another study using an alternative transgenic model of IL-7 where

GFP is knocked into the IL-7 locus and therefore IL-7 expressing cells also express GFP. A high proportion of VCAM-1 staining was observed on GFP positive cells and an endosteal location of the cells was suggestive of a mesenchymal cell identification (Hara et al, 2012). A large proportion of GFP positive cells were also identified as $PDGFR^{+}$ $Sca\text{-}1^{+}$, markers which have previously been used as part of a panel to identify mMSCs that were found to be quiescent and located in a perivascular region (Morikawa et al, 2009a). If the GFP positive cells were MSCs, they would be ideally located to provide HSCs in a perivascular niche with IL-7 to promote lymphopoiesis while the GFP positive cells at the endosteum could be osteoblastic cells that exert a regulatory effect on osteoclastic activity.

Two mechanisms of bone formation known as intramembranous and endochondral ossification are employed in the developing skeleton, therefore bones formed by each process were examined to determine if IL-7 reporter expression was located in the same regions. In each case, MSCs initially form condensations during development that then either directly differentiate to form bone in the case of intramembranous ossification, or create an intermediary cartilage template before bone mineralisation occurs (endochondral). Little is known about this initial aggregation of MSCs and the subsequent initiation of bone modelling. If the MSCs were to express IL-7 at this point, it would follow that all of the bone and cartilage tissue would express YFP. In chapter 3, examination of embryonic tissue found only a small proportion to be YFP positive cells in the femur (formed by endochondral ossification), indicating that IL-7 is not expressed until the cartilage template is complete. Interestingly, YFP cells were not detected in the embryonic sternum (formed by intramembranous ossification) that was at the same developmental stage as the femur, indicating anatomical differences in the onset of IL-7 expression in bones and between bones that are formed by different processes.

Analysis of the adult sternum showed a distinct expression pattern of YFP in the hypertrophic chondrocytes next to the cartilage costal regions. At the knee joint surface, IL-7 reporter was expressed in the layer of articular chondrocytes and, less

extensively in the hypertrophic chondrocytes compared to the sternum. These findings suggest further anatomical variation in IL-7 expression by chondrocytes in the adult. IL-7 has been reported to be increased in chondrocytes with age, which may explain some of the YFP expression in the adult mice. Chondrocytes also play an important role in the progression of RA and are therefore of interest to determine the interaction of IL-7 in this, and other, inflammatory conditions. As the long bones develop, the primary ossification centre initiates bone formation in a collar that extends from the centre to the ends of the bone. The chondrocytes are replaced with bone, apart from at each distal end of the bones where articular cartilage is not calcified and remains covering the joint surface. Secondary sites of ossification appear within the ends of the bone where chondrocytes also remain in the growth plate to increase bone length into adulthood. Therefore, traditional concepts of bone formation are challenged and either bone formation can be initiated by a mixed population of MSCs, or IL-7 expression may be restricted to more committed progenitors and mature cells.

As a gene associated with haematopoietic support, IL-7 transcript expression was found to be high in $CD271^+$ MSCs isolated from bone marrow aspirates of healthy individuals. A non-significant decrease in its expression was detected in cultured MSCs (Churchman et al, 2012) . This is consistent with the role of MSCs being intrinsic to haematopoietic function and importantly shows the expression of IL-7 in freshly isolated MSCs. IL-7 production from MSCs has also been reported in MSCs derived from the human periodontal ligament (PDL) (Trubiani et al, 2008) which were able to support *in vitro* haematopoietic progenitors in long-term culture initiating cell assays. IL-7 was detected by ELISA in the supernatants of cultured MSCs at concentrations of approximately 10 pg/ml, which were higher than reports of IL-7 in cultures of bone marrow MSCs (Isgro et al, 2005). The level of IL-7 detected increased to 20 pg/ml and 120 pg/ml after several weeks of osteogenic and adipogenic differentiation, respectively (Trubiani et al, 2008). This differential expression is the opposite to this study, which has shown at the transcript level where adipogenesis induced a decrease in IL-7 mRNA in some donors and suggests

that MSCs from different sources have different characteristics and distinct functional attributes. It is suggested that IL-7 expression from PDL-MSCs may contribute to tooth development or regeneration but has yet to be explicitly determined and highlights the requirement for fully investigating cell potential and defining key cell surface markers for their accurate isolation with consistency between tissues.

IL-7 expression by differentiated mesenchymal cells.

Despite charting the fate of IL-7 expressing cells as they differentiate, the IL-7Cre Rosa26-eYFP mouse model cannot explicitly demonstrate the current IL-7 expression status of cells that are YFP^+. Therefore, it remains a possibility that IL-7 may be expressed at the time of analysis by a proportion of the YFP^+ cells and is required for the functional roles of these mature cells in the bone marrow. Based on the physical location of YFP positive cells and information that is reported about IL-7 in the bone marrow, several candidates could be proposed as the source of IL-7, including osteocytes, osteoblasts and endothelial cells.

Under certain situations, such as PTH stimulation, osteoblasts are known to express IL-7 (Zhu et al, 2007). Some IL-7 reporter-expressing cells have the potential to be osteoblasts given their endosteal and bone lining location identified in chapter 3. In order to confirm the presence of YFP in osteoblastic cells, immunostaining with markers osteocalcin and osteopontin was performed on femoral sections from IL-7Cre Rosa26-eYFP mice. Unfortunately, staining was not successful and echoes similar problems that have been reported in staining osteoblasts for these molecules (Mazzucchelli et al, 2009). With so many osteoblasts present at the endosteum, discerning which ones make a functional contribution to the niche is a complicated process and has resulted in contradictory evidence regarding whether or not they are essential in the HSC niche. Recently, two papers have been published with evidence to support the theory that distinct niches exist for HSC progenitors as well as stem cells. CXCL12 is expressed by osteoblasts, stromal cells and endothelial cells. Cell-specific selective depletion was performed in a similar

mechanism of Cre mediated depletion in both studies to determine the key niche cells that are the essential sources of this chemokine. It was revealed that CXCL12 expression comes predominantly from CAR cells with a minor contribution from mature osteoblasts and endothelial cells. Osterix Cre mediated CXCL12 depletion in mature osteoblasts and CAR cells which led to HSC mobilisation and a loss of B lymphopoiesis, indicating these cells are required for HSC retention and supportive function in B cell development. Osteocalcin Cre activity demonstrated no effect of the depletion of CXCL12 in mineralising osteoblasts.

Surprisingly, when Prx-1 Cre mediated CXCL12 depletion in mesodermally derived cells, dramatic effects were noted in the loss of HSCs, their quiescence and common lymphoid progenitors. Prx-1 Cre was found to target $PDGFR^{+}Sca\text{-}1^{+}$ cells that were capable of high CFU-F forming efficiencies (much higher than those determined in nestin-GFP^{+} MSCs). Perivascular cell markers: CD146, leptin receptor and nestin were not detected in these $PDGFR^{+}Sca\text{-}1^{+}$ cells. Common haematopoietic maintenance gene expression of kit ligand and ang-1 was also absent in these cells and could point to IL-7 being the key factor in both HPC retention and B lymphopoiesis mechanisms (Greenbaum et al, 2013). Similar cell types showed expression of CXCL12 when reported using a dsRed knock-in into the CXCL12 locus. Cell-specific deletion of CXCL12 in haematopoietic cells and nestin-cre expressing cells had little effect on HSCs or restricted progenitors, questioning the role of CXCL12 expression or secretion by these cells. Leptin receptor expressing cells that were specifically deleted for CXCL12 resulted in the mobilisation of HSCs, indicating their role in the retention of HSCs (Ding & Morrison, 2013).

Osteocytes are derived from osteoblasts that become embedded in bone matrix and remain in communication with the bone-lining cells through long cytoplasmic processes and a network of channels called canaliculi. The mechanism for osteoblast conversion into osteocyte is not well understood. Osteocytes represent 95% of all cells in the bone and approximately a fifth of osteocytes examined in tissue sections were found to express YFP. As it is known that osteoblasts can

express IL-7, so it is reasonable to accept that a proportion of these cells are enveloped into the bone and could account for the YFP^+ osteocytes and, additionally, that IL-7 signalling has no functional role in these terminally differentiated cells. However, some similarities exist between the signalling mechanisms involved in osteoclastogenesis mediated by osteocytes and T cells. IL-7 production from stromal cells has been seen to induce RANKL in T cells, resulting in the subsequent activation of osteoclasts and bone resorption (Weitzmann et al, 2000). Osteocytes have also been reported to increase RANKL expression in response to microdamage of bone in order to initiate osteoclastogenesis in the process of bone remodelling (Kennedy et al, 2012). As IL-7 and its receptor mRNA have been reported in osteocytes, they may be able to respond to IL-7 by up-regulating RANKL and potentially express IL-7 themselves to perpetuate the signal. However, IL-7 gene expression in osteocytes with activated PTH receptor was not altered compared to wild type mice (Calvi et al, 2012). PTH stimulates bone formation and increases the number of osteoblasts and osteocytes and subsequent IL-7 expression from osteoblasts. As IL-7 is reported to reduce bone formation and increase osteoclastogenesis, a threshold level may occur that initially promotes bone remodelling in a regulatory mechanism but that breaching a critical level results in sustained bone resorption and a decrease in bone mass. Osteocytes are worthy of further investigation as it becomes clear they are not just retired osteoblasts but have a pivotal role in initiating bone remodelling.

YFP was detected throughout the central bone marrow and associated to vessel-like structures. Others have demonstrated this concentration of IL-7 reporter cells around vasculature in the bone marrow using a similar transgenic mouse that directly marked IL-7 producing cells with eCFP on account of a BAC transgene containing eCFP in the IL-7 locus (Mazzucchelli et al, 2009). Homing in on the cells that express IL-7 in the bone marrow will lead to the refinement of the cells considered to be part of the HSC niche.

YFP was not detected in adipose tissue surrounding the leg bones in IL-7Cre Rosa26-eYFP mice. Mice overexpressing IL-7 have a decreased adipose tissue mass associated with a higher number of smaller adipocytes than controls. PCR detected similar levels of IL-7 mRNA in adipocytes and the stromal vascular fraction (SVF) of adipose tissue but higher levels of the IL-7 receptor in SVF cells (Lucas et al, 2012). This indicates that these cells may be able to express and respond to IL-7 signals and that the SVF cells are more likely to be responsive to IL-7 regulation of fat tissue. This fraction contains endothelial cells, macrophages and adipo-progenitors that are potentially stimulated by IL-7 to differentiate into adipocytes. The observation that adipocytes were not YFP^+ suggests that they do not arise from an MSC that has expressed IL-7. IL-7 expressing MSCs may therefore be restricted in their differentiation capacity. In the differentiated cell type, it may be explained by the IL-7 reporter that may not be expressed in these cells due to a level of IL-7 expression too low to initiate reporter expression, or it may be expressed differently in various adipose regions. Regulation of the adipogenic differentiation pathway is largely unknown but IL-7 clearly has an indirect role on the fate of adipocytes at least.

Similarities between IL-7Cre expression and nestin-GFP expression

Originally identified as a marker of central nervous system stem cells, which is then downregulated and replaced during their differentiation into the mature cells of the nervous system, nestin has been reported in stem cells and progenitors in the adult brain, heart and pancreas (Reviewed by Wiese et al, 2004). In an attempt to uniquely characterise murine MSCs, nestin was used as a marker of MSCs whose progeny show a remarkable similarity to the distribution of YFP^+ cells in the IL-7Cre Rosa26-eYFP mice (Mendez-Ferrer et al, 2010). Of particular note was the feature that not all cells of a certain lineage expressed nestin; for example, only a fraction of the osteocytes were derived from $nestin^+$ MSCs, which is comparable to the YFP expression in IL-7Cre Rosa26-eYFP mice demonstrated in this study. This was also highlighted in histological images of 4-week-old mouse femurs (Mendez-Ferrer et al, 2010). Hypertrophic chondrocytes were visibly distinct in origin from their

neighbours and in contrast to the vast majority of YFP^+ articular chondrocytes that have been demonstrated in this study, very few articular chondrocytes appeared derived from $nestin^+$ MSCs. $Nestin^+$ cells have been detected by immunohistochemistry as spindle-shaped cells located at the endosteum and throughout the central marrow, which were increased in wild type mice treated with PTH but not in mice with activated PTH1R. However, not all of these spindle-shaped cells were positive for nestin (Calvi et al, 2012). This suggests another subset of MSCs distinct from $nestin^+$ cells that are also expanded in response to PTH treatment. IL-7 is well placed to mark this unique subset of MSCs. The authors propose that the nestin positive cells that associated with trabeculae were potentially osteoblastic cells and their gradual decline from the bone marrow of transgenic mice with constitutively activated PTH1R contributed to the loss of bone marrow HSC support (Calvi et al, 2012).

Can MSCs respond to IL-7?

An altruistic mechanism is proposed in T cell populations that promotes the maximal survival of T cell numbers. It is thought that this is achieved by a dowregulation of IL-7Rα in response to an IL-7 signal which allows further IL-7 to be shared with remaining T cells (Park et al, 2004). A significant downregulation of IL-7Rα was observed after incubation with 20 pg/ml IL-7 for 24 hours in human MSCs (Figure 5.23). Higher doses of IL-7 treatment did not have any effect on the expression of IL-7Rα, suggesting that a negative feedback response is not initiated in MSCs in the presence of IL-7. A different effect may have been observed analysing the samples after a shorter period in culture.

Results detailed in chapter 5 also indicate that addition of IL-7 to *in vitro* cultures and its continued presence throughout had no impact on the differentiation of MSCs. As IL-7 reportedly downregulates bone formation upon administration in vivo, this was unexpected. The two concentrations of 20 pg/ml and 20 ng/ml are above those reported in serum screens from normal patients and those with arthritis but may not present a high enough tissue specific dose to exert its effect,

or IL-7 may indirectly cause the block of bone formation and the linking cell type is missing from the *in vitro* situation. IL-7 also had no effect on the proliferation of MSCs. The lack of responsiveness to IL-7 is coupled with the finding that the γc co-receptor could not be detected by PCR. However, IL-7Rα transcript was detected and MSCs could efficiently bind IL-7 as demonstrated in the flow cytometric binding assay and although further investigation would need to assess the functional signalling of IL-7 by detection of phosphorylated JAK/STAT proteins, the basis of the signalling pathway is present in these MSCs. Potentially, IL-7 could also signal through Flt3 and c-kit receptors (Cosenza et al, 2002).

Does IL-7 and nestin expression predict MSC function?

Bone marrow flushes of IL-7Cre Rosa26-eYFP mice were sorted by flow cytometry and it was predicted that a small number of the $CD45^-$ YFP^+ cells may be MSCs capable of multipotent differentiation. Unfortunately, attempts at osteogenic and adipogenic differentiation and CFU-F assays were unsuccessful. Whilst some cells initially adhered to the plates, further growth or proliferation was not observed. A combination of growth factors was added to the medium to encourage MSC expansion but again this was unsuccessful. It is possible that the appropriate growth factors that would be provided by a heterogeneous cell population from the bone marrow were not fully compensated for and a critical factor remained absent, which led to the death of the cells. Others have reported that the IL-7 reporter cells from bone marrow are very fragile (Mazzucchelli et al, 2009) and they may have been irreparably damaged during the processing. Murine MSCs are generally more difficult than their human counterparts to culture *in vitro* and variations in culture requirements and growth properties have been shown to be dependent on mouse strain and the presence of haematopoietic cells during initial expansion (Peister et al, 2004). As the proportion of progenitor cells in the YFP^+ fraction is likely to be small even when plated at high density, there may not have been sufficient number of MSCs to support paracrine stimulation and survival. Similar to the culture method used for neural stem cells, $nestin^+$ MSCs were able to form cell aggregates or 'mesenspheres' when seeded out at low densities (Mendez-Ferrer et al, 2010).

Although isolated YFP^+ cells were not sufficiently maintained to generate cellular aggregates from clonal seeding methods, they did successfully form spheroids when cultured in methyl-cellulose media. YFP negative cells were also able to form spheroids, indicating an intrinsic factor was met in 3D culture that enabled murine stromal cell survival *in vitro*.

Additionally, CAR cells identified by GFP expressed under the promoter of the CXCL12 locus have been reported to die immediately in culture when sorted from transgenic mice. The investigators therefore used whole bone marrow cultures *in vitro* that maintained the CAR cells in a viable state and allowed them to undergo differentiation. GFP^+ pre-adipocytic cells and cells expressing ALP were identified after adipogenic and osteogenic differentiation respectively (Omatsu et al, 2010). It is therefore conceivable that a subset of the YFP^+ cells isolated might be CAR cells and that their culture *in vitro* would be assisted by heterogeneous culture with the whole bone marrow. It will also be interesting to examine the CXCL12 expression status of YFP^+ cells.

CD146 is an adhesion molecule that was first identified in melanoma cells and recognised for its association with tumour progression (Lehmann et al, 1989). CD146 has since been reported in human endothelial cells in the thymus and on circulating endothelial progenitor cells (Duda et al, 2006). Bone marrow-derived CD146-expressing human subendothelial cells have been demonstrated to recapitulate the bone and marrow at ectopic sites when transplanted in irradiated mice (Sacchetti et al, 2007) but CD146 has not been reported on murine MSCs. Studies in mice have reported CD146 expression on endothelial cells in a range of tissues including kidney, spleen, heart and liver but relatively little is known about its function (Schrage et al, 2008). A population of natural killer (NK) cells in the bone marrow have also been isolated with CD146 expression (Despoix et al, 2008).

Immunostaining of IL-7Cre Rosa26-eYFP bone sections revealed cells throughout the bone marrow that expressed CD146 which were small, round cells but did not

seem to be organised around vascular areas or have an expected spindle-shaped appearance. The CD146 positive cells detected may be NK cells or perhaps neutrophils but are unlikely to be other lymphocytes as murine B, T and monocytes reportedly do not express CD146 (Despoix et al, 2008). Further investigation would be required to evaluate the localisation of CD146 in the bone marrow and if these cells were in any way associated with IL-7 cells. CD146 is expressed by stem cells and progenitor cells in humans and has been reported in a variety of murine cells that contribute to the HSC niche such as endothelial cells. Therefore, although CD146 was not co-localised with YFP in the tissue examined, it remains conceivable that CD146 has a role to play in the bone marrow microenvironment.

Examination of the YFP^+ cells determined that they were in close proximity to $CD169^+$ macrophages in the bone marrow. $CD169^+$ macrophages are reported to support the retention of HSCs by $nestin^+$ MSC. Macrophage depletion did not alter numbers of $nestin^+$ MSCs or osteoblasts after 7 days but it decreased the gene expression of CXCL12, Ang-1, KitL and VCAM-1 in MSCs (Chow et al, 2011). As an important factor in the attraction and retention of HSCs, CXCL12 is expressed by osteoblasts and stromal cells. Its expression in osteoblasts was not changed upon macrophage deletion, adding some weight to the argument that osteoblasts are not essential components of the HSC niche. VCAM-1 was also detected on approximately half of the YFP^+ cells, indicating these cells may be involved in the retention of HSCs in the bone marrow.

Cells *in vitro* have altered behaviour depending on their culture environment including growth substrate, nutrient medium and co-culture with additional cell types. Therefore, considering MSCs in a 3D model will improve the understanding of the interactions and regulatory mechanisms of MSCs in the HSC niche. The use of a simple 3D cellular spheroid model bridges the gap between the *in vivo* environment and traditional 2D culture by providing greater cell-cell contact and additional mechanical forces in the structure created. This study has focused on a model of simple cellular spheroids that were reproducibly formed in static culture

using 4 x 10^4 C3H10T1/2 cells, a common murine cell model of MSCs. Cells within the spheroids were found to be quiescent after 48 hours and able to differentiate down osteo-, chondro-, and adipogenic lineages.

Addition of primary murine HPCs to C3H10T1/2 cells also resulted in the spontaneous formation of spheroids. In work presented in this thesis, cells were observed leaving the main body of the spheroid after 3 days of co-culture and congregating and expanding around the spheroid, preferentially attaching to the tissue culture plastic. Further examination demonstrated that the cells were F4/80$^+$ macrophages. Whilst the source of the macrophages was not determined, they were potentially either contaminants in the HPC fraction or were differentiated from them in the spheroid; they may provide a beneficial additive to the 3D model given the reported roles of niche macrophages. The macrophages may support the MSC function of HPC maintenance and further analysis would be required to measure the impact of their presence.

Fluorescent labelling of the HPCs allowed monitoring of their location within the spheroids. A proportion of these cells were identified outside of the main body of the spheroid and further characterisation would confirm if they are HPCs and not differentiated cells. It remains a possibility that they were also able to re-enter the spheroid in a manner similar to that *in vivo* that allows a small proportion of HSCs to enter the peripheral circulation from the bone marrow and back again. As the HPCs were isolated from the foetal liver, where HPCs are known to extensively proliferate before homing to the bone marrow, the tissue source of origin may have an impact on the mobilisation characteristics of these cells. Further characterisation is needed to assess the level of mobility that the HPCs have within the spheroid model and the role played by the stromal and macrophage cells in retaining HPCs.

Nestin is increasingly becoming regarded as a marker of stem cells and progenitors. In order to address if nestin was expressed by human MSCs, gene expression analysis and immunohistochemistry was performed on primary MSCs. In agreement

with these findings, results in chapter 5 demonstrate nestin mRNA is expressed by bone marrow MSCs and is subsequently decreased during osteogenic and adipogenic differentiation. This pattern was not noted in chondrogenic cells and nestin was in fact increased in some cases, when compared to the control. Cellular spheroids are believed to enhance the *in vitro* stem cell environment and enable cells to retain a more immature phenotype compared to traditional 2D culture. Chondrogenic differentiation is carried out in a 3D pellet structure and may therefore have altered gene expression and potentially improved conditions to sustain primitive stem cell features. Therefore, it might be expected that nestin expression would be increased in this situation. Indeed, when assessed at day 0, two of the three donors had nestin levels at least 4-fold more than that of the monolayer culture. During differentiation, however, nestin levels were detected above that of the appropriate control at each time point, although this was not always statistically significant. Therefore, nestin expression was highest in 3D compared to 2D culture but the factors contributing to the upregulation in 3D were not over-ridden by the chondrogenic differentiation of the cells as might be expected.

Nestin is reported to be re-expressed in stem cells that respond to tissue demand for regeneration and remodelling (El-Helou et al, 2005). MSC populations may exist as a reservoir of cells ready to be activated and generate bone and cartilage tissue and be induced to up-regulate nestin to acquire a more immature phenotype, rendering them more able to proliferate and differentiate into the required cells. The *in vitro* situation of osteogenesis and bone remodelling is somewhat artificial, whereas the chondrogenic process involves deposition of ECM from the cells undergoing differentiation. Additionally, cells are under different mechanical forces and as nestin is an intermediate filament, it may have a more functional role in the changes in the cytoskeleton that occur in cells cultured in 3D. A combination of these factors may contribute to the observed increase in nestin during 3D culture and differentiation.

Alternatively, other culture conditions such as time in culture and factors present in the growth medium could account for the observed differences, as described in studies carried out in mice. Nestin expression has been reported on 50% of murine MSCs isolated to study the expression of nestin as a marker of neuronal differentiation potential and in a population of mMSCs that were first immunodepleted to exclude the presence of endothelial and haematopoietic cells (Baddoo et al, 2003; Tropel et al, 2006). However, it has also been reported that nestin expression is upregulated in a number of cell types following culture *in vitro* and therefore its expression in bone marrow MSCs may be an artefact of culture. In both cases mentioned above, the cells were cultured for 10-20 passages or 8 days respectively, before analysis, which may have allowed the expression of nestin. Nestin was upregulated in rat MSCs after several population doublings *in vitro* or upon neuronal differentiation which was carried out in serum-free medium (Wislet-Gendebien et al, 2003). Serum removal also independently induced nestin expression in another study of bone marrow MSCs (Wautier et al, 2007). Chondrogenic culture is performed in serum-free medium which may be responsible for inducing nestin expression in this instance and suggests the presence of a factor in serum that inhibits the expression of nestin.

MSCs – a heterogeneous population of IL-7 and nestin expressing cells

This study generated a total of 36 clones from two patient donors, which revealed a varying level of nestin and IL-7 mRNA expression between MSCs. Induction of osteogenic, adipogenic and chondrogenic pathways also determined variation in the differentiation potential of clonally derived cells. Of the 26 clones that were assessed for osteogenic potential, all were able to show some degree of osteogenic differentiation with only one out of seven clones showing a distinct lack of Oil Red O staining to indicate the absence of adipogenic differentiation. Chondrogenic differentiation was not confidently determined and improved cell numbers would be required for further assessment. As the clones were cultured *in vitro* before analysis, a necessity to obtain enough cells to analyse, a possible explanation for the loss of adipogenic potential and the decreased ability to differentiate

osteogenically is that the multipotency which the cells had when first isolated was reduced or lost in culture and therefore not representative of the original cells. It is also possible that the cells which were able to form colonies were committed progenitors only capable of restricted differentiation and that the initial CFU-F assay selected for these cells.

As nestin has been previously proposed as a marker of stem cells and bone marrow MSCs, it is hypothesised that cells with the highest expression levels of nestin would be the most immature cells and therefore have the greatest potential to perform as stem cells in their self-renewal and proliferation in culture and the widest differentiation potential. In the clones that were generated this did not appear to be the case. It may be that at the time of RNA extraction, the cells were not in a state that was representative of homeostatic nestin expression, which would therefore skew the subsequent results. Nestin is downregulated in the stationary growth phase (Zimmerman et al, 1994). Although cells were seeded at the same density and collected at the same time point, some cells were certainly more proliferative than others. This supports the theory that some clones lose their stemness in culture and began to 'age'.

Immunohistochemistry was carried out in order to determine the presence of nestin protein in MSC cultures and, as demonstrated in chapter 5, nestin expression has been detected in the cytoplasm of MSCs, consistent with its expected cellular location as an intermediate filament. However, in donor K6 cells, nestin was weakly expressed in the nucleus of most of the cells, suggesting its mis-localisation or an alternative cellular function. A similar distribution has been reported in neurogenic tumour lines where nuclear staining was observed in cells with a weakly staining cytoplasm. Nuclear nestin was determined in 3/11 tumour lines and had variable expression between cells and lines as detected by Immunofluorescence and cellular fractionation followed by Western blot analysis (Krupkova et al., 2011). However, within their study only 10% of cells in each line expressed nuclear nestin and these cells were lost during culture in favour of purely cytoplasmic expression of the

protein, suggesting no benefit of the nuclear expression in culture at least (Krupkova et al, 2011). Relatively little is known about the nuclear localisation of nestin and the evidence that is presented is contradictory, highlighting the need for further characterisation.

Antisense transfected nestin clones from neuroblastoma lines reduced the expression of nestin approximately 1.5 fold but the level of N-myc protein was unchanged. This led to the reduced motility and colony-forming efficiency of the neuroblastoma clones compared to the parental line, suggesting the roles of tumour migration and cell proliferation that were previously attributed to N-Myc expression were in fact regulated by nestin, presumably downstream of N-Myc (Thomas et al, 2004). However, another study analysed over 30 paraffin embedded neuroblastoma samples and found no association between nestin expression and proliferation or tumour malignancy and only 1/7 neuroblastomas expressed nestin (Korja et al, 2005). As nestin cannot be transported into the nucleus by nucleopores, an alternative suggestion is that the ancestral gene of nestin was lamin-like and that other intermediate filaments arose and lost the nuclear localisation signal. (Dahlstrand et al, 1992; Dodemont et al, 1990). Nuclear interaction of nestin and DNA has been suggested (Hartig et al, 1998) but essentially, the functional role of nestin is still not well understood. This study has shown that bone marrow MSCs express nestin, which is subsequently downregulated upon osteogenic and adipogenic differentiation and therefore supports the theory that nestin is a marker of stem cells. Evidence suggesting roles for nestin in the proliferation and migration of cells is inconsistent and results from this study can only hint at an effect of nestin on proliferation due to the small number of clones generated.

6.1 Thesis conclusions

MSCs and their progeny have been described as essential components of the HSC niche. The HSC niche has been proposed to be located in close proximity to the endosteum or alternatively near blood vessels in the bone marrow. Furthermore, this theory is currently being extended to include niches that exist for progenitors that overlap and interplay. Each niche location has a different composition of cell types and availability of factors such as oxygen concentration, and consequently the microenvironment is thought to control different aspects of HSC renewal and differentiation. In a logical extension, MSCs present at each location may also be differentially activated to regulate HSC fate. Evidence to suggest that MSCs are derived from distinct embryonic origins such as the neural crest (Nagoshi et al, 2008) and the mesoderm (Vodyanik et al, 2010) supports the theory that the bone marrow is host to a number of different subsets of MSCs that may have variable expression profiles and different functional attributes.

IL-7 has been examined in this study as a potential marker of bone marrow derived MSCs. A novel IL-7Cre BAC transgenic mouse model facilitated the identification of cells that appeared to arise from a subset of MSCs given the distribution of the mature cells in the bone marrow that were YFP (IL-7 reporter) positive.
Understanding and acquiring information about the key components involved in the HSC niche will lead to more accurate representations of the microenvironment that can potentially be exploited to manipulate haematopoiesis in a clinical setting. For example, the number of HSCs is known to be a limiting factor in bone marrow transplantation. Therefore, the ability to expand these HSCs in culture would offer greater potential for therapeutic use. Maintaining the ability of stem cells to self renew *ex vivo* is difficult and the challenge now is to imitate these complex stem cell niches *in vitro* in order to better control stem cell renewal and differentiation.

The generation of an *in vitro* spheroid model reproduced *in vivo* attributes of the stem cell niche such as cell quiescence and stromal organisation but was unable to sufficiently maintain HPCs in culture and requires further modification. The

functional roles of IL-7 and nestin in MSCs are still to be determined but the work presented here supports published data about nuclear expression of nestin and the potential of IL-7 to be expressed by MSCs to regulate a range of haematopoietic niches but not necessarily be affected by its expression. Together with reported studies, the evidence suggests that IL-7 is expressed by osteoprogenitors that have perivascular locations close to the endosteum and that they support B-lymphopoiesis and HPC maintenance in the niche.

Abbreviations

°C	degrees Celsius
2D	2 dimensional
3D	3 dimensional
α-MEM	minimum essential medium – alpha
β3-tub	beta III tubulin
µg	microgram
µL	microlitre
ACPA	anti citrullinated peptides antibodies
ADSC	adipose derived stem cell
AGM	aorta-gonad-mesonephros
ALP	alkaline phosphatase
Ang-1	angiopoietin
APLNR	apelin receptor
ARC	adventitial reticular cell
ATP	adenosine triphosphate
BABB	benzyl alcohol: benzyl benzoate
BAC	bacterial artificial chromosome
Bcl2	B cell lymphoma-2
bFGF	basic fibroblastic growth factor
BMP	bone morphogenic protein
BMPR1A	bone morphogenic protein receptor 1A
bp	base pair
BSA	bovine serum albumin
CAR cell	CXCL12 abundant reticular cell
CCK-8	cell counting kit -8
cDNA	complementary deoxyribonucleic acid
C/EBP	CCAAT-enhancer-binding protein
CFSE	carboxyfluorescein diacetate succinimidyl ester
CFU	colony forming unit

CFU-F	colony forming unit - fibroblast
CFU-M	colony forming unit - macrophage
CNS	central nervous system
Ct	cycle threshold
CXCL12	CXC chemokine ligand 12
CXCR4	CXC chemokine receptor 4
DAPI	4',6-diamidino-2-phenylindole
dATP	2’-deoxyadenosine-5’-triphosphate
dCTP	2’-deoxycytidine-5’-triphosphate
dGTP	2’-deoxyguanosine-5’-triphosphate
dH_2O	distilled water
DMARD	disease modifying anti-rheumatic drug
DMEM	Dulbecco’s modified Eagle’s medium
DNA	deoxyribonucleic acid
dNTP	deoxyribonucleotide triphosphate
DTT	dithiothreitol
dTTP	2’-deoxythymidine-5’-triphosphate
EB	embryoid body
eCFP	enhanced cyan fluorescence protein
ECM	extra cellular matrix
EDTA	ethylenediaminetetraacetic acid
Epo	erythropoietin
ESC	embryonic stem cell
EthD-1	ethidium homodimer-1
FABP4	fatty-acid-binding protein 4
FACS	fluorescence-activated cell sorting
FBS	foetal bovine serum
FGF	fibroblast growth factor
FITC	fluorescein isothiocyanate
g	acceleration due to gravity
G	gauge

GAG	glycosaminoglycan
G-CSF	granulocyte-colony stimulating factor
GFAP	glial fibrillary acidic protein
H&E	haematoxylin and eosin
HPC	haematopoietic progenitor cell
HSC	haematopoietic stem cell
IBMX	3-isobutyl-1-methylxanthine
ICAM-1	inter-cellular adhesion molecule 1
IgG	immunoglobulin G
IL	interleukin
IMS	industrial methylated spirit
ISCT	international society for cellular therapy
JAK	janus kinase
kDa	kilodalton
KO	knockout
LT-HSC	long term-haematopoietic stem cell
MACS	magnetic-activated cell sorting
Mcl-1	myeloid cell leukaemia sequence 1
M-CSF	macrophage colony stimulating factor
MHC	major histocompatibility complex
MMP	matrix metalloproteinase
mRNA	messenger ribonucleic acid
MSC	mesenchymal stem cell
MPP	multipotent progenitor
NCSC	neural crest stem cell
NEAA	non essential amino acid
NF-L	neurofilament
ng	nanogram
nm	nanometre
NSC	neural stem cell
OC	osteoclast

OCT	optimal cutting temperature compound
OPG	osteoprotegerin
P/S	penicillin/streptomycin
PBS	phosphate buffered saline
PBS-T	phosphate buffered solution – Triton X-100
PCR	polymerase chain reaction
PDGFR	platelet derived growth factor receptor
PDL	periodontal ligament
PE	phycoerythrin
PFA	paraformaldehyde
pg	picogram
pNP	p-nitrophenol
pNPP	p-nitrophenyl phosphate
PNS	peripheral nervous system
PPARγ	peroxisome proliferator-activated receptor gamma
PTH	parathyroid hormone
PVA	polyvinyl acetate
qPCR	quantitative polymerase chain reaction
RA	rheumatoid arthritis
RANKL	receptor activator of NF-κB ligand
RNA	ribonucleic acid
rpm	revolutions per minute
RPS27a	ribosomal protein S27a
RT	reverse transcriptase
RT-PCR	reverse-transcription polymerase chain reaction
SCF	stem cell factor
SDF-1	stromal cell-derived factor-1
SCID	severe combined immunodeficient
SLAM	signalling lymphocytic activation molecule
SNS	sympathetic nervous system
SOCS	suppressors of cytokine signalling

STAT	signal transducers and activators of transcription
ST-HSC	short term-haematopoietic stem cell
SVF	stromal vascular fraction
TEC	thymic epithelial cell
TEM	transmission electron microscopy
TRAP	tartrate resistant acid phosphatase
TSLP	thymic stromal lymphopoietin
VCAM-1	vascular cell adhesion molecule 1
VE-cadherin	vascular endothelial cadherin
YFP	yellow fluorescent protein

References

Adams GB, Chabner KT, Alley IR, Olson DP, Szczepiorkowski ZM, Poznansky MC, Kos CH, Pollak MR, Brown EM, Scadden DT (2006) Stem cell engraftment at the endosteal niche is specified by the calcium-sensing receptor. *Nature* **439:** 599-603

Aihara M, Sugawara K, Torii S, Hosaka M, Kurihara H, Saito N, Takeuchi T (2004) Angiogenic endothelium-specific nestin expression is enhanced by the first intron of the nestin gene. *Lab Invest* **84:** 1581-1592

Alves NL, Richard-Le Goff O, Huntington ND, Sousa AP, Ribeiro VS, Bordack A, Vives FL, Peduto L, Chidgey A, Cumano A, Boyd R, Eberl G, Di Santo JP (2009) Characterization of the thymic IL-7 niche in vivo. *Proc Natl Acad Sci U S A* **106:** 1512-1517

Anjos-Afonso F, Siapati EK, Bonnet D (2004) In vivo contribution of murine mesenchymal stem cells into multiple cell-types under minimal damage conditions. *J Cell Sci* **117:** 5655-5664

Arai F, Hirao A, Ohmura M, Sato H, Matsuoka S, Takubo K, Ito K, Koh GY, Suda T (2004) Tie2/angiopoietin-1 signaling regulates hematopoietic stem cell quiescence in the bone marrow niche. *Cell* **118:** 149-161

Avecilla ST, Hattori K, Heissig B, Tejada R, Liao F, Shido K, Jin DK, Dias S, Zhang F, Hartman TE, Hackett NR, Crystal RG, Witte L, Hicklin DJ, Bohlen P, Eaton D, Lyden D, de Sauvage F, Rafii S (2004) Chemokine-mediated interaction of hematopoietic progenitors with the bone marrow vascular niche is required for thrombopoiesis. *Nat Med* **10:** 64-71

Baddoo M, Hill K, Wilkinson R, Gaupp D, Hughes C, Kopen GC, Phinney DG (2003) Characterization of mesenchymal stem cells isolated from murine bone marrow by negative selection. *J Cell Biochem* **89:** 1235-1249

Baksh D, Yao R, Tuan RS (2007) Comparison of proliferative and multilineage differentiation potential of human mesenchymal stem cells derived from umbilical cord and bone marrow. *Stem Cells* **25:** 1384-1392

Banerjee M, Bhonde RR (2006) Application of hanging drop technique for stem cell differentiation and cytotoxicity studies. *Cytotechnology* **51:** 1-5

Baune BT, Rothermundt M, Ladwig KH, Meisinger C, Berger K (2011) Systemic inflammation (Interleukin 6) predicts all-cause mortality in men: results from a 9-year follow-up of the MEMO Study. *Age (Dordr)* **33:** 209-217

Beguin PC, El-Helou V, Assimakopoulos J, Clement R, Gosselin H, Brugada R, Villeneuve L, Rohlicek CV, Del Duca D, Lapointe N, Rouleau JL, Calderone A (2009) The phenotype and potential origin of nestin+ cardiac myocyte-like cells following infarction. *J Appl Physiol* **107:** 1241-1248

Beguin PC, El-Helou V, Gillis MA, Duquette N, Gosselin H, Brugada R, Villeneuve L, Lauzier D, Tanguay JF, Ribuot C, Calderone A (2011) Nestin (+) stem cells independently contribute to neural remodelling of the ischemic heart. *J Cell Physiol* **226:** 1157-1165

Bhandoola A, Sambandam A (2006) From stem cell to T cell: one route or many? *Nat Rev Immunol* **6:** 117-126

Birgersdotter A, Sandberg R, Ernberg I (2005) Gene expression perturbation in vitro--a growing case for three-dimensional (3D) culture systems. *Semin Cancer Biol* **15:** 405-412

Bixby S, Kruger GM, Mosher JT, Joseph NM, Morrison SJ (2002) Cell-intrinsic differences between stem cells from different regions of the peripheral nervous system regulate the generation of neural diversity. *Neuron* **35:** 643-656

Bondurand N, Kobetz A, Pingault V, Lemort N, Encha-Razavi F, Couly G, Goerich DE, Wegner M, Abitbol M, Goossens M (1998) Expression of the SOX10 gene during human development. *FEBS Lett* **432:** 168-172

Bonnet D, Dick JE (1997) Human acute myeloid leukemia is organized as a hierarchy that originates from a primitive hematopoietic cell. *Nat Med* **3:** 730-737

Calderone A (2012) Nestin+ cells and healing the infarcted heart. *Am J Physiol Heart Circ Physiol* **302:** H1-9

Calvi LM, Adams GB, Weibrecht KW, Weber JM, Olson DP, Knight MC, Martin RP, Schipani E, Divieti P, Bringhurst FR, Milner LA, Kronenberg HM, Scadden DT (2003) Osteoblastic cells regulate the haematopoietic stem cell niche. *Nature* **425:** 841-846

Calvi LM, Bromberg O, Rhee Y, Weber JM, Smith JN, Basil MJ, Frisch BJ, Bellido T (2012) Osteoblastic expansion induced by parathyroid hormone receptor signaling in murine osteocytes is not sufficient to increase hematopoietic stem cells. *Blood* **119:** 2489-2499

Caplan AI (1991) Mesenchymal stem cells. *J Orthop Res* **9:** 641-650

Cattaneo E, McKay R (1990) Proliferation and differentiation of neuronal stem cells regulated by nerve growth factor. *Nature* **347:** 762-765

Chan CK, Chen CC, Luppen CA, Kim JB, DeBoer AT, Wei K, Helms JA, Kuo CJ, Kraft DL, Weissman IL (2009) Endochondral ossification is required for haematopoietic stem-cell niche formation. *Nature* **457:** 490-494

Chang MK, Raggatt LJ, Alexander KA, Kuliwaba JS, Fazzalari NL, Schroder K, Maylin ER, Ripoll VM, Hume DA, Pettit AR (2008) Osteal tissue macrophages are intercalated throughout human and mouse bone lining tissues and regulate osteoblast function in vitro and in vivo. *J Immunol* **181:** 1232-1244

Choi K (1998) Hemangioblast development and regulation. *Biochem Cell Biol* **76:** 947-956

Chotinantakul K, Leeanansaksiri W (2012) Hematopoietic stem cell development, niches, and signaling pathways. *Bone Marrow Res* **2012:** 270425

Chow A, Lucas D, Hidalgo A, Mendez-Ferrer S, Hashimoto D, Scheiermann C, Battista M, Leboeuf M, Prophete C, van Rooijen N, Tanaka M, Merad M, Frenette PS (2011) Bone

marrow CD169+ macrophages promote the retention of hematopoietic stem and progenitor cells in the mesenchymal stem cell niche. *J Exp Med* **208:** 261-271

Christensen JL, Wright DE, Wagers AJ, Weissman IL (2004) Circulation and chemotaxis of fetal hematopoietic stem cells. *PLoS Biol* **2:** E75

Churchman SM, Ponchel F (2008) Interleukin-7 in rheumatoid arthritis. *Rheumatology (Oxford)* **47:** 753-759

Churchman SM, Ponchel F, Boxall SA, Cuthbert R, Kouroupis D, Roshdy T, Giannoudis PV, Emery P, McGonagle D, Jones EA (2012) Transcriptional profile of native CD271+ multipotential stromal cells: evidence for multiple fates, with prominent osteogenic and Wnt pathway signaling activity. *Arthritis Rheum* **64:** 2632-2643

Colucci-Guyon E, Portier MM, Dunia I, Paulin D, Pournin S, Babinet C (1994) Mice lacking vimentin develop and reproduce without an obvious phenotype. *Cell* **79:** 679-694

Corfe SA, Rottapel R, Paige CJ (2011) Modulation of IL-7 thresholds by SOCS proteins in developing B lineage cells. *J Immunol* **187:** 3499-3510

Cosenza L, Gorgun G, Urbano A, Foss F (2002) Interleukin-7 receptor expression and activation in nonhaematopoietic neoplastic cell lines. *Cell Signal* **14:** 317-325

Cuthbert R, Boxall SA, Tan HB, Giannoudis PV, McGonagle D, Jones E (2012) Single-platform quality control assay to quantify multipotential stromal cells in bone marrow aspirates prior to bulk manufacture or direct therapeutic use. *Cytotherapy* **14:** 431-440

Dahlstrand J, Zimmerman LB, McKay RD, Lendahl U (1992) Characterization of the human nestin gene reveals a close evolutionary relationship to neurofilaments. *J Cell Sci* **103 (Pt 2):** 589-597

Danielian PS, Muccino D, Rowitch DH, Michael SK, McMahon AP (1998) Modification of gene activity in mouse embryos in utero by a tamoxifen-inducible form of Cre recombinase. *Curr Biol* **8:** 1323-1326

Despoix N, Walzer T, Jouve N, Blot-Chabaud M, Bardin N, Paul P, Lyonnet L, Vivier E, Dignat-George F, Vely F (2008) Mouse CD146/MCAM is a marker of natural killer cell maturation. *Eur J Immunol* **38:** 2855-2864

Dillon N, Grosveld F (1993) Transcriptional regulation of multigene loci: multilevel control. *Trends Genet* **9:** 134-137

Ding L, Morrison SJ (2013) Haematopoietic stem cells and early lymphoid progenitors occupy distinct bone marrow niches. *Nature* **495:** 231-235

Ding L, Saunders TL, Enikolopov G, Morrison SJ (2012) Endothelial and perivascular cells maintain haematopoietic stem cells. *Nature* **481:** 457-462

Dodemont H, Riemer D, Weber K (1990) Structure of an invertebrate gene encoding cytoplasmic intermediate filament (IF) proteins: implications for the origin and the diversification of IF proteins. *EMBO J* **9:** 4083-4094

Dominici M, Le Blanc K, Mueller I, Slaper-Cortenbach I, Marini F, Krause D, Deans R, Keating A, Prockop D, Horwitz E (2006) Minimal criteria for defining multipotent mesenchymal stromal cells. The International Society for Cellular Therapy position statement. *Cytotherapy* **8:** 315-317

Dougall WC, Glaccum M, Charrier K, Rohrbach K, Brasel K, De Smedt T, Daro E, Smith J, Tometsko ME, Maliszewski CR, Armstrong A, Shen V, Bain S, Cosman D, Anderson D, Morrissey PJ, Peschon JJ, Schuh J (1999) RANK is essential for osteoclast and lymph node development. *Genes Dev* **13:** 2412-2424

Duda DG, Cohen KS, di Tomaso E, Au P, Klein RJ, Scadden DT, Willett CG, Jain RK (2006) Differential CD146 expression on circulating versus tissue endothelial cells in rectal cancer patients: implications for circulating endothelial and progenitor cells as biomarkers for antiangiogenic therapy. *J Clin Oncol* **24:** 1449-1453

Eaton CL, Colombel M, van der Pluijm G, Cecchini M, Wetterwald A, Lippitt J, Rehman I, Hamdy F, Thalman G (2010) Evaluation of the frequency of putative prostate cancer stem cells in primary and metastatic prostate cancer. *Prostate* **70:** 875-882

Ebihara Y, Masuya M, Larue AC, Fleming PA, Visconti RP, Minamiguchi H, Drake CJ, Ogawa M (2006) Hematopoietic origins of fibroblasts: II. In vitro studies of fibroblasts, CFU-F, and fibrocytes. *Exp Hematol* **34:** 219-229

Echelard Y, Vassileva G, McMahon AP (1994) Cis-acting regulatory sequences governing Wnt-1 expression in the developing mouse CNS. *Development* **120:** 2213-2224

Ehninger A, Trumpp A (2011) The bone marrow stem cell niche grows up: mesenchymal stem cells and macrophages move in. *J Exp Med* **208:** 421-428

El-Helou V, Beguin PC, Assimakopoulos J, Clement R, Gosselin H, Brugada R, Aumont A, Biernaskie J, Villeneuve L, Leung TK, Fernandes KJ, Calderone A (2008) The rat heart contains a neural stem cell population; role in sympathetic sprouting and angiogenesis. *J Mol Cell Cardiol* **45:** 694-702

El-Helou V, Dupuis J, Proulx C, Drapeau J, Clement R, Gosselin H, Villeneuve L, Manganas L, Calderone A (2005) Resident nestin+ neural-like cells and fibers are detected in normal and damaged rat myocardium. *Hypertension* **46:** 1219-1225

Engel P, Eck MJ, Terhorst C (2003) The SAP and SLAM families in immune responses and X-linked lymphoproliferative disease. *Nat Rev Immunol* **3:** 813-821

Ferrari G, Cusella-De Angelis G, Coletta M, Paolucci E, Stornaiuolo A, Cossu G, Mavilio F (1998) Muscle regeneration by bone marrow-derived myogenic progenitors. *Science* **279:** 1528-1530

Filbin MT, Walsh FS, Trapp BD, Pizzey JA, Tennekoon GI (1990) Role of myelin P0 protein as a homophilic adhesion molecule. *Nature* **344:** 871-872

Florenes VA, Holm R, Myklebost O, Lendahl U, Fodstad O (1994) Expression of the neuroectodermal intermediate filament nestin in human melanomas. *Cancer Res* **54:** 354-356

Foster K, Sheridan J, Veiga-Fernandes H, Roderick K, Pachnis V, Adams R, Blackburn C, Kioussis D, Coles M (2008) Contribution of neural crest-derived cells in the embryonic and adult thymus. *J Immunol* **180:** 3183-3189

Friedenstein AJ, Chailakhjan RK, Lalykina KS (1970) The development of fibroblast colonies in monolayer cultures of guinea-pig bone marrow and spleen cells. *Cell Tissue Kinet* **3:** 393-403

Frith JE, Thomson B, Genever PG (2010) Dynamic Three-Dimensional Culture Methods Enhance Mesenchymal Stem Cell Properties and Increase Therapeutic Potential. *Tissue Eng Part C-Me* **16:** 735-749

Fruehauf S, Veldwijk MR, Seeger T, Schubert M, Laufs S, Topaly J, Wuchter P, Dillmann F, Eckstein V, Wenz F, Goldschmidt H, Ho AD, Calandra G (2009) A combination of granulocyte-colony-stimulating factor (G-CSF) and plerixafor mobilizes more primitive peripheral blood progenitor cells than G-CSF alone: results of a European phase II study. *Cytotherapy* **11:** 992-1001

Fry TJ, Mackall CL (2002) Interleukin-7: from bench to clinic. *Blood* **99:** 3892-3904

Fry TJ, Mackall CL (2005) The many faces of IL-7: from lymphopoiesis to peripheral T cell maintenance. *J Immunol* **174:** 6571-6576

Giri JG, Ahdieh M, Eisenman J, Shanebeck K, Grabstein K, Kumaki S, Namen A, Park LS, Cosman D, Anderson D (1994) Utilization of the beta and gamma chains of the IL-2 receptor by the novel cytokine IL-15. *EMBO J* **13:** 2822-2830

Goeb V, Aegerter P, Parmar R, Fardellone P, Vittecoq O, Conaghan PG, Emery P, Le Loet X, Ponchel F (2012) Progression to rheumatoid arthritis in early inflammatory arthritis is associated with low IL-7 serum levels. *Ann Rheum Dis*

Gohel A, McCarthy MB, Gronowicz G (1999) Estrogen prevents glucocorticoid-induced apoptosis in osteoblasts in vivo and in vitro. *Endocrinology* **140:** 5339-5347

Goodman JW, Hodgson GS (1962) Evidence for stem cells in the peripheral blood of mice. *Blood* **19:** 702-714

Grabstein KH, Waldschmidt TJ, Finkelman FD, Hess BW, Alpert AR, Boiani NE, Namen AE, Morrissey PJ (1993) Inhibition of murine B and T lymphopoiesis in vivo by an anti-interleukin 7 monoclonal antibody. *J Exp Med* **178:** 257-264

Grand RJ, Turnell AS, Grabham PW (1996) Cellular consequences of thrombin-receptor activation. *Biochem J* **313 (Pt 2):** 353-368

Greenbaum A, Hsu YM, Day RB, Schuettpelz LG, Christopher MJ, Borgerding JN, Nagasawa T, Link DC (2013) CXCL12 in early mesenchymal progenitors is required for haematopoietic stem-cell maintenance. *Nature* **495:** 227-230

Gronthos S, Zannettino AC, Hay SJ, Shi S, Graves SE, Kortesidis A, Simmons PJ (2003) Molecular and cellular characterisation of highly purified stromal stem cells derived from human bone marrow. *J Cell Sci* **116:** 1827-1835

Habib T, Senadheera S, Weinberg K, Kaushansky K (2002) The common gamma chain (gamma c) is a required signaling component of the IL-21 receptor and supports IL-21-induced cell proliferation via JAK3. *Biochemistry* **41:** 8725-8731

Hara T, Shitara S, Imai K, Miyachi H, Kitano S, Yao H, Tani-ichi S, Ikuta K (2012) Identification of IL-7-producing cells in primary and secondary lymphoid organs using IL-7-GFP knock-in mice. *J Immunol* **189:** 1577-1584

Haringman JJ, Gerlag DM, Zwinderman AH, Smeets TJ, Kraan MC, Baeten D, McInnes IB, Bresnihan B, Tak PP (2005) Synovial tissue macrophages: a sensitive biomarker for response to treatment in patients with rheumatoid arthritis. *Ann Rheum Dis* **64:** 834-838

Hartig R, Shoeman RL, Janetzko A, Tolstonog G, Traub P (1998) DNA-mediated transport of the intermediate filament protein vimentin into the nucleus of cultured cells. *J Cell Sci* **111 (Pt 24):** 3573-3584

Hattori K, Heissig B, Tashiro K, Honjo T, Tateno M, Shieh JH, Hackett NR, Quitoriano MS, Crystal RG, Rafii S, Moore MA (2001) Plasma elevation of stromal cell-derived factor-1 induces mobilization of mature and immature hematopoietic progenitor and stem cells. *Blood* **97:** 3354-3360

Haylock DN, Williams B, Johnston HM, Liu MC, Rutherford KE, Whitty GA, Simmons PJ, Bertoncello I, Nilsson SK (2007) Hemopoietic stem cells with higher hemopoietic potential reside at the bone marrow endosteum. *Stem Cells* **25:** 1062-1069

Herrera MB, Bussolati B, Bruno S, Morando L, Mauriello-Romanazzi G, Sanavio F, Stamenkovic I, Biancone L, Camussi G (2007) Exogenous mesenchymal stem cells localize to the kidney by means of CD44 following acute tubular injury. *Kidney Int* **72:** 430-441

Horwitz EM, Le Blanc K, Dominici M, Mueller I, Slaper-Cortenbach I, Marini FC, Deans RJ, Krause DS, Keating A (2005) Clarification of the nomenclature for MSC: The International Society for Cellular Therapy position statement. *Cytotherapy* **7:** 393-395

Huber TL, Kouskoff V, Fehling HJ, Palis J, Keller G (2004) Haemangioblast commitment is initiated in the primitive streak of the mouse embryo. *Nature* **432:** 625-630

Isgro A, Marziali M, Mezzaroma I, Luzi G, Mazzone AM, Guazzi V, Andolfi G, Cassani B, Aiuti A, Aiuti F (2005) Bone marrow clonogenic capability, cytokine production, and thymic output in patients with common variable immunodeficiency. *J Immunol* **174:** 5074-5081

Jones E, English A, Churchman SM, Kouroupis D, Boxall SA, Kinsey S, Giannoudis PG, Emery P, McGonagle D (2010) Large-scale extraction and characterization of CD271+ multipotential stromal cells from trabecular bone in health and osteoarthritis: implications for bone regeneration strategies based on uncultured or minimally cultured multipotential stromal cells. *Arthritis Rheum* **62:** 1944-1954

Jones EA, Kinsey SE, English A, Jones RA, Straszynski L, Meredith DM, Markham AF, Jack A, Emery P, McGonagle D (2002) Isolation and characterization of bone marrow multipotential mesenchymal progenitor cells. *Arthritis Rheum* **46:** 3349-3360

Jung Y, Song J, Shiozawa Y, Wang J, Wang Z, Williams B, Havens A, Schneider A, Ge C, Franceschi RT, McCauley LK, Krebsbach PH, Taichman RS (2008) Hematopoietic stem cells regulate mesenchymal stromal cell induction into osteoblasts thereby participating in the formation of the stem cell niche. *Stem Cells* **26:** 2042-2051

Kachinsky AM, Dominov JA, Miller JB (1995) Intermediate filaments in cardiac myogenesis: nestin in the developing mouse heart. *J Histochem Cytochem* **43:** 843-847

Kaiserling E (2001) Newly-formed lymph nodes in the submucosa in chronic inflammatory bowel disease. *Lymphology* **34:** 22-29

Katayama Y, Battista M, Kao WM, Hidalgo A, Peired AJ, Thomas SA, Frenette PS (2006) Signals from the sympathetic nervous system regulate hematopoietic stem cell egress from bone marrow. *Cell* **124:** 407-421

Kawaguchi A, Miyata T, Sawamoto K, Takashita N, Murayama A, Akamatsu W, Ogawa M, Okabe M, Tano Y, Goldman SA, Okano H (2001) Nestin-EGFP transgenic mice: visualization of the self-renewal and multipotency of CNS stem cells. *Mol Cell Neurosci* **17:** 259-273

Kennedy OD, Herman BC, Laudier DM, Majeska RJ, Sun HB, Schaffler MB (2012) Activation of resorption in fatigue-loaded bone involves both apoptosis and active pro-osteoclastogenic signaling by distinct osteocyte populations. *Bone* **50:** 1115-1122

Kennison JA (1993) Transcriptional activation of Drosophila homeotic genes from distant regulatory elements. *Trends Genet* **9:** 75-79

Khaled AR, Durum SK (2002) Lymphocide: cytokines and the control of lymphoid homeostasis. *Nat Rev Immunol* **2:** 817-830

Kiel MJ, Acar M, Radice GL, Morrison SJ (2008) Hematopoietic Stem Cells Do Not Depend on N-Cadherin to Regulate Their Maintenance *Cell Stem Cell* **4:** 170-179

Kiel MJ, Yilmaz OH, Iwashita T, Terhorst C, Morrison SJ (2005) SLAM family receptors distinguish hematopoietic stem and progenitor cells and reveal endothelial niches for stem cells. *Cell* **121:** 1109-1121

Kim GY, Hong C, Park JH (2011) Seeing is believing: illuminating the source of in vivo interleukin-7. *Immune Netw* **11:** 1-10

Kollet O, Dar A, Shivtiel S, Kalinkovich A, Lapid K, Sztainberg Y, Tesio M, Samstein RM, Goichberg P, Spiegel A, Elson A, Lapidot T (2006) Osteoclasts degrade endosteal components and promote mobilization of hematopoietic progenitor cells. *Nat Med* **12:** 657-664

Korja M, Finne J, Salmi TT, Kalimo H, Karikoski R, Tanner M, Isola J, Haapasalo H (2005) Chromogenic in situ hybridization-detected hotspot MYCN amplification associates with Ki-

67 expression and inversely with nestin expression in neuroblastomas. *Mod Pathol* **18:** 1599-1605

Kruger GM, Mosher JT, Bixby S, Joseph N, Iwashita T, Morrison SJ (2002) Neural crest stem cells persist in the adult gut but undergo changes in self-renewal, neuronal subtype potential, and factor responsiveness. *Neuron* **35:** 657-669

Krupkova O, Jr., Loja T, Redova M, Neradil J, Zitterbart K, Sterba J, Veselska R (2011) Analysis of nuclear nestin localization in cell lines derived from neurogenic tumors. *Tumour Biol* **32:** 631-639

Kuhlbrodt K, Herbarth B, Sock E, Hermans-Borgmeyer I, Wegner M (1998) Sox10, a novel transcriptional modulator in glial cells. *J Neurosci* **18:** 237-250

Lapidot T, Petit I (2002) Current understanding of stem cell mobilization: the roles of chemokines, proteolytic enzymes, adhesion molecules, cytokines, and stromal cells. *Exp Hematol* **30:** 973-981

Laterveer L, Lindley IJ, Hamilton MS, Willemze R, Fibbe WE (1995) Interleukin-8 induces rapid mobilization of hematopoietic stem cells with radioprotective capacity and long-term myelolymphoid repopulating ability. *Blood* **85:** 2269-2275

Lee G, Kim H, Elkabetz Y, Al Shamy G, Panagiotakos G, Barberi T, Tabar V, Studer L (2007) Isolation and directed differentiation of neural crest stem cells derived from human embryonic stem cells. *Nat Biotechnol* **25:** 1468-1475

Lehmann JM, Riethmuller G, Johnson JP (1989) MUC18, a marker of tumor progression in human melanoma, shows sequence similarity to the neural cell adhesion molecules of the immunoglobulin superfamily. *Proc Natl Acad Sci U S A* **86:** 9891-9895

Leistad L, Ostensen M, Faxvaag A (1998) Detection of cytokine mRNA in human, articular cartilage from patients with rheumatoid arthritis and osteoarthritis by reverse transcriptase-polymerase chain reaction. *Scand J Rheumatol* **27:** 61-67

Leonard WJ (2001) Cytokines and immunodeficiency diseases. *Nat Rev Immunol* **1:** 200-208

Li W, Johnson SA, Shelley WC, Yoder MC (2004) Hematopoietic stem cell repopulating ability can be maintained in vitro by some primary endothelial cells. *Exp Hematol* **32:** 1226-1237

Lin RC, Matesic DF, Marvin M, McKay RD, Brustle O (1995) Re-expression of the intermediate filament nestin in reactive astrocytes. *Neurobiol Dis* **2:** 79-85

Lo Celso C, Fleming HE, Wu JW, Zhao CX, Miake-Lye S, Fujisaki J, Cote D, Rowe DW, Lin CP, Scadden DT (2009) Live-animal tracking of individual haematopoietic stem/progenitor cells in their niche. *Nature* **457:** 92-96

Lo Celso C, Scadden DT (2011) The haematopoietic stem cell niche at a glance. *J Cell Sci* **124:** 3529-3535

Long D, Blake S, Song XY, Lark M, Loeser RF (2008) Human articular chondrocytes produce IL-7 and respond to IL-7 with increased production of matrix metalloproteinase-13. *Arthritis Res Ther* **10:** R23

Lord BI, Testa NG, Hendry JH (1975) The relative spatial distributions of CFUs and CFUc in the normal mouse femur. *Blood* **46:** 65-72

Lucas S, Taront S, Magnan C, Fauconnier L, Delacre M, Macia L, Delanoye A, Verwaerde C, Spriet C, Saule P, Goormachtigh G, Heliot L, Ktorza A, Movassat J, Polakowska R, Auriault C, Poulain-Godefroy O, Di Santo J, Froguel P, Wolowczuk I (2012) Interleukin-7 regulates adipose tissue mass and insulin sensitivity in high-fat diet-fed mice through lymphocyte-dependent and independent mechanisms. *PLoS One* **7:** e40351

Mackie EJ (2003) Osteoblasts: novel roles in orchestration of skeletal architecture. *Int J Biochem Cell Biol* **35:** 1301-1305

Manabe N, Kawaguchi H, Chikuda H, Miyaura C, Inada M, Nagai R, Nabeshima Y, Nakamura K, Sinclair AM, Scheuermann RH, Kuro-o M (2001) Connection between B lymphocyte and osteoclast differentiation pathways. *J Immunol* **167:** 2625-2631

Manolagas SC (2000) Birth and death of bone cells: basic regulatory mechanisms and implications for the pathogenesis and treatment of osteoporosis. *Endocr Rev* **21:** 115-137

Marine JC, Topham DJ, McKay C, Wang D, Parganas E, Stravopodis D, Yoshimura A, Ihle JN (1999) SOCS1 deficiency causes a lymphocyte-dependent perinatal lethality. *Cell* **98:** 609-616

Massberg S, Schaerli P, Knezevic-Maramica I, Kollnberger M, Tubo N, Moseman EA, Huff IV, Junt T, Wagers AJ, Mazo IB, von Andrian UH (2007) Immunosurveillance by hematopoietic progenitor cells trafficking through blood, lymph, and peripheral tissues. *Cell* **131:** 994-1008

Mazzucchelli R, Durum SK (2007) Interleukin-7 receptor expression: intelligent design. *Nat Rev Immunol* **7:** 144-154

Mazzucchelli RI, Warming S, Lawrence SM, Ishii M, Abshari M, Washington AV, Feigenbaum L, Warner AC, Sims DJ, Li WQ, Hixon JA, Gray DH, Rich BE, Morrow M, Anver MR, Cherry J, Naf D, Sternberg LR, McVicar DW, Farr AG, Germain RN, Rogers K, Jenkins NA, Copeland NG, Durum SK (2009) Visualization and identification of IL-7 producing cells in reporter mice. *PLoS One* **4:** e7637

Mendez-Ferrer S, Lucas D, Battista M, Frenette PS (2008) Haematopoietic stem cell release is regulated by circadian oscillations. *Nature* **452:** 442-447

Mendez-Ferrer S, Michurina TV, Ferraro F, Mazloom AR, Macarthur BD, Lira SA, Scadden DT, Ma'ayan A, Enikolopov GN, Frenette PS (2010) Mesenchymal and haematopoietic stem cells form a unique bone marrow niche. *Nature* **466:** 829-834

Mercier FE, Ragu C, Scadden DT (2012) The bone marrow at the crossroads of blood and immunity. *Nat Rev Immunol* **12:** 49-60

Mignone JL, Kukekov V, Chiang AS, Steindler D, Enikolopov G (2004) Neural stem and progenitor cells in nestin-GFP transgenic mice. *J Comp Neurol* **469:** 311-324

Milner DJ, Weitzer G, Tran D, Bradley A, Capetanaki Y (1996) Disruption of muscle architecture and myocardial degeneration in mice lacking desmin. *J Cell Biol* **134:** 1255-1270

Miyamoto K, Yoshida S, Kawasumi M, Hashimoto K, Kimura T, Sato Y, Kobayashi T, Miyauchi Y, Hoshi H, Iwasaki R, Miyamoto H, Hao W, Morioka H, Chiba K, Yasuda H, Penninger JM, Toyama Y, Suda T, Miyamoto T (2011) Osteoclasts are dispensable for hematopoietic stem cell maintenance and mobilization. *J Exp Med* **208:** 2175-2181

Miyamoto T, Ohneda O, Arai F, Iwamoto K, Okada S, Takagi K, Anderson DM, Suda T (2001) Bifurcation of osteoclasts and dendritic cells from common progenitors. *Blood* **98:** 2544-2554

Miyaura C, Onoe Y, Inada M, Maki K, Ikuta K, Ito M, Suda T (1997) Increased B-lymphopoiesis by interleukin 7 induces bone loss in mice with intact ovarian function: similarity to estrogen deficiency. *Proc Natl Acad Sci U S A* **94:** 9360-9365

Moitra J, Mason MM, Olive M, Krylov D, Gavrilova O, Marcus-Samuels B, Feigenbaum L, Lee E, Aoyama T, Eckhaus M, Reitman ML, Vinson C (1998) Life without white fat: a transgenic mouse. *Genes Dev* **12:** 3168-3181

Moore MA, Metcalf D (1970) Ontogeny of the haemopoietic system: yolk sac origin of in vivo and in vitro colony forming cells in the developing mouse embryo. *Br J Haematol* **18:** 279-296

Morikawa S, Mabuchi Y, Kubota Y, Nagai Y, Niibe K, Hiratsu E, Suzuki S, Miyauchi-Hara C, Nagoshi N, Sunabori T, Shimmura S, Miyawaki A, Nakagawa T, Suda T, Okano H, Matsuzaki Y (2009a) Prospective identification, isolation, and systemic transplantation of multipotent mesenchymal stem cells in murine bone marrow. *J Exp Med* **206:** 2483-2496

Morikawa S, Mabuchi Y, Niibe K, Suzuki S, Nagoshi N, Sunabori T, Shimmura S, Nagai Y, Nakagawa T, Okano H, Matsuzaki Y (2009b) Development of mesenchymal stem cells partially originate from the neural crest. *Biochem Biophys Res Commun* **379:** 1114-1119

Morrison SJ, White PM, Zock C, Anderson DJ (1999) Prospective identification, isolation by flow cytometry, and in vivo self-renewal of multipotent mammalian neural crest stem cells. *Cell* **96:** 737-749

Morrissey PJ, Conlon P, Charrier K, Braddy S, Alpert A, Williams D, Namen AE, Mochizuki D (1991) Administration of IL-7 to normal mice stimulates B-lymphopoiesis and peripheral lymphadenopathy. *J Immunol* **147:** 561-568

Morshead CM, Reynolds BA, Craig CG, McBurney MW, Staines WA, Morassutti D, Weiss S, van der Kooy D (1994) Neural stem cells in the adult mammalian forebrain: a relatively quiescent subpopulation of subependymal cells. *Neuron* **13:** 1071-1082

Mosnier JF, Degott C, Marcellin P, Henin D, Erlinger S, Benhamou JP (1993) The intraportal lymphoid nodule and its environment in chronic active hepatitis C: an immunohistochemical study. *Hepatology* **17:** 366-371

Nagoshi N, Shibata S, Kubota Y, Nakamura M, Nagai Y, Satoh E, Morikawa S, Okada Y, Mabuchi Y, Katoh H, Okada S, Fukuda K, Suda T, Matsuzaki Y, Toyama Y, Okano H (2008) Ontogeny and multipotency of neural crest-derived stem cells in mouse bone marrow, dorsal root ganglia, and whisker pad. *Cell Stem Cell* **2:** 392-403

Namen AE, Lupton S, Hjerrild K, Wignall J, Mochizuki DY, Schmierer A, Mosley B, March CJ, Urdal D, Gillis S (1988) Stimulation of B-cell progenitors by cloned murine interleukin-7. *Nature* **333:** 571-573

Naveiras O, Nardi V, Wenzel PL, Hauschka PV, Fahey F, Daley GQ (2009) Bone-marrow adipocytes as negative regulators of the haematopoietic microenvironment. *Nature* **460:** 259-263

Nilsson SK, Johnston HM, Whitty GA, Williams B, Webb RJ, Denhardt DT, Bertoncello I, Bendall LJ, Simmons PJ, Haylock DN (2005) Osteopontin, a key component of the hematopoietic stem cell niche and regulator of primitive hematopoietic progenitor cells. *Blood* **106:** 1232-1239

Nosaka T, van Deursen JM, Tripp RA, Thierfelder WE, Witthuhn BA, McMickle AP, Doherty PC, Grosveld GC, Ihle JN (1995) Defective lymphoid development in mice lacking Jak3. *Science* **270:** 800-802

O'Malley DP (2007) Benign extramedullary myeloid proliferations. *Mod Pathol* **20:** 405-415

Olsen BR, Reginato AM, Wang W (2000) Bone development. *Annu Rev Cell Dev Biol* **16:** 191-220

Omatsu Y, Sugiyama T, Kohara H, Kondoh G, Fujii N, Kohno K, Nagasawa T (2010) The essential functions of adipo-osteogenic progenitors as the hematopoietic stem and progenitor cell niche. *Immunity* **33:** 387-399

Onoe Y, Miyaura C, Kaminakayashiki T, Nagai Y, Noguchi K, Chen QR, Seo H, Ohta H, Nozawa S, Kudo I, Suda T (1996) IL-13 and IL-4 inhibit bone resorption by suppressing cyclooxygenase-2-dependent prostaglandin synthesis in osteoblasts. *J Immunol* **156:** 758-764

Park D, Xiang AP, Mao FF, Zhang L, Di CG, Liu XM, Shao Y, Ma BF, Lee JH, Ha KS, Walton N, Lahn BT (2010) Nestin is required for the proper self-renewal of neural stem cells. *Stem Cells* **28:** 2162-2171

Park JH, Yu Q, Erman B, Appelbaum JS, Montoya-Durango D, Grimes HL, Singer A (2004) Suppression of IL7Ralpha transcription by IL-7 and other prosurvival cytokines: a novel mechanism for maximizing IL-7-dependent T cell survival. *Immunity* **21:** 289-302

Park LS, Martin U, Garka K, Gliniak B, Di Santo JP, Muller W, Largaespada DA, Copeland NG, Jenkins NA, Farr AG, Ziegler SF, Morrissey PJ, Paxton R, Sims JE (2000) Cloning of the murine

thymic stromal lymphopoietin (TSLP) receptor: Formation of a functional heteromeric complex requires interleukin 7 receptor. *J Exp Med* **192:** 659-670

Parmar K, Mauch P, Vergilio JA, Sackstein R, Down JD (2007) Distribution of hematopoietic stem cells in the bone marrow according to regional hypoxia. *Proc Natl Acad Sci U S A* **104:** 5431-5436

Parrish YK, Baez I, Milford TA, Benitez A, Galloway N, Rogerio JW, Sahakian E, Kagoda M, Huang G, Hao QL, Sevilla Y, Barsky LW, Zielinska E, Price MA, Wall NR, Dovat S, Payne KJ (2009) IL-7 Dependence in human B lymphopoiesis increases during progression of ontogeny from cord blood to bone marrow. *J Immunol* **182:** 4255-4266

Peister A, Mellad JA, Larson BL, Hall BM, Gibson LF, Prockop DJ (2004) Adult stem cells from bone marrow (MSCs) isolated from different strains of inbred mice vary in surface epitopes, rates of proliferation, and differentiation potential. *Blood* **103:** 1662-1668

Petit I, Szyper-Kravitz M, Nagler A, Lahav M, Peled A, Habler L, Ponomaryov T, Taichman RS, Arenzana-Seisdedos F, Fujii N, Sandbank J, Zipori D, Lapidot T (2002) G-CSF induces stem cell mobilization by decreasing bone marrow SDF-1 and up-regulating CXCR4. *Nat Immunol* **3:** 687-694

Ponchel F, Verburg RJ, Bingham SJ, Brown AK, Moore J, Protheroe A, Short K, Lawson CA, Morgan AW, Quinn M, Buch M, Field SL, Maltby SL, Masurel A, Douglas SH, Straszynski L, Fearon U, Veale DJ, Patel P, McGonagle D, Snowden J, Markham AF, Ma D, van Laar JM, Papadaki HA, Emery P, Isaacs JD (2005) Interleukin-7 deficiency in rheumatoid arthritis: consequences for therapy-induced lymphopenia. *Arthritis Res Ther* **7:** R80-92

Ponomaryov T, Peled A, Petit I, Taichman RS, Habler L, Sandbank J, Arenzana-Seisdedos F, Magerus A, Caruz A, Fujii N, Nagler A, Lahav M, Szyper-Kravitz M, Zipori D, Lapidot T (2000) Induction of the chemokine stromal-derived factor-1 following DNA damage improves human stem cell function. *J Clin Invest* **106:** 1331-1339

Qian H, Le Blanc K, Sigvardsson M (2012) Primary mesenchymal stem and progenitor cells from bone marrow lack expression of CD44 protein. *J Biol Chem* **287:** 25795-25807

Rafii S, Mohle R, Shapiro F, Frey BM, Moore MA (1997) Regulation of hematopoiesis by microvascular endothelium. *Leuk Lymphoma* **27:** 375-386

Repass JF, Laurent MN, Carter C, Reizis B, Bedford MT, Cardenas K, Narang P, Coles M, Richie ER (2009) IL7-hCD25 and IL7-Cre BAC transgenic mouse lines: new tools for analysis of IL-7 expressing cells. *Genesis* **47:** 281-287

Roland M, Rao SR, Sibbald B, Hann M, Harrison S, Walter A, Guthrie B, Desroches C, Ferris TG, Campbell EG (2011) Professional values and reported behaviours of doctors in the USA and UK: quantitative survey. *BMJ Qual Saf* **20:** 515-521

Russell SM, Johnston JA, Noguchi M, Kawamura M, Bacon CM, Friedmann M, Berg M, McVicar DW, Witthuhn BA, Silvennoinen O, et al. (1994) Interaction of IL-2R beta and gamma c chains with Jak1 and Jak3: implications for XSCID and XCID. *Science* **266:** 1042-1045

Sacchetti B, Funari A, Michienzi S, Di Cesare S, Piersanti S, Saggio I, Tagliafico E, Ferrari S, Robey PG, Riminucci M, Bianco P (2007) Self-renewing osteoprogenitors in bone marrow sinusoids can organize a hematopoietic microenvironment. *Cell* **131:** 324-336

Salati S, Lisignoli G, Manferdini C, Pennucci V, Zini R, Bianchi E, Norfo R, Facchini A, Ferrari S, Manfredini R (2013) Co-culture of hematopoietic stem/progenitor cells with human osteblasts favours mono/macrophage differentiation at the expense of the erythroid lineage. *PLoS One* **8:** e53496

Saleh FA, Frith JE, Lee JA, Genever PG (2012) Three-dimensional in vitro culture techniques for mesenchymal stem cells. *Methods Mol Biol* **916:** 31-45

Sato T, Watanabe K, Masuhara M, Hada N, Hakeda Y (2007) Production of IL-7 is increased in ovariectomized mice, but not RANKL mRNA expression by osteoblasts/stromal cells in bone, and IL-7 enhances generation of osteoclast precursors in vitro. *J Bone Miner Metab* **25:** 19-27

Sauer B (1998) Inducible gene targeting in mice using the Cre/lox system. *Methods* **14:** 381-392

Scadden DT (2006) The stem-cell niche as an entity of action. *Nature* **441:** 1075-1079

Schmits R, Filmus J, Gerwin N, Senaldi G, Kiefer F, Kundig T, Wakeham A, Shahinian A, Catzavelos C, Rak J, Furlonger C, Zakarian A, Simard JJ, Ohashi PS, Paige CJ, Gutierrez-Ramos JC, Mak TW (1997) CD44 regulates hematopoietic progenitor distribution, granuloma formation, and tumorigenicity. *Blood* **90:** 2217-2233

Schofield R (1978) The relationship between the spleen colony-forming cell and the haemopoietic stem cell. *Blood Cells* **4:** 7-25

Schrage A, Loddenkemper C, Erben U, Lauer U, Hausdorf G, Jungblut PR, Johnson J, Knolle PA, Zeitz M, Hamann A, Klugewitz K (2008) Murine CD146 is widely expressed on endothelial cells and is recognized by the monoclonal antibody ME-9F1. *Histochem Cell Biol* **129:** 441-451

Scobioala S, Klocke R, Kuhlmann M, Tian W, Hasib L, Milting H, Koenig S, Stelljes M, El-Banayosy A, Tenderich G, Michel G, Breithardt G, Nikol S (2008) Up-regulation of nestin in the infarcted myocardium potentially indicates differentiation of resident cardiac stem cells into various lineages including cardiomyocytes. *FASEB J* **22:** 1021-1031

Scott LM, Priestley GV, Papayannopoulou T (2003) Deletion of alpha4 integrins from adult hematopoietic cells reveals roles in homeostasis, regeneration, and homing. *Mol Cell Biol* **23:** 9349-9360

Serafini B, Rosicarelli B, Magliozzi R, Stigliano E, Aloisi F (2004) Detection of ectopic B-cell follicles with germinal centers in the meninges of patients with secondary progressive multiple sclerosis. *Brain Pathol* **14:** 164-174

Shalapour S, Deiser K, Sercan O, Tuckermann J, Minnich K, Willimsky G, Blankenstein T, Hammerling GJ, Arnold B, Schuler T (2010) Commensal microflora and interferon-gamma promote steady-state interleukin-7 production in vivo. *Eur J Immunol* **40:** 2391-2400

Shizuya H, Birren B, Kim UJ, Mancino V, Slepak T, Tachiiri Y, Simon M (1992) Cloning and stable maintenance of 300-kilobase-pair fragments of human DNA in Escherichia coli using an F-factor-based vector. *Proc Natl Acad Sci U S A* **89:** 8794-8797

Silver IA, Murrills RJ, Etherington DJ (1988) Microelectrode studies on the acid microenvironment beneath adherent macrophages and osteoclasts. *Exp Cell Res* **175:** 266-276

Simmons PJ, Torok-Storb B (1991) Identification of stromal cell precursors in human bone marrow by a novel monoclonal antibody, STRO-1. *Blood* **78:** 55-62

Sims JE, Williams DE, Morrissey PJ, Garka K, Foxworthe D, Price V, Friend SL, Farr A, Bedell MA, Jenkins NA, Copeland NG, Grabstein K, Paxton RJ (2000) Molecular cloning and biological characterization of a novel murine lymphoid growth factor. *J Exp Med* **192:** 671-680

Sorrentino A, Ferracin M, Castelli G, Biffoni M, Tomaselli G, Baiocchi M, Fatica A, Negrini M, Peschle C, Valtieri M (2008) Isolation and characterization of CD146+ multipotent mesenchymal stromal cells. *Exp Hematol* **36:** 1035-1046

Starr R, Hilton DJ (1998) SOCS: suppressors of cytokine signalling. *Int J Biochem Cell Biol* **30:** 1081-1085

Stemple DL, Anderson DJ (1992) Isolation of a stem cell for neurons and glia from the mammalian neural crest. *Cell* **71:** 973-985

Stier S, Ko Y, Forkert R, Lutz C, Neuhaus T, Grünewald E, Cheng T, Dombkowski D, Calvi LM, Rittling SR, Scadden DT (2005) Osteopontin is a hematopoietic stem cell niche component that negatively regulates stem cell pool size *JEM* **201:** 1781-1791

Sugawara K, Kurihara H, Negishi M, Saito N, Nakazato Y, Sasaki T, Takeuchi T (2002) Nestin as a marker for proliferative endothelium in gliomas. *Lab Invest* **82:** 345-351

Sugiyama T, Kohara H, Noda M, Nagasawa T (2006) Maintenance of the hematopoietic stem cell pool by CXCL12-CXCR4 chemokine signaling in bone marrow stromal cell niches. *Immunity* **25:** 977-988

Sun S, Guo Z, Xiao X, Liu B, Liu X, Tang PH, Mao N (2003) Isolation of mouse marrow mesenchymal progenitors by a novel and reliable method. *Stem Cells* **21:** 527-535

Taichman RS, Emerson SG (1994) Human osteoblasts support hematopoiesis through the production of granulocyte colony-stimulating factor. *J Exp Med* **179:** 1677-1682

Taichman RS, Reilly MJ, Emerson SG (1996) Human osteoblasts support human hematopoietic progenitor cells in vitro bone marrow cultures. *Blood* **87:** 518-524

Takashima Y, Era T, Nakao K, Kondo S, Kasuga M, Smith AG, Nishikawa S (2007) Neuroepithelial cells supply an initial transient wave of MSC differentiation. *Cell* **129:** 1377-1388

Takemura S, Braun A, Crowson C, Kurtin PJ, Cofield RH, O'Fallon WM, Goronzy JJ, Weyand CM (2001) Lymphoid neogenesis in rheumatoid synovitis. *J Immunol* **167:** 1072-1080

Takeshita T, Asao H, Ohtani K, Ishii N, Kumaki S, Tanaka N, Munakata H, Nakamura M, Sugamura K (1992) Cloning of the gamma chain of the human IL-2 receptor. *Science* **257:** 379-382

Takubo K, Goda N, Yamada W, Iriuchishima H, Ikeda E, Kubota Y, Shima H, Johnson RS, Hirao A, Suematsu M, Suda T (2010) Regulation of the HIF-1alpha level is essential for hematopoietic stem cells. *Cell Stem Cell* **7:** 391-402

Tanabe BK, Abe LM, Kimura LH, Reinker KA, Yamaga KM (1996) Cytokine mRNA repertoire of articular chondrocytes from arthritic patients, infants, and neonatal mice. *Rheumatol Int* **16:** 67-76

Taniguchi H, Toyoshima T, Fukao K, Nakauchi H (1996) Presence of hematopoietic stem cells in the adult liver. *Nat Med* **2:** 198-203

Tavassoli M, Crosby WH (1968) Transplantation of marrow to extramedullary sites. *Science* **161:** 54-56

Teglund S, McKay C, Schuetz E, van Deursen JM, Stravopodis D, Wang D, Brown M, Bodner S, Grosveld G, Ihle JN (1998) Stat5a and Stat5b proteins have essential and nonessential, or redundant, roles in cytokine responses. *Cell* **93:** 841-850

Thomas SK, Messam CA, Spengler BA, Biedler JL, Ross RA (2004) Nestin is a potential mediator of malignancy in human neuroblastoma cells. *J Biol Chem* **279:** 27994-27999

Timmer TC, Baltus B, Vondenhoff M, Huizinga TW, Tak PP, Verweij CL, Mebius RE, van der Pouw Kraan TC (2007) Inflammation and ectopic lymphoid structures in rheumatoid arthritis synovial tissues dissected by genomics technology: identification of the interleukin-7 signaling pathway in tissues with lymphoid neogenesis. *Arthritis Rheum* **56:** 2492-2502

Tokoyoda K, Egawa T, Sugiyama T, Choi BI, Nagasawa T (2004) Cellular niches controlling B lymphocyte behavior within bone marrow during development. *Immunity* **20:** 707-718

Tomita Y, Matsumura K, Wakamatsu Y, Matsuzaki Y, Shibuya I, Kawaguchi H, Ieda M, Kanakubo S, Shimazaki T, Ogawa S, Osumi N, Okano H, Fukuda K (2005) Cardiac neural crest cells contribute to the dormant multipotent stem cell in the mammalian heart. *J Cell Biol* **170:** 1135-1146

Toraldo G, Roggia C, Qian WP, Pacifici R, Weitzmann MN (2003) IL-7 induces bone loss in vivo by induction of receptor activator of nuclear factor kappa B ligand and tumor necrosis factor alpha from T cells. *Proc Natl Acad Sci U S A* **100:** 125-130

Tormin A, Li O, Brune JC, Walsh S, Schutz B, Ehinger M, Ditzel N, Kassem M, Scheding S (2011) CD146 expression on primary nonhematopoietic bone marrow stem cells is correlated with in situ localization. *Blood* **117:** 5067-5077

Trivedi P, Hematti P (2008) Derivation and immunological characterization of mesenchymal stromal cells from human embryonic stem cells. *Exp Hematol* **36:** 350-359

Tropel P, Platet N, Platel JC, Noel D, Albrieux M, Benabid AL, Berger F (2006) Functional neuronal differentiation of bone marrow-derived mesenchymal stem cells. *Stem Cells* **24:** 2868-2876

Trubiani O, Isgro A, Zini N, Antonucci I, Aiuti F, Di Primio R, Nanci A, Caputi S, Paganelli R (2008) Functional interleukin-7/interleukin-7Ralpha, and SDF-1alpha/CXCR4 are expressed by human periodontal ligament derived mesenchymal stem cells. *J Cell Physiol* **214:** 706-713

Tzeng YS, Li H, Kang YL, Chen WC, Cheng WC, Lai DM (2011) Loss of Cxcl12/Sdf-1 in adult mice decreases the quiescent state of hematopoietic stem/progenitor cells and alters the pattern of hematopoietic regeneration after myelosuppression. *Blood* **117:** 429-439

Uy GL, Rettig MP, Cashen AF (2008) Plerixafor, a CXCR4 antagonist for the mobilization of hematopoietic stem cells. *Expert Opin Biol Ther* **8:** 1797-1804

van Roon JA, Verweij MC, Wijk MW, Jacobs KM, Bijlsma JW, Lafeber FP (2005) Increased intraarticular interleukin-7 in rheumatoid arthritis patients stimulates cell contact-dependent activation of CD4(+) T cells and macrophages. *Arthritis Rheum* **52:** 1700-1710

Veselska R, Kuglik P, Cejpek P, Svachova H, Neradil J, Loja T, Relichova J (2006) Nestin expression in the cell lines derived from glioblastoma multiforme. *BMC Cancer* **6:** 32

Visnjic D, Kalajzic Z, Rowe DW, Katavic V, Lorenzo J, Aguila HL (2004) Hematopoiesis is severely altered in mice with an induced osteoblast deficiency. *Blood* **103:** 3258-3264

Vodyanik MA, Yu J, Zhang X, Tian S, Stewart R, Thomson JA, Slukvin, II (2010) A mesoderm-derived precursor for mesenchymal stem and endothelial cells. *Cell Stem Cell* **7:** 718-729

Wang Y, Zhang Y, Zeng Y, Zheng Y, Fu G, Cui Z, Yang T (2006) Patterns of nestin expression in human skin. *Cell Biol Int* **30:** 144-148

Watt SM, Forde SP (2008) The central role of the chemokine receptor, CXCR4, in haemopoietic stem cell transplantation: will CXCR4 antagonists contribute to the treatment of blood disorders? *Vox Sang* **94:** 18-32

Wautier F, Wislet-Gendebien S, Chanas G, Rogister B, Leprince P (2007) Regulation of nestin expression by thrombin and cell density in cultures of bone mesenchymal stem cells and radial glial cells. *BMC Neurosci* **8:** 104

Weitzmann MN, Cenci S, Rifas L, Brown C, Pacifici R (2000) Interleukin-7 stimulates osteoclast formation by up-regulating the T-cell production of soluble osteoclastogenic cytokines. *Blood* **96:** 1873-1878

Weitzmann MN, Roggia C, Toraldo G, Weitzmann L, Pacifici R (2002) Increased production of IL-7 uncouples bone formation from bone resorption during estrogen deficiency. *J Clin Invest* **110:** 1643-1650

Wiese C, Rolletschek A, Kania G, Blyszczuk P, Tarasov KV, Tarasova Y, Wersto RP, Boheler KR, Wobus AM (2004) Nestin expression--a property of multi-lineage progenitor cells? *Cell Mol Life Sci* **61:** 2510-2522

Winkler IG, Sims NA, Pettit AR, Barbier V, Nowlan B, Helwani F, Poulton IJ, van Rooijen N, Alexander KA, Raggatt LJ, Levesque JP (2010) Bone marrow macrophages maintain hematopoietic stem cell (HSC) niches and their depletion mobilizes HSCs. *Blood* **116:** 4815-4828

Wislet-Gendebien S, Laudet E, Neirinckx V, Alix P, Leprince P, Glejzer A, Poulet C, Hennuy B, Sommer L, Shakhova O, Rogister B (2012) Mesenchymal stem cells and neural crest stem cells from adult bone marrow: characterization of their surprising similarities and differences. *Cell Mol Life Sci* **69:** 2593-2608

Wislet-Gendebien S, Leprince P, Moonen G, Rogister B (2003) Regulation of neural markers nestin and GFAP expression by cultivated bone marrow stromal cells. *J Cell Sci* **116:** 3295-3302

Wright DE, Wagers AJ, Gulati AP, Johnson FL, Weissman IL (2001) Physiological migration of hematopoietic stem and progenitor cells. *Science* **294:** 1933-1936

Yamauchi Y, Abe K, Mantani A, Hitoshi Y, Suzuki M, Osuzu F, Kuratani S, Yamamura K (1999) A novel transgenic technique that allows specific marking of the neural crest cell lineage in mice. *Dev Biol* **212:** 191-203

Yang XH, Wu QL, Yu XB, Xu CX, Ma BF, Zhang XM, Li SN, Lahn BT, Xiang AP (2008) Nestin expression in different tumours and its relevance to malignant grade. *J Clin Pathol* **61:** 467-473

Yang XW, Model P, Heintz N (1997) Homologous recombination based modification in Escherichia coli and germline transmission in transgenic mice of a bacterial artificial chromosome. *Nat Biotechnol* **15:** 859-865

Yao L, Yokota T, Xia L, Kincade PW, McEver RP (2005) Bone marrow dysfunction in mice lacking the cytokine receptor gp130 in endothelial cells. *Blood* **106:** 4093-4101

Yoshida S, Shimmura S, Nagoshi N, Fukuda K, Matsuzaki Y, Okano H, Tsubota K (2006) Isolation of multipotent neural crest-derived stem cells from the adult mouse cornea. *Stem Cells* **24:** 2714-2722

Zamisch M, Moore-Scott B, Su DM, Lucas PJ, Manley N, Richie ER (2005) Ontogeny and regulation of IL-7-expressing thymic epithelial cells. *J Immunol* **174:** 60-67

Zhang J, Niu C, Ye L, Huang H, He X, Tong WG, Ross J, Haug J, Johnson T, Feng JQ, Harris S, Wiedemann LM, Mishina Y, Li L (2003) Identification of the haematopoietic stem cell niche and control of the niche size. *Nature* **425:** 836-841

Zhu J, Garrett R, Jung Y, Zhang Y, Kim N, Wang J, Joe GJ, Hexner E, Choi Y, Taichman RS, Emerson SG (2007) Osteoblasts support B-lymphocyte commitment and differentiation from hematopoietic stem cells. *Blood* **109:** 3706-3712

Zimmerman L, Parr B, Lendahl U, Cunningham M, McKay R, Gavin B, Mann J, Vassileva G, McMahon A (1994) Independent regulatory elements in the nestin gene direct transgene expression to neural stem cells or muscle precursors. *Neuron* **12:** 11-24